Late Mesozoic-Cenozoic tectono-stratigraphic evolution of the Vesterålen margin, offshore northern Norway

Juan Camilo Meza

Master Thesis in Geosciences
Petroleum Geoscience
60 credits

Department of Geosciences
Faculty of Mathematics and Natural Sciences

UNIVERSITY OF OSLO
June 2020

Late Mesozoic-Cenozoic tectono-stratigraphic evolution of the Vesterålen margin, offshore northern Norway

Juan Camilo Meza

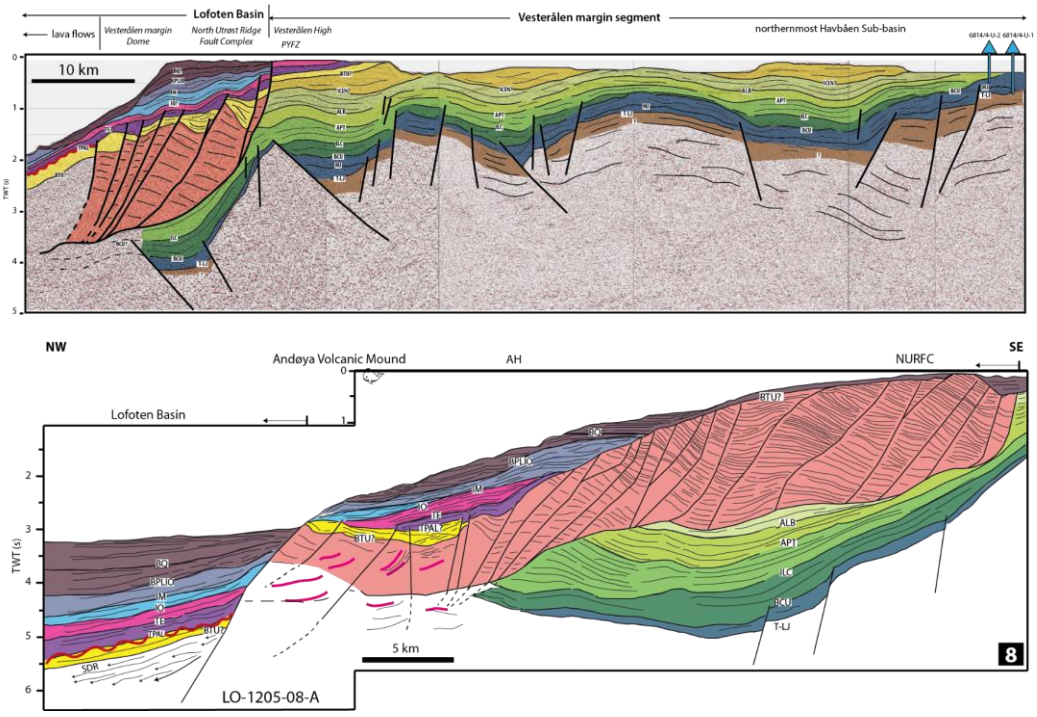

Master Thesis in Geosciences
Petroleum Geoscience
60 credits

Department of Geosciences
Faculty of Mathematics and Natural Sciences

UNIVERSITY OF OSLO

June 2020

2020

Late Mesozoic-Cenozoic tectono-stratigraphic evolution of the Vesterålen margin, offshore northern Norway

Juan Camilo Meza

http://www.duo.uio.no/

Trykk: Reprosentralen, Universitetet i Oslo

Abstract

Available 2D multi-channel seismic profiles and a 3D seismic survey are utilized together with potential field and limited well data to study the Late Mesozoic-Cenozoic tectono-stratigraphic evolution of the Vesterålen margin offshore northern Norway. The analysis resulted in an updated structural and stratigraphic framework, together with new and better refined structural elements for the Vesterålen margin. Distinct along-margin basin segmentation is evident through NW-SE trending curvilinear transfer zones informally named as the Jennegga transfer zone, Vesterålen transfer zone system, and Andøya transfer zone. These divide the study area into three main margin segments, namely the northern Lofoten, Vesterålen, and Andøya segments. Five main rift phases of varying intensity have been recognised and refined, and they are evidenced by eight mapped fault families: pre-Jurassic, Late Jurassic-earliest Cretaceous, Aptian-Albian, Albian-Cenomanian, three individual fault families within Late Cretaceous, and Paleocene. Furthermore, fault heave and displacement measurements were undertaken within the North Utrøst Ridge Fault Complex (NURFC) that exhibits prominent low-angle detachment faults of Cretaceous strata. The analysis demonstrated a progressively northwards increase of fault heave and displacement intensity from ~3 km in the south to ~7-8 km in the north of the study area, and a maximum stretching factor defined by fault geometry (β_f) of ~1.7. These values when compared to the crustal stretching (i.e. >3) and thinning (0.7-0.9) factors required to achieve the observed extension on the >300-km-width extended NE Greenland-Vesterålen conjugate margins reveal an apparent extension discrepancy. Fault population analysis suggests that only ~14% of extension is seen from the faults on seismic profiles in the NURFC. Finally, a conceptual tectonic multiphase evolution model for lithospheric extension is proposed for the NE Greenland-Vesterålen conjugate margins, consisting of a lower and upper plate configuration. This model elaborates the more ductile mode of deformation evidenced by the Late Cretaceous-Paleocene low-angle detachment fault complexes on both conjugate margins and the asymmetry in crustal structure at the time of continental rupture at the Paleocene-Eocene transition. The study shows that the Vesterålen margin represents an essential area to study the tectono-stratigraphic evolution of the NE Atlantic margins.

Preface

This master thesis (60 ECTS) has been submitted as the final part of the two-years master program in Geosciences with specialization in “Petroleum Geoscience” at the University of Oslo (UiO). The thesis has been supervised by Professor Filippos Tsikalas and Professor Jan Inge Faleide.

Acknowledgements

I would like to express my gratitude to my supervisors at the University of Oslo for their guidance and feedback during the work of this thesis. Their knowledge has been critical for the completion of this project. I want to also acknowledge Kristoffer Løvstad and Dr. Mansour Abdelmalak for preparing and providing, respectively the seismic, and the gravity and magnetic datasets. TGS and NPD are acknowledged for providing access to seismic and the potential field data, and Schlumberger for making the Petrel software available. Some figures are courtesy of Prof. Filippos Tsikalas, Prof. Jan Inge Faleide, and Dr. Mansour Abdelmalak. I would like to thank as well the University of Oslo IT-crew at the Department of Geosciences for making it possible to work at home under the special circumstances of the Covid-19.

Thank you to all my fellow peers and friends for motivation during this work, and for making it easier to adapt here in Oslo: Hanne, Yuanwei, Shajahat, Markus, Emil, and Michael; and to Ivan and his family.

Special thanks to my partner Aaf for all her love, companionship and support she has given me since we first met, and thanks to her family for the warm welcome I have received from them. Finally, I express my deep gratitude to my family in Colombia; my parents Juan and Luz, and my sister Laura, for helping me with costing my life expenses in Oslo, but most importantly, thank you for your unconditional love and support. I then dedicate this work to all of you, and to my grandma Alicia-you will always be in my heart.

Juan Camilo Meza

Contents

1 Introduction

The Vesterålen margin is located at ~67°N off mainland Norway and is the northern part of the ~400-km-long composite Lofoten-Vesterålen continental margin (LVM) (Fig. 1.1). The latter is separated to the south and north, respectively, from the wide Vøring volcanic passive margin by the Bivrost Lineament (BL) and from the SW Barents Sea sheared margin by the Senja Fracture Zone (SFZ) (Blystad et al., 1995; Bergh et al., 2007). The LVM represents the link between the mid-Norwegian, SW Barents and conjugate NE Greenland margins, and is a key area to study the rift-basin architecture and the tectono-stratigraphic evolution of the NE Atlantic margins (Fig. 1.1) (Faleide et al., 2008; Tsikalas et al., 2012).

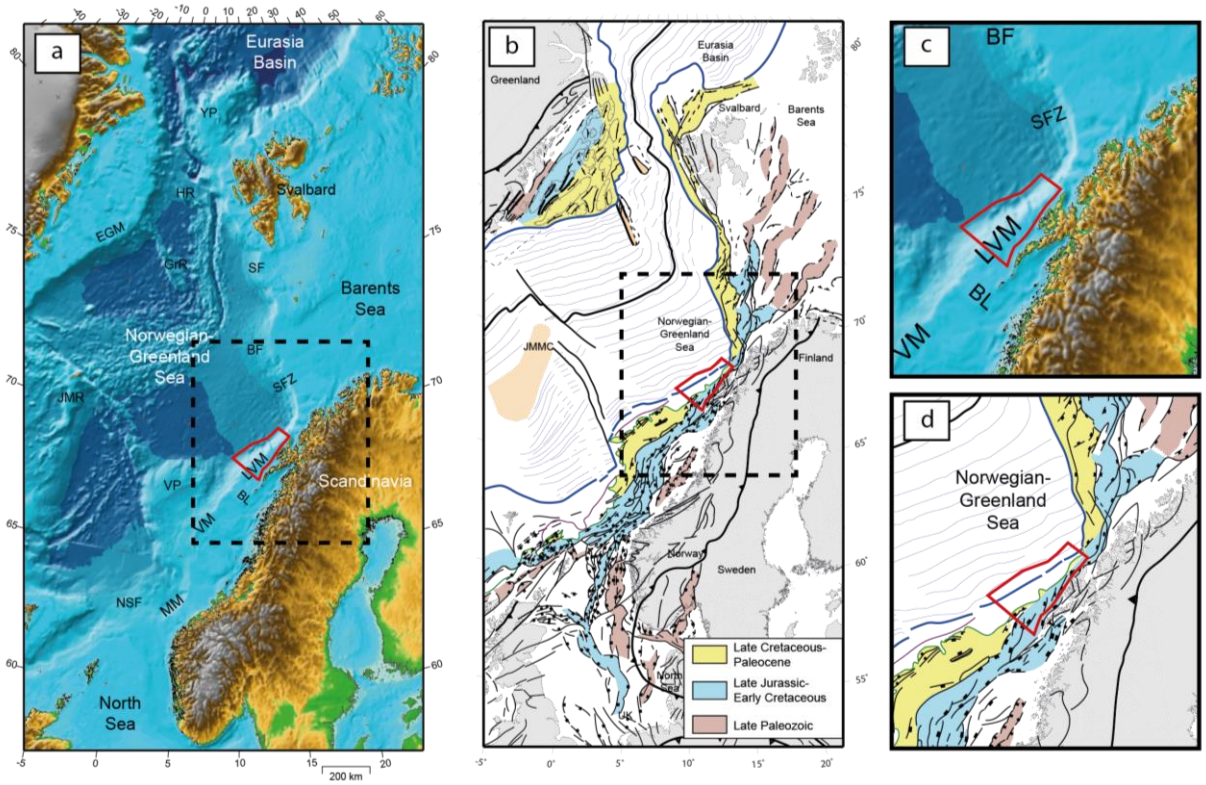

***Fig. 1.1**: **(a)** Regional setting of the Norwegian continental margin. The location of the study area is marked with a red polygon. BF: Bjørnøya Fan; BL: Bivrost Lineament; EGM: East Greenland Margin; GR: Greenland Ridge; HR: Hovgård Ridge; JMR: Jan Mayen Ridge; LVM: Lofoten-Vesterålen Margin; MM: Møre Margin; NSF: North Sea Fan; SF: Storfjorden Fan; SFZ: Senja Fracture Zone; VM: Vøring Margin; VP: Vøring Plateau; YP: Yermak Plateau. **(b)** Main structural elements of the Norwegian continental shelf and adjacent areas. The structural elements are related to the main rift phases affecting the NE Atlantic region. JMMC: Jan Mayen micro-continent. **(c)** and **(d)** zoomed portions marked with black-dashed boxes in **(a)** and **(b)**, respectively, showing the area of interest. Modified from Faleide et al. (2015).*

The Lofoten and Vesterålen segments are characterized by a narrow shelf and steep slope, with an elevated rifted complex of margin-parallel basement ridges, and shallow Mesozoic sedimentary basins (Blystad et al., 1995). The LVM physiographic attributes, crustal structure, and sedimentary infill history and distribution distinctly contrast with the adjacent margins, making the LVM a separate and one of the least understood tectono-stratigraphic provinces within the Norwegian Continental Shelf (Eldholm et al., 2002; Faleide et al., 2008). The situation is even worse for the Vesterålen margin segment where, prior to the current study, only vintage 2D seismic reflection profiles have been available. Furthermore, the study area within the Vesterålen margin segment (Fig. 1.1) is defined as the Nordland VII petroleum province west of the Lofoten, Vesterålen and Andøya archipelagos. This area is considered among the top areas with yet-to-find prospective resources in the Norwegian Sea (~127 Mill. Sm3 o.e; NPD, 2010). However, the area has never been opened for petroleum exploration, and thus no conventional exploration wells were ever drilled there.

In this study, reprocessed vintage 2D multi-channel seismic (MCS) reflection profiles, and the most recently acquired 2D MCS dataset and a 3D seismic survey that are for the first time available to academia, are utilized together with well (exploration and stratigraphic shallow boreholes) and potential-field (gravity and magnetic) data. The main aim is to study the Cretaceous-Cenozoic tectono-sedimentary evolution of the Vesterålen margin segment in the context of the LVM. Through seismic and structural interpretations, the study objectives are as follows:

- Refine rift phases affecting the study area
- Map along-margin tectono-stratigraphic changes
- Decipher role of transfer zones in margin evolution
- Investigate possible structural inheritance
- View the study area in a conjugate setting for margin evolution considerations

2 Geological setting

The Lofoten-Vesterålen margin (LVM) is part of the NE Atlantic margins, which have evolved through multiple rift episodes since the collapse of the Caledonides in Devonian (Fig. 2.1) (Faleide et al., 2008). The culmination of lithospheric extension was accompanied with regional magmatic events near the Paleocene-Eocene transition (~55 Ma), where complete lithospheric break-up took place (Eldholm et al., 2002). Consequently, the continental separation between Eurasia and Greenland led to a rifted conjugate passive margin that, in response to subsidence and sediment loading during the widening and deepening of the Norwegian-Greenland Sea, gave rise to the Vøring and Lofoten-Vesterålen margins (Faleide et al., 2015). The subsequent tectonic history from earliest Eocene to Present is characterized by active seafloor spreading (Lundin and Doré, 2002).

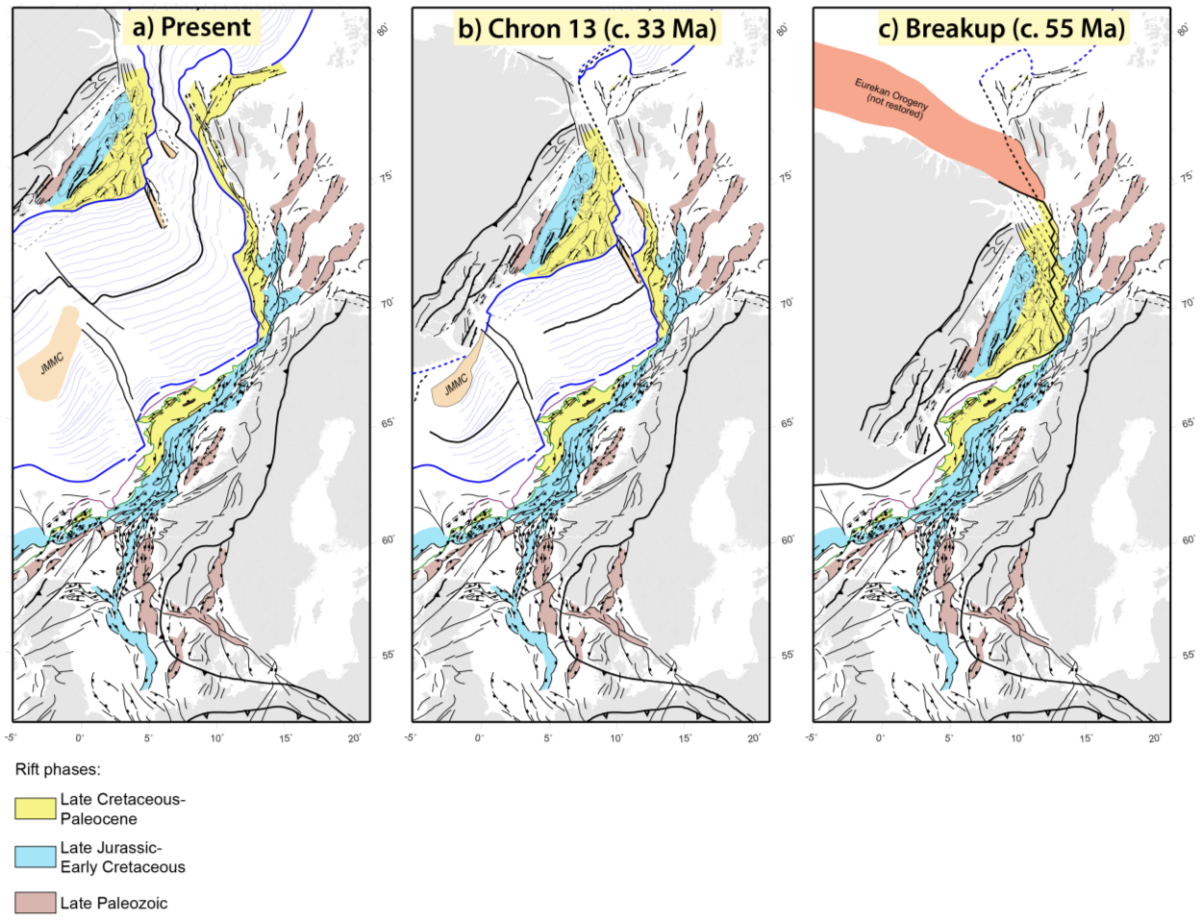

***Fig. 2.1**: Plate tectonic reconstructions of the NE Atlantic (modified from Faleide et al. 2015). (a) Present, (b) ~33 Ma, (c) ~55 Ma, time of breakup. JMMC: Jan Mayen micro-continent.*

2.1 Lofoten-Vesterålen margin

The LVM lies west of the Lofoten and Vesterålen archipelagos and consists of a narrow shelf with a steep slope composed of several NE trending shelf-parallel basement ridges and horsts (Blystad et al., 1995). In addition, gravity and magnetic potential-field maps correlate with main structural elements (Berndt et al., 2002), showing them as elongated anomaly belts with similar NE-SW trends. The ridges are deeply eroded, and Precambrian crystalline rocks are exposed on the seabed and on the islands along the margin (Blystad et al., 1995). A small Mesozoic rift basin is, however, preserved on Andøya (Dalland, 1981), and Mesozoic rift basins occur locally in the fjords in the Lofoten-Vesterålen area. This indicates that the Lofoten and Vesterålen archipelagos were previously covered by Mesozoic sedimentary sequences (Hansen et al., 2012). Moreover, the widest portion of LVM (~150 km in south Lofoten margin) is positioned just north of the Bivrost Lineament and close to the Vøring margin, while the LVM narrows towards the north (~35 km offshore Andøya) when approaching the Senja Fracture Zone in the vicinity of the SW Barents Sea (Rise et al., 2013). Crustal thicknesses have been estimated for the LVM with values corresponding up to ~30 km beneath the continental shelf, while for the oceanic crust up to ~8 km (Mjelde et al., 1993; Tsikalas et al., 2005a; Breivik et al., 2017 and 2020).

Time constraints for Mesozoic rift phases in this particular part of the Norwegian Continental Shelf (NCS) are challenging to establish, due to the lack of deep exploration wells, scarcity of high-resolution seismic coverage, and absence of onshore sedimentary outcrops across the area. Nonetheless, there is some agreement that the main rift phases occurred in Late Permian-earliest Triassic, Late Jurassic-Early Cretaceous, mid Cretaceous, and Late Cretaceous-Paleocene (Færseth, 2012). As each rift phase developed, three different NNE-SSW, ENE-WSW to NW-SE-trending fault set systems were stablished along the LVM (Tsikalas et al., 2005a). Some models have been postulated to account for these deformation events within the margin, including a time-progressive evolution (Fig. 2.2a) (Bergh et al., 2007; Eig and Bergh, 2011), and transtension or oblique-normal faulting with multi-phase rifting (Fig. 2.2b) (Wilson et al., 2006; Henstra et al., 2015, 2019).

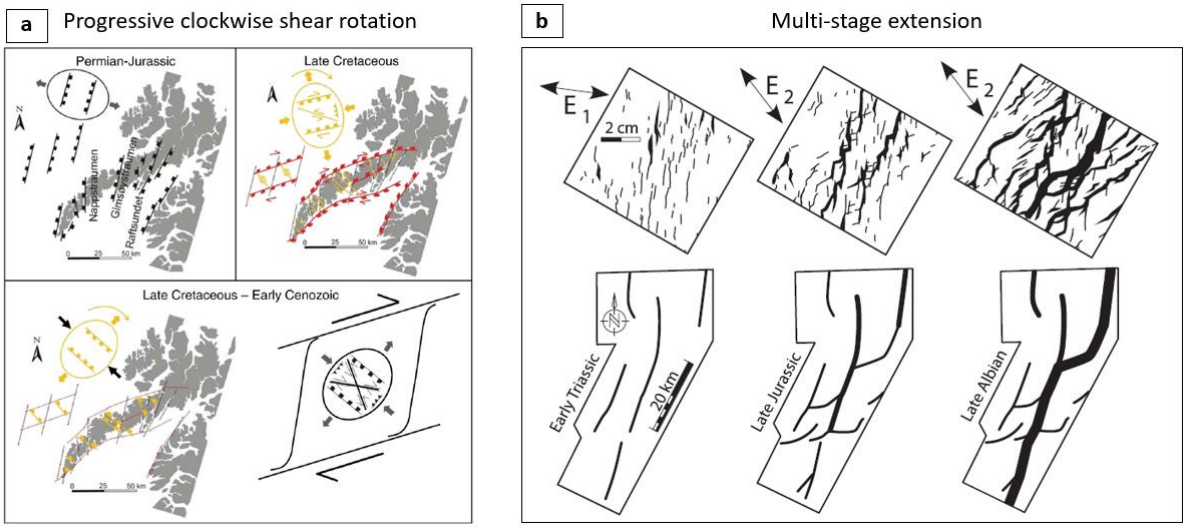

***Fig. 2.2**: **(a)** Regional strain-stress model for the LVM that combines extension and shear rotation of stress fields (after Eig and Bergh, 2011). **(b)** Schematic representation of the multi-stage extension tectonic model (after Henstra et al., 2015). E1 and E2 indicate extension direction.*

2.2 Margin segmentation

The present-day basin architecture of the LVM displays a strong geometrical relationship between a set of graben or half-graben basins and elevated structural elements, typical of rift basins. A change in along-margin structural style, fault dip and polarity, depth-to-Moho, and sediment distribution occurs between the islands of Lofoten, Vesterålen, and Andøya (Løseth and Tventen, 1996; Olesen et al., 2002 and 2007). Consequently, three tectonic models to account for the margin evolution have been proposed and the models mainly focus on the lateral along-margin segmentation (Fig. 2.3):

- Tsikalas et al. (2001) divided the LVM margin into three different rifted segments (Lofoten, Vesterålen, and Andøya) defined by border fault geometry and polarity changes across NW-SE trending transfer zones (Fig. 2.3a). The transfer zones are the Bivrost Lineament, separating the southernmost part of the Lofoten margin from the northernmost part of the Vøring margin, the Jennengga transfer zone, separating the Lofoten and Vesterålen margin segments, and the Vesterålen transfer zone, separating the Vesterålen and Andøya margin segments.
- Bergh et al. (2007) proposed a multi-phase fault initiation with progressive clockwise shear rotation of the stress field from E-W to NNW-SSE that started in the Permo-Jurassic and finalized at Mesozoic-Paleogene times. The proposed lateral segmentation of the margin takes place based on the timing of fault initiation, and their

corresponding distribution (Fig. 2.3b). Hence, fault populations are genetically related to distinct rift episodes.

- Færseth (2012) suggested two rift segments within the LVM bounded by an E-W trending accommodation zone just between the Lofoten and Vesterålen segments (Fig. 2.3c). The change in dip direction of the Jurassic faults across this zone took place without any evidence of strike-slip motion.

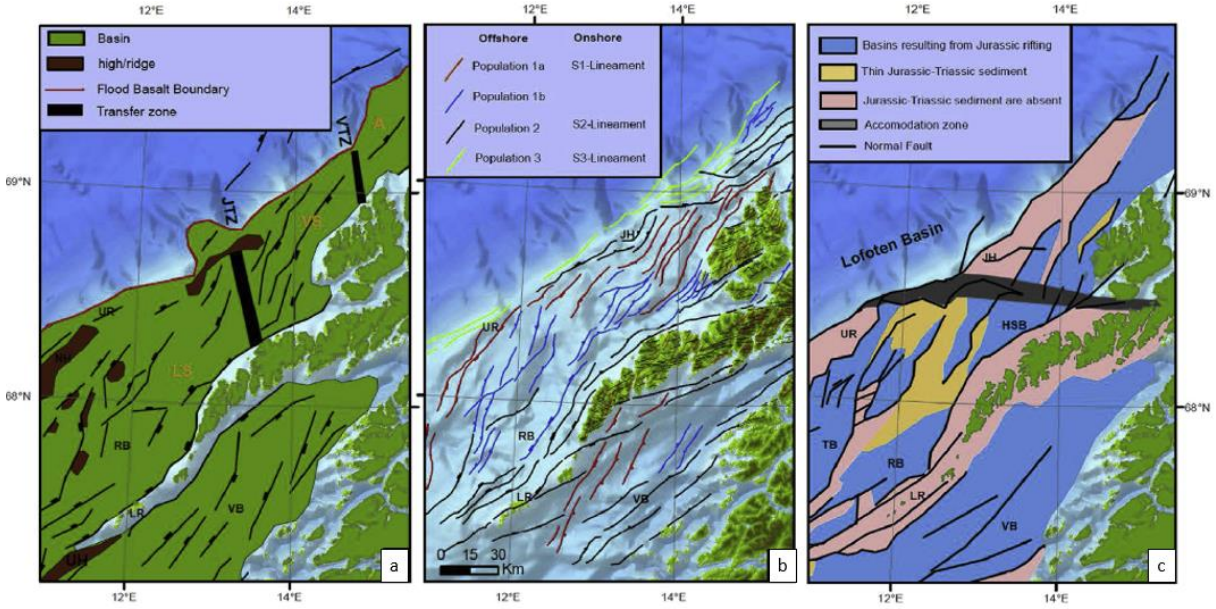

Fig. 2.3*: Previous segmentation models for the evolution of the LVM (after Tasrianto and Escalona, 2015).* ***(a)*** *Tsikalas et al. (2001) model.* ***(b)*** *Bergh et al. (2007) model.* ***(c)*** *Færseth (2012) model. AS: Andøya segment; JTZ: Jennengga transfer zone; LS: Lofoten segment; NH: Nyk High; RB: Ribban Basin; UH: Utgard High; UR: Utrøst Ridge; VB: Vestfjorden Basin; VS: Vesterålen segment; VTZ: Vesterålen transfer zone.*

Several other studies have attempted to propose different styles of margin segmentation following some of the principles of the three models described above. Hansen et al. (2012) related the change in dominant fault polarity and basin architecture across a broad E-W trending zone, similar to that of Færseth (2012), but with dextral offsetting of the Lofoten and Vesterålen islands denoted as soft-linked transfer zones (e.g. Eig and Bergh 2011), and coupled with NE-SW hard-linked transfer zones (e.g. Tsikalas et al., 2001). Tasrianto and Escalona (2015) supported the model of Tsikalas et al. (2001) and separated the LVM into three time-transgressive segments: Southern Lofoten, Northern Lofoten and Vesterålen-Andøya. In more recent studies in the southern part of the Lofoten margin (e.g. Wilhelmsen, 2016; Kalač, 2017; Tsikalas et al., 2019), the Bivrost Lineament has been interpreted has a low-relief Late Jurassic-Early Cretaceous accommodation zone, acting as a rift propagation barrier towards the north and evidenced in diminishing fault throw intensity, fault termination,

and depocenter thickness variations across it. Furthermore, it was suggested that during Late Cretaceous-Paleocene the Bivrost Lineament has experienced a major role on uplift and doming within the area, as more heat flow circulated this susceptive weak zone (Mjelde et al., 2003).

In this study, three different segments within the LVM will be contemplated in order to better describe the study area: Lofoten, Vesterålen, and Andøya segments (as in Tsikalas et al., 2001). The Lofoten segment is dominated by westward dipping faults, and includes the Lofoten islands and the part of the margin to the northeast and southwest. The Vesterålen segment, which is the focus study area, is dominated by eastward dipping faults, and there are no pronounced boundary fault separating the offshore rift basins from the Vesterålen islands. The Andøya segment is dominated by westward dipping faults, possibly linked to a master fault through common detachment planes, and includes the Andøya island area.

2.3 Structural elements and basin configuration

Figure 2.4 illustrates the structural elements of the study area. Some of them have been already formalized by Blystad et al. (1995), and others will be refined and/or informally defined in this study in light of the new conducted observations (cf. Chapter 4, Results). The inner and outer parts of the LVM are divided by the roughly NE-SW oriented landward lava boundary (Fig. 2.4). This mapped boundary represents the extent of basaltic flows related to lithospheric break-up at the Paleocene-Eocene transition (Tsikalas et al., 2001). The maximum landward extension of these flows culminates near the western border of the basement highs and the shelf edge.

Several N-S to NE-SW striking graben and half-graben basins and sub-basins, infilled with, mainly, Early Cretaceous sedimentary successions constitute the inner part of the LVM (Figs. 2.4 to 2.7). In the study area, the main depocenter is the Ribban Basin. This basin is flanked and bounded by deeply eroded, Mesozoic basement horsts and their respective culminations, such as the Lofoten Ridge and the Utrøst Ridge (Fig. 2.5). On the other hand, the outer part of the margin is dominated by highly eroded Cenozoic sedimentary sequences covering the Late Mesozoic structures (Fig. 2.4). Crustal thickness variations between the inner and outer part of adjacent margins to the south and near the study area suggest that the lithosphere has been

stretched, at least by a β-factor of ~3 in the Møre Margin (Theissen-Krah et al., 2017), ~1.5 in the Vøring Margin, and ~2.12 in the southern LVM (Skogseid, 1994) (Fig. 2.5a and 2.6).

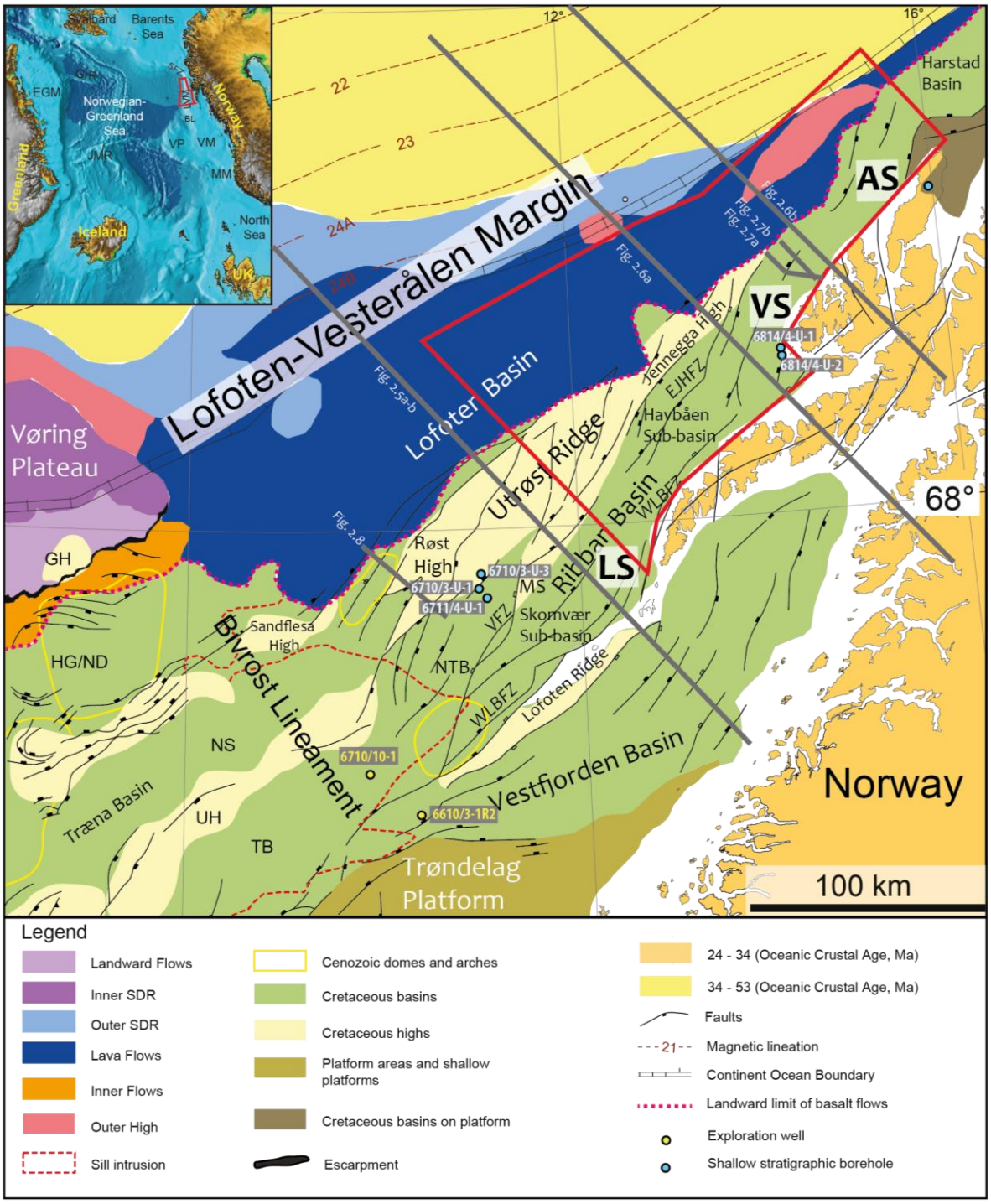

Fig. 2.4: *Main structural elements on the Lofoten-Vesterålen and adjacent margins (modified from Abdelmalak et al., 2017). Inset map from Faleide et al. (2015). The study area is defined by the red polygon. Seismic profiles examples and crustal transects are marked in gray lines. AS: Andøya segment; EJHFZ: East Jennegga High Fault Zone; GH: Grimm High; HG/ND: Hel Graben/Nagfar Dome; LS: Lofoten segment; MS: Marmæle Spur; NS: Någrind Syncline; NTB: North Træna Basin; SDR: Seaward dipping reflectors; UH: Utgard High; VFZ: Vesterdjupet Fault Zone; VS: Vesterålen segment; WLBFZ: West Lofoten Border Fault Zone. Inset map abbreviations in Fig. 1.1.*

The Ribban Basin is subdivided into the Skomvær and Havbåen sub-basins to the south and north, respectively. The Ribban Basin is bounded to the east by the West Lofoten Border Fault Zone (WLBFZ) to the Lofoten Ridge and to the west by the Vesterdjupet Fault Zone (VFZ) to the Marmæle Spur, which is the south-eastward termination of the Utrøst Ridge. The Lofoten Ridge is one of the most prominent structural elements within the study area (Fig. 2.4). It is a ~350 km long set of horsts formed during Late Jurassic-Early Cretaceous. To the south, the ridge becomes narrower (< ~15 km) and terminates against the Bivrost Lineament. The role of the lineament is still debatable, but there is an apparent structural control of lower-crust high-velocity bodies emplacement beneath it (Figs. 2.5a and 2.6) (Planke et al., 1991, Abdelmalak et al., 2017). The Træna Basin is structurally segmented north of this lineament into the North Træna Basin (Fig. 2.4), and it terminates against the Røst High, the south-west prolongation of the Utrøst Ridge. Concerning the Havbåen Sub-basin, its western termination is defined by the gently eastward-dipping East Jennegga High Fault Zone (EJHFZ) to the Utrøst Ridge, and to the east the sub-basin is bounded by a west-dipping fault (i.e. WLBFZ) along the Lofoten Ridge.

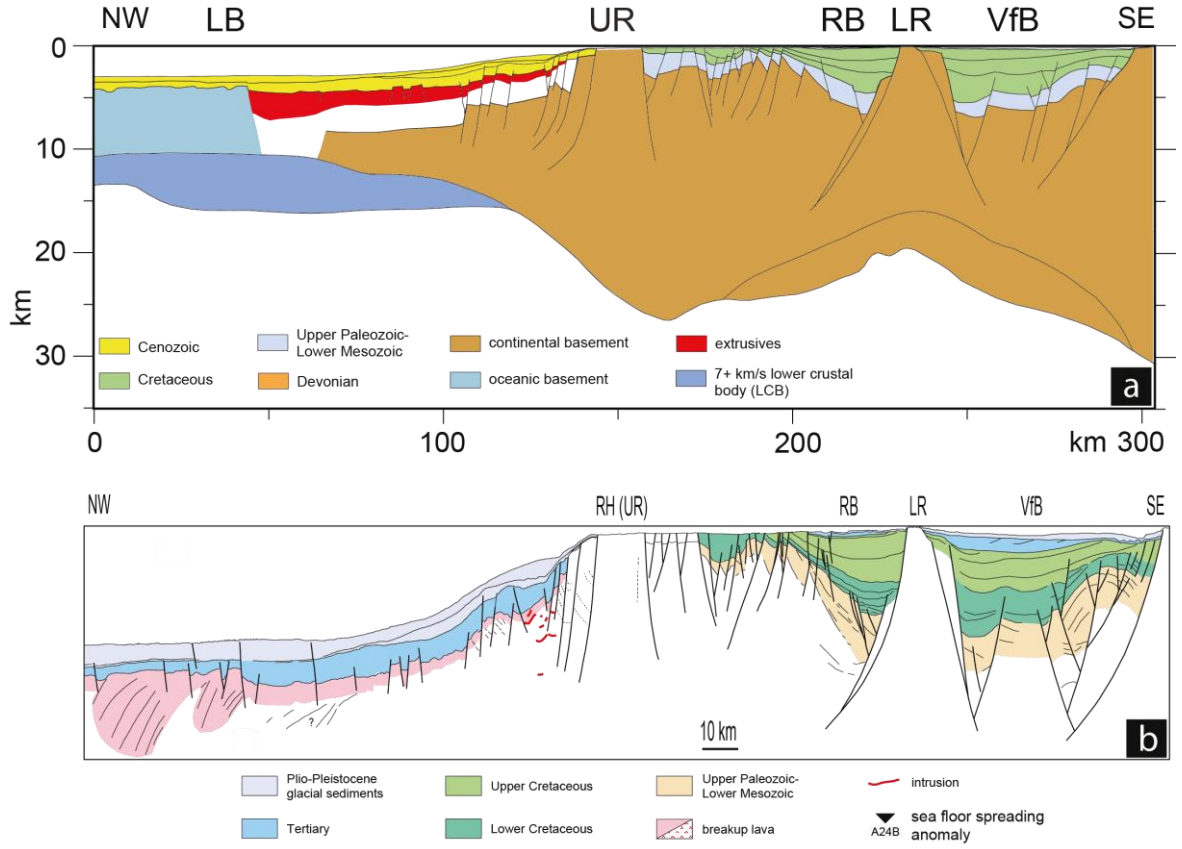

Fig. 2.5: (a) *Regional crustal transect across the south part of the Lofoten-Vesterålen margin,* ***(b)*** *Regional profile across the south part of the Lofoten-Vesterålen margin. COB: continent-ocean boundary; LR: Lofoten Ridge; RB: Ribban Basin; RH: Røst High; UR: Utrøst Ridge; VB: Vestfjorden Basin. Modified from Faleide et al. (2015). Profile locations in Fig. 2.4.*

Close to the Vesterålen island and north of the Havbåen Sub-basin, the dominant fault polarity changes to easterly-dipping faults with a NNE-SSW orientation (i.e. EJHFZ) that determine the basin geometry (Fig. 2.6 and 2.7) (Blystad et al., 1995). This area of fault polarity-shift marks the transition of the Lofoten to the Vesterålen margin segment (Fig. 2.4). Tsikalas et al. (2001) indicated that this shift in structural style is defined by the NW-SE-trending Jennegga Transfer Zone, named after the elevated element located in the proximity, the Jennegga High, or the northeastern termination of the Utrøst Ridge. In contrary, Hansen et al. (2012) indicated that the shift occurs at an E-W transfer zone that extends from the northern part of the Lofoten islands across the Havbåen Sub-basin and the Jennegga High. Regardless of the preferred tectonic model, it is clear that the Jennegga High area constitutes a distinctive border between two different rifted segments.

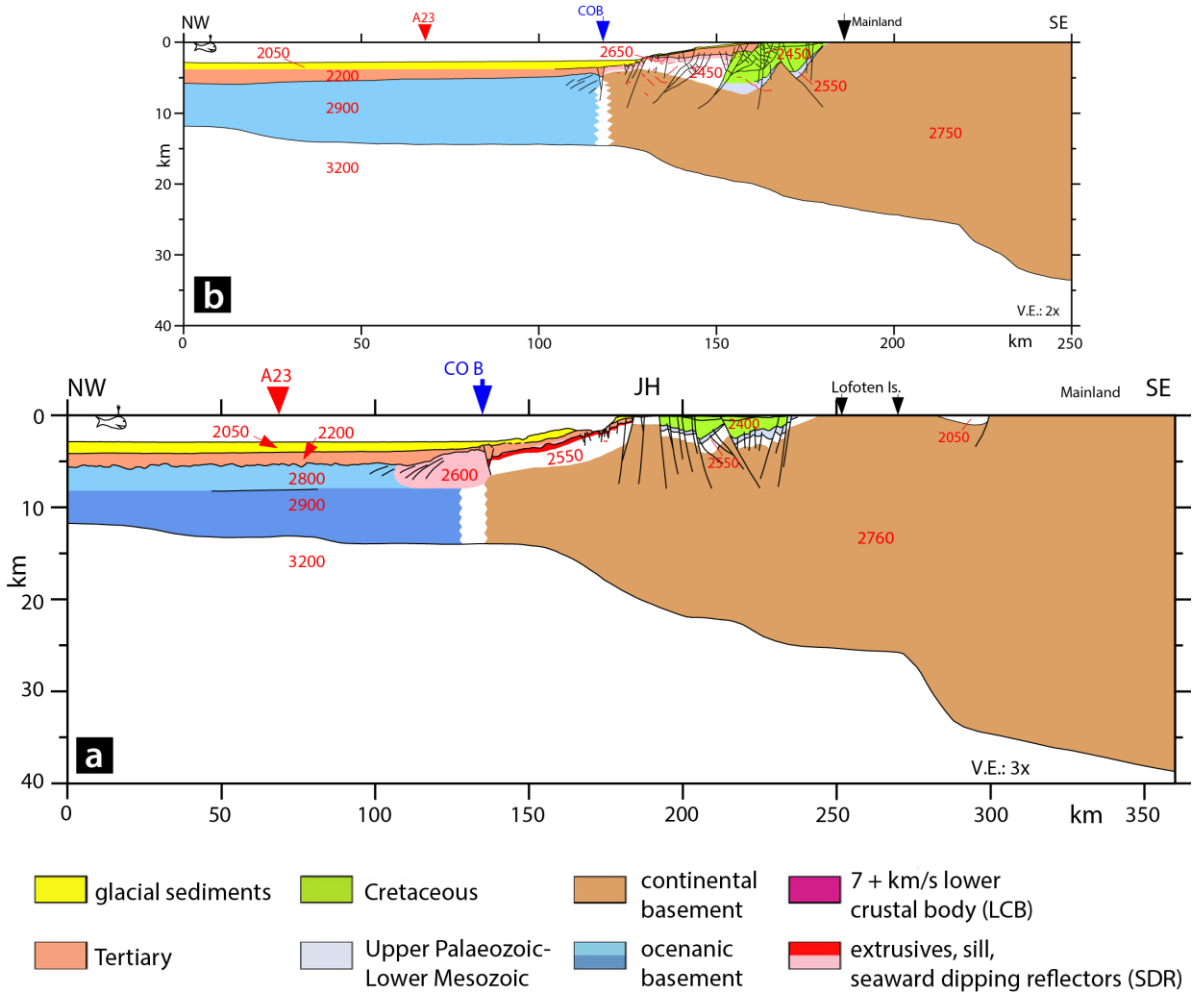

Fig. 2.6: *Regional gravity-modelled crustal transect for the Lofoten-Vesterålen margin (after Tsikalas et al., 2005a).* ***(a)*** *crustal transect between the Lofoten and Vesterålen islands.* ***(b)*** *crustal transect north of the Vesterålen islands. Densities (kg/cc) are bolded in red. Note the absence of high seismic velocity Lower Crustal Bodies in comparison to the southern part of the LVM (Fig. 2.5). A23: Seafloor spreading anomaly; COB: continent-ocean boundary. JH: Jennegga High. Profile locations in Fig. 2.4.*

On the Vesterålen margin segment, the Lower Cretaceous strata show prominent growth on the hanging-walls of rotated-fault blocks (Fig. 2.7). The faults display listric downthrow to the east and they rotate the blocks to the west (Færseth, 2012). The wedge-shaped sediment layers vary gradually from thin on the crests into thick in the basins, and thickness variations across faults demonstrate the syn-tectonic sedimentation. Subsequently, faults developed during the Early Cretaceous and the main uplift commenced in the latest Cretaceous to early Tertiary times (Løseth and Tveten, 1996). Late Cretaceous-Paleocene rifting is also evidenced within the same margin segment as Paleogene seismic reflectors onlap towards faults in the vicinity of the Jennegga High (Fig. 2.7b). Undifferentiated Mesozoic sequences arranged as intense low-angle west-dipping structures appear also near the northern part of the Vesterålen margin segment. These structures become more prominent and dominant towards the Andøya area (Fig. 2.7b) (e.g. Bergh et al., 2007). In the southern part of the LVM, similar structures can be observed near the western part of the Røst High, where a local Campanian deformation episode for these reflectors have been suggested (Blystad et al., 1995). Moreover, doming and truncation of the Cenozoic sequences covering these latter structures is common, and occurs close to the transition between the inner and the outer part of the LVM (Fig. 2.8) (Tsikalas et al., 2019).

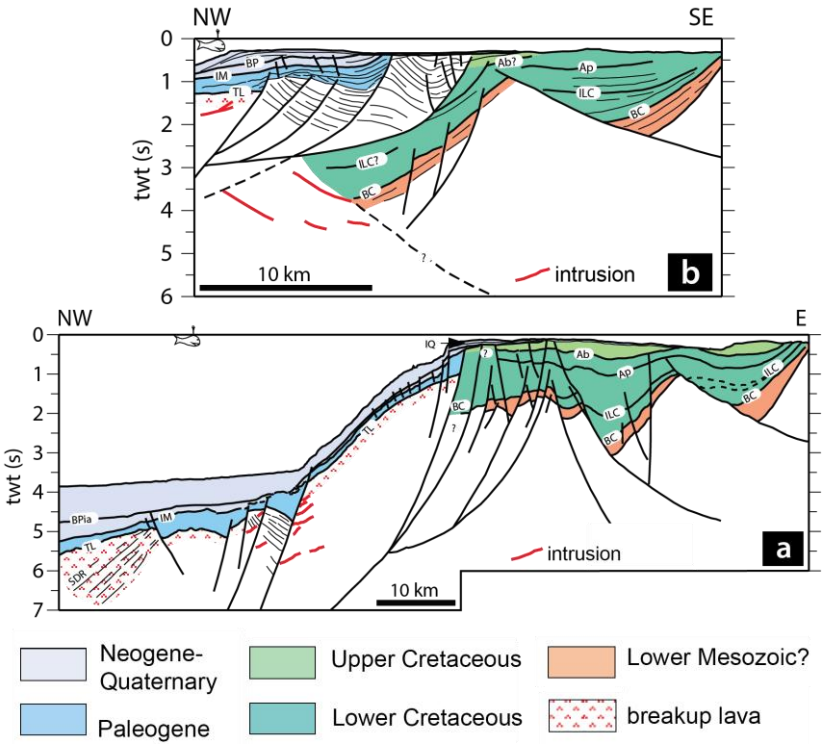

Fig. 2.7: *Geoseismic profile examples from the Vesterålen margin segment (after Tsikalas et al., 2001). Ab: Intra Albian; Ap: Intra Aptian; BC: Base Cretaceous; BP: Base Upper Pliocene; ILC: Intra Lower Cretaceous; IM: Intra Miocene; IQ: Intra Quaternary; TL: Top Lava; SDR: Seaward dipping reflectors. Profile locations in Fig. 2.4.*

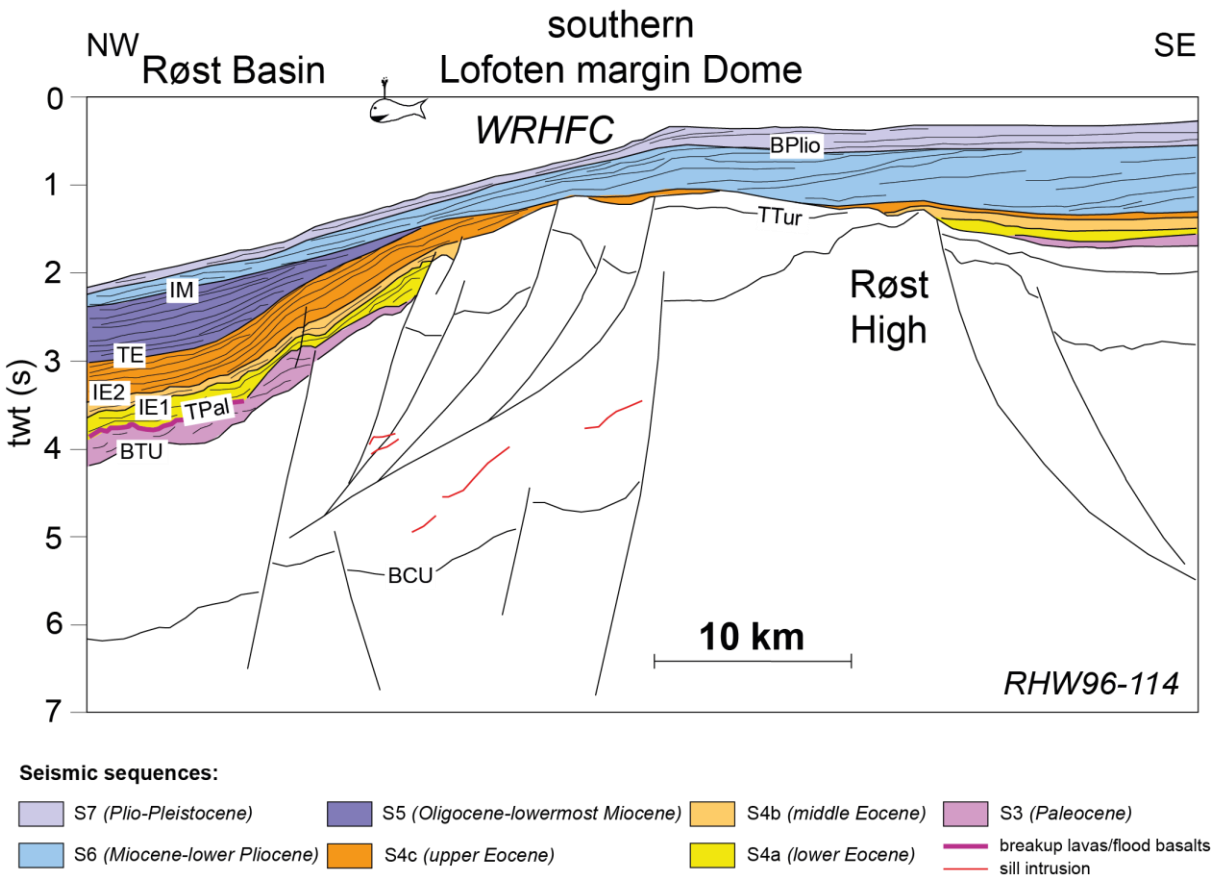

Fig. 2.8: *Geoseismic profile example illustrating doming and truncation of Cenozoic sequences on top of the fault complexes (after Tsikalas et al., 2019). BCU: Base Cretaceous Unconformity; BPlio: Base Pliocene; BTU: Base Tertiary Unconformity; IE1 and IE2: Intra Eocene; IM: Intra Miocene; TPal: Top Paleocene; TTur: Top Turonian; WRHFC: West Røst High Fault Complex. Profile location in Fig. 2.4.*

Above the lava flows, a thick sedimentary sequence (~2 km) is deposited in the outer part of the LVM (Sellevoll et al., 1988). These sediments make up the main depocenter of the area, named as the Lofoten Basin (Fig. 2.4). The latter mainly developed after the post-early Eocene break-up tectonism (Løseth and Tveten, 1996), and includes a series of magmatic structures arranged as volcanic mounds, which characterize the outer part of the Andøya margin segment (Fig. 2.4). Sediments have easily by-passed from the proximity of the LVM shelf towards this area due to the absence of marginal highs and to the unstable depositional environment on the steep slope, resulting in gradual widening and deepening of the basin (Eldholm et al., 2002). A series of canyons developed during Tertiary times as uplift and erosion dominated the shelf (Rise et al., 2013). Below the lava flows, and further west of the LVM outer part, the continent-ocean boundary (COB) can be traced on seismic data (Fig. 2.4), in close proximity to the seaward dipping reflectors (SDR; Fig. 2.5b and 2.7a) (Sellevoll et al., 1988).

2.4 Stratigraphic framework

The development and evolution of major Cretaceous sedimentary basins in the LVM and adjacent areas, such as the Vøring and SW Barents Sea margins, are directly linked to the evolution of the tectonic framework of the NE Atlantic-Arctic Late Jurassic–Early Cretaceous rift episodes (Fig. 2.9) (Faleide et al., 2015). Following the end of the orogenic processes around Silurian-Devonian times, the tectono-magmatic history of the margin was that of general extension and rifting of the continent, ending with a final lithospheric rupture and opening of the northern North Atlantic by seafloor spreading in Early Eocene times (Brekke et al., 2001).

Pre-Cretaceous

Permian–Triassic extension is generally poorly dated and there is limited evidence of this event in the LVM (Færseth, 2012). However, it is best constrained onshore East Greenland where a major phase of normal faulting culminated in the mid-Permian and further block faulting took place in the Early Triassic (Faleide et al., 2015). The later Triassic basin evolution was characterized by regional subsidence and deposition of large continental sediment volumes. These sequences consist mainly of sandstones and conglomerates (Fig. 2.9) (Tasrianto and Escalona, 2015) and were deposited under dry climate. By Late Triassic times, the climate became more arid, and the sediments were more influenced by marine processes. Towards the Early to Middle Jurassic the stratigraphy reflects a relative sea-level rise that caused the entire margin to be dominated by shallow clastic shelf environments (Brekke et al., 2001). Evidence of influx of sand, for example from Andøya, strongly indicates a delta prograding towards the south being fed by clastic sediments from hinterlands to the west, north and east. This resulted in deposition of some of the most important reservoir rocks, including the Åre-Tilje-Tofte-Ile-Garn formations, which have been producing in hydrocarbon fields in the Trøndelag Platform, situated south of the LVM (Faleide et al., 2015). The end of the Jurassic marks the initial phase of the major extensional tectonic period that caused the break-up of the NE Atlantic. As a consequence, a major sea-level rise flooded the entire margin, and marine shales were deposited (Fig. 2.9). These represent some of the most important source rocks in the shelf, such as the Draupne/Spekk Formation, a Kimmeridgian Clay Formation (North Sea) equivalent (NPD, 2010).

Lower Cretaceous

Deep basinal areas continued to develop by subsidence along the rift axis by Late Jurassic-Early Cretaceous, together with the main infill of the sediments found presently in the LVM rift basins (Brekke et al., 2001). The increasing sea level led to widespread deposition of marine claystones and siltstones facies (Fig. 2.9) (Løseth and Tveten, 1996) that, in turn, shows a gradual increase in thickness from south to north in the Lofoten segment. By Aptian times, a new pulse of regional transgression started and continued into the Late Cretaceous slowly drowning emergent intra-basinal highs and surrounding land areas throughout the entire area of the margin. Erosion of basin flanks and sedimentary rocks took place during this period (NPD, 2010).

Upper Cretaceous

The Upper Cretaceous sedimentary succession is hundreds of meters thick at the south of the Lofoten segment, and consists mainly of fine-grained clastics represented by claystones and siltstones (Fig. 2.9). These sequences represent outer shelf deposits, also containing some sandstones. In contrast to the case of the Early Cretaceous rocks, towards the northern parts of the segment there is a gradual removal of the Upper Cretaceous sedimentary succession, probably as a response of uplift of the Utrøst Ridge between Early and Late Cretaceous (NPD, 2010). This is indicated by the pinching out of the Upper Cretaceous sedimentary sequences towards the Utrøst Ridge. The top of the Upper Cretaceous sequence is marked by the Base Tertiary Unconformity (BTU).

Cenozoic

The Paleogene succession contains sandstones and claystones in shallowing upward sequences (Fig. 2.9) (Tasrianto and Escalona, 2015). These sequences contain upper slope to inner shelf deposits that can be found in the Vøring margin and Ribban Basin, and are sourced from the elevated Utrøst Ridge area (Hansen et al., 2012). Along the outer Vøring and Lofoten-Vesterålen margins, most of the Late Cretaceous–Paleocene deformation is masked by the break-up-related lavas, but the structures appear to continue seawards underneath them (Sellevoll et al., 1988). Plio-Pleistocene glacial sediments overlie the Paleogene successions and are much thicker in the western part of the LVM (Faleide et al., 2015).

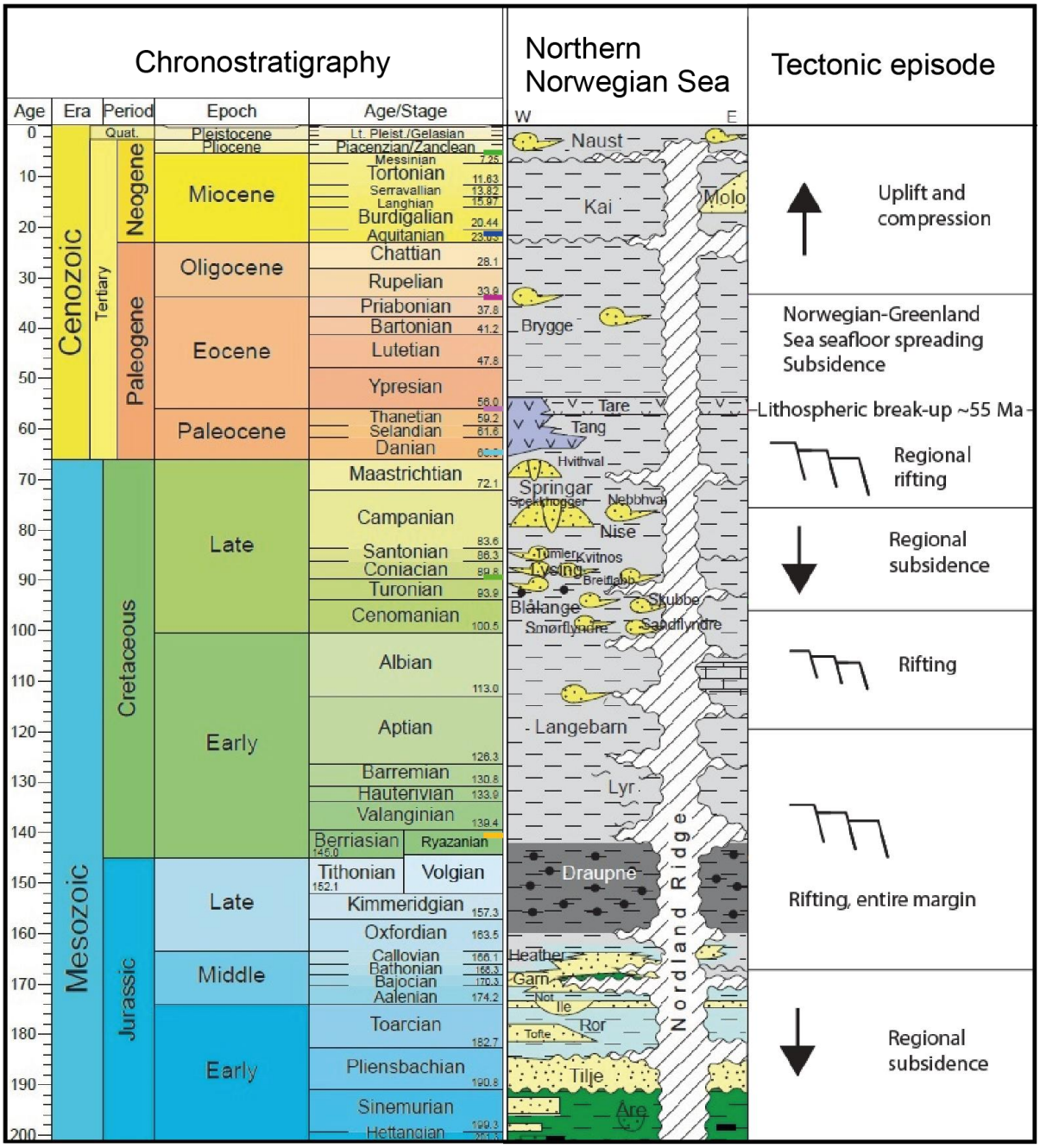

***Fig. 2.9**: Chronostratigraphic and lithostratigraphic charts of the Northern Norwegian Sea (modified from Norlex, 2012 and Tsikalas et al., 2012).*

2.5 Nordland VII petroleum province

The study area is located within the defined Nordland VII petroleum province that was never opened for petroleum exploration and, as a consequence, no deep commercial wells were ever drilled (Fig. 2.10a). Shallow stratigraphic boreholes 6814/04-U-1 and 6814/04-U-2 off the coast of Vesterålen are the only available ground-truth of litho-stratigraphic information, together with the Andøya outcrop located onshore (Dalland, 1981). Nonetheless, wells 6710/10-1 and 6610/3-1 R2, together with shallow stratigraphic boreholes (6710/3-U-1; 6710/3-U-3; 6711/4-U-1), all located south of the study area have been also included in this study for seismic-to-well ties of key horizons (Fig. 2.4). The Norwegian Sea area was opened for exploration in 1980, and the first discover fields were put in production since 1993. Well 6610/3-1 R2 was drilled in 1993 (TD: Upper Triassic) and revealed shows/traces of hydrocarbons, whereas well 6710/10-1 was drilled in 2001 (TD: uppermost Cretaceous) and resulted dry. Shortly after, the area was closed for petroleum exploration in the same year (2001), due to a comprehensive environmental impact assessment that declared any petroleum activity was no longer permitted in the Nordland VI, Nordland VII and Troms II areas, and has remained like that until today (NPD, 2010) (Fig. 2.10).

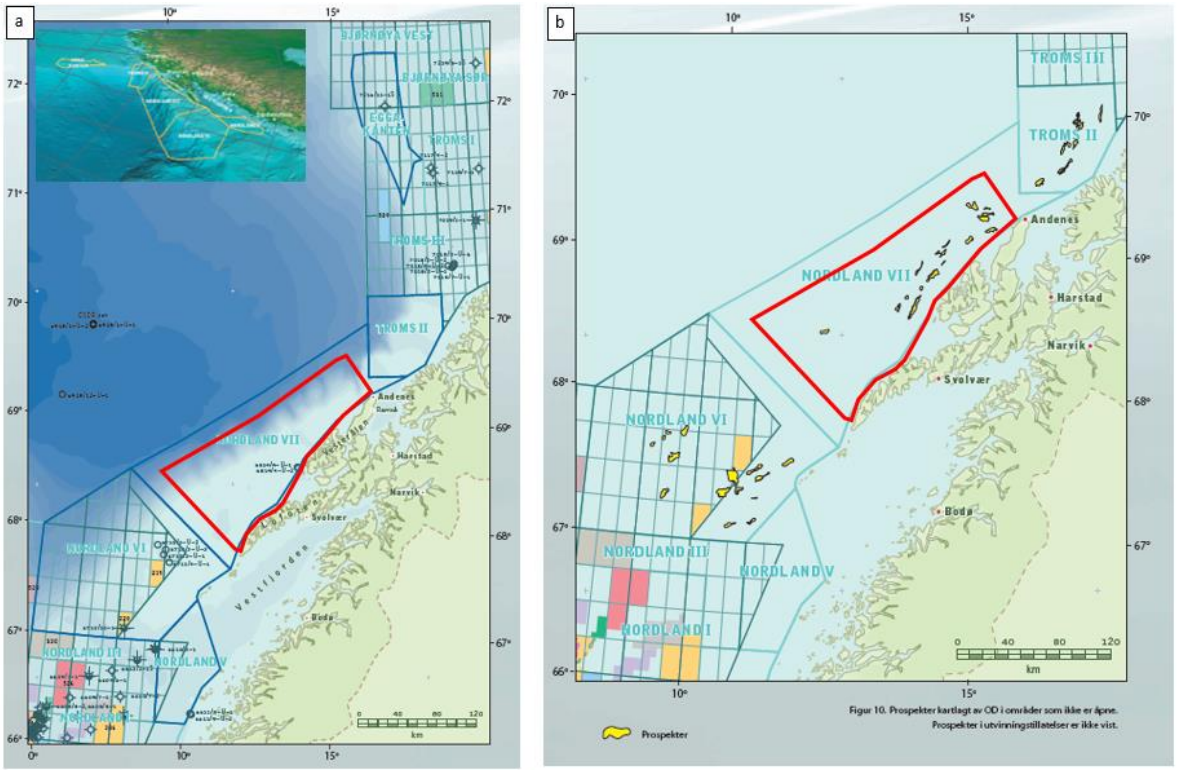

Fig. 2.10*: Oil and gas exploration areas and wells on the Lofoten-Vesterålen and adjacent margins (maps retrieved from NPD, 2010). Red polygon represents the study area. Note location and distribution of wells in* ***(a)****, and hydrocarbon prospections marked in yellow raster in* ***(b)****. Inset: bathymetry data depicting the margin morphology (NPD, 2010).*

Typical trap types drilled so far in the available petroleum provinces on the mid-Norwegian continental shelf are rotated fault blocks of Jurassic age in the horst-and-graben terranes of the Halten Terrace, and complex fault-blocks within the major fault zones (NPD, 2010). The source rock feeding the petroleum system was formed during rifting in Late Jurassic (Faleide et., 2015). Reservoirs from the Åre-Tilje-Tofte-Ile-Garn formations are situated in the Trøndelag Platform, far south of the LVM. Hence, the hydrocarbon exploration field trend extends towards the north and is indicative that the Lower-Middle Jurassic play is considered the one with the highest potential for success, followed by the Lower Cretaceous syn-rift sequences (Tasrianto and Escalona, 2015). All these in hand, put the LVM, specially the Vesterålen margin segment, as a high yet-to-find prospective resource area in the northern Norwegian Sea (Fig. 2.10b). At the Jurassic level, the greatest uncertainty is related to the lateral extent of the source rock and reservoir rock. For the Cretaceous prospects, the greatest uncertainty is related to weather there is a reservoir sandstone present (NPD, 2010). Ongoing exploration on the open petroleum provinces of the Norwegian Sea are, however, promising. Six new discoveries were made in 2019, and the unproven resources are estimated at 720 million Sm3 o.e. (NPD, 2020a).

3 Data

3.1 Seismic data

The seismic data utilised in the present study comprise ~25,000 km 2D multi-channel seismic reflection profiles (MCS), including both vintage (1986-1998) profiles and the most recently acquired (2007-2008) profiles, together with a 3D survey (2009) of ~1,258 km^2 (Table 3.1 and Fig. 3.1). The seismic coverage extends from south to north, respectively, into the Skomvær Sub-basin and the Harstad Basin. Line-spacing of the various 2D surveys ranges in average between 2-6 km. The most dense line coverage is found within the Andøya margin segment in the north and the sparsest towards the southernmost outer part of the LVM in the Lofoten Basin. The most recently acquired (2007-2008) 2D MCS dataset and the 3D survey (2009) are for the first time available to academia (Fig. 3.1c). The 3D survey (NPD-LOF-1-09) extends within the Vesterålen and southern Andøya margin segments, and has been utilized for further structural interpretations and time-constrains on tectonic episodes in the LVM, particularly around the Vesterålen margin segment.

Table 3.1*: Seismic reflection surveys utilized in this study. Surveys in bold-italics are the ones inside the study area.*

Survey	Type	Year	Company/authority	Recording time (TWT, s)	Resolution quality
LO-86	2D	1986	NPD	7	Moderate
LO-87	2D	1987	NPD	7	Moderate
LO-88	2D	1988	NPD	6	Moderate
LO-89	2D	1989	NPD	8	Moderate
LO-07	2D	2007	NPD	9	Moderate
LO-08	2D	2008	NPD	8	Poor
NPD-LOF-1-09	3D	2009	NPD	8	Moderate
TB-87	2D	1987	NPD	7	Good (reprocessed)
LIVB89	2D	1989	NPD	8	Very good (reprocessed)
AMR-N6T	2D	1992	TGS	8	Very good
N6-92R00	2D	1994	TGS	7	Good
GMNR-94	2D	1994	Geco	14	Good
UH-94R00	2D	1994	TGS	7	Good
AMR_TBN96	2D	1996	TGS	8	Very good (reprocessed)
AMR_RHW96	2D	1996	TGS	8	Very good (reprocessed)
RHW96	2D	1996	Geoteam Exploration	8	Very good (reprocessed)
RHS98	2D	1998	Geoteam Exploration	8	Very good (reprocessed)

The resolution quality in the study area is, in general, moderate (Table 3.1), except below the lava flows which is an acoustic barrier that absorbs most of the seismic energy and the imaging below this level is thus poor. The recording time of the various surveys (2D and 3D) range between 6-8 s TWT (two-way travel-time) in the study area, but it was possible to map with confidence the deepest reflections just down to ~2.5 to ~3 s TWT in the 2D surveys, and down to ~4 s TWT in the 3D survey. In addition, the signal-to-noise ratio is decreasing towards the north of the study area, possibly because of shallow water depths that increase the presence of seismic artefacts, including sea-bottom multiples which can be seen on most of the 2D MCS and 3D dataset, especially in the vintage LO-surveys. Some other aspect to consider regarding the quality of the seismic imaging may be due to the low variability in lithology, which makes the acoustic impedance more or less uniform with depth through the shale-dominant facies (Fig. 2.9). The relatively best seismic resolution (in average very good) is found south of the study area within the south Lofoten margin segment.

3.2 Well data

Five offshore shallow stratigraphic boreholes and one ~700 m outcrop onshore Andøya have been utilized in the study (Table 3.2 and Fig. 3.1). The stratigraphic boreholes were drilled by the Institute of Continental Shelf Research (IKU), and each of them contains ~200 m of individual rock cores. In addition, two exploration wells (6610/3-1R2 and 6710/10-1; Table 3.2) located in the southernmost part of the LVM were included in order to obtain reliable stratigraphic control and to transfer that into the study area. The absence of widely distributed wells within the study area leads to limitations in stratigraphic and sedimentological constraints. Despite this, the available wells have been used to define the best possible well-to-seismic ties and correlation, although the confidence of age constraints is naturally somewhat reduced, especially towards the north and the outer part of the study area. The available well-tops are provided in true vertical depth sub-sea (TVDSS; meters) by the Norwegian Petroleum Directorate (NPD; factpages, 2020). Interval velocity information for the area (Table 3.3) and the limited available well-logs were used to calculate depth-time conversions. These were used to constrain the necessary well-to-seismic ties in the utilised wells and 2D seismic profiles.

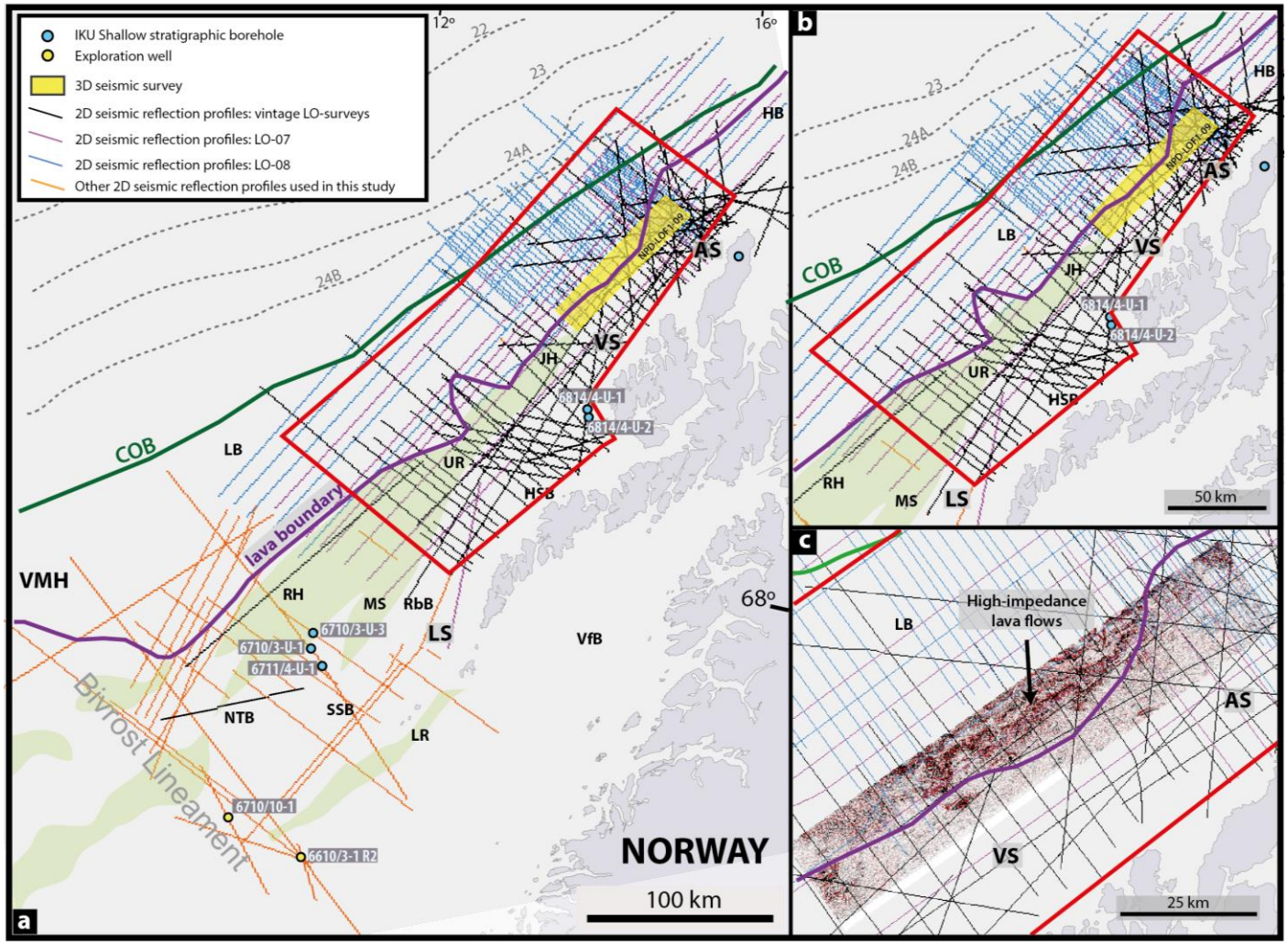

Fig. 3.1*: Seismic reflection coverage and location of utilised wells, overlain on main structural elements defined in the NPD map. Red polygon indicates study area.* ***(a)*** *Study area and south part of the LVM.* ***(b)*** *Zoom-in of the study area.* ***(c)*** *Zoom-in of the 3D survey (NPD-LOF-1-09). Note distribution of high-impedance lava flows and lava boundary. AS: Andøya segment; COB: continent-ocean boundary; HB: Harstad Basin; HSB: Havbåen Sub-Basin; JH: Jennegga High; LB: Lofoten Basin; LR: Lofoten Ridge; LS: Lofoten segment; MS: Marmæle Spur; NTB: North Træna Basin; RbB: Ribban Basin; RH: Røst High; SSB: Skomvær Sub-basin; UR: Utrøst Ridge; VfB: Vestfjorden Basin; VMH: Vøring Marginal High; VS: Vesterålen segment.*

Table 3.2: *Utilised wells.*

Well name	Location	Type	Operator	Coordinates
6710/3-U-1	North Træna Basin	Shallow stratigraphic	IKU	67° 48' 16.4 " N 10° 57' 25.3 " E
6710/3-U-3	Røst High	Shallow stratigraphic	IKU	67° 53' 34.7 " N 10° 48' 6.4 " E
6711/4-U-1	North Træna Basin	Shallow stratigraphic	IKU	67° 44' 12.2 " N 11° 6' 34.3 " E
6814/4-U-1	Vesterålen margin	Shallow stratigraphic	IKU	68° 39' 10.9 " N 14° 11' 8.9 " E
6814/4-U-2	Vesterålen margin	Shallow stratigraphic	IKU	68° 39' 45.8 " N 14° 9' 47.1 " E
6610/3-1R2	Vestfjorden Basin	Exploration	Statoil/Equinor	66° 55' 29.7" N 10° 54' 6.28" E
6710/10-1	North Træna Basin	Exploration	Statoil/Equinor	67° 5' 51.7" N 10° 8' 46.8" E

Table 3.3: *Interval velocities for the LVM area used in depth-time conversion (Tsikalas et al., 2005a).*

Sequence/Unit	Interval velocity (km/s)
Water	1.46
Plio-Pleistocene glacial sediments	1.80-1.85
Tertiary	2.45
Upper Cretaceous	2.70-2.80
Aptian-Albian	3.30
Lower Cretaceous	3.75-8.80
Pre-Cretaceous	4.10-4.45
Continental crystalline crust	6.0-6.8/7.1

3.3 Potential field anomaly data

Gravity and magnetic data (courtesy of TGS) were available for this study (Fig. 3.2). Both potential field anomaly grids have been high-pass filtered with a cut-off wavelength of 50 km (e.g. Abdelmalak et al., 2017). Magnetic anomalies are a measure of local variations in the Earth's magnetic field, as a result of rocks being composed with differences in chemistry and magnetism. Gravimetric anomalies are a means to measure lateral density differences between the observed gravity value and the theoretically calculated value at a given point on Earth (Olesen et al., 2010).

The potential field anomaly data are being applied to a wide variety of exploration problems, and are complimentary to seismic methods. Basement highs with thin sedimentary cover often appear as a strong positive anomaly, while sediment-filled basins display negative anomalies. Consequently, these data helped to support the interpretation of structural trends, basement highs, lateral distribution of sediments, and to constrain interpolation of defined faults where seismic coverage is sparse (Paterson and Reeves, 1985).

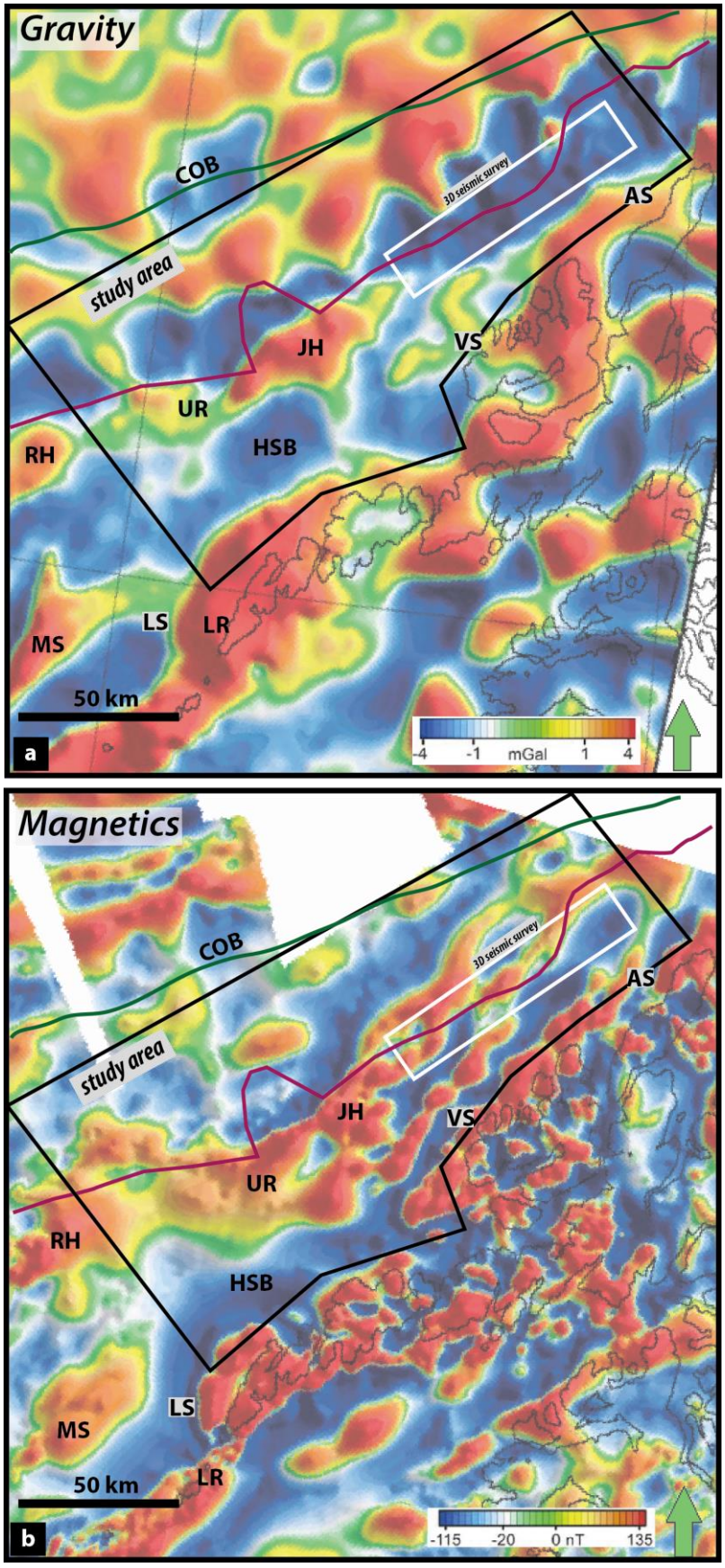

***Fig. 3.2**: Potential field data utilised in this study. **(a)** 50 km high-pass filtered gravity anomaly data. **(b)** 50 km high-pass filtered magnetic anomaly data. Black polygon indicates study area. White polygon indicates 3D seismic survey (NPD-LOF-1-09) area. Lava boundary is indicated in purple line. Abbreviations in Fig. 3.1. Gravity and magnetic data courtesy of TGS.*

4 Seismic and structural interpretation

4.1 Methodology and workflow

The focus of the study is on the Cretaceous-Cenozoic evolution and development of the LVM and, in particular, the Vesterålen margin segment. In doing so, the available 2D/3D seismic datasets have been interpreted using the Schlumberger's Petrel E&P Software Platform. The initial stage of the work includes stratigraphic control for the study area with well-to-seismic ties, and general seismic and structural interpretation. This was performed as a primary objective of getting a better understanding of the evolution and basin architecture on the study area. As a result, thirteen (fourteen including the seabed) main horizons were mapped along the study area (Fig 4.1). Mapping of the Base Cretaceous Unconformity (BCU) provided the outline of the Late Jurassic-earliest Cretaceous structural elements in the study area. Three distinct main horizons representing the Lower Cretaceous basin infill were traced, together with two main horizons representing the Upper Cretaceous sequences. Mapping of pre-Cretaceous horizons was also carried out, providing additional information on events prior to Cretaceous times. In addition, six Cenozoic main horizons were mapped in order to decipher the Tertiary tectono-stratigraphic evolution of the study area.

The basis for the mapped horizons was seismic and structural interpretation of equivalent seismic reflectors. Subsequently, time-structure maps and time-thickness maps were also generated in order to provide the lateral and vertical configurations of the sedimentary successions, and to visualize better the tectono-stratigraphic evolution. Potential field anomaly data have been used to identify new and refine existing structural elements and to extrapolate structural trends during seismic and structural/fault interpretation.

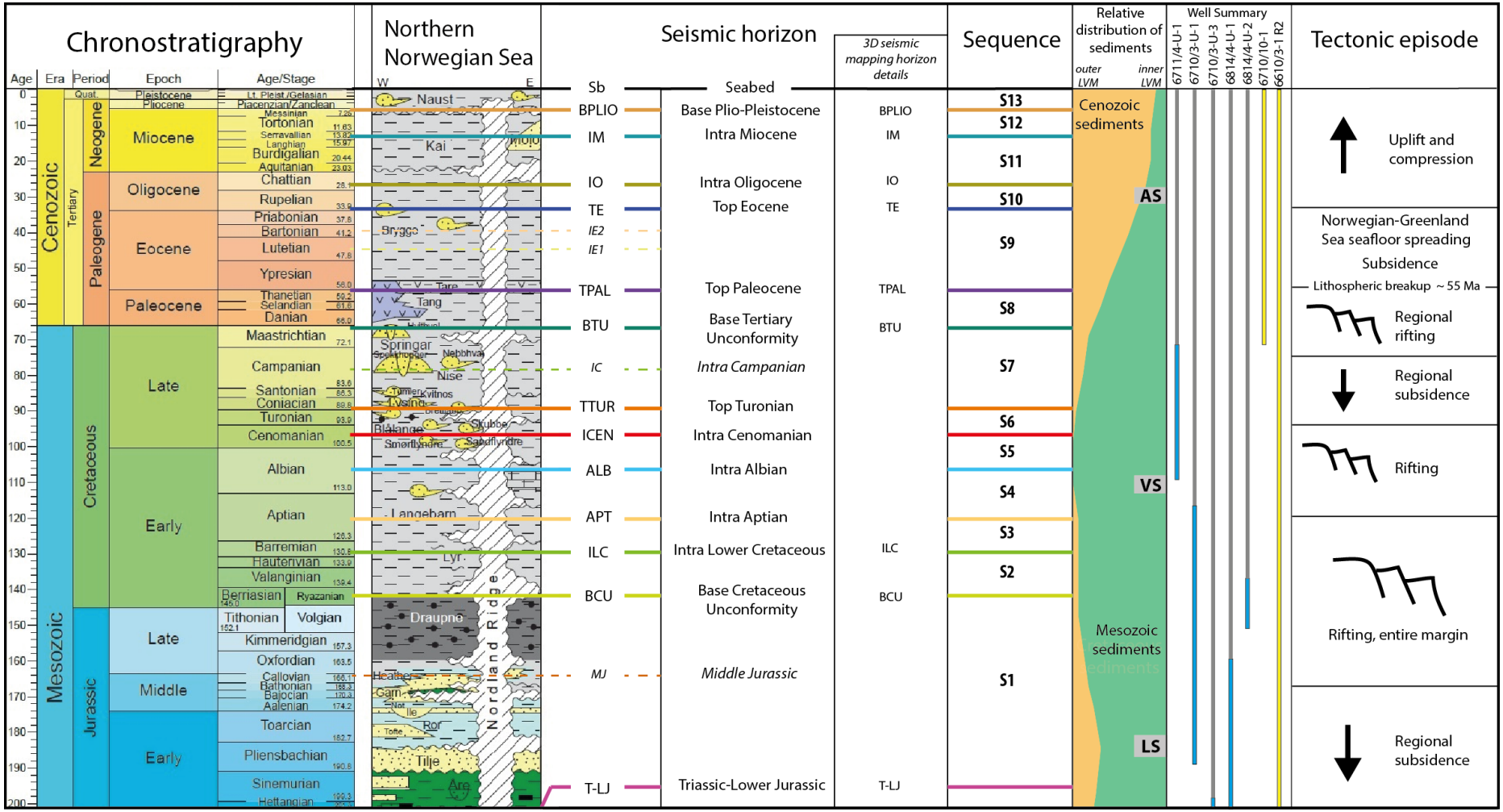

Fig. 4.1*: Seismic stratigraphic framework for the Lofoten-Vesterålen margin. Thirteen (fourteen including the seabed) interpreted main horizons bound thirteen seismic sequences. Secondary horizons are marked with dashed lines. Areal extent of Mesozoic sedimentary sequences decreases towards the northern part of the study area. Both exploration and IKU shallow boreholes are indicated in yellow and blue, respectively. AS: Andøya segment; LS: Lofoten segment; VS: Vesterålen segment. Chronostratigraphic and lithostratigraphic charts of the Northern Norwegian Sea modified from Norlex (2012). Tectonic episodes based on Tsikalas et al. (2012).*

4.2 Well correlation

The LVM contains no exploration wells in the study area and only a limited amount of shallow stratigraphic boreholes, which causes large uncertainties when attempting stratigraphic correlations in the study area. Adding to that, the structural complexity of the area, combined with the low resolution of the seismic data, brings additional interpretation challenges. The two utilized exploration wells to the south of the study area (Fig. 4.2 and 4.3), and the IKU shallow stratigraphic boreholes and onshore Andøya outcrop (Fig. 4.4), all provided the ties for the reflections mapped in the study area. Interval velocities from stacking velocities (Table 3.3) have been used in rough depth conversions from depth in meters to TWT in milliseconds, and vice-versa, for the well-to-seismic ties, thickness, burial and fault-throw estimates. Earlier interpretations were also used as reference and guidance (Tsikalas et al., 2001, 2019; Wilson et al., 2006; Hansen et al., 2012; Wilhelmsen, 2016; Kalač, 2017).

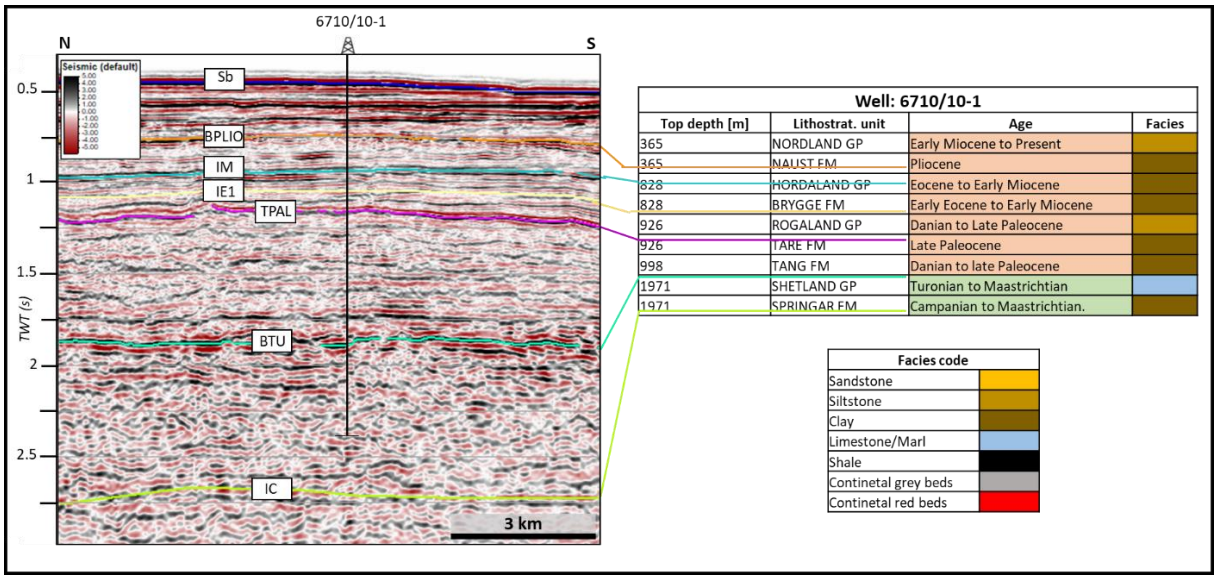

***Fig. 4.2**: Well-to-seismic tie of exploration well 6710/10-1 to profile TBS2000. Lithological information from NPD (factpages.npd.no-Wellbore). Facies represent the overall lithology of the lithostratigraphic group or formation. Interpreted horizons and abbreviations in Fig. 4.1 and Table 4.1. Location of well and seismic profile in Fig. 4.5.*

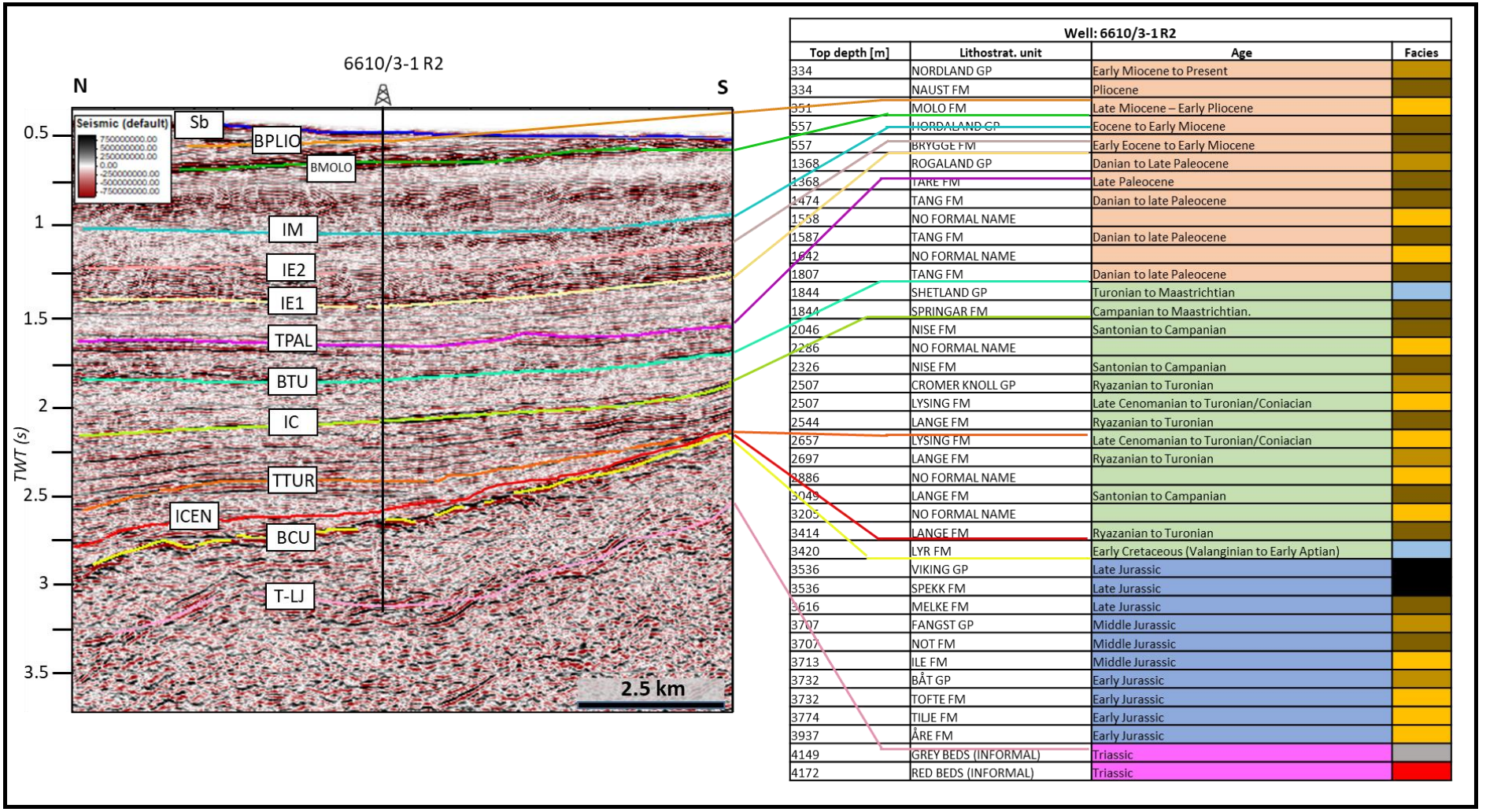

Well: 6610/3-1 R2			
Top depth [m]	Lithostrat. unit	Age	Facies
334	NORDLAND GP	Early Miocene to Present	
334	NAUST FM	Pliocene	
351	MOLO FM	Late Miocene – Early Pliocene	
557	HORDALAND GP	Eocene to Early Miocene	
557	BRYGGE FM	Early Eocene to Early Miocene	
1368	ROGALAND GP	Danian to Late Paleocene	
1368	TARE FM	Late Paleocene	
1474	TANG FM	Danian to late Paleocene	
1558	NO FORMAL NAME		
1587	TANG FM	Danian to late Paleocene	
1642	NO FORMAL NAME		
1807	TANG FM	Danian to late Paleocene	
1844	SHETLAND GP	Turonian to Maastrichtian	
1844	SPRINGAR FM	Campanian to Maastrichtian.	
2046	NISE FM	Santonian to Campanian	
2286	NO FORMAL NAME		
2326	NISE FM	Santonian to Campanian	
2507	CROMER KNOLL GP	Ryazanian to Turonian	
2507	LYSING FM	Late Cenomanian to Turonian/Coniacian	
2544	LANGE FM	Ryazanian to Turonian	
2657	LYSING FM	Late Cenomanian to Turonian/Coniacian	
2697	LANGE FM	Ryazanian to Turonian	
2886	NO FORMAL NAME		
3049	LANGE FM	Santonian to Campanian	
3205	NO FORMAL NAME		
3414	LANGE FM	Ryazanian to Turonian	
3420	LYR FM	Early Cretaceous (Valanginian to Early Aptian)	
3536	VIKING GP	Late Jurassic	
3536	SPEKK FM	Late Jurassic	
3616	MELKE FM	Late Jurassic	
3707	FANGST GP	Middle Jurassic	
3707	NOT FM	Middle Jurassic	
3713	ILE FM	Middle Jurassic	
3732	BÅT GP	Early Jurassic	
3732	TOFTE FM	Early Jurassic	
3774	TILJE FM	Early Jurassic	
3937	ÅRE FM	Early Jurassic	
4149	GREY BEDS (INFORMAL)	Triassic	
4172	RED BEDS (INFORMAL)	Triassic	

***Fig. 4.3**: Well-to-seismic tie of exploration well 6610/3-1 R2 to profile ST9104. Lithological information from NPD (factpages.npd.no-Wellbore). Facies represent the overall lithology of the lithostratigraphic group or formation. Facies legend in Fig. 4.2. Interpreted horizons and abbreviations in Fig. 4.1 and Table 4.1. Location of well and seismic profile in Fig. 4.5.*

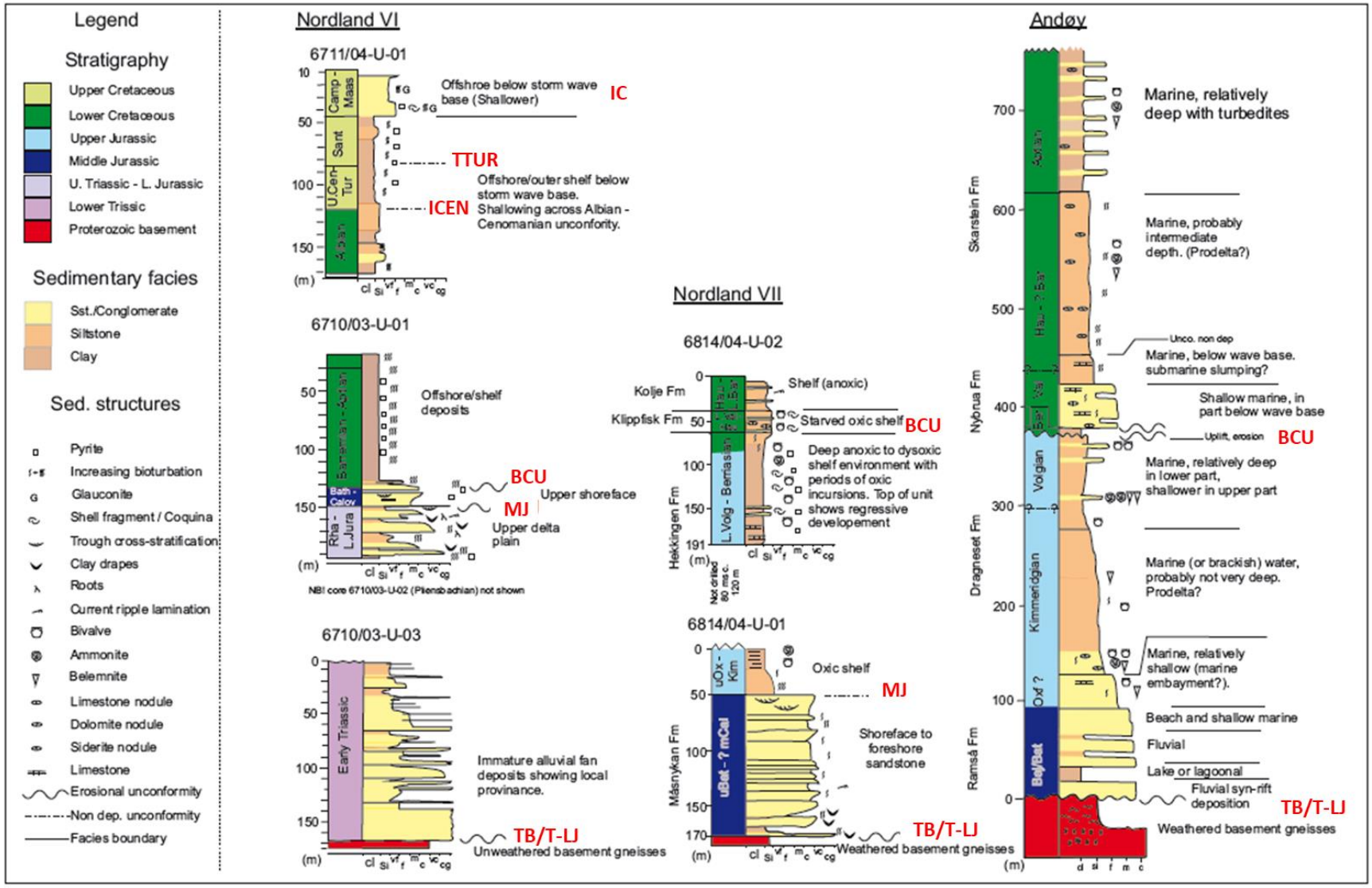

***Fig. 4.4**: Stratigraphic information from the IKU shallow stratigraphic boreholes compiled from Hansen et al. (1992) and Smelror et al. (2001) with the stratigraphy from Andøya described by Dalland (1981) (after Hansen et al., 2012). Seismic ties (Table 4.1) are shown with red letters. Location for boreholes in Fig. 4.5.*

4.3 Interpreted key seismic horizons/reflectors and sequences

4.3.1 General setting

Well correlation helped to define the seismic stratigraphic framework (Fig. 4.1), which enabled a detailed interpretation of the seismic data. The interpreted horizons are summarized in Table 4.1 and are following the well-to-seismic ties utilized in this thesis.

Table 4.1: *Summary of mapped seismic horizons/reflectors in the study area. Main horizons are marked in bold letters (Abbr.).*

Seismic horizon	Abbr.	Character/Properties	Well tie
Base Plio-Pleistocene	**BPLIO**	Semi-continuous reflector, high amplitude; is truncated towards Quaternary seismic units (BQ)	6610/3-1 R2 6710/10-1
Intra Miocene	**IM**	Semi-continuous to continuous reflector, with medium-to-high amplitude	6610/3-1 R2 6710/10-1
Intra Oligocene	**IO**	Semi-continuous reflector (mainly in the inner-outer margin transition), medium amplitude	Not drilled in study area
Top Eocene	**TE**	Semi-continuous reflector (south of LVM), high amplitude	6610/3-1 R2 6710/10-1
Intra Eocene 1, Intra Eocene 2	IE1, IE2	Semi-continuous reflectors, medium amplitude, confined to the Skomvær Sub-basin	6610/3-1 R2 6710/10-1
Top Paleocene	**TPAL**	Semi-continuous to continuous reflector, high amplitude; correlates with the top of breakup lavas	6610/3-1 R2 6710/10-1
Base Tertiary Unconformity	**BTU**	Chaotic and discontinuous reflector, low to medium amplitude	6610/3-1 R2 6710/10-1
Intra Campanian	IC	Continuous high amplitude reflector, confined to the Skomvær Sub-basin and North Træna Basin	6711/4-U-1 6610/3-1 R2
Top Turonian	**TTUR**	Semi-continuous reflector with a low to medium amplitude strength, confined to the southern LVM	6711/4-U-1 6610/3-1 R2
Intra Cenomanian	**ICEN**	Semi-continuous reflector with a low to medium amplitude strength, confined to the southern LVM and parts of the Vesterålen segment	6610/3-1 R2 6711/4-U-1
Intra Albian	**ALB**	Semi-continuous reflector in the southern Lofoten segment, with medium amplitude strength	6711/4-U-1
Intra Aptian	**APT**	Semi-continuous reflector in the Lofoten segment, with medium amplitude strength	6710/3-U-1
Intra Lower Cretaceous	**ILC**	Semi-continuous reflector with varying amplitude in the deepest part of basins	Not drilled
Base Cretaceous Unconformity	**BCU**	Regional erosional unconformity, semi-continuous reflector and varying middle-to-high amplitude	6710/3-U-3 6814/4-U-1 6610/3-1 R2
Middle Jurassic	MJ	Semi-continuous and low amplitude reflector, confined to the southern LVM and parts of the Vesterålen segment	6710/3-U-3 6814/4-U-1
Top Basement/Triassic-Lower Jurassic	**TB/ T-LJ**	Semi-continuous to continuous, varying amplitude and frequency reflector generally overlying more chaotic or transparent reflectivity	6710/3-U-3 6814/4-U-1 6610/3-1 R2

The geo-seismic sections in Figs. 4.6 to 4.9 illustrate the well-to-seismic ties that provide stratigraphic control for the study area. Some of them are long-distance ties with correlations of several hundreds of kilometres due to the lack of wells in the northern part of the LVM and in the study area. In addition, these sections have been built trying to avoid elevated structural highs as much as possible. No mapping was performed under the breakup lava flows due to the poor seismic resolution.

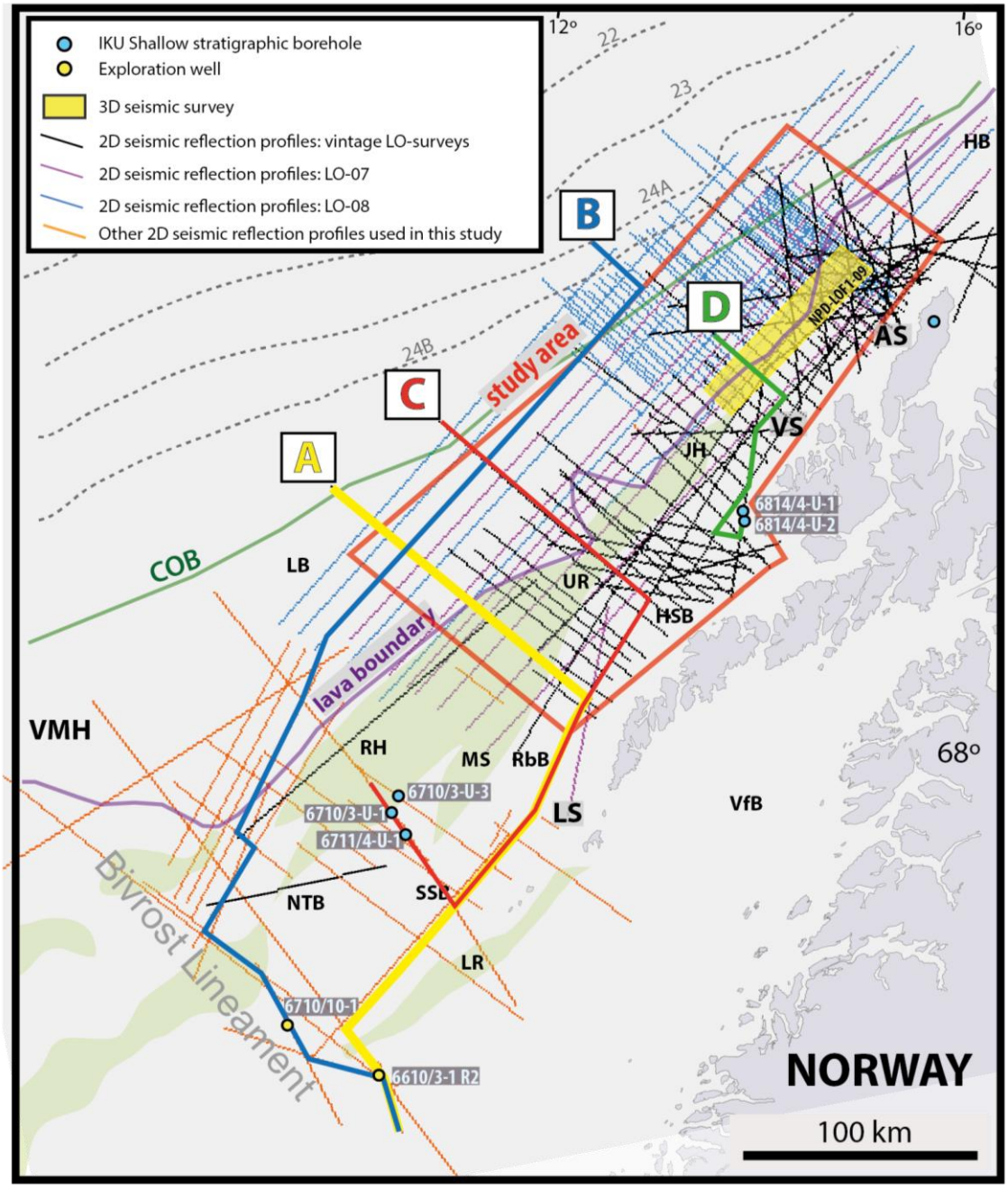

Fig. 4.5: *Location of composite seismic profiles for the well-to-seismic ties and stratigraphic control on the study area. The different sections are labelled as A to D and displayed successively in Figs. 4.6 to 4.9, respectively. The light-red polygon represents the focus study area. Abbreviations in Fig. 3.1.*

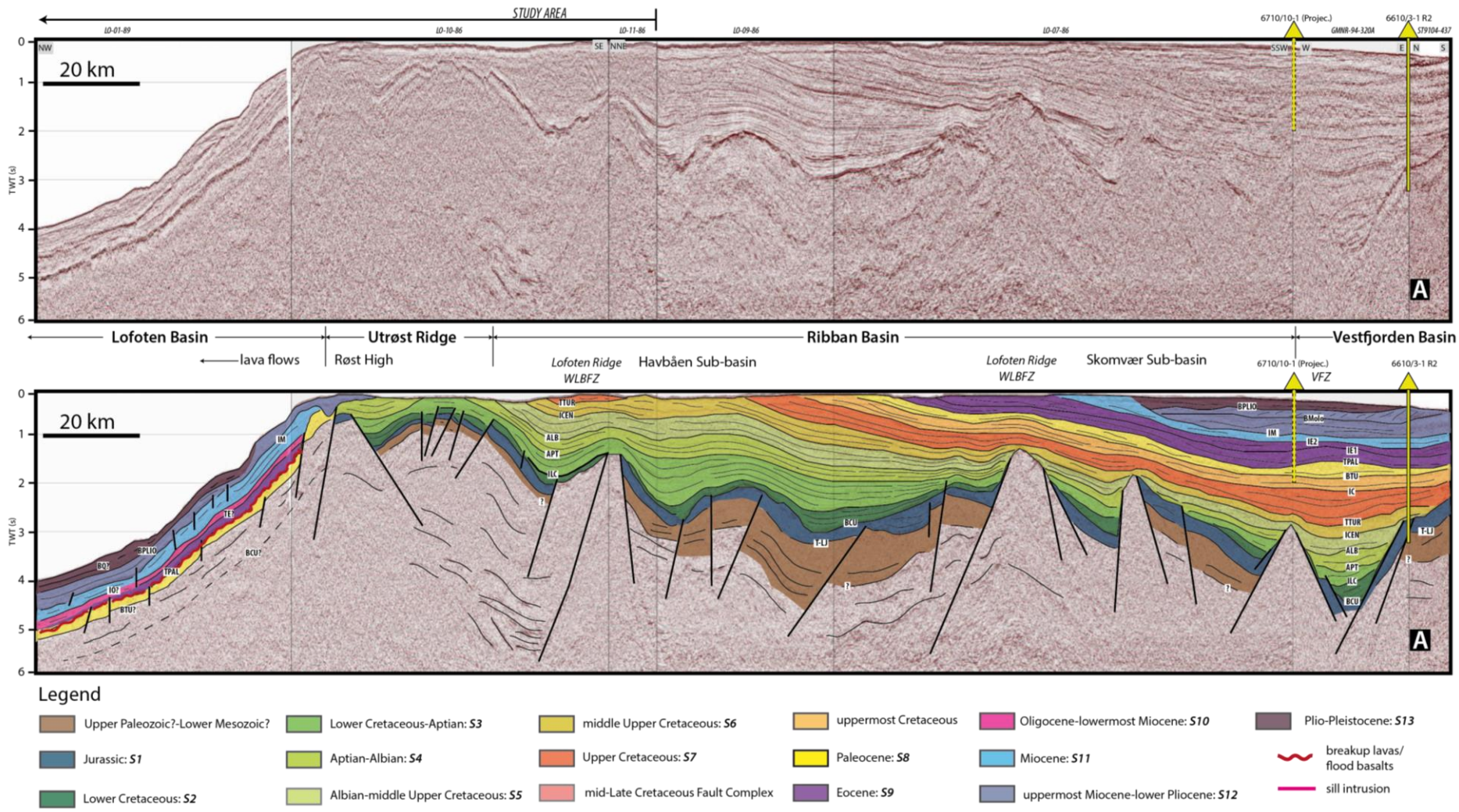

Fig 4.6: *Composite seismic reflection profile and line drawing interpretation illustrating the well-to-seismic ties to exploration wells 6610/3-1 R2 and 6710/10-1, and correlations within the study area. Abbreviations in Fig. 4.1 and Table 4.1.*

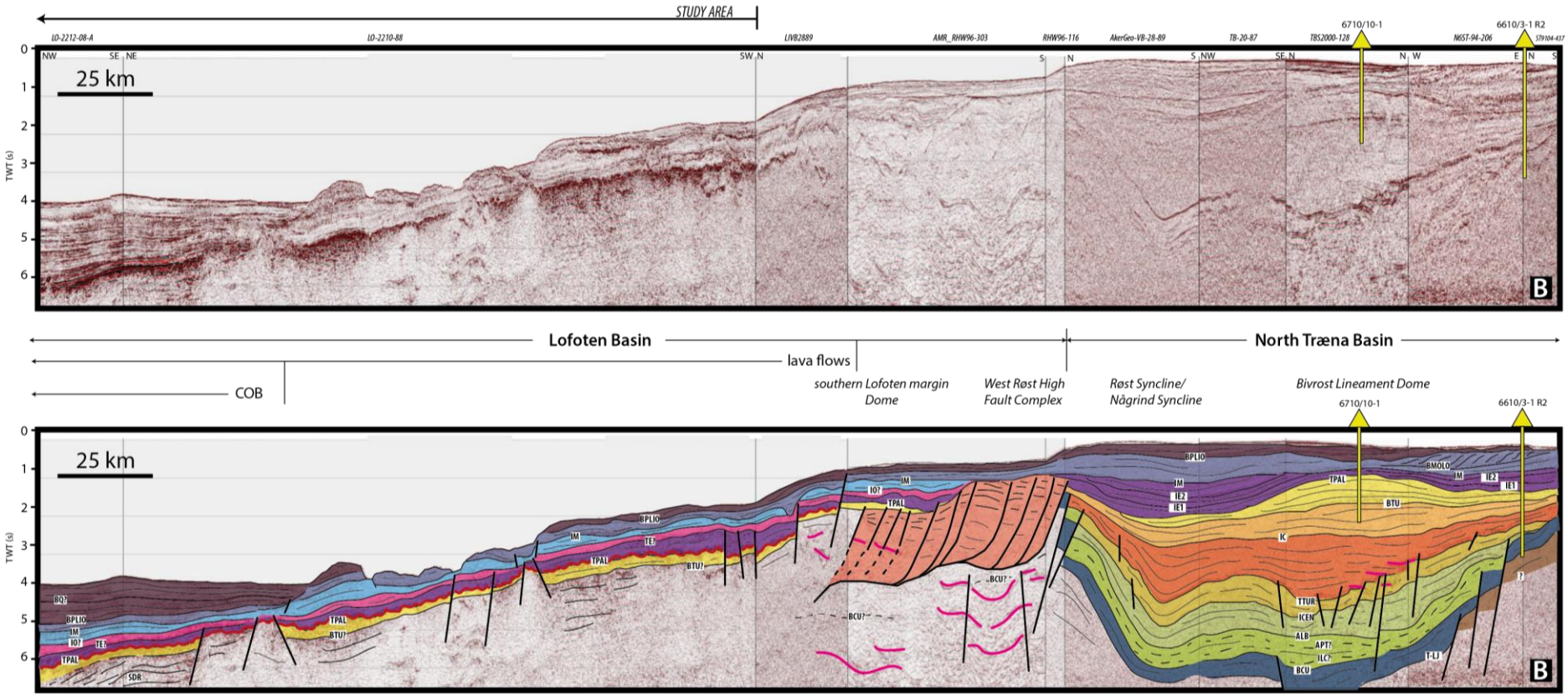

Fig 4.7: *Composite seismic reflection profile and line drawing interpretation illustrating the well-to-seismic ties to exploration wells 6610/3-1 R2 and 6710/10-1, and correlations within the study area. Abbreviations in Fig. 4.1 and Table 4.1. Colour legend in Fig. 4.6. SDR: sea-dipping reflectors.*

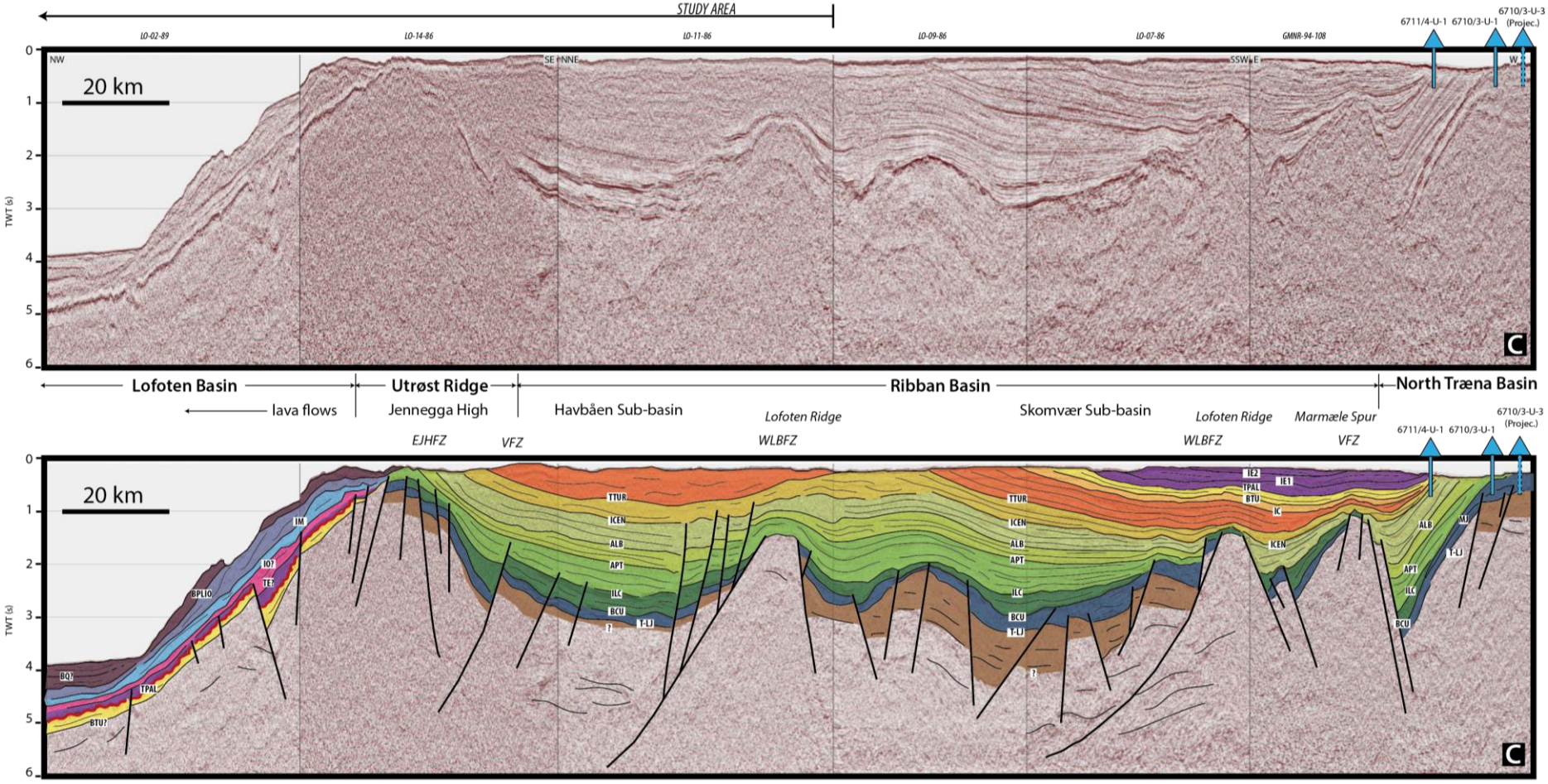

Fig 4.8: *Composite seismic reflection profile and line drawing interpretation illustrating the well-to-seismic ties to shallow stratigraphic boreholes 67710/3-U-3, 6710/3-U-1 and 6711/4-U-1, and correlations within the study area. Abbreviations in Fig. 4.1 and Table 4.1. Colour legend in Fig. 4.6.*

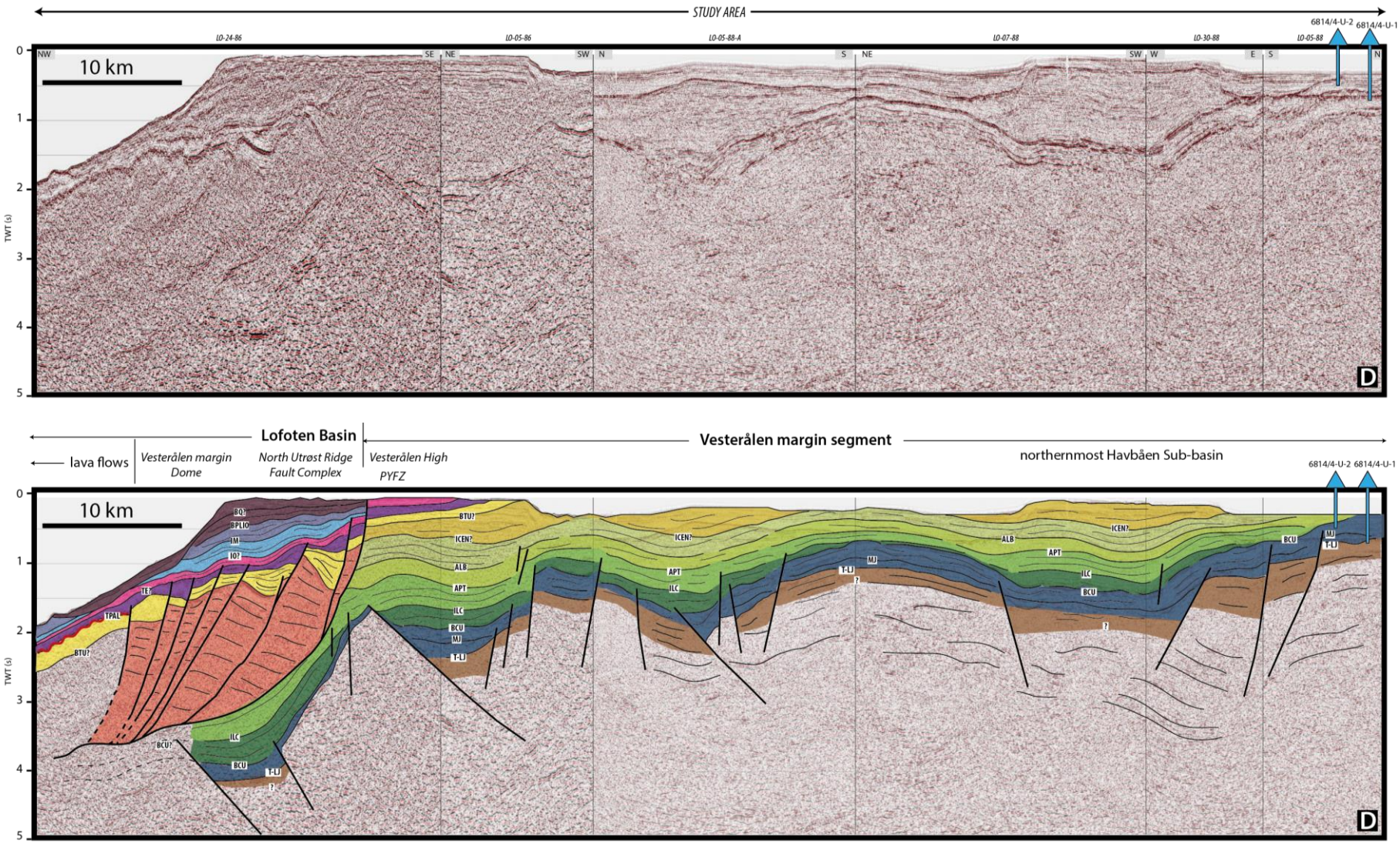

Fig 4.9: *Composite seismic reflection profile and line drawing interpretation illustrating the well-to-seismic ties to shallow stratigraphic boreholes 6814/4-U-1 and 6814/4-U-2, and correlations within the study area. Abbreviations in Fig. 4.1 and Table 4.1. Colour legend in Fig. 4.6. PYFZ: Pyramiden Fault Zone.*

As seen from the well-to-seismic ties, the main infill of the basins located in the inner part of the LVM comprises Cretaceous successions. The pre-Cretaceous and Cretaceous seismic sequences show syn-rift character, which is expressed in the growth of strata towards fault planes (Figs. 4.6 to 4.9). In Fig. 4.6, the syn-sedimentary faulting is evidenced in the deepest parts of the Vestfjorden and Ribban basins and is also preserved in rotated fault-blocks (Fig. 4.9). In the central part of the Ribban Basin, the pre-Cretaceous and mid- to Upper Cretaceous units onlap onto the West Lofoten Border Fault Zone (WLBFZ), and in addition a significant growth of Lower Cretaceous seismic sequences is evident in a northward direction. Consequently, the Lofoten Ridge must have been an elevated structural element by Early Cretaceous times sourcing adjacent areas (Løseth and Tveten, 1996), that, in turn, may have continued to be uplifted until mid-Cretaceous as evidenced by the frequent concave down geometries of seismic units (Figs. 4.6 and 4.8). Furthermore, by Cenomanian time the previous rift topography is observed to be covered, and Upper Cretaceous units were deposited (Figs. 4.6 and 4.8). In the study area, the Havbåen Sub-basin is confined to the east by the WLBFZ and to the west by the Utrøst Ridge/Røst High. Within the Havbåen Sub-basin, the Upper Cretaceous seismic units are thin (~0.5-1 s TWT) compared to their thickness in the south on the Skomvær Sub-basin and Vestfjorden Basin (~2 s TWT), and on the North Træna Basin (~2.5 s TWT) (Fig. 4.7). These observations are in line with a Late Cretaceous major phase of uplift/erosion on the LVM (Breivik et al., 2020), that seems to be intensified towards the north of the study area. The Upper Cretaceous strata are absent in the majority on the Vesterålen segment and farther north (Fig. 4.9).

In the transition between the inner to outer margin parts, fault complexes are often found (Figs. 4.7 and 4.9). They are observed as low-angle detachment fault complexes of undifferentiated Cretaceous successions. In this region, there are observations of mid- and Upper Cretaceous seismic sequences that are abruptly truncated to the east of these fault complexes, together with truncation of Cenozoic units to the west of them, and all are indicative of Late Cretaceous-Paleocene deformation (this study; Tsikalas et al., 2019).

Thick Cenozoic units are found on the Skomvær Sub-basin (~1.7 s TWT) and North Træna Basin (~2.5 s TWT) (Figs. 4.6 and 4.7). However, the Cenozoic seismic sequences seem to be confined to the outer part of the margin in the study area, together with Paleocene breakup lavas (Figs. 4.6 to 4.9). It is interesting to notice how the lava flows do not surpass neither the Utrøst Ridge nor the observed fault complexes in the inner/outer margin transition and, thus,

do not spread towards the inner LVM (Figs. 4.7 and 4.9). Thus, these structural elements must have been elevated structures prior to Tertiary breakup.

4.3.2 Pre-Cretaceous reflectors and sequences

Top Basement (TB)/Triassic-Lower Jurassic (T-LJ) reflector

The offshore presence of basement is confirmed by the IKU shallow stratigraphic boreholes 6710/3-U-3 and 6814/4-U-1 in the Røst High and in the northernmost part of the Havbåen Sub-basin, respectively (Figs. 4.6 to 4.9). The boreholes revealed that the basement consists of gneisses formed during Caledonian orogeny (Fig. 4.4). Borehole 6814/4-U-1 (Vesterålen margin) indicates weathering in the drilled basement, whereas in the southern part of the Lofoten segment there is no evidence of such alteration. The Top Basement (TB) is, however, a semi-transparent reflector and its existence in the deepest part of the basins can be evidenced within few rotated fault-blocks in the central parts of the Ribban and North Træna basins. Moreover, the TB reflector has a discontinuous seismic character and cannot be followed towards the northern parts of the study area. In particular, the TB reflector is observed beneath Triassic and Middle Jurassic units in most of the study area due to the extensive erosional regimes in this part of the LVM. Therefore, the Triassic-Lower Jurassic (T-LJ) reflector has been established in this study as the base of the sedimentary successions and the deepest mapped horizon within the entire extent of the study area (Table 4.1), which may occasionally overlap at a similar stratigraphic level as the TB reflector.

The T-LJ seismic reflector is confirmed by exploration well 6610/3-1 R2 that represents the top of the Late Triassic “Grey Beds” Group (Fig. 4.3) (factpages.npd.no-Wellbores). In general, the T-LJ reflector displays a semi-continuous seismic character and medium-to-strong amplitude, and progressively the reflector becomes more discontinuous towards the north within the study area. In addition, this reflector is overlying more transparent reflections with, occasionally, wedge-shaped internal configuration (Figs. 4.6, 4.8 and 4.9). Blystad et al. (1995) interpreted the above reflections as Paleozoic rift basins. Little focus has been given to possible Paleozoic-Lower Mesozoic strata due to their limited areal extent and low seismic resolution. However, since the focus of this study lies within the Late Mesozoic and Cenozoic rift basin evolution, this does not have major implications in the work presented in this thesis. Mapping of this horizon becomes progressively more difficult towards the northwest part of the LVM and the study area due to the weaker amplitude it displays.

Middle Jurassic (MJ) reflector

The MJ seismic reflector has been tied to IKU boreholes 6710/3-U-1 and 6814/4-U-1 at ~0.55 seconds in the North Træna Basin and the northern part of the Havbåen Sub-basin, respectively (Figs. 4.4, 4.8 and 4.9). The seismic character of the MJ reflector is, in general, of middle-to-high intensity seismic amplitude, and the reflector is often found down-faulted (Fig. 4.9). Due to uplift and erosion, the MJ reflector is mainly confined to the southern part of the LVM, and occasionally found at the Vesterålen margin, thus this reflector is defined in this study as of subordinate importance. Hansen et al. (2012) referred to the MJ reflector as the Callovian Unconformity, and it can be assumed to be near the top of the Jurassic reservoir rocks (Fig. 4.1; e.g. Båt and Fangst lithostratigraphic groups including the Åre/Tilje/Tofte/Ile/Garn sandstone formations) (NPD, 2010).

Seismic sequence S1

Seismic sequence S1 is defined at the base by the T-LJ horizon, which separates it from basement reflections, and is bounded at the top by the Base Cretaceous Unconformity (BCU) (Fig. 4.1). The MJ horizon roughly divides this sequence in lower and upper stratigraphic units, but seismic resolution does not allow to properly map this separation within the study area. Sedimentary rocks of the Upper Triassic-Lower Jurassic Båt and Fangst lithostratigraphic groups constitute the S1 lower unit in the southern Lofoten segment, and these have been confirmed by well 6610/3-1 R2 in the Vestfjorden Basin and IKU borehole 6710/3-U-3 in the North Træna Basin (Figs. 4.2 and 4.3). The sedimentary facies include immature alluvial fan deposits showing local provenance. Towards the northern parts of the Lofoten segment, the facies become sandier and show more marine influence, representing shoreface to foreshore deposits of the Måsnykan Formation confirmed by the IKU borehole 6814/4-U-1 in the Vesterålen margin (Fig. 4.4). The onshore equivalent of the S1 lower unit has been interpreted as the fluvial syn-rift sandstones of the Ramså Formation found on Andøya (Fig. 4.4). Syn-rift character is also observed offshore in the northern part of the Havbåen Sub-basin, where wedge-shaped internal geometries can be locally observed in rotated-fault blocks in the Vesterålen margin (Fig. 4.9).

The upper unit of seismic sequence S1 is tied to IKU boreholes 6710/3-U-1 in the North Træna Basin and 6814/4-U-2 in the northern Havbåen Sub-basin (Fig. 4.4). It mainly consists of dark-grey muddy siltstones of the Upper Jurassic Spekk/Hekkingen Formation deposited under deep anoxic to dysoxic shelf environment. In addition, well 6610/3-1 R2 (Vestfjorden

Basin) confirmed at the top of sequence S1 a black shale with high organic content of the Spekk Formation (Fig. 4.3), whereas shallow marine prodelta deposits of the Kimmeridgian Dragneset Formation are found onshore in Andøya and constitute the onshore equivalent of sequence S1. The overall thickness of sequence S1 is variable, with less than 20 meters in the North Træna Basin and up to 170 meters in the Havbåen Sub-basin. Internal geometries within this seismic sequence are often chaotic and transparent, but in some cases the geometries are sub-parallel within the lower member due to the dominance of sandy facies over the silty/shaley facies in the upper unit (Fig. 4.9). The thickness of reservoir sandstone in this Jurassic seismic sequence is uncertain.

4.3.3 Lower Cretaceous reflectors and sequences

The presence of Lower Cretaceous sedimentary successions on the LVM is confirmed by IKU boreholes 6711/4-U-1, 6710/3-U-1 and 6814/4-U-2, and exploration well 6610/3-1 R2 (Figs. 4.3 and 4.4). They can be found in the south Lofoten segment as infills of deep depocenters (>4 s TWT) that are separated by shelf-parallel ridges (Figs. 4.6 and 4.8). In general, mapping of the Lower Cretaceous reflectors is restricted to the inner margin and to the west by the Utrøst Ridge. Core information reveals that the Lower Cretaceous rocks consist of shelf deposits of siltstone and clay facies.

Base Cretaceous Unconformity (BCU) reflector

The BCU is tied in the south LVM to exploration well 6610/3-1 R2 in the Vestfjorden Basin and IKU borehole 6710/3-U-1 in the North Træna Basin, as well as to IKU borehole 6814/4-U-1 in the northern Havbåen Sub-basin (Figs. 4.3 and 4.4). BCU is a regional erosional unconformity that marks the base of the Cretaceous successions in all the LVM (Fig. 4.1). It can be recognized as a distinctive strong amplitude and semi-continuous seismic reflector, with reflections onlapping on it near the basin flanks (Figs. 4.6 to 4.9). Faults and highs offset this reflector, but it is possible to map it in all the study area and to correlate it across structural elements. Additionally, prospects and prospect opportunities are grossly defined at this level (easier interpretable) for the Jurassic reservoirs below (NPD, 2010).

Seismic sequence S2

Seismic sequence S2 is bounded at the base by the BCU reflector, while its upper boundary has been interpreted as the Intra Lower Cretaceous (ILC) reflector (Fig. 4.1). The sequence is preserved to some degree in almost the entire study area, and it is found in fault-bounded

depocenters, located within the deepest basinal parts (Figs. 4.6, 4.8 and 4.9). Thickness variations are often observed as a progressively thinning of sedimentary accumulations towards the crest of rotated fault-blocks where they pinch-out. As a result, wedge-shaped geometries are present in this seismic sequence; for example, in the south of the study area on the Røst High (Fig. 4.6) and in the Havbåen Sub-basin (Fig. 4.8). Interpreted seismic sequences with similar characteristics as the one described above have been reported south of the Lofoten segment in the Någrind Syncline (Fig. 4.7), where a local Neocomian rift phase is believed to be responsible for the basin infill pattern (Zastrozhnov et al., 2018). In the south Lofoten segment, only a minor amount of sequence S2 is preserved in the North Træna Basin (Fig. 4.8), but becomes thicker towards north and within the study area. Stratigraphic correlation for this seismic sequence is limited, however core information from IKU borehole 6814/4-U-2 (Havbåen Sub-basin) suggests that it may contain rocks from the late Valanginian to Hauterivian Klippfisk Formation (Fig. 4.4). This formation consists of dark-grey to grey-green, calcareous siltstones interbedded with limestone layers that overlie the Hekkingen Formation. Marine fossil fauna and lack of sedimentary structures suggest that the sediments were deposited under a starved oxic shelf environment. The internal configuration of this sequence is in general transparent and chaotic, but more reflections are often observed towards the upper boundary of the sequence, and particularly in areas of the Vesterålen margin where some stratigraphy can be followed (Fig. 4.9).

Intra Lower Cretaceous (ILC) reflector

The ILC reflector is only observed in the deepest part of the basins (e.g. Figs. 4.6 and 4.8), and it is not possible to correlate it with the available well data since it has not been penetrated by drilling. Hence, the presence of this seismic reflector on some portions of the North Træna Basin is uncertain (Fig. 4.7). Overall, this reflector is semi-continuous up to some degree, with variations in its lateral distribution and seismic amplitude intensity within the deepest part of the basins.

Seismic sequence S3

The base of seismic sequence S3 is bounded by the ILC reflector (Fig. 4.1). This seismic reflector onlaps within the study area against the BCU reflector (Fig. 4.9) and onto elevated structural elements, such as the Marmæle Spur in the south Lofoten segment and the Lofoten Ridge in the south of the study area (Fig. 4.8). As a consequence, this seismic sequence is flanked towards the borders of the depocenter, and its lower boundary may be in contact with

BCU, such as in the Utrøst Ridge area (Figs. 4.6 and 4.8). Similar as for seismic sequence S1, lateral thickness variations (thinning/expansion) across rotated-fault blocks in the Skomvær and Havbåen sub-basins are also evident in seismic sequence S3.

The top of the sequence S3 is bounded by the Intra Aptian (APT) seismic reflector (Fig. 4.1). Thus, the age for this sequence is constrained as Barremian-Aptian. In addition, IKU borehole 6710/3-U-1 drilled in the North Træna Basin (Fig. 4.8) has penetrated offshore (shelf) deposits constituted by claystone formations with Barremian to Aptian ages (Fig. 4.4). The internal configuration of sequence S3 is observed to be stratified or laminated due to a set of parallel and semi-continuous to continuous reflections, as for example in the Ribban Basin (Fig. 4.6). In the Vesterålen margin and towards the north of the study area, these internal geometries gradually become more chaotic and transparent, but the overall lamination tendency is preserved.

Intra Aptian (APT) reflector

The APT reflector has been tied to IKU borehole 6710/3-U-1 in the North Træna Basin, where core information revealed Aptian sediments (Fig. 4.4). In general, this horizon is a semi-continuous to continuous reflector with medium-to-strong seismic amplitude, often near structural highs (Figs. 4.6 and 4.8). However, north of the Ribban Basin the APT seismic character is that of a more discontinuous and low amplitude intensity reflector. Mapping of this reflector becomes restricted to the west by the Utrøst Ridge (Figs. 4.6 and 4.8). The northerly reduced seismic amplitude trend in the study area makes it difficult to correlate the APT reflector in this part of the margin, especially near/inside low-angle detachment fault complexes where the APT reflector is abruptly truncated against the former (Fig. 4.9).

Seismic sequence S4

Seismic sequence S4 is bounded at the base and top by the Intra Aptian (APT) and the Intra Albian (ALB) reflectors, respectively (Fig. 4.1). Thus, the indicative age for this sequence is Aptian-Albian. Shales and probably sandstones deposited in an offshore/shelf environment constitute seismic sequence S4 (Fig. 4.4). The sequence is interpreted to overlay conformably seismic sequence S3 with a similar internal geometry. However, thickness variations within S4 is relatively absent in the majority of the study area and south of the Lofoten segment (Figs. 4.6, 4.8, and 4.9). Hence, sequence S4 represents sediments deposited in a period of tectonic stability (NPD, 2010), and the majority of faults terminate below or within it (Figs.

4.6 and 4.8). In addition, this sequence fills the rift topography effectively, and possible wedge-shaped geometries in the Skomvær Sub-basin lack indications of growth strata (Fig. 4.6). Sequence S4 often subcrops close to the sea-floor (Fig. 4.8), and in particular in the northern part of the Lofoten segment (Fig. 4.9).

Intra Albian (ALB) reflector

The ALB reflector has been tied to IKU borehole 6711/4-U-1 in the North Træna Basin, where core information revealed Albian sediments (Fig. 4.4). Seismic characteristics are similar to those of the Intra Aptian (APT) reflector, with a semi-continuous and middle amplitude strength in the Lofoten segment (Figs. 4.6 and 4.8). However, its discontinuous character is much more accentuated than that of the APT reflector, especially in the northern portions of the study area, where the margin becomes narrow with a limited areal mapping extent and the reflector is also truncated to the northwest by fault complexes in the Vesterålen and Andøya margin segments (Fig. 4.9). The ALB reflector is the top of the seismic sequence S4, and defines the top of the Lower Cretaceous seismic reflectors and sequences in this study.

4.3.4 Upper Cretaceous reflectors and sequences

The Lower and Upper Cretaceous sequences share a similar depositional environment, consisting of offshore/outer shelf mud and siltstone facies. Exploration wells 6710/10-1 and 6610/3-1 R2, together with IKU borehole 6711/4-U-1 confirm the existence of Upper Cretaceous strata in the LVM (Figs. 4.2 to 4.4). Shallower sedimentary environment conditions in the study area during Late Cretaceous are indicated by the presence of limestone and sandstones in the cores of the above wells. The shelf in the LVM has been exposed to major uplift and erosion events during Late Cretaceous-Paleocene (Breivik et al., 2020), and the transition between Lower to Upper Cretaceous sedimentary successions is debatable. Considerable uplift in the study area has led to a very intense erosion and removal of most of the Upper Cretaceous sequences, as seen on the well-to-seismic ties (Figs. 4.6 to 4.9) and on the onshore Andøya outcrop (Fig. 4.4). Nonetheless, for simplicity and correlation between the northern and southern parts of the study area, the Intra Albian (ALB) reflector has been defined as a good candidate to represent the transition between the Lower and Upper Cretaceous successions in the studied portion of the LVM (Fig. 4.1).

Seismic sequence S5

Seismic sequence S5 is bounded at the base and top by the Intra Albian (ALB) and the Intra Cenomanian reflectors, respectively (Fig. 4.1). A Cenomanian age is interpreted for this sequence, and is correlated by well 6610/3-1 R2 in the Vestfjorden Basin to the Berrasian-Late Turonian Lange Formation (Fig. 4.3). Core information from this exploration well depicts marine rocks with a clay-dominated lithology. Additionally, in the proximity of the North Træna Basin, this sequence onlaps on the BCU (Fig. 4.7), and marl facies of the Lyr Formation are also present. However, IKU borehole 6711/4-U-1 drilled in the northern North Træna Basin and close to the Marmæle Spur, shows more silt and coarser grain size lithologies towards the top of the sequence (Fig. 4.4). East of that area, sequence S5 shows strong sub-parallel internal reflections with sag geometry (Fig. 4.8). There, the Vesterdjupet Fault Zone may be responsible for the thickness expansion of this sequence (Fig. 4.8). The S5 sequence is subcropping close to the seafloor in the northern part of the Lofoten margin and along the Vesterålen margin (Figs. 4.6, 4.8, and 4.9).

Intra Cenomanian (ICEN) reflector

The ICEN reflector has been tied to exploration well 6610/3-1 R2 in the Vestfjorden Basin to the base of the Lange Formation, and correlated to IKU borehole 6711/4-U-1 in the North Træna Basin (Figs. 4.3 and 4.4). The reflector is eroded when it approaches to the Utrøst Ridge/Røst High in the Lofoten segment, while it gradually becomes absent towards the Vesterålen margin and the northern parts of the study area (Figs. 4.6 to 4.9). In the proximity of the Marmæle Spur, the reflector drapes above the elevated local structural highs and younger reflections/sequences appear to onlap/pinch-out onto it (Fig. 4.8), hence a local unconformity character is observed. The ICEN reflector is semi-continuous with a medium amplitude strength that increases in the fault-blocks in the southwestern part of the Røst High.

Seismic sequence S6

The base of seismic sequence S6 is characterized by a sag geometry, represented by the Intra Cenomanian (ICEN) reflector (Fig. 4.8). This is clearly observed in the Røst Syncline/Någrind Syncline and in the Marmæle Spur area (both located in the North Træna Basin) and where the thickest successions of sequence S6 are preserved in the entire study area (~2 s TWT) (Figs. 4.7 and 4.8). The sequence is correlated to the Lange and Lysing formations penetrated by well 6610/3-1 R2 in the Vestfjorden Basin, thus, a Late Cenomanian to Turonian/Coniacian age has been assigned to sequence S6 (Fig. 4.3). The Lysing

Formation consists of fine to medium, occasionally coarse grained, white-grey sandstones interbedded with shales, and deposited in a shallow marine to deep marine environment, possibly as submarine fan deposits (NPD, 2020b). More clay sedimentary facies are found towards the North Træna Basin in cores from IKU borehole 6711/4-U-1 (Fig. 4.4). The sequence is bounded at the top by the Top Turonian (TTUR) reflector, and younger reflections progressively onlap this surface (Figs. 4.1 and 4.8). The internal configuration of the sequence is, in general, semi-transparent in some places, and occasional sill intrusions mask even more the seismic amplitude, in particular in the North Træna Basin (Fig. 4.7). However, clear and distinct internal reflections are observed in the Ribban Basin, together with aggradational build-up geometries towards the West Lofoten Border Fault Zone (WLBFZ) in the Lofoten Ridge (Fig. 4.8). Reflections generally become more apparent and distinct towards the upper boundary of the sequence, but disappear towards the north of the study area in the Vesterålen margin (Fig. 4.9).

Top Turonian (TTUR) reflector

The TTUR reflector is tied by exploration well 6610/3-1 R2 to the top of the Lysing Formation (Fig. 4.3), and correlated to IKU borehole 6711/4-U-1 (Fig. 4.4). It is a semi-continuous and medium-to-high amplitude intensity seismic reflector in the Ribban and North Træna basins. TTUR has an onlap character onto the Intra Cenomanian (ICEN) reflector in the North Træna Basin (Fig 4.8), and it is often found to be down-faulted and cross-cut by sill intrusions (Fig. 4.7). It has been mapped to the northern parts of the study area following geometrical relationships and the seismic character since it cannot be directly followed on the seismic data due to uplift and erosion between the Skomvær and the Havbåen sub-basins in the Lofoten segment (Figs. 4.6 and 4.8). The TTUR represents the youngest Upper Cretaceous reflector interpreted within the study area (Fig. 4.1).

Seismic sequence S7

Seismic sequence S7 is bounded at the base by the Top Turonian (TTUR) reflector (Fig. 4.1). This sequence has been correlated by exploration well 6610/3-1 R2 (Fig. 4.3) and IKU borehole 6711/4-U-1 (Fig. 4.4) to the Springar Formation. The Springar Formation (Campanian to Maastrichtian age) predominantly consists of greyish-green claystones interbedded with stringers of carbonates and sandstones deposited under an open marine environment (NPD, 2020b). IKU core information, however, shows predominance of sandstones and conglomerates. The internal configuration of sequence S7 is similar to that of

the seismic sequence S6, where semi-continuous and medium-to-high amplitude intensity reflections stratify the sequence. Nonetheless, sequence S7 becomes chaotic and transparent in the study area (Fig. 4.9). In the south of the Lofoten segment, sequence S7 is bounded on the top by the Intra Campanian (IC) reflector, and in the northern parts of the margin the sequence subcrops close to the seafloor. Sequence S7 is the youngest Upper Cretaceous seismic sequence that was able to be mapped in the study area (Fig. 4.1).

Intra Campanian (IC) reflector

The IC reflector is tied by exploration wells 6710/10-1 and 6610/3-1 R2 to the base of the Springar Formation (Figs. 4.2 and 4.3), and was correlated to IKU borehole 6711/4-U-1 (Fig. 4.4). It has a continuous and high amplitude reflection character. However, it was only possible to map IC in the south Lofoten segment and not within the focus study area, hence it is defined as a subordinate importance reflector (Fig. 4.1 and Table 4.1). In the Skomvær Sub-basin and the North Træna Basin, the IC reflector constitutes the top boundary of seismic sequence S7, and represents the youngest Upper Cretaceous reflector interpreted in the Lofoten segment area (Figs. 4.6 and 4.7). In addition, an uppermost Cretaceous sequence has been interpreted in the south of the study area with the purpose to better reveal and define the tectono-sedimentary history on the LVM, but as the IC reflector, it is confined just to the southern basins.

4.3.5 Cenozoic reflectors and sequences

The Cenozoic sedimentary successions were confirmed in the LVM by exploration wells 6710/10-1 and 6610/3-1 R2 located in the North Træna and Vestfjorden basins, respectively (Figs. 4.2 and 4.3). These Tertiary successions represent sediments that were by-passed from the narrow and elevated shelf and were rapidly deposited and buried into the Lofoten Basin located in the outer LVM margin (Eldholm et al., 2002). Glacial Plio-Pleistocene submarine canyons were developed and the deposited sediments overlaid the shelf (Faleide et al., 2015). Mass transport processes within these canyons resulted in high erosional rates in the LVM continental slope (Rise et al., 2013). Thus, the seismic-to-well ties for the Cenozoic reflectors and sequences are difficult tasks to perform. The challenges in the mapping imposed by erosion, together with the moderate-to-poor seismic resolution in the outer margin, make the Cenozoic reflectors and sequences to have the highest degree of uncertainty compared to all other interpreted horizon and seismic sequences in this study (Fig. 4.1). However, Fig. 4.7 illustrates a composite seismic section that was used to bring the Cenozoic stratigraphy from

the south to the northern parts of the LVM and to the study area, and represents a good approximation for the ties of these successions.

Base Tertiary Unconformity (BTU) reflector

The BTU reflector is tied by exploration wells 6710/10-1 and 6610/3-1 R2 to the base of the Tang Formation (Figs. 4.2 and 4.3). It represents the top of the uppermost Cretaceous sequences interpreted south of the inner part of the LVM, whereas it constitutes the base for the interpreted Cenozoic reflectors/sequences within the entire study area (both inner and outer parts). The reflector is interpreted as an unconformity because it overlies both Lower and Upper Cretaceous strata, and its seismic character is discontinuous and with low seismic amplitude. Hence, the interpretation of the reflector has often been assisted by the observed downlaping/onlapping reflections onto it in the southern part of the LVM, and near fault complexes.

Seismic sequence S8

Seismic sequence S8 is bounded at the base by the Base Tertiary Unconformity (BTU) reflector (Fig. 4.1). Exploration wells 6710/10-1 and 6610/3-1 R2 helped to correlate this sequence to the Paleocene Tang Formation (Figs. 4.2 and 4.3). The Tang Formation consists of claystones with minor sandstones and limestones layers at a deep marine depositional environment (NPD, 2020b). Sequence S8 in the south LVM exhibits its thickest accumulations within the Bivrost Lineament Dome located in the North Træna Basin (Fig. 4.7) (Tsikalas et al., 2019). In the same area, the internal configuration of this sequence is that of sub-parallel to wavy medium-to-high amplitude reflections that downlap and onlap the BTU horizon. However, in the north and outer part of the LVM the internal reflections of sequence S8 are chaotic. Similarly, towards the upper boundary of the sequence, the Top Paleocene (TPAL) reflector, high concentration of lava flows hampers the seismic resolution (Table 4.1).

Top Paleocene (TPAL) reflector

The TPAL reflector has been tied by exploration wells 6710/10-1 and 6610/3-1 R2 to the top of the Tare Formation (Figs. 4.2 and 4.3). This reflector is interpreted as the top of seismic sequence S8 (Fig. 4.1). Within the study area, the TPAL reflector is mainly restricted to the outer part of the LVM and west of the Utrøst Ridge, where it has been mapped just on top of the high-impedance breakup lava-flows (Figs. 4.6 to 4.9) (e.g. Eldholm et al., 2002). Thus, the

TPAL reflector is in general a high amplitude intensity and semi-continuous seismic reflector that can be followed with no major problems through the entire outer part of the LVM. In addition, a local unconformity character is observed towards fault complexes and structural highs in the inner-to-outer margin transition, with younger and older strata downlaping and top-lapping, respectively, onto it (Figs. 4.7 and 4.9).

Seismic sequence S9

Seismic sequence S9 is interpreted to be Eocene in age, bounded at its base by the Top Paleocene (TPAL) reflector (Fig. 4.1). Exploration wells 6710/10-1 and 6610/3-1 R2 correlate the lower part of the sequence to the Tare Formation (Figs. 4.2 and 4.3). The Tare Formation belongs to the Rogaland Group, and consists of deep marine dark grey, green or brown claystones with some thin sandstone stringers with a variable content of tuff (NPD, 2020b). Sedimentary rocks from the Brygge Formation are also present in this sequence, and they concentrate on the upper parts of this seismic sequence (Figs. 4.2 and 4.3). The Brygge Formation consists of marine claystone with stringers of sandstone, siltstone, limestone and marl. Pyrite, glauconite and shell fragments are also seen in the sandstones (NPD, 2020b). The thickest part of sequence S9 is found in the south of the Lofoten segment, where it is bounded on the top by the Intra Miocene (IM) reflector (Figs. 4.6 to 4.8). On the other hand, sequence S9 thins considerably towards the outer part of the LVM, and its top has been interpreted as the Top Eocene (TE) reflector (Figs. 4.1 and 4.7). The internal configuration of this sequence exhibits slightly wavy reflections and the sequence becomes more transparent in the outer margin part. In this part of the margin, several reflections often toplap the S9 upper boundary, especially near fault complexes (Figs. 4.7 and 4.9).

Intra Eocene 1 (IE1) and Intra Eocene 2 (IE2) reflectors

The IE1 and IE2 reflectors have been tied by exploration wells 6710/10-1 and 6610/3-1 R2 and are interpreted as Intra Brygge Formation horizons (Figs. 4.2 and 4.3). They are only mapped in the southern part of the Lofoten segment for better stratigraphic control (Figs. 4.6 and 4.8), thus they are considered as subordinate horizons in this study (Fig. 4.1 and Table 4.1). A semi-continuous and medium seismic reflection character is observed in both horizons. IE1 and IE2 are interpreted within seismic sequence S9 in the North Træna Basin and the Skomvær Sub-basin (Figs. 4.6 to 4.8).

Top Eocene (TE) reflector

The TE reflector has been tied to exploration wells 6710/10-1 and 6610/3-1 R2, and is interpreted as a top Brygge Formation horizon (Figs. 4.2 and 4.3). TE bounds the top of seismic sequence S9 in the outer part of the LVM (Figs. 4.1 and 4.7). However, the reflector is eroded in the inner margin, thus the Intra Miocene (IM) reflector is depicted as a better candidate for the top of sequence S9 in this studied portion (e.g. Fig. 4.6) (NPD, 2020b). This horizon exhibits a discontinuous and medium-amplitude intensity seismic reflector character. An onlapping/downlaping (unconformity) character of younger reflections onto TE is observed near fault complexes in the inner-to-outer margin transition (Figs. 4.7 and 4.9).

Seismic sequence S10

Seismic sequence S10 is bounded at the base by the Top Eocene (TE) reflector, and is only observed in the outer part of the LVM due to erosion of the inner part (Figs. 4.1 and 4.7). No exploration wells available in this study have penetrated this sequence, however, wells 6710/10-1 and 6610/3-1 R2 show Eocene to Early Miocene Hordaland Group sedimentary successions (Figs. 4.2 and 4.3). Thus, an Oligocene age has been assigned to sequence S10. The internal configuration of the sequence is, in general, chaotic and transparent, with some minor wavy reflections that are visible towards the inner-to-outer margin transition where the sequence pinches-out (Fig. 4.7). In addition, close to fault complexes the seismic reflection character in sequence S10 gradually shifts from onlapping near the base of the sequence to a top-lapping towards the top of it (Figs. 4.7 and 4.9). The top of sequence S10 is interpreted as the Intra Oligocene (IO) reflector (Fig. 4.1).

Intra Oligocene (IO) reflector

The IO reflector has not been drilled in the study area, but exploration wells 6710/10-1 and 6610/3-1 R2 show Eocene to Early Miocene Hordaland Group sedimentary successions (Figs. 4.2 and 4.3). This seismic reflector is, thus, only mapped in the outer part of the LVM (Figs. 4.6 to 4.9). It is truncated towards the east onto the Utrøst Ridge and/or near fault complexes (Figs. 4.7 and 4.9). The IO reflector is a discontinuous and medium-amplitude intensity seismic reflector. A toplap seismic character onto the Intra Miocene (IM) reflector is often observed for the IO reflector near the inner-to-outer margin transition (Figs. 4.7 and 4.9).

Seismic sequence S11

Seismic sequence S11 has been penetrated by exploration wells 6710/10-1 and 6610/3-1 R2, and shows mainly clay-dominated lithologies (Hordaland Group sedimentary rocks) (Figs. 4.2 and 4.3). Thus, the assigned age for this sequence is Miocene. Similar characteristics to those of the seismic sequences S9 and S10 are observed in sequence S11, as well. These include the transparency in internal reflection geometries, and the onlapping/top-lapping character for the base/top reflections (Figs. 4.7 and 4.9). Seismic sequence S11 is also truncated towards the east onto the Utrøst Ridge and/or near fault complexes (Figs. 4.7 and 4.9). The Intra Oligocene (IO) and the Intra Eocene 2 (IE2) reflectors correspond to the base of this sequence in the outer and inner parts of the margin, respectively, whereas the Intra Miocene (IM) reflector is bounded to the top of it (Figs. 4.6 to 4.8).

Intra Miocene (IM) reflector

The IM reflector is tied to exploration wells 6710/10-1 and 6610/3-1 R2 in the south Lofoten segment to the top of the Hordaland Group (Figs. 4.2 and 4.3). It is possible to map this seismic reflector in the entire area of the outer part of the LVM, and up to some extent in the south inner part of the margin due to its semi-continuous and medium-amplitude intensity character (Figs. 4.6 to 4.8). Towards the northwest of the margin, the IM reflector is truncated towards the Utrøst Ridge/Røst High (Fig. 4.9). Younger strata are observed to downlap and onlap the IM reflector, thus, a local angular unconformity character is evident (Figs. 4.7 and 4.9). The IM reflector overlies also both Eocene and Oligocene strata (Miocene canyons/channels) (Figs. 4.6 and 4.7).

Seismic sequence S12

Seismic sequence S12 is bounded at the base by the Intra Miocene (IM) reflector and is tied to the Hordaland Group (Figs. 4.1 to 4.3). S12 is extended in most of the studied LVM area, except for the Havbåen Sub-basin and the northern inner margin part (Fig. 4.9). The thickness of this sequence is variable, but the thickest successions are found in the North Træna Basin, where internal geometries of gently and westward prograding clinoforms are observed (Fig. 4.7). This internal configuration corresponds to the Late Miocene-Early Pliocene Molo Formation (BMOLO; Fig. 4.7) (Tsikalas et al., 2019). The Molo Formation consists of red to yellow coloured sand, with some sections also containing well-rounded, rust-tinted pebbles, and glauconitic and mica-rich sand (Fig. 4.3). The formation has been deposited in a coastal, shallow marine to prograding deltaic depositional environment, probably with strong wave

influence (NPD, 2020b). In addition, sequence S12 has been interpreted as the sedimentary infill of submarine canyons located on the continental slope of the LVM. The top of this seismic sequence is assigned to the Base Plio-Pleistocene (BPLIO) reflector, but it often subcrops on the seafloor in the outer part of the margin (Figs. 4.1 and 4.7).

Base Plio-Pleistocene (BPLIO) reflector

The BPLIO reflector is tied to exploration wells 6710/10-1 and 6610/3-1 R2 in the south Lofoten segment to the base of the Naust Formation (Figs. 4.2 and 4.3). The seismic character of BPLIO is that of a semi-continuous and medium-amplitude intensity reflector. It was only mapped in the outer part of the margin along the study area, as the other Cenozoic reflectors/sequences are truncated towards the west side of the Utrøst Ridge or the observed fault complexes. However, in the south Lofoten segment the seismic character of the reflector is more continuous and with high-amplitude. Younger strata are observed to downlap and onlap the BPLIO reflector, thus, a local angular unconformity character is evident. In addition, this reflector represents the lower boundary of the glacial sedimentary sequence. The BPLIO is the youngest Cenozoic main reflector that was mapped in the study area.

Seismic sequence S13

Seismic sequence S13 is bounded at the base by the Base Plio-Pleistocene (BPLIO) reflector (Fig. 4.1). Sedimentary successions of the Naust Formation are mainly composing this sequence (Figs. 4.2 and 4.3). The Naust Formation consists of glacio-marine deposits of interbedded claystone, siltstone and sand, occasionally with very coarse clastics in the upper part (NPD, 2020b). In the upper part of the sequence a distinct seismic contrast is often observed and this has been interpreted as the Base Quaternary (BQ) reflector (Figs. 4.7 and 4.9). In the south of the study area, sequence S13 often lies at the top of the main Cretaceous deposits of the North Træna Basin and the Skomvær Sub-basin (Figs. 4.6 and 4.7). On the other hand, this sequence was only mapped on the Lofoten Basin in the outer part of the margin and the study area (Figs. 4.8 and 4.9). The internal configuration of the sequence is often chaotic. Sequence S13 is the youngest Cenozoic sequence that was mapped in the study area, and is bounded to the top by the seabed reflector (Sb) (Fig. 4.1).

4.4 Time-structure maps

Time structure maps were generated for each of the interpreted main horizons in order to visualize in an easier way the areal distribution of the seismic reflectors, and the time-space evolution of the structural elements within the LVM. A total of fourteen (including the seabed) time-structure maps were gridded as a means of illustrating the geological events in the study area. The time-structure maps cannot be used as a direct representation of topographical relief at the specific time intervals, as they are the result of accumulated geo-tectonic events. All these maps are restricted in their lateral distribution by topography and faults. In addition, it is not possible to confidently map reflectors in the area west of the Utrøst Ridge beneath the breakup lavas. In the inner part of the margin, the T-LJ and BCU are the most continuous horizons that generate continuous time-structure maps across the entire study area, and give a good representation of the interpreted structural elements.

4.4.1 Pre-Cretaceous

Triassic-Lower Jurassic (T-LJ) **[Fig. 4.10]**

The T-LJ time-structure map represents the deepest interpreted level in the study area. The overall impression is that all the present-day structural elements are evident, together with a northward shelf narrowing expression. NNE-SSW trending faults dominate the area of the T-LJ map. In addition, elevated structural highs can be correlated to major basement involved faults and are indicated in thicker black lines. In the Lofoten segment (LS), the Havbåen Sub-Basin (HSB) is the deepest area in the inner part of the margin. It reaches a time-depth level of ~3500 ms, and is bounded to the east by the West Lofoten Border Fault Zone (WLBFZ) to the Lofoten Ridge (LR) and to the west by the northern continuation of the Vesterdjupet Fault Zone (VFZ) to the Røst High (RH)/Utrøst Ridge (UR). Towards the north and in the proximity of the Vesterålen segment (VS), two prominent highs are found at less than ~500 ms time-depth and constitute the main inner margin physiography and shallowest time-structure levels. One of them is the Jennegga High (JH), located west of the margin and just east of the lava boundary/shelf edge. The other is a more elongated NNE-SSW striking high that extends along the eastern VS. Both structural highs delineate, respectively, two other master faults that are named the East Jennegga High Fault Zone (EJHFZ) and the Pyramiden Fault Zone (PYFZ). On the other hand, the Andøya segment (AS) represents a very narrow shelf relief with time-depth contours that abruptly drop from ~1000 ms to more than ~3000 ms, and extend gradually towards the outer margin.

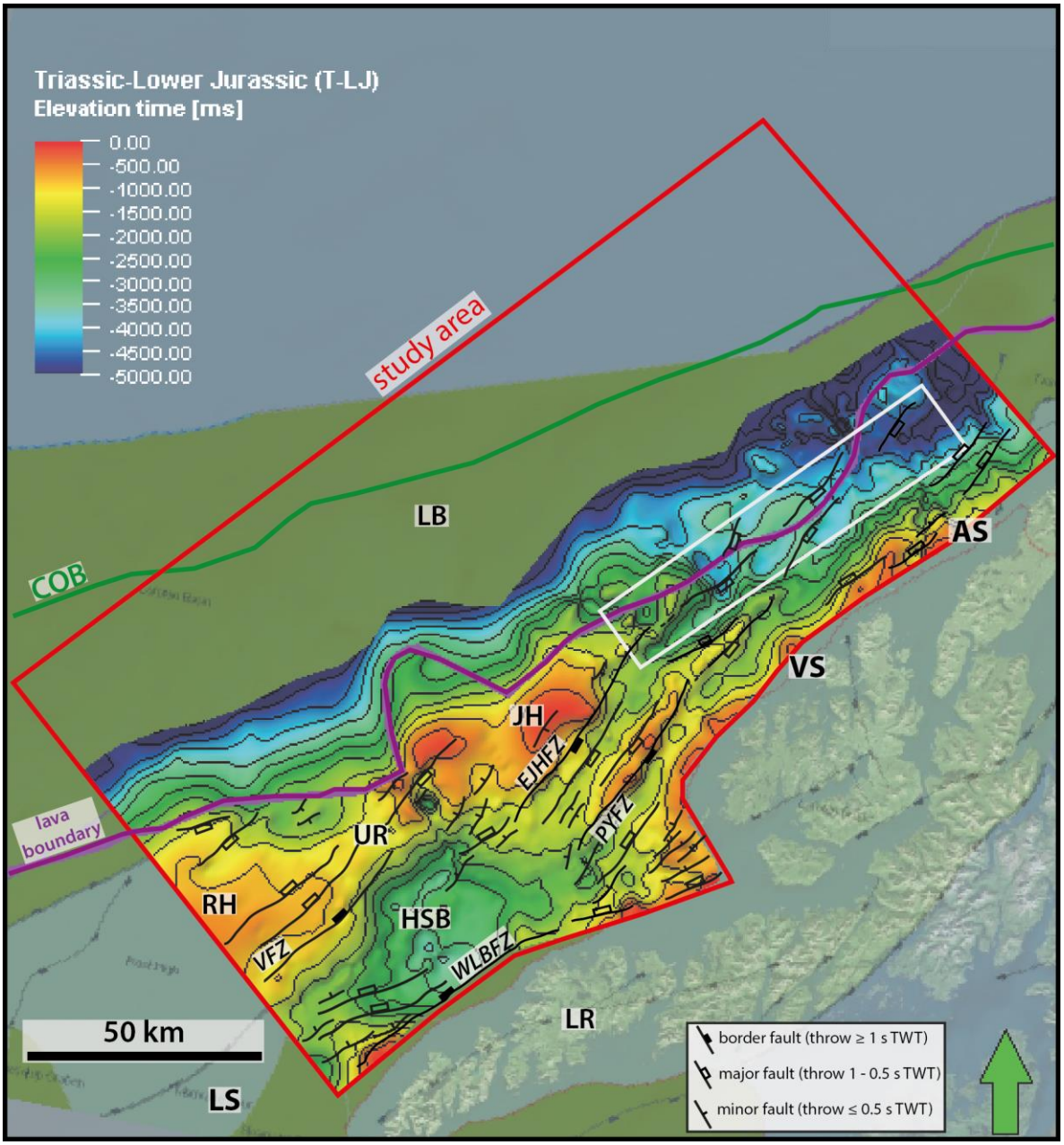

Fig 4.10: *Time-structure map of the Triassic-Lower Jurassic (T-LJ) horizon (contour interval 450 ms). All faults are displayed in black and draped above the surface. The white polygon indicates NPD-LOF1-09 3D seismic survey. The NPD structural map is included in the background for comparison. AS: Andøya segment; COB: continent-ocean boundary; EJHFZ: East Jennegga High Fault Zone; HSB: Havbåen Sub-basin; JH: Jennegga High; LB: Lofoten Basin; LS: Lofoten segment; PYFZ: Pyramiden Fault Zone; RH: Røst High; UR: Utrøst Ridge; VFZ: Vesterdjupet Fault Zone; VS: Vesterålen segment; WLBFZ: West Lofoten Border Fault Zone.*

4.4.2 Lower Cretaceous

Base Cretaceous Unconformity (BCU) **[Fig. 4.11]**

The BCU time-structure map represents the deepest Cretaceous interpreted level in the study area, and it delineates the base for the Cretaceous basins in the inner part of the LVM. In general, all the present-day structural elements are evident in the map. The generated time-structure surface differs slightly compared to that of the T-LJ time-structure map (Fig. 4.10). Hence, the main characteristics of the T-LJ map are also appreciated on the BCU map. This is possible due to reactivation of faults, and lower confidence in the T-LJ time-structure surface, as it is located at a greater depth. Still, the general NNW-SSE fault trend is also dominant in this time-structure surface. The Utrøst Ridge area appears as a slightly more continuous elevated structural element. Contour lines also differ a little, illustrating larger closures of approximately the same depth in areas of deep inner margin depocenters. Furthermore, the Jennegga High is more dominated by local-scale and frequent alteration of the contour line interval. The deepest area at around ~3200 ms time-depth is observed in the Havbåen Sub-basin, whereas the shallowest is observed at ~500 ms time-depth in the Jennegga High area. Further mapping to the west and northwest is restricted due to poor seismic resolution below the lava flows.

Intra Lower Cretaceous (ILC) **[Fig. 4.12]**

The ILC time-structure map still depicts the present-day structural elements, however, extensive erosion towards the western parts of the Utrøst Ridge become clearer. Thus, the ILC map shows a decrease in areal lateral coverage compared to the BCU map. The NNE-SSW oriented master faults that bound the major basins are still clear, together with a decreased contour interval that better defines and delimits the different structural elements. The deepest levels depicted in this map are observed within the Havbåen Sub-basin at ~2500 ms and ~3500 ms time-depths in the Andøya segment, respectively. The shallowest level of the reflector is still found in the Jennegga High at ~500 ms time-depth.

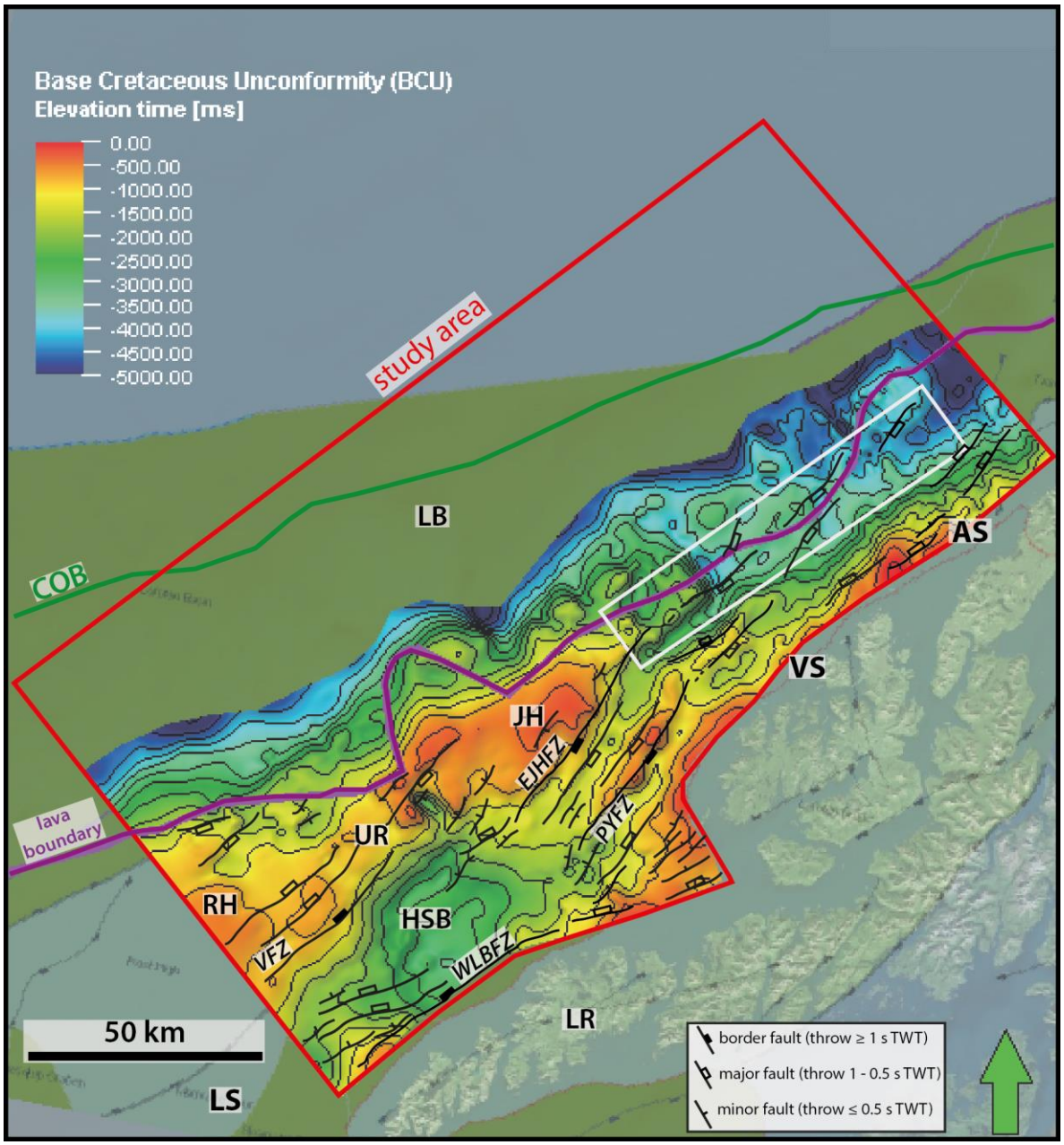

Fig 4.11: *Time-structure map of the Base Cretaceous Unconformity (BCU) horizon (contour interval 400 ms). All faults are displayed in black and draped above the surface. The NPD structural map is included in the background for comparison. Abbreviations in Fig. 4.10.*

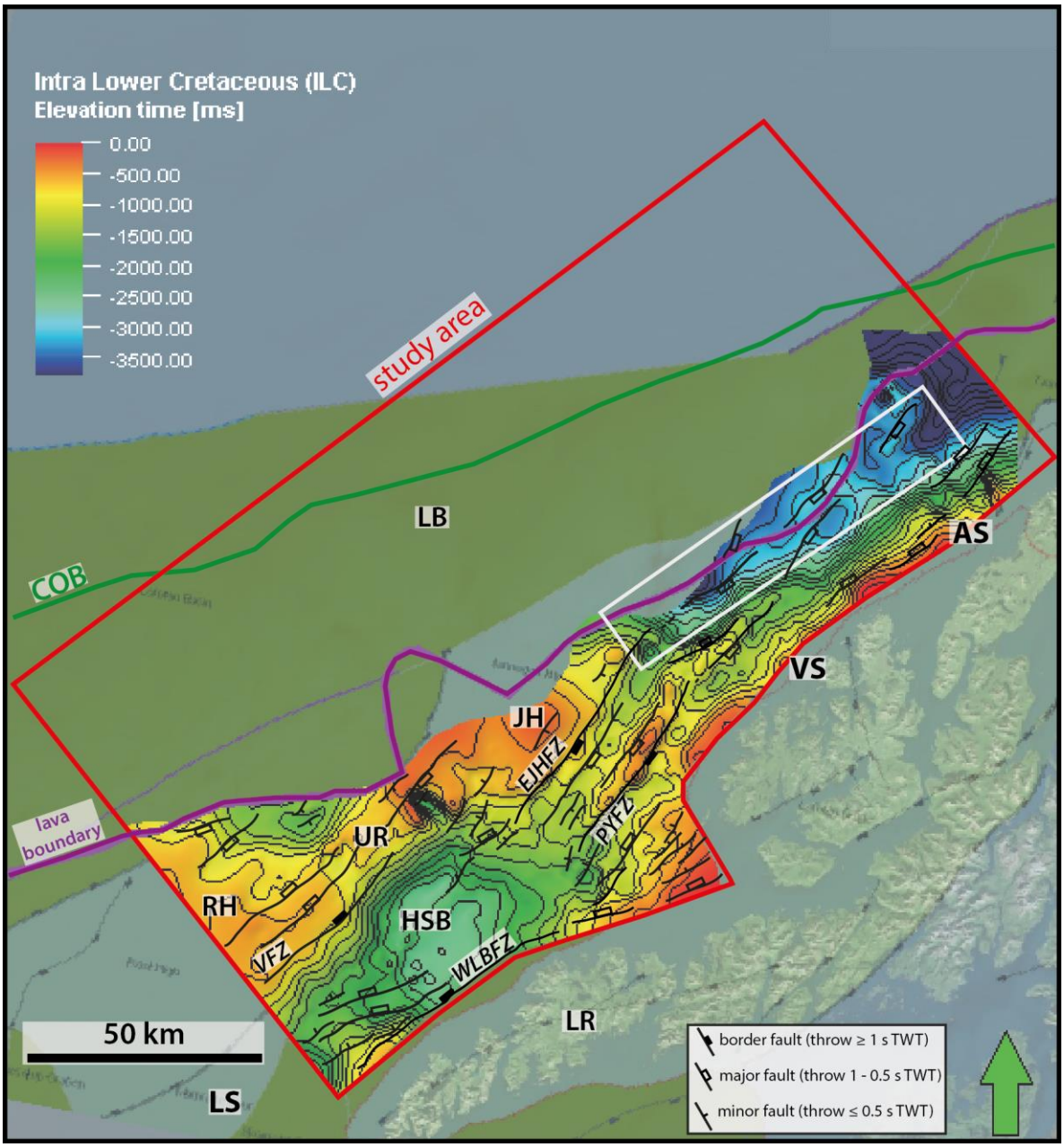

Fig 4.12: *Time-structure map of the Intra Lower Cretaceous (ILC) horizon (contour interval 200 ms). All faults are displayed in black and draped above the surface. The NPD structural map is included in the background for comparison. Abbreviations in Fig. 4.10.*

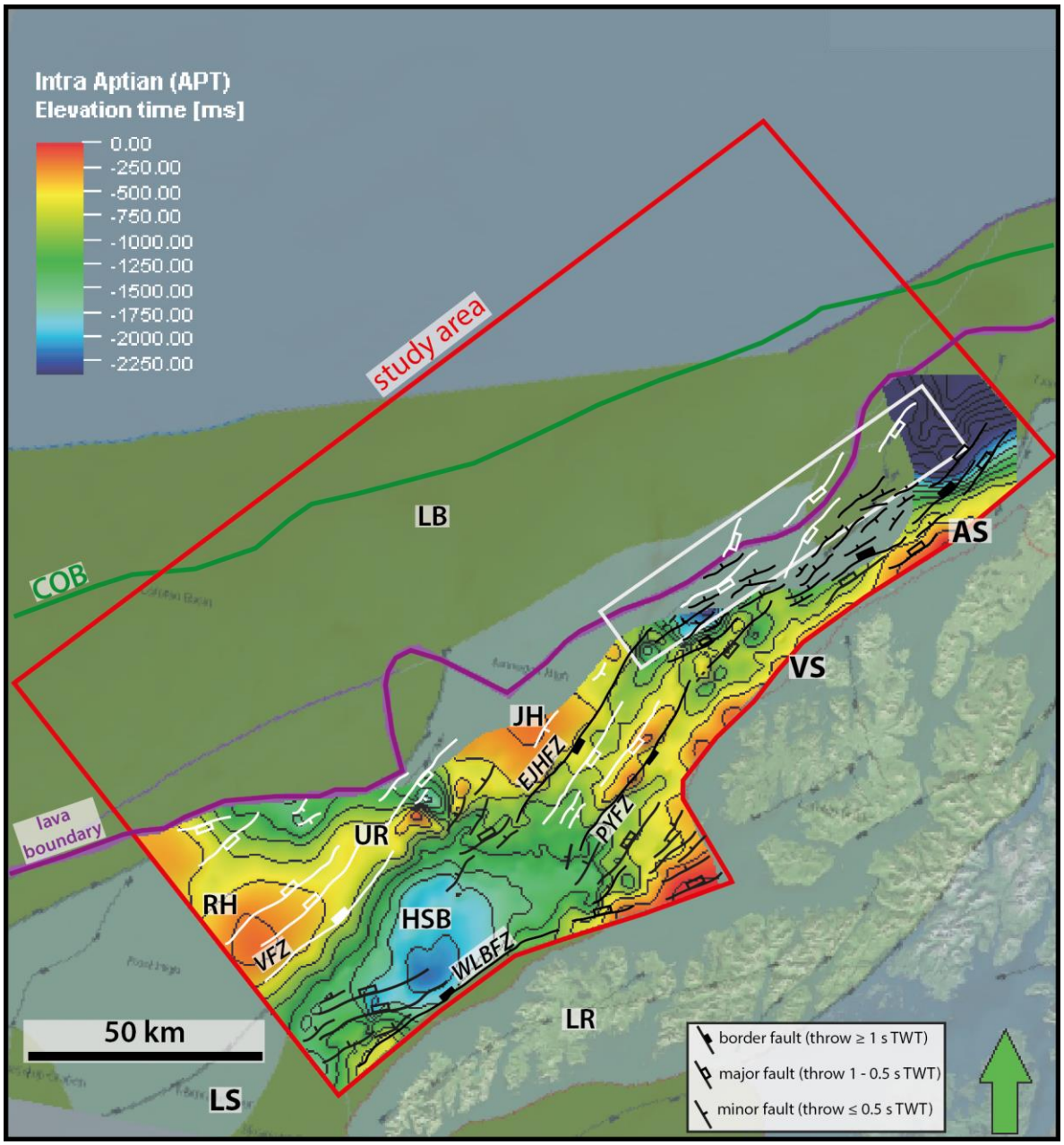

Fig 4.13: *Time-structure map of the Intra Aptian (APT) horizon (contour interval 250 ms). Faults are displayed in black. Inactive faults are in white. All faults are draped above the surface. The NPD structural map is included in the background for comparison. Abbreviations in Fig. 4.10.*

Intra Aptian (APT) **[Fig. 4.13]**

The APT time-structure map illustrates a general shallowing upwards character in the basin architecture towards mid-Cretaceous times. The margin becomes narrower and more eroded towards the north, and the interpretable part of the horizon is limited to the west by the Utrøst Ridge and the lava boundary. The same set of master and minor faults previously observed in the deepest horizons (Figs. 4.10 to 4.12) are commenced to be inactive, such as the VFZ and minor pre-Jurassic and Late Jurassic-Early Cretaceous faults. The WLBFZ still bounds the active depocenter of the Havbåen Sub-basin (~2000 ms time-depth; cf. to be shown later in subchapter 5.1). Farther north, and in particular at the north Vesterålen segment, the map is abruptly interrupted due to the activation of a new set of west-dipping faults with similar NE-SW orientation and low-angle detachment character that are detached to a common fault plane extending up to the Andøya segment.

Intra Albian (ALB) **[Fig. 4.14]**

The ALB time-structure map is more intensified than the character of the APT time-structure map (Fig. 4.13), and in general there are no major changes between them. In addition, the ALB time-structure map largely shows the present-day structural elements, as the map is further reduced in lateral extent in comparison to the APT surface/map, especially near the new and more active fault complexes in the Vesterålen and Andøya margin segments. Up to this point in time, the Havbåen Sub-Basin (~1800 ms) constitutes the largest and most important depocenter, and exhibits a rather constant extent still in mid-Cretaceous times.

4.4.3 Upper Cretaceous

Intra Cenomanian (ICEN) **[Fig. 4.15]**

The ICEN time-structure map represents the deepest Upper Cretaceous horizon mapped in the study area. Intense uplift/erosion northwards are evidenced by the lack of interpretation in the northern part of the study area, and most of the interpretation is restricted to the region of the Havbåen Sub-Basin (~1300 ms time-depth) located south of the study area. Most of the Utrøst Ridge area remains an elevated structural element, hence the ICEN horizon is more exposed to erosion. The west-dipping master fault of the WLBFZ in the Lofoten segment appears to be active, together with the faults ligated to the complexes in the northern segments. On the other hand, the east-dipping master faults (EJHFZ and PYFZ) on the Vesterålen segment have ceased in activity.

Top Turonian (TTUR) **[Fig. 4.16]**

The TTUR time-structure map illustrates the progressive uplift/erosion northwards that continued to evolve in mid-Upper Cretaceous times. Hence, the TTUR was only able to be mapped on the still active depocenter of the Havbåen Sub-basin (~1000 ms time-depth). The active faults include the WLBFZ in the Lofoten segment, together with the faults ligated to the complexes in the northern segments. The TTUR time-structure maps represents the shallowest Upper Cretaceous horizon mapped in the study area.

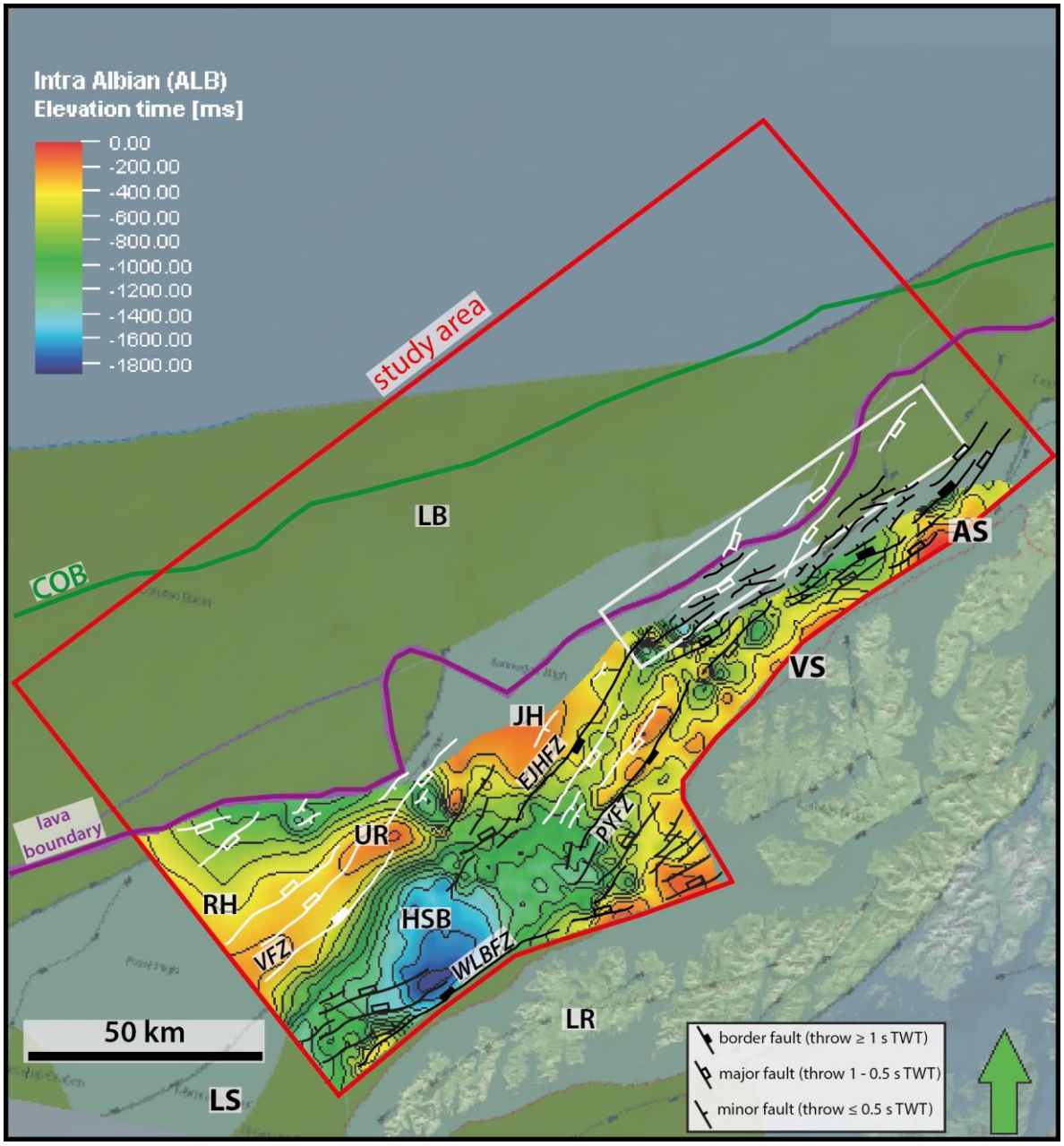

Fig 4.14: *Time-structure map of the Intra Albian (ALB) horizon (contour interval 150 ms). Faults are displayed in black. Inactive faults are in white. All faults are draped above the surface. The NPD structural map is included in the background for comparison. Abbreviations in Fig. 4.10.*

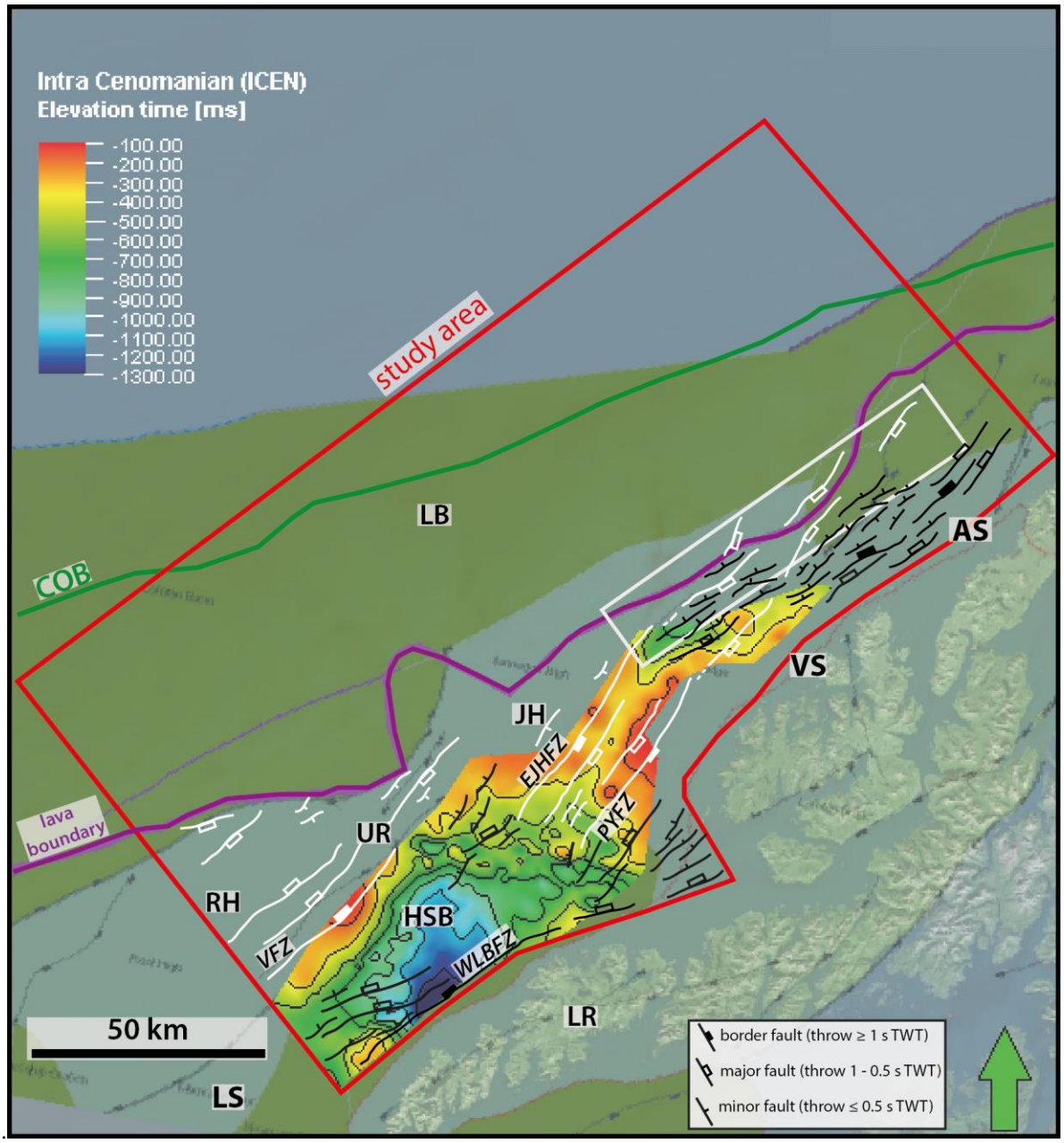

Fig 4.15: *Time-structure map of the Intra Cenomanian (ICEN) horizon (contour interval 150 ms). Faults are displayed in black. Inactive faults are in white. All faults are draped above the surface. The NPD structural map is included in the background for comparison. Abbreviations in Fig. 4.10.*

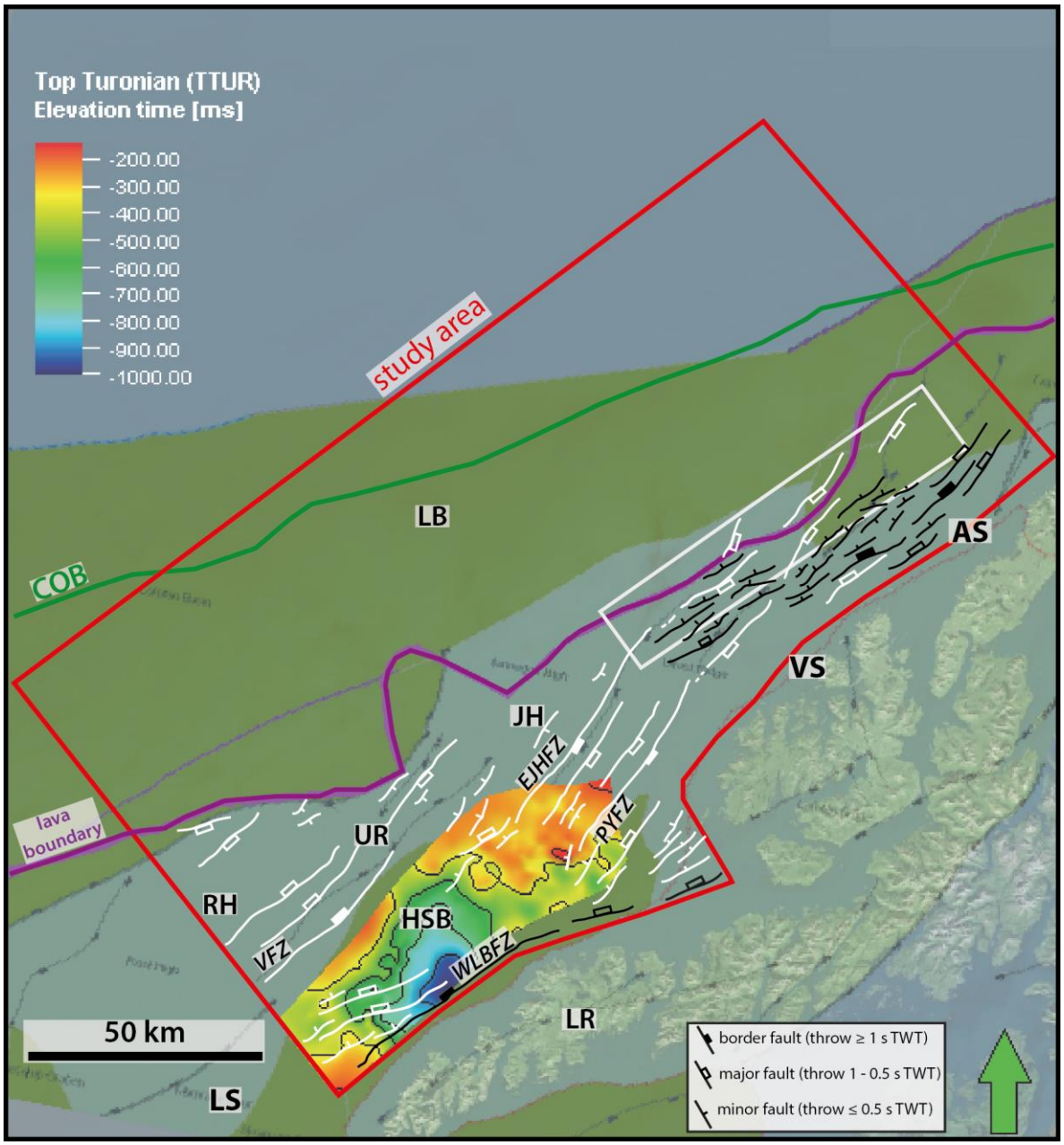

Fig 4.16: *Time-structure map of the Top Turonian (TTUR) horizon (contour interval 150 ms). Faults are displayed in black. Inactive faults are in white. All faults are draped above the surface. The NPD structural map is included in the background for comparison. Abbreviations in Fig. 4.10.*

4.4.4 Cenozoic

In general, all the Cenozoic time-structure maps are restricted to the Lofoten Basin (LB), located in the outer part of the LVM and west of the roughly NE-SW oriented landward boundary of the lava flows. Additionally, the Cenozoic time-structure maps show a semi-smooth deepening towards the northwest corner of the study area.

Base Tertiary Unconformity (BTU) **[Fig. 4.17]**

The BTU time-structure map represents the deepest Cenozoic horizon mapped in the study area. As stated earlier, most of the lateral distribution is restricted to the outer part of the margin, with the exception of the Vesterålen and Andøya segments, where some information has been gridded, in particular towards the northernmost parts. The wavy contour lines present a more or less even spacing and separation, and are indicative of a semi-smooth westward deepening trend. In addition, the margin seems to be gradually more elevated in the northern part of the study area, reaching a maximum time-elevation of ~500 ms, while the deepest area has been interpreted at more than ~6500 ms in the northwest corner. Faults located in the transition between the inner to outer margin parts are indicated to be active, in particular within the fault complex on the northern part of the LVM.

Top Paleocene (TPAL) **[Fig. 4.18]**

The TPAL time-structure map displays much more smooth contour lines than those of the BTU surface. Fault activity is again registered by this time, in particular to the eastern border of the lava boundary. Farther to the north of the study area, in the outer part of the Andøya segment, more faulting is evidenced. The new fault sets were activated during Paleocene and, in general, show the same NE-SW orientation of the older faults that have shaped the inner part of the margin. The shallowest horizon level is observed in the Jennegga High (~500 ms time-depth), whereas the deepest part is in the northwest corner of the study area (~6000 ms time-depth).

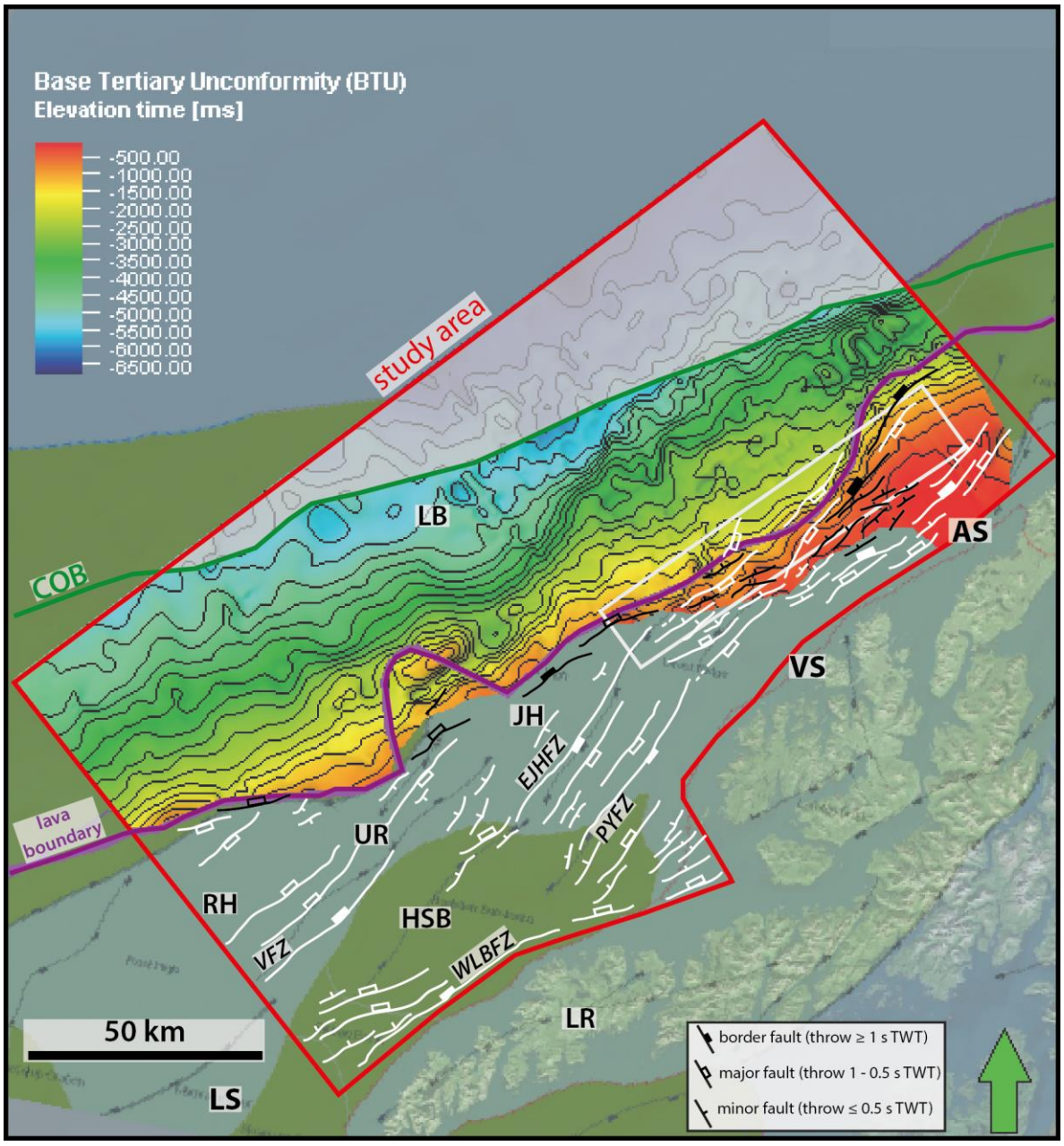

Fig 4.17: *Time-structure map of the Base Tertiary Unconformity (BTU) horizon (contour interval 300 ms). Faults are displayed in black. Inactive faults are in white. All faults are draped above the surface. The NPD structural map is included in the background for comparison. Abbreviations in Fig. 4.10.*

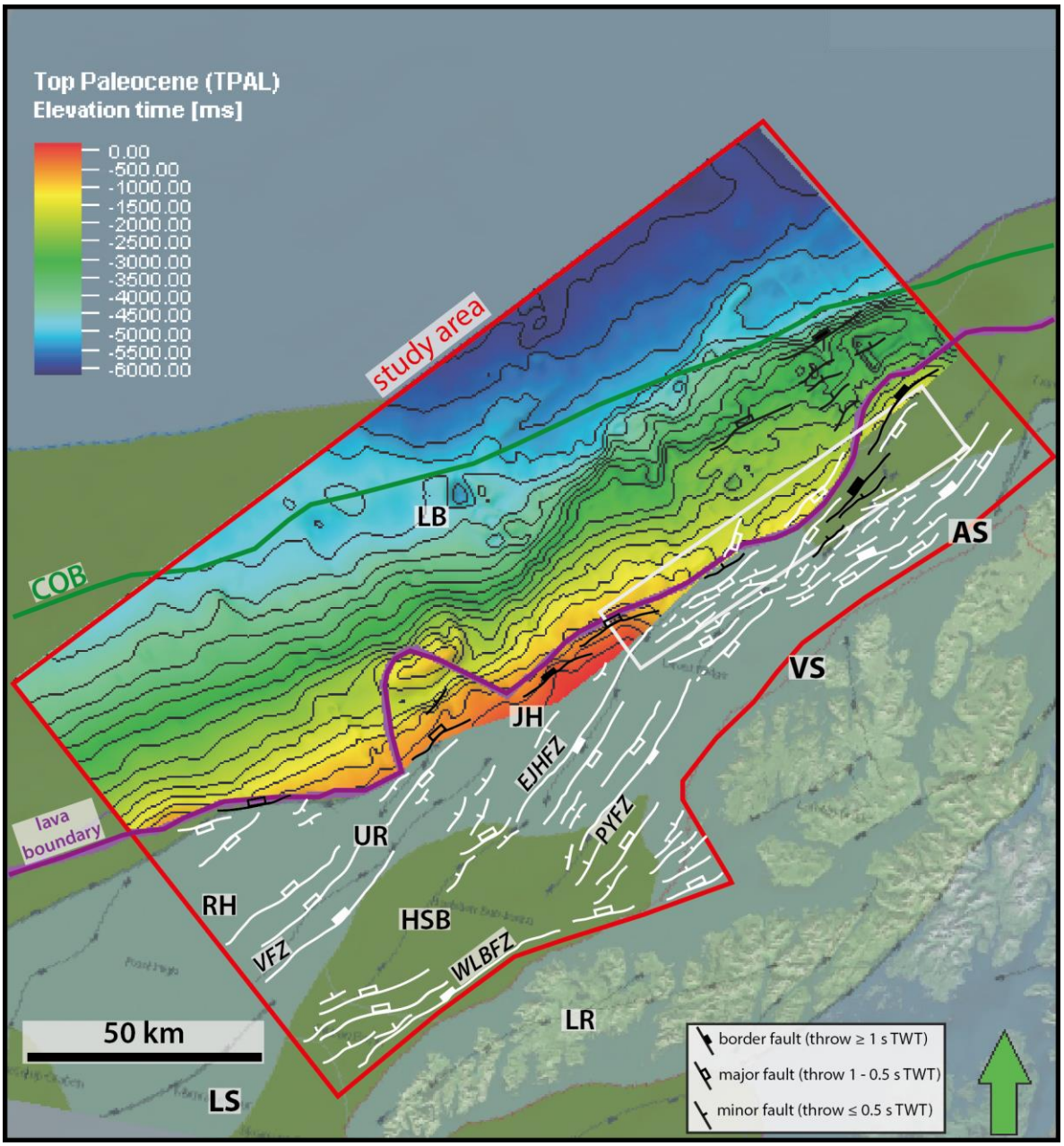

Fig 4.18: *Time-structure map of the Top Paleocene (TPAL) horizon (contour interval 300 ms). Faults are displayed in black. Inactive faults are in white. All faults are draped above the surface. The NPD structural map is included in the background for comparison. Abbreviations in Fig. 4.10.*

Top Eocene (TE) **[Fig. 4.19]**

The TE time-structure map displays an overall similar trend to that of the BTU (Fig. 4.17) and TPAL (Fig. 4.17) maps. Fault systems from Paleocene times appear to be still active. Deepening towards the northwest is still evident. However, contour lines have become very smooth and with wider closures compared to the previous Cenozoic time-structure surfaces. In addition, mapping uncertainty is increased for this horizon, as it becomes a discontinuous and weak intensity reflector towards the north. The shallowest horizon level is observed in the Jennegga High (~500 ms time-depth), whereas the deepest part is in the northwest corner of the study area (~5500 ms time-depth).

Intra Oligocene (IO) **[Fig. 4.20]**

The IO time-structure map continues to exhibit similar characteristics as the TE time-structure map (Fig. 4.19), with few faults just east of the lava boundary and the ones towards the west part of the study area interpreted to be active across the LVM. The shallowest horizon level is observed in the Jennegga High (~500 ms time-depth), whereas the deepest part is in the northwest corner of the study area (~5500 ms time-depth). A distinct canyon is indicated by the V-shaped contour lines in the continental slope of the Vesterålen segment at ~3200 ms time-depth.

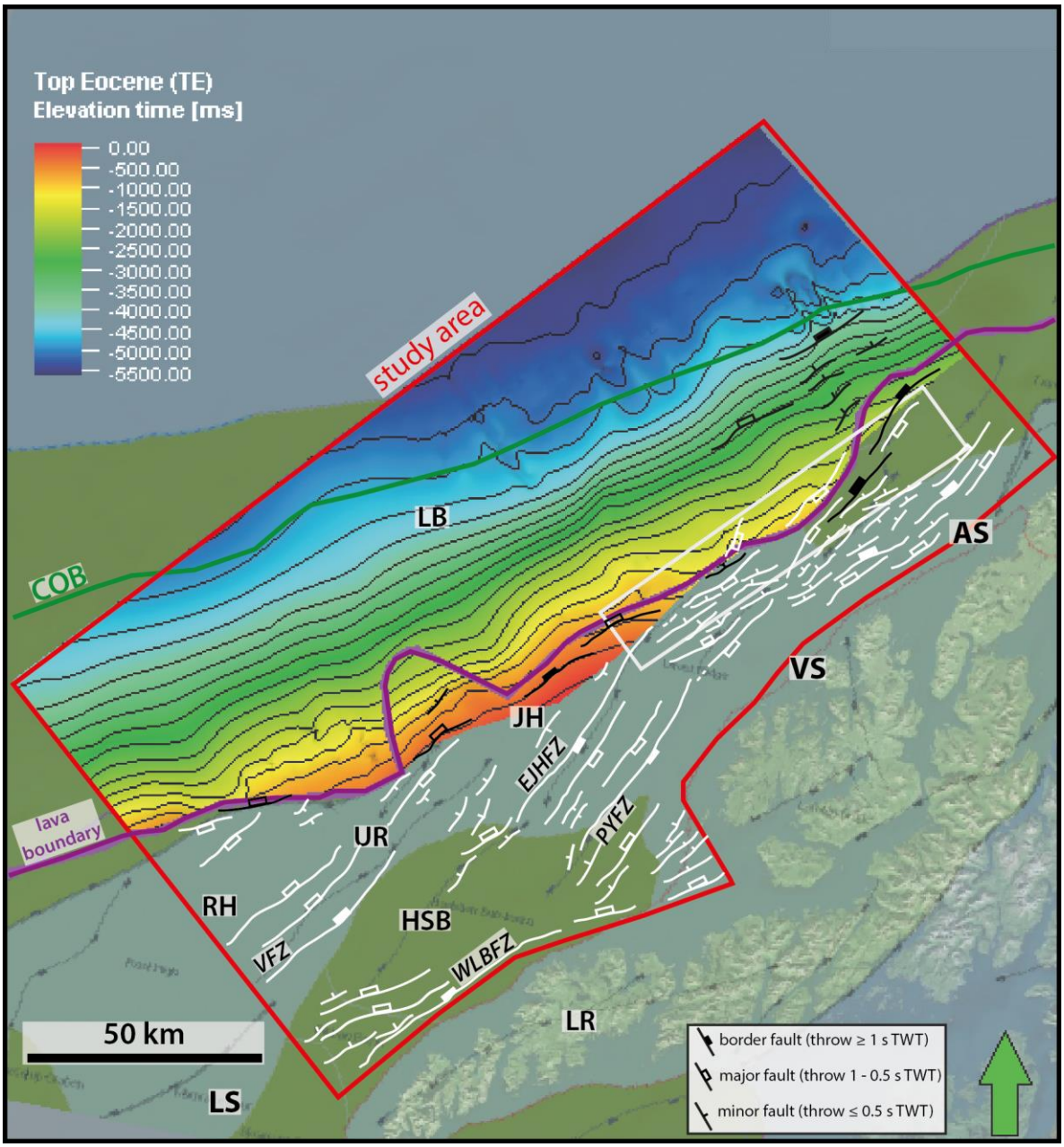

Fig 4.19: *Time-structure map of the Top Eocene (TE) horizon (contour interval 300 ms). Faults are displayed in black. Inactive faults are in white. All faults are draped above the surface. The NPD structural map is included in the background for comparison. Abbreviations in Fig. 4.10.*

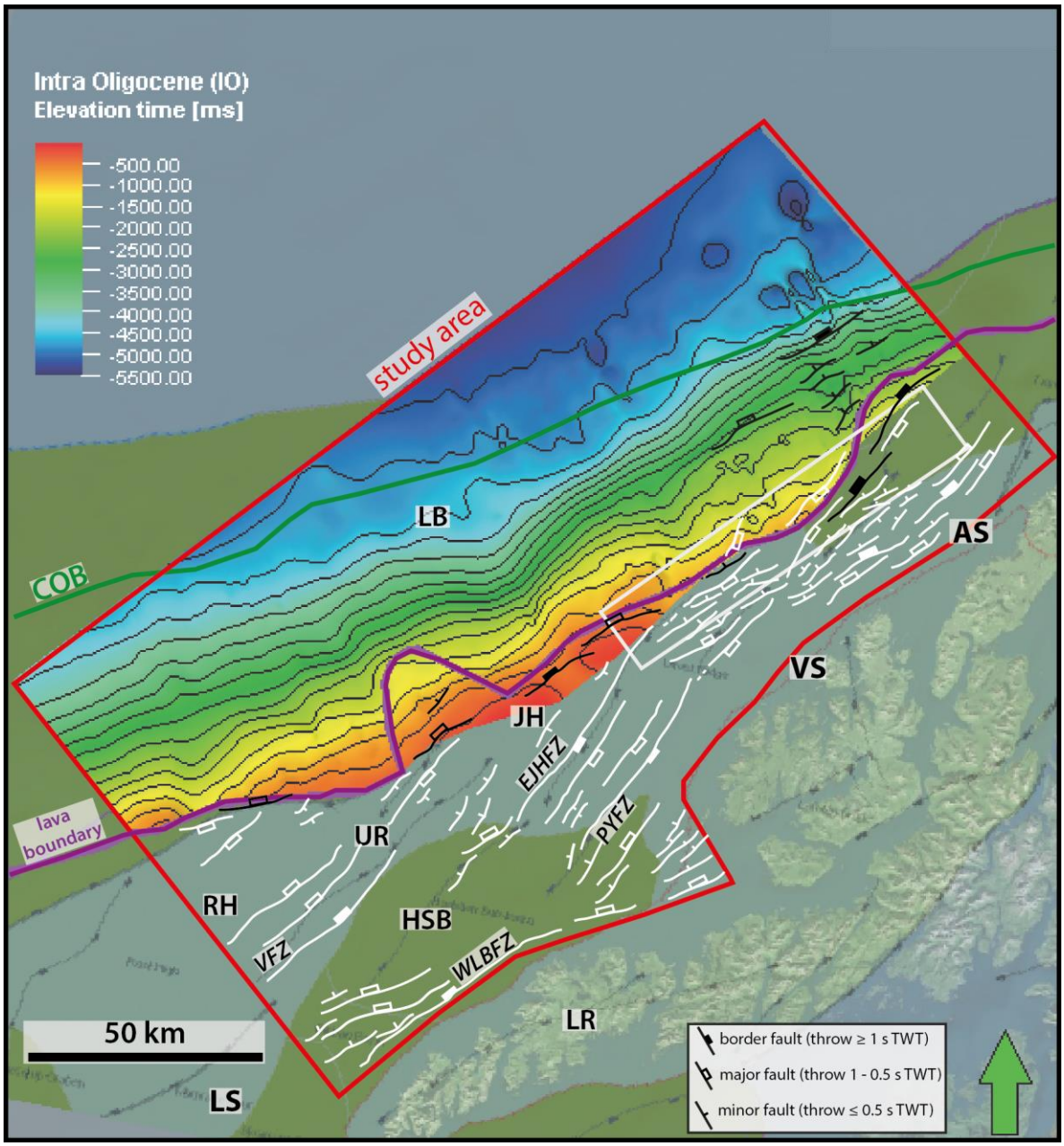

Fig 4.20: *Time-structure map of the Intra Oligocene (IO) horizon (contour interval 300 ms). Faults are displayed in black. Inactive faults are in white. All faults are draped above the surface. The NPD structural map is included in the background for comparison. Abbreviations in Fig. 4.10.*

Intra Miocene (IM) **[Fig. 4.21]**

The IM time-structure map exhibits similar characteristics as the IO time-structure map (Fig. 4.20). Both faults just east of the lava boundary and the ones towards the western part of the margin are interpreted to be the only ones active. The shallowest horizon level is observed in the Jennegga High (~500 ms time-depth), whereas the deepest part is in the northwest corner of the study area (~5000 ms time-depth). In addition, V-shaped contours towards the Lofoten segment become more apparent at ~3000 ms time-depth.

Base Plio-Pleistocene (BPLIO) **[Fig. 4.22]**

The BPLIO time-structure map exhibits similar characteristics as the IM time-structure map (Fig. 4.21). Active faults are interpreted to be just in the northwestern part of the study area. The shallowest horizon level is observed in the Jennegga High (~500 ms time-depth), whereas the deepest part is in the northwest corner of the study area (~4500 ms time-depth). In addition, the V-shaped contours become more apparent in the entire continental slope at ~2700 ms time-depth. The BPLIO represents the uppermost Cenozoic horizon interpreted in this study.

Seabed (Sb) **[Fig. 4.23]**

The time-structure map represents the present-day seafloor bathymetry (in TWT) of the studied LVM area. An interest feature to notice is the set of submarine canyons that are disposed into the entire continental slope, and may be connected to the inner parts of the shelf, as seen, for example on the Vesterålen segment. These are related to the last glaciation event during Plio-Pleistocene and they continue to develop until present time (Faleide et al., 2015).

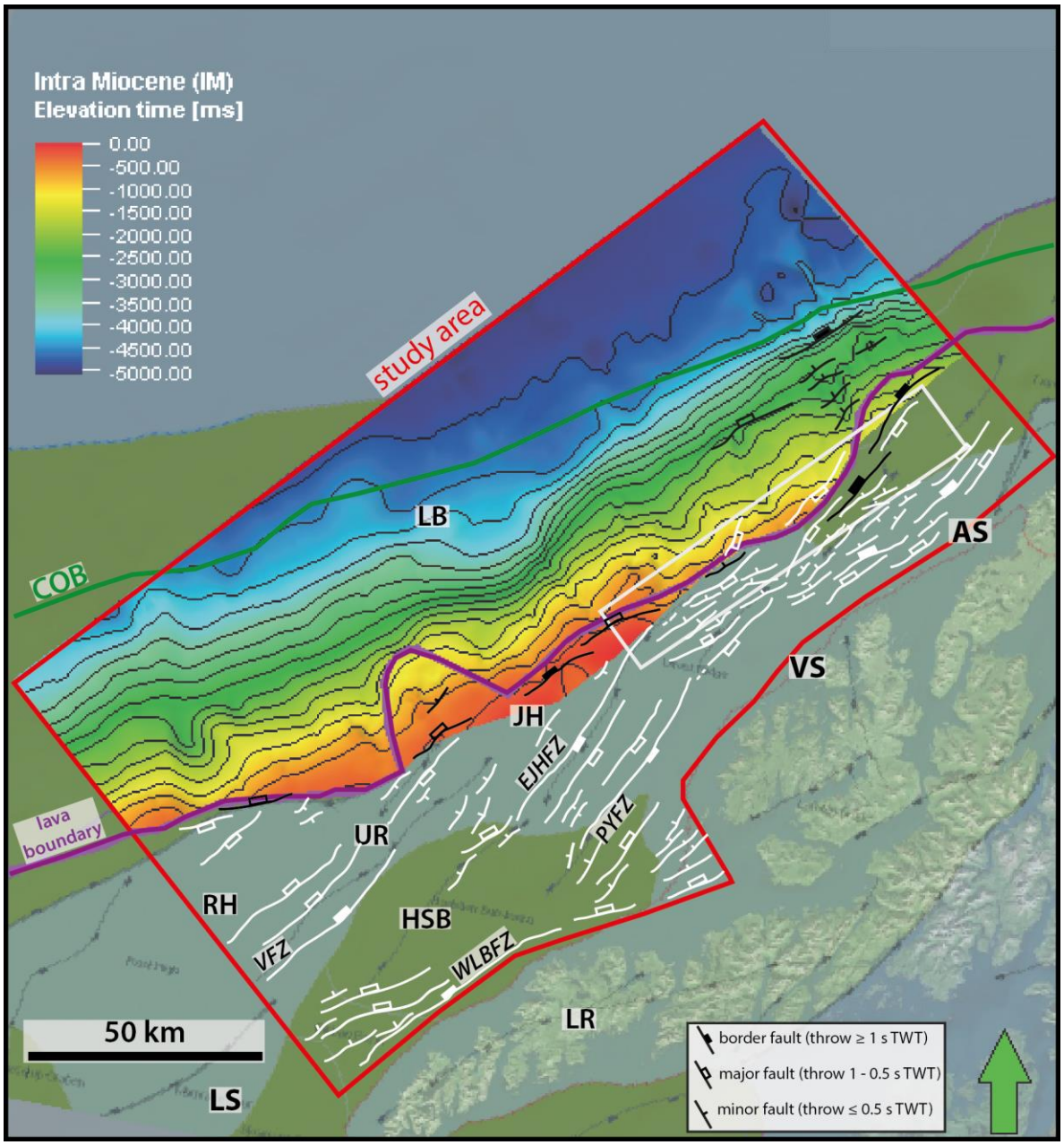

Fig 4.21: *Time-structure map of the Intra Miocene (IM) horizon (contour interval 300 ms). Faults are displayed in black. Inactive faults are in white. All faults are draped above the surface. The NPD structural map is included in the background for comparison. Abbreviations in Fig. 4.10.*

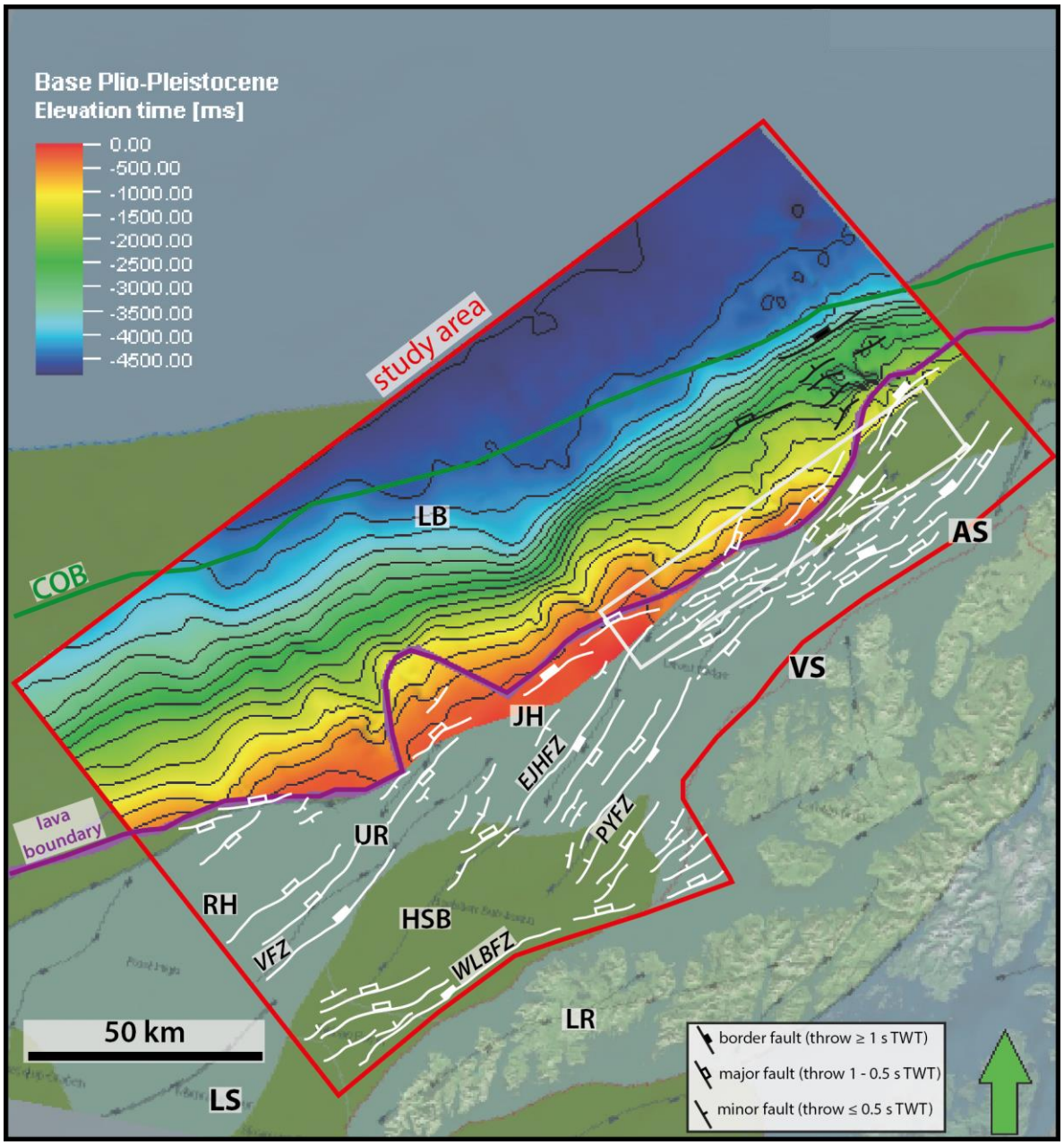

Fig 4.22: *Time-structure map of the Base Plio-Pleistocene (BPLIO) horizon (contour interval 300 ms). Faults are displayed in black. Inactive faults are in white. All faults are draped above the surface. The NPD structural map is included in the background for comparison. Abbreviations in Fig. 4.10.*

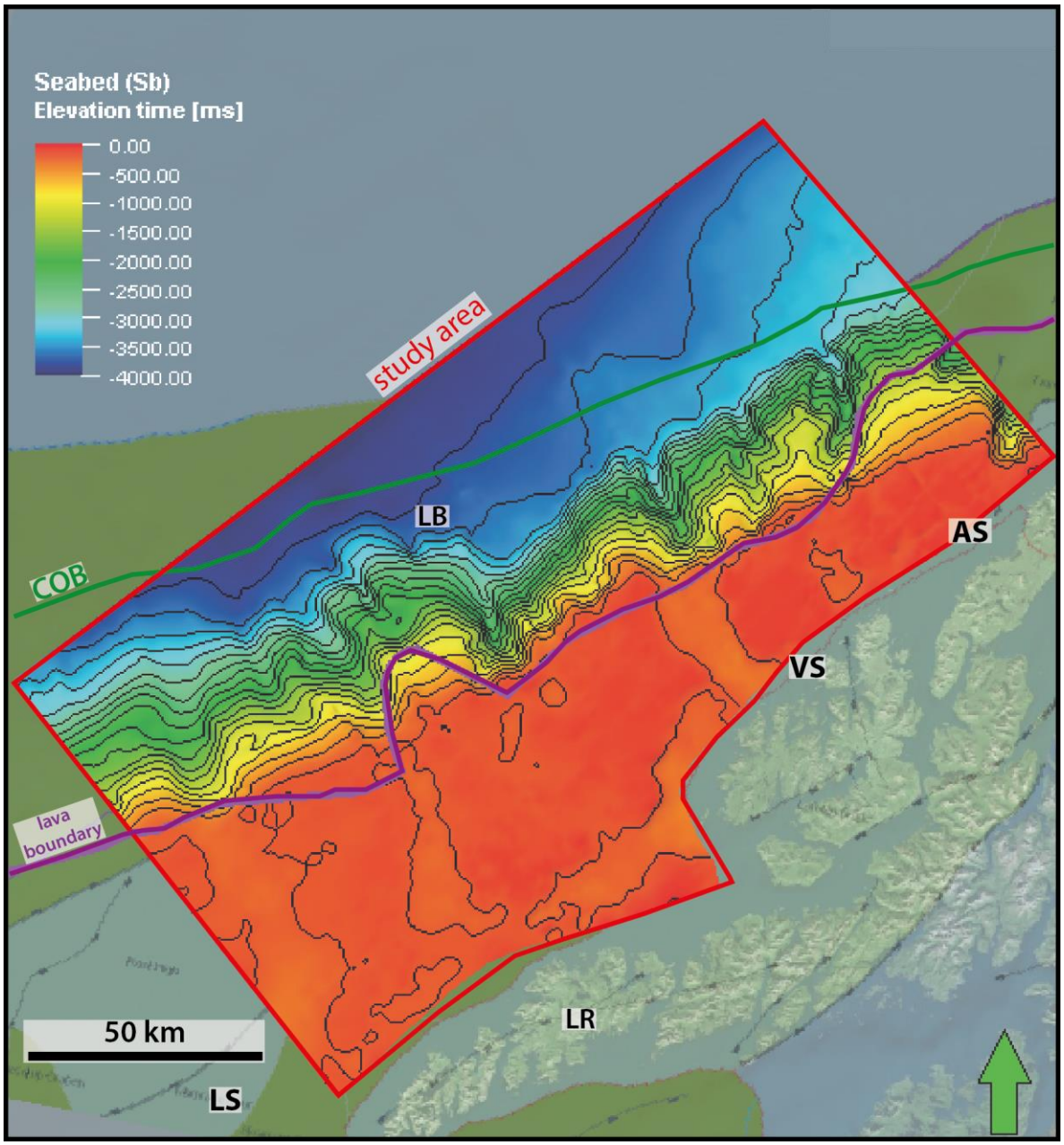

Fig 4.23: *Time-structure map of the Seabed (Sb) horizon (contour interval 200 ms). The NPD structural map is included in the background for comparison. Abbreviations in Fig. 4.10.*

4.5 New and refined structural elements

On the basis of seismic and potential field data integration, new and better refined structural elements have been mapped within the study area and are described below.

Jennegga High

The Jennegga High (JH) is a basement high located in the northeast part of the Utrøst Ridge, near the landward breakup lava boundary. It was first described by Blystad et al. (1995) on the basis of seismic data, and defined as an elevated structural high during Early Cretaceous revealed by onlapping Lower Cretaceous sediments. The Jennegga High remained an elevated structural element also during the latest Cretaceous-earliest Tertiary and is related to the tectonic activity accompanying the opening of the Norwegian Sea. Subsequent studies (e.g. Tsikalas et al., 2001; Hansen et al., 2012) have highlighted the role of the Jennegga High area on various margin segmentation models within the LVM. In this study, the Jennegga High is better defined in its areal extent towards north (Fig. 4.25), and it appears to coincide with a strong positive anomaly in both gravity and magnetic data (Fig. 4. 26), and it is further refined in seismic data due to the abrupt elevation changes of the Base Cretaceous Unconformity (BCU) (Fig. 4.24). The eastern flank of the high is bounded by a curvilinear fault zone here termed the East Jennegga High Fault Zone (EJHFZ), and which is found as NNE-SSW trending and E-dipping border fault along the Vesterålen margin segment (VS) (Fig. 4.11). Towards the transition of the Lofoten and Vesterålen margin segments, the Jennegga High is observed to be fairly buried in depth and a low-angle detachment fault complex appears to develop in the west (Fig. 4.24). This area, thus, may represent a distinct tectono-sedimentary shift in basin architecture (Fig. 4.25).

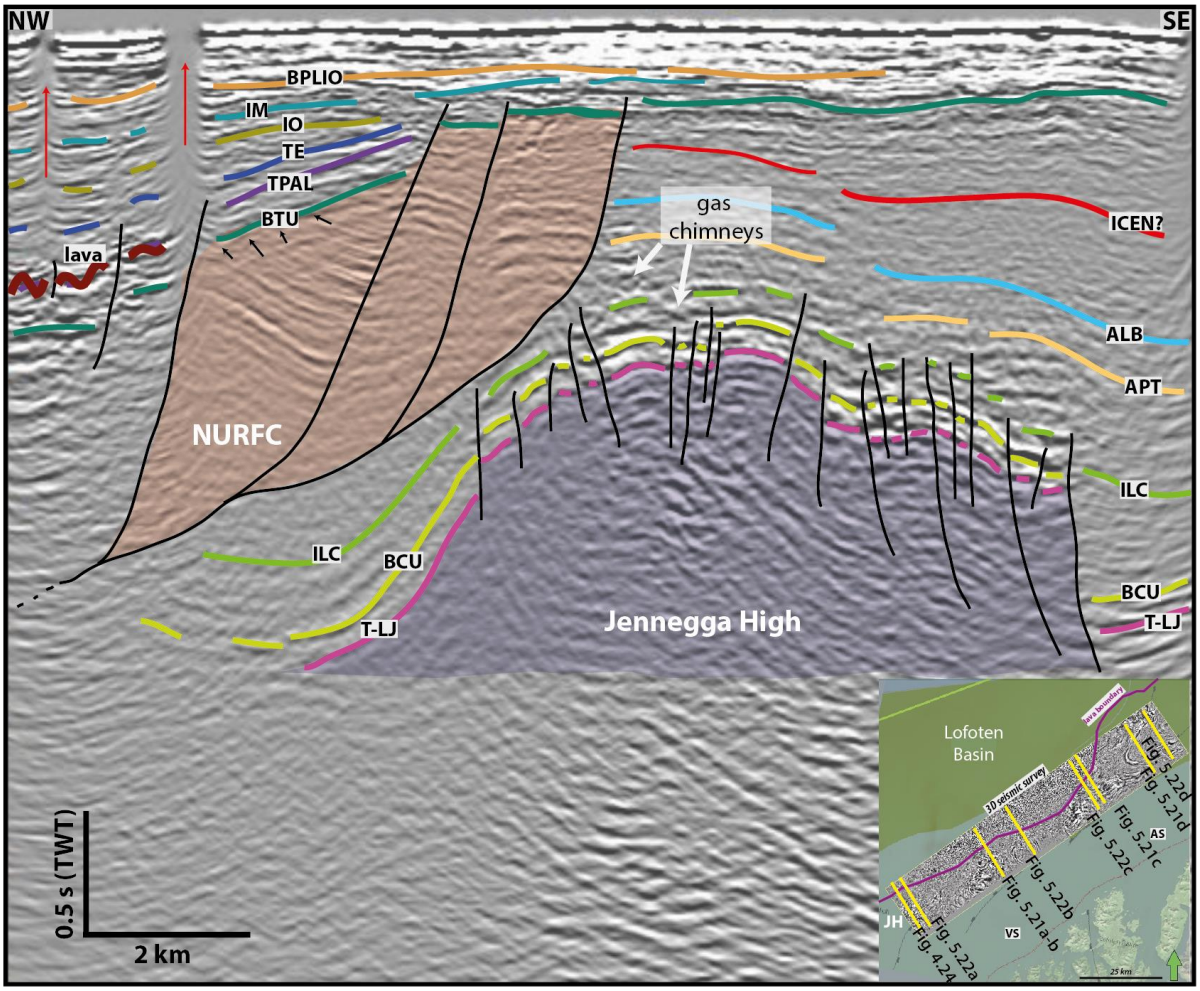

Fig 4.24: *Seismic profile example (x-line 2000, NPD-LOF1-09 3D seismic survey) of the Jennegga High (JH). Note initiation of the North Utrøst Ridge Fault Complex (NURFC) just on top of the JH. Black arrows within the NURFC indicate toplap/truncation of undifferentiated Cretaceous units onto the Base Tertiary Unconformity (BTU). Red arrows indicate venting events. Profile location on inset map. Abbreviations in Table 4.1.*

Myre High

The Myre High (MH) is a new structural element informally named in this study, located just north of the Utrøst Ridge/Jennegga High (Figs. 4.26-b and 5.18). Initially, mapping of the Base Cretaceous Unconformity (BCU) on the westernmost areas of the Vesterålen margin segment indicated a buried, but distinct structural element with a fault plane bordering its eastern flank, where Jurassic and Lower Cretaceous seismic units were observed to onlap onto. Further potential field data integration, utilising mainly the magnetic anomaly map, showed a strong positive anomaly north of the Jennegga High (Fig. 4.26-b). The geometry and areal distribution of the Myre High on the magnetic anomaly map may be interpreted to be the northward continuation of the Utrøst Ridge. However, seismic interpretation suggests that the Myre High is an individual structural element separated from the Jennegga High (Fig.

5.18). Furthermore, an apparent NW-SE trending divider line where there is a very small shift in the magnetic anomaly is traced between the Jennegga and Myre highs, and can be extended towards the Vesterålen islands. This is interpreted as an accommodation/transfer zone; the Vesterålen transfer zone (cf. Figs. 5.18 and 5.19 and discussion below).

Vesterålen High

The Vesterålen High (VH) is a refined structural element, and informally named in this study. It was interpreted in early publications (e.g. Løseth and Tveten, 1996; Tsikalas et al., 2001) as a prominent fault-block rotated up to ~15° to the west, and extending ~70 km along the Vesterålen margin segment (Fig. 4.25). It is bounded on the eastern flank by a basement-involved, NNE-trending and E-dipping listric fault zone termed by Hansen et al. (2012) as the Pyramiden Fault Zone (PYFZ) (Figs. 4.9, 4.27, 5.17-3, 5.18-4 and 5.18-5). This fault zone is characterized by having a syn-sedimentary faulting character associated to the Late Jurassic-Early Cretaceous rift event on the LVM (Løseth and Tveten, 1996; this study). On seismic data, the VH is clearly observed as a pyramid shape-like, and intra-basin elevated horst where Jurassic and Cretaceous seismic units onlap onto both of its eastern and western flanks (Fig. 4.27). In this study, this element is better defined in its areal extent towards the north of the margin (Fig. 4.25), and it appears to coincide with a strong positive and elongated anomaly in both gravity and magnetic data (Fig. 4.26). Furthermore, structural segmentation within this high is observed, and this may be related to burial as seen on the gravity map (Fig. 4.26-a), and/or by a possible transfer fault that slightly offsetting this high (Fig. 4.25, 4.26). Note that the segmentation occurs at a local gravity and magnetic anomaly shift at a NW-SE trending area extended to the zone of apparent division between the Myre and Jennegga highs (Fig. 4.26).

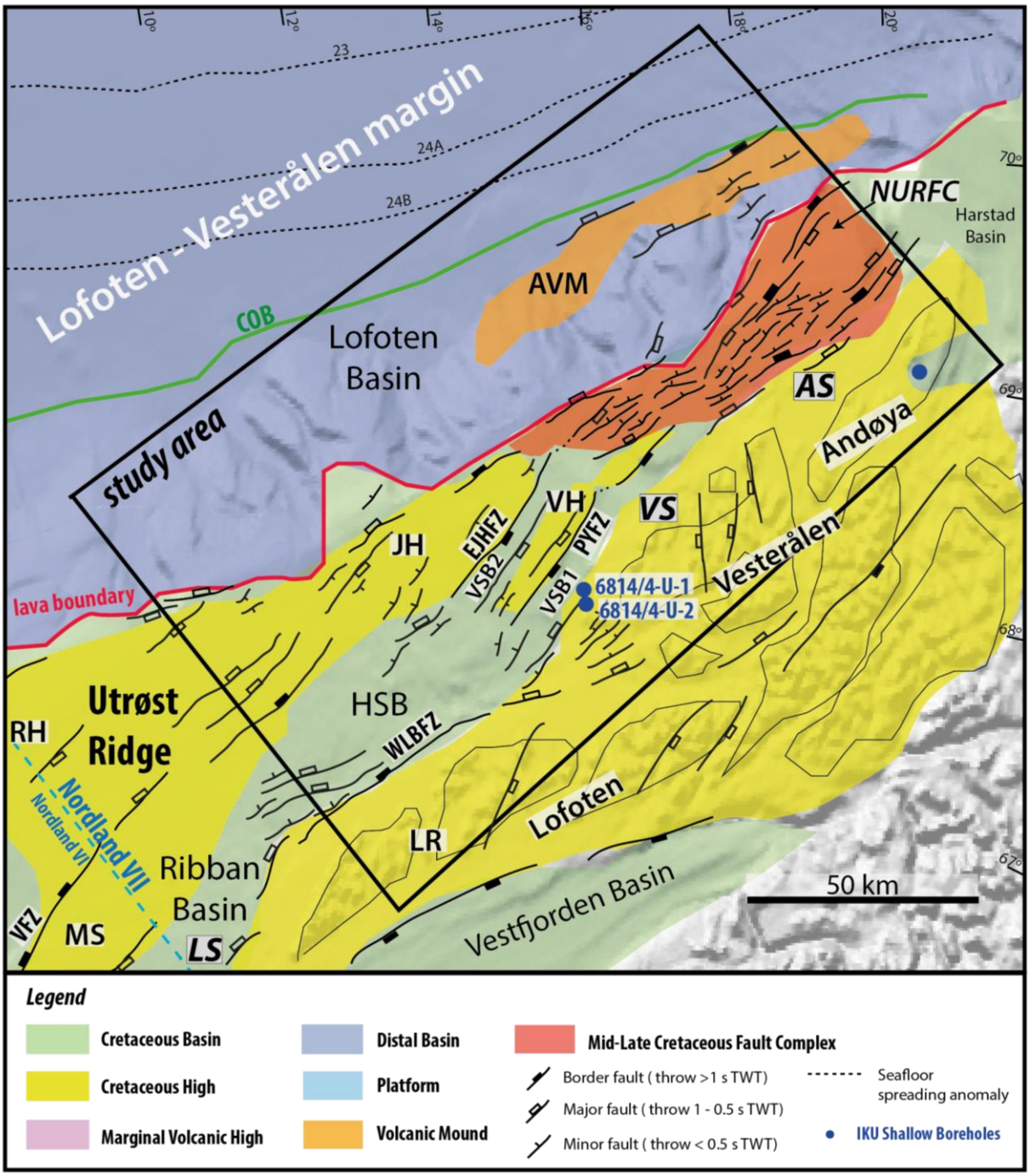

Fig 4.25: *Structural map indicating the location and extent of the new and refined structural elements of this study. AVM: Andøya Volcanic Mound; NURFC: North Utrøst Ridge Fault Complex; VSB1: Vesterålen Sub-basin 1; VSB2: Vesterålen Sub-basin 2. Other abbreviations in Fig. 4.10.*

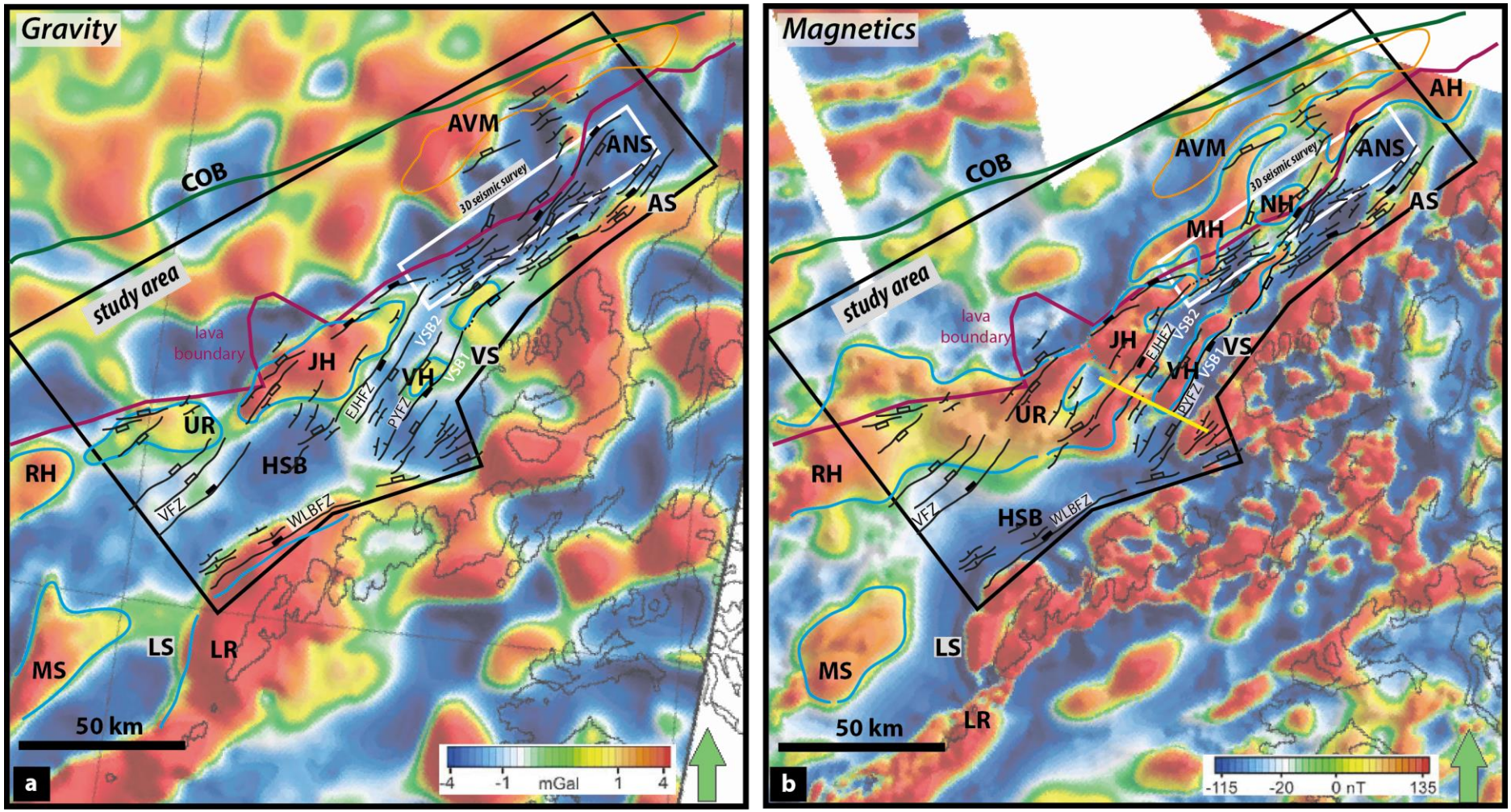

Fig 4.26: *Potential field anomaly data with interpreted faults, and new and refined structural elements of this study. Structural highs on Base Cretaceous Unconformity (BCU) level are indicated in blue outline. Note how major faults coincide at the edges of strong positive anomalies. White polygon indicates the NPD-LOF1-09 3D seismic survey.* ***(a)*** *50 km high-pass filtered gravity anomaly.* ***(b)*** *50 km high-pass filtered magnetic anomaly. Yellow line indicates profile location on Fig. 4.27. Gravity and magnetic data courtesy of TGS. AH: Andenes High; ANS: Andøya Syncline; MH: Myre High; NH: Nøss High. Other abbreviations in Figs. 3.1 and 4.10.*

Vesterålen Sub-basins 1 and 2

The Vesterålen Sub-basins 1 and 2 (VSB1 and VSB2) are new sub-basins informally named in this study. They are the narrow and elongated depocenters locally found to the east and west of the Vesterålen High (VH), respectively, and represent the northern continuation of the Havbåen Sub-basin (Fig. 4.25). The two sub-basins exhibit wedge-shaped sediment layers in the seismic data with the thickest parts in the central part of the sub-basins and gradual thinning towards the crests of the VH (Fig. 4.27). Thickness variations across fault planes of the EJHFZ and PYFZ, demonstrate the syn-tectonic sedimentation during the Late Jurassic-Early Cretaceous rifting. The VB1 and VB2 are further correlated with strong negative anomalies in both the gravity and magnetic data (Figs. 4.26 and 4.27).

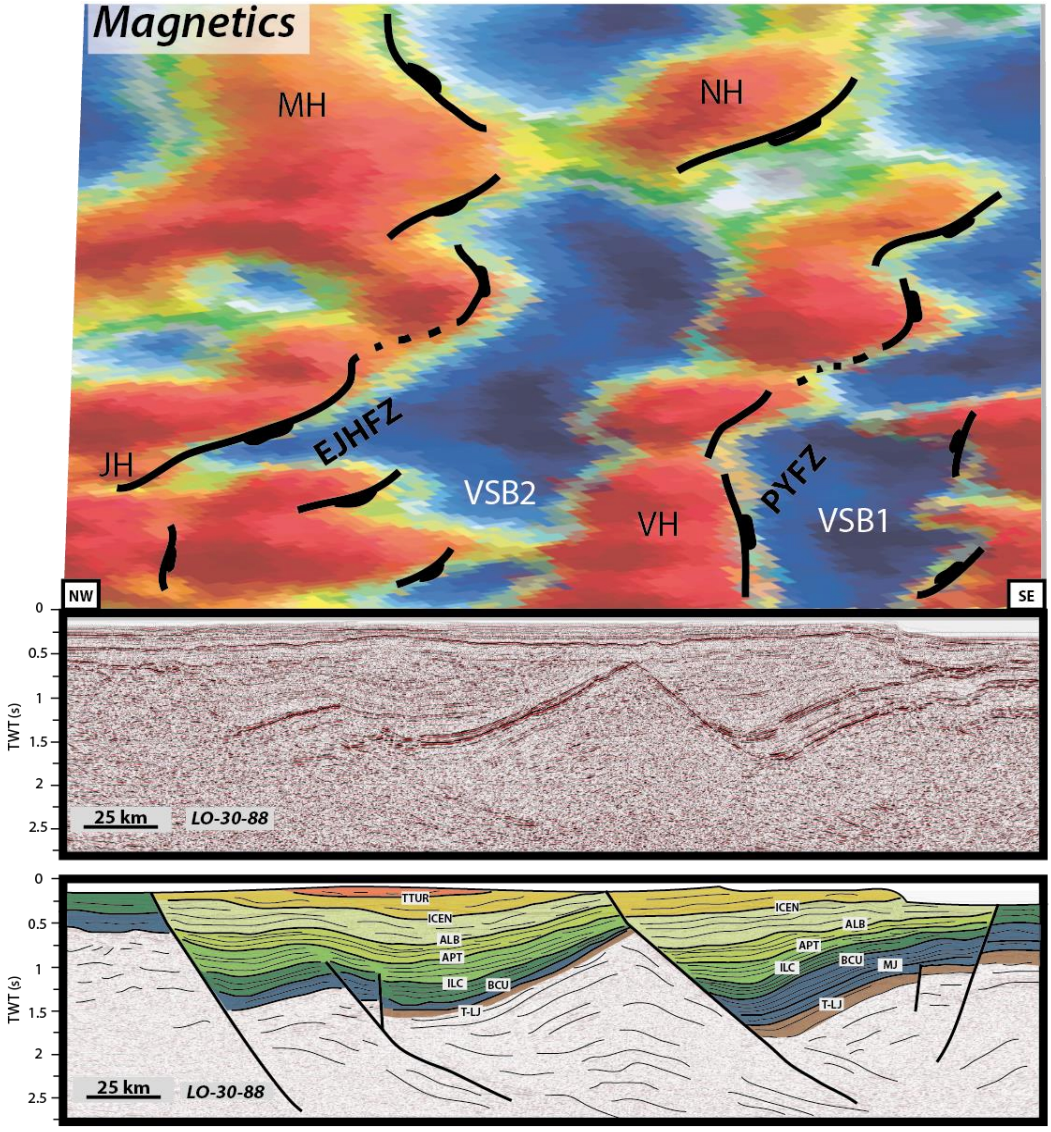

Fig 4.27: *Magnetic anomaly map and seismic data integration example. The structural highs are correlated with strong positive anomalies, while the basins with strong negative anomalies. Profile location in Fig. 4.26. Colour scale and abbreviations as in Figs. 3.1, 4.26 and 4.6.*

North Utrøst Ridge Fault Complex

Prominent and intense faulting is observed along the northern part of the LVM (Fig. 4.25). There, we define a new structural element that is informally named in this study, as North Utrøst Ridge Fault Complex (NURFC). The existence of a fault complex was earlier indicated in the area (Blystad et al., 1995; Tsikalas et al., 2001; Hansen et al., 2012). However, in this study the NPD-LOF1-09 3D seismic survey is used for the first time to properly study the NURFC. Therefore, in light of the observations of this study, the NURFC is more properly defined on the basis of detailed seismic interpretation. Note that both gravity and magnetic anomaly maps illustrate NURFC as strong negative anomalies (Fig. 4.26) and this is in accordance with the large thickness of sediments involved in the fault complex and the equivalent burial of basement at large depths. The NURFC is mainly characterized by NE-SW trending and W-dipping faults that extend across the Vesterålen margin segment for less than ~7 km, and more than ~25 km towards the northeast of the Andøya margin segment (Fig. 4.25).

Nøss High

The Nøss High (NH) is a new and informally named basement high defined in this study, located NE of the Myre High (MH) (Fig. 4.26-b). Mapping of the Base Cretaceous Unconformity (BCU) led to observations of a prominent but deeply buried horst beneath the North Utrøst Ridge Fault Complex (NURFC). Jurassic and Lower Cretaceous seismic units are also observed to be truncated by a fault plane bordering the eastern flank of this high (Fig. 4.26-b). The gravity anomaly map does not show presence of a high due to the thick sedimentary cover (Fig. 4.26-a). The magnetic anomaly map, on the other hand, correlates the Nøss High with a strong positive anomaly (Fig. 4.26-b).

Andenes High

The Andenes High (AH) is a new and informally named basement high defined in this study, located in the northwestern part of the Andøya margin segment close to the landward breakup lava boundary (Fig. 4.26-b). Mapping of the Base Cretaceous Unconformity (BCU) led to observations of a prominent but buried horst beneath the North Utrøst Ridge Fault Complex (NURFC). Due to the extensive and thick sedimentary cover, the Andenes High is further correlated with a strong positive anomaly on the magnetic anomaly map (Fig. 4.26b). The Andenes High is often observed intruded in the west by sills that may conform to a volcanic complex termed here the Andøya Volcanic Mound (AVM) (Fig. 4.26).

Andøya Syncline

The Andøya Syncline (ANS) is a new and informally named depocenter defined in this study, located in the northwestern part of the Andøya margin segment (Fig. 4.28). It is a narrow basin between the Andenes High and the basement structure on the Andøya island that may represent the southernmost part of the Harstad Basin (Fig. 4.25). The Andøya Syncline is filled with Jurassic and Lower Cretaceous seismic units affected by Late Jurassic-Early Cretaceous rifting. High rates of subsidence may be responsible for the narrow character of the evolved depocenter. The Andøya Syncline is observed in both vintage 2D and the new 3D (NPD-LOF1-09) seismic datasets (Figs. 4.9, 4.28), as well as in both gravity and magnetic anomaly maps that indicate an area of strong negative anomalies beneath the North Utrøst Ridge Fault Complex (NURFC; Fig. 4.26-b).

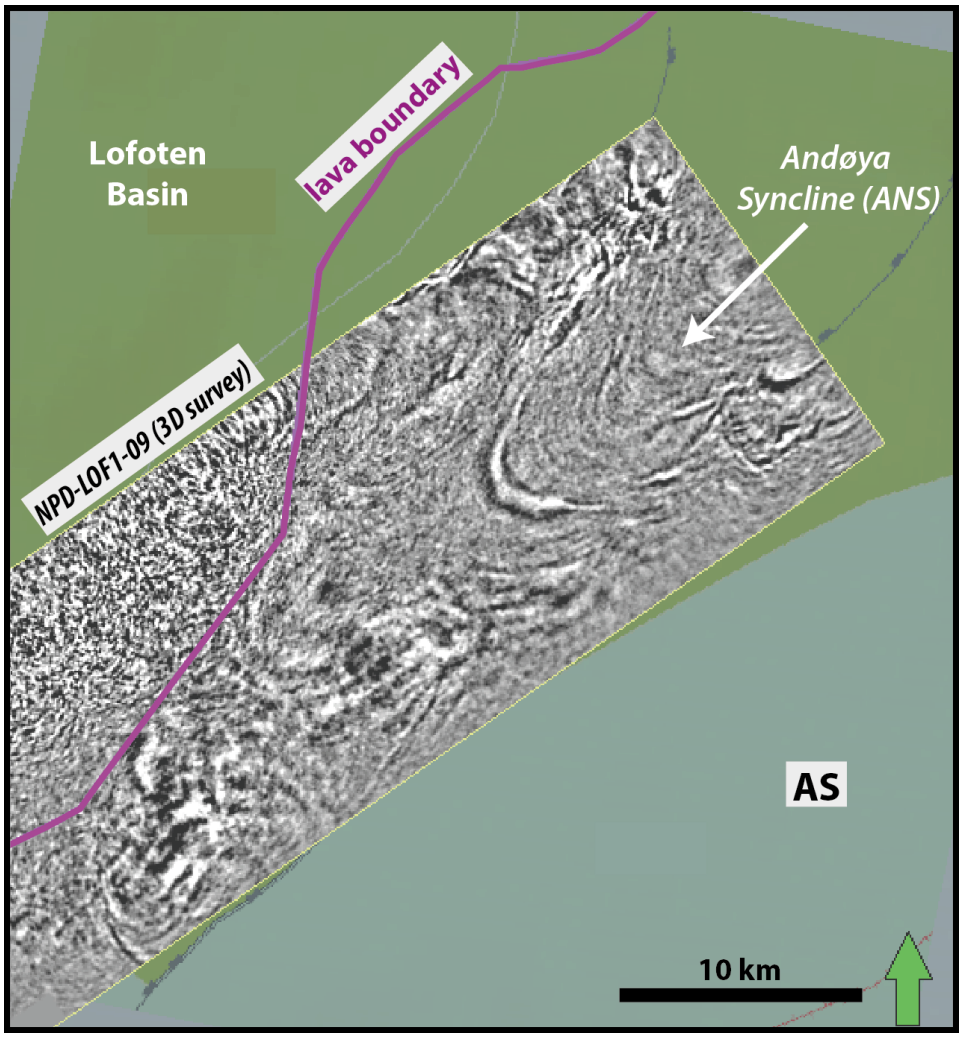

Fig 4.28: *Time-slice (Z=4180 ms, TWT) illustrating seismic expression and areal extend of the Andøya Syncline (ANS). AS: Andøya segment.*

5 Discussion

5.1 Late Mesozoic-Cenozoic tectono-stratigraphic evolution

The fault activity and basin infill history of the Lofoten-Vesterålen margin (LVM) are of the least understood and most debated topics on the northern Norwegian Sea. This section aims to discuss and compare the observations of this study in the context of sediment thickness distribution, and the inter-relationships with structural highs and basin-bounding faults through time-thickness isochore maps (Figs. 5.1-5.13). Each of these time-thickness maps are in addition presented in both, colour and monochromatic scale in order to intonate possible changes in depocenter location and morphological features. Following earlier studies (Blystad et al., 1995; Tsikalas et al., 2001; Bergh et al., 2007; Færseth, 2012), the resolvable (on seismic reflection data) most important tectonic events on the LVM following the Caledonian orogeny (cf. Chapter 2) took place during: Permo-Triassic, Late Jurassic-earliest Cretaceous, Early Cretaceous, and Late Cretaceous-Early Cenozoic.

5.1.1 Pre-Jurassic tectonism

Seismic sequence S1: T-LJ to BCU **[Fig. 5.1]**

The time-thickness map of the seismic sequence S1 shows the depositional trend from the near top basement reflection (TB/T-LJ) to the Base Cretaceous Unconformity (BCU). In general, a widespread deposition of sediments is observed in the area within this time interval. Maximum time-thickness values for sequence S1 are observed just on the western parts of the composite Utrøst Ridge (~900 ms time-thickness), while at the same time sediments pinch-out towards the terminations of the prominent parts of Utrøst Ridge, the Røst (RH) and Jennegga (JH) highs. However, these westernmost accumulations may not represent accurate values for this unit since they are located below the lava flows where the seismic data resolution and hence precise mapping are obscured. Significant thicknesses of sequence S1 can also be found on the Havbåen Sub-basin area (~400 ms time-thickness), and in the northern part of the study area (~600 ms time-thickness) related to the formation of the Andøya Syncline. The former depocenters appear to be structurally controlled by W-dipping faults, such as the West Lofoten Border Fault Zone (WLBFZ) bounding to the east the Havbåen Sub-basin on the Lofoten margin segment.

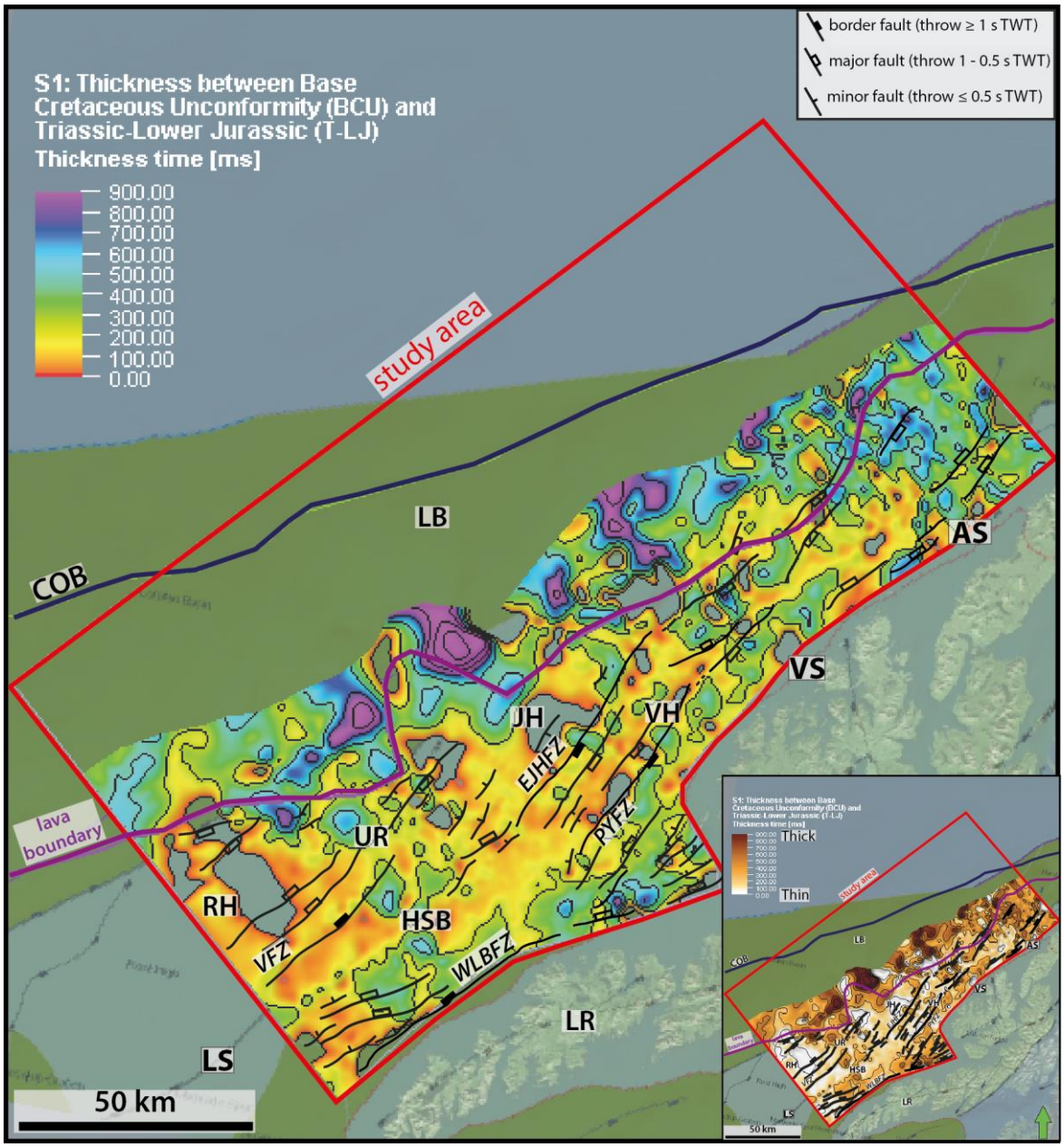

***Fig. 5.1**: Time-thickness map of seismic sequence S1 (BCU – T-LJ). Contour interval 250 ms. Inset: the same map in a monochromatic colour scale intonating thick (darker colours) versus thin (lighter colours) accumulations of the. Abbreviations in Figs. 3.1 and 4.10.*

5.1.2 Late Jurassic-earliest Cretaceous tectonic episode

***Seismic sequence S2: BCU to ILC* [Fig. 5.2]**

The seismic sequence S2 time-thickness map represents the depositional interval between the Base Cretaceous Unconformity (BCU) and the Intra Lower Cretaceous (ILC) horizon. During this period of time, the main depocenters for this seismic unit started to develop and is mainly represented by the Havbåen Sub-basin, with some minor contribution of the Vesterålen sub-basins 1 and 2, and the Andøya Syncline. On the southern part of the study area, the Havbåen Sub-basin (~400 ms time- thickness) is a well delimited depocenter, and the West Lofoten

Border Fault Zone is seen as an active structural element that controls the sedimentation of the area. In a similar way, the East Jennegga High Fault Zone is observed to be responsible for the sediment distribution and deposition on the Vesterålen Sub-basin 2 (~500 ms time-thickness). Major thinning/absence of sequence S2 is, however, observed towards the Jennegga High. The other main depocenter of sequence S2 appears at the northern part of the Vesterålen margin segment and the studied portion of the Andøya margin segment. There, the Andøya Syncline is developed where sequence S2 reaches its maximum thickness (~700 time-thickness). In addition, an apparent NW-prograding depositional trend in the area is indicated by the contour lines of the time-thickness map.

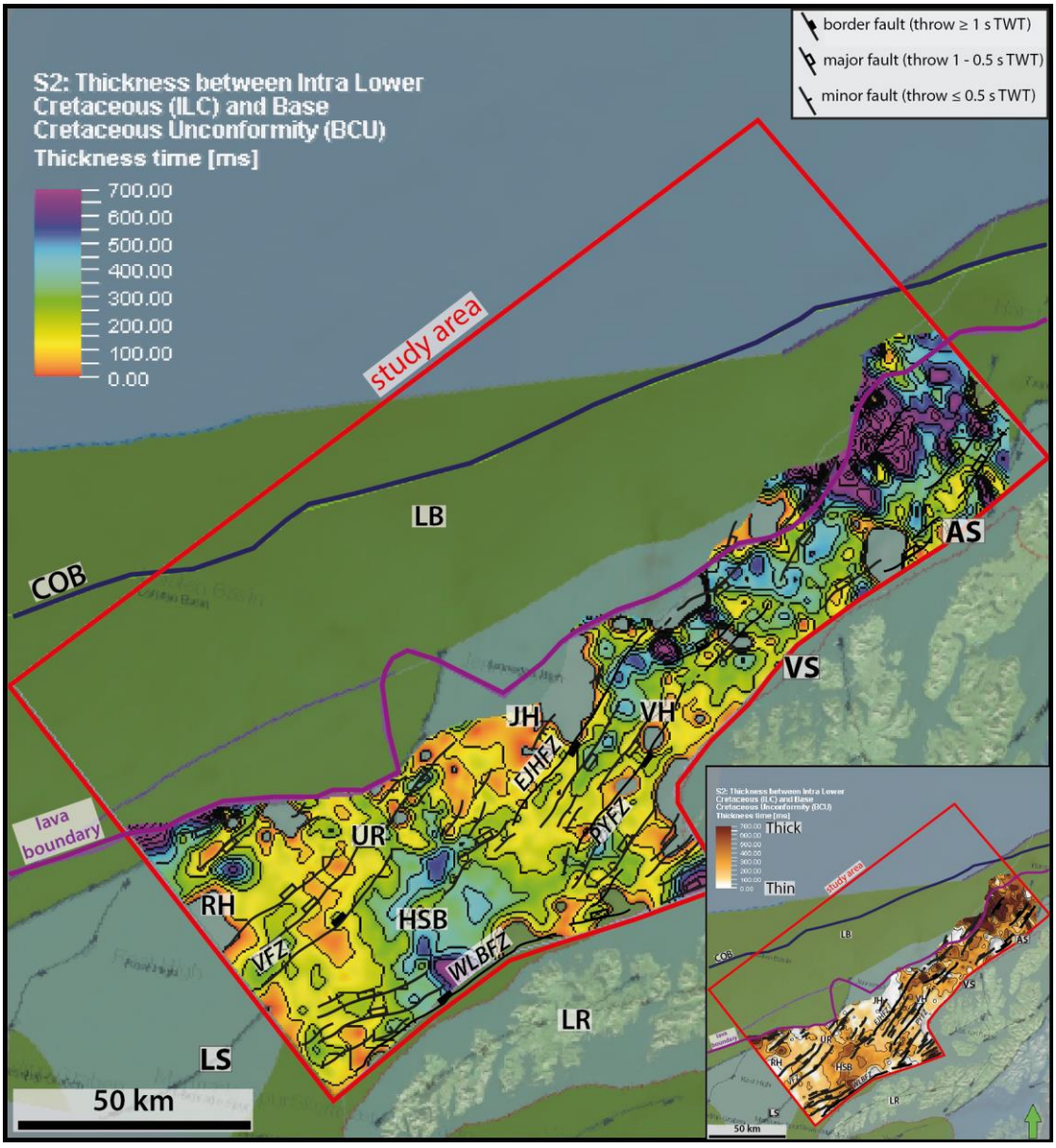

***Fig. 5.2**: Time-thickness map of seismic sequence S2 (ILC – BCU). Contour interval 100 ms. Inset: the same map in a monochromatic colour scale intonating thick (darker colours) versus thin (lighter colours) accumulations of the sequence. Abbreviations in Figs. 3.1 and 4.10.*

5.1.3 Early Cretaceous

Seismic sequence S3: ILC to APT **[Fig. 5.3]**

By Early-to-mid Cretaceous times, the Havbåen Sub-basin on the Lofoten margin segment represented a more concentrated and better delimited major fault-controlled (West Lofoten Border Fault Zone, WLBFZ) depocenter for seismic sequence S3 (~600 ms time-thickness) compared to earliest Cretaceous (Fig. 5.2). The Vesterålen sub-basins 1 and 2 are observed to be still active, but exhibit only minor depocenters for sequence S3 (~400 ms time-thickness). Thinning and erosion of sedimentary successions is even more evident within the western parts of the Utrøst Ridge/Jennegga High area. In the central part of the studied area marked by the Vesterålen margin segment, the sedimentation/deposition of seismic unit S3 appears to be, in overall, larger (> 700 ms time-thickness) compared to that in the southern parts of the study area. The same sedimentary trend is also observed during earliest Cretaceous (S2, Fig. 5.2). However, the intense faulting of the North Utrøst Ridge Fault Complex (NURFC) obscures mapping of sequence S3 in the north part of the study area.

Seismic sequence S4: APT to ALB **[Fig. 5.4]**

The seismic sequence S4 time-thickness map represents the depositional time interval from Aptian to Albian in the study area. In general, the tectono-sedimentary character is that of a wider deposition of sediments in the Havbåen Sub-basin on the Lofoten margin segment. Accumulations of seismic sequence S4 at this part of the LVM appear to be less thick (~450 ms time-thickness), but with more areal extent and uniformity compared to the earliest Cretaceous sequence (S3, Fig. 5.3). The Vesterålen sub-basins 1 and 2 are interpreted as minor depocenters, and with thinner accumulations of sequence S4 (~200 ms time-thickness). The Utrøst Ridge area is observed as a more prominent and elevated structure in the entire LVM, where little or non-deposition of sediments occurred above this high and its terminations. Similar to the time period represented by seismic sequence S3 time-thickness map, by Aptian-Albian time the North Utrøst Ridge Fault Complex (NURFC) is seen as an intense deformation structure dominating the northern parts of the study area. However, more faulting activity involving the North Utrøst Ridge Fault Complex NURFC is observed towards the north of the Vesterålen segment due to the larger discontinuity of sequence S4 time-thickness map. In addition, slightly more sediments were deposited at this latter part of the study area (> 500 ms time-thickness).

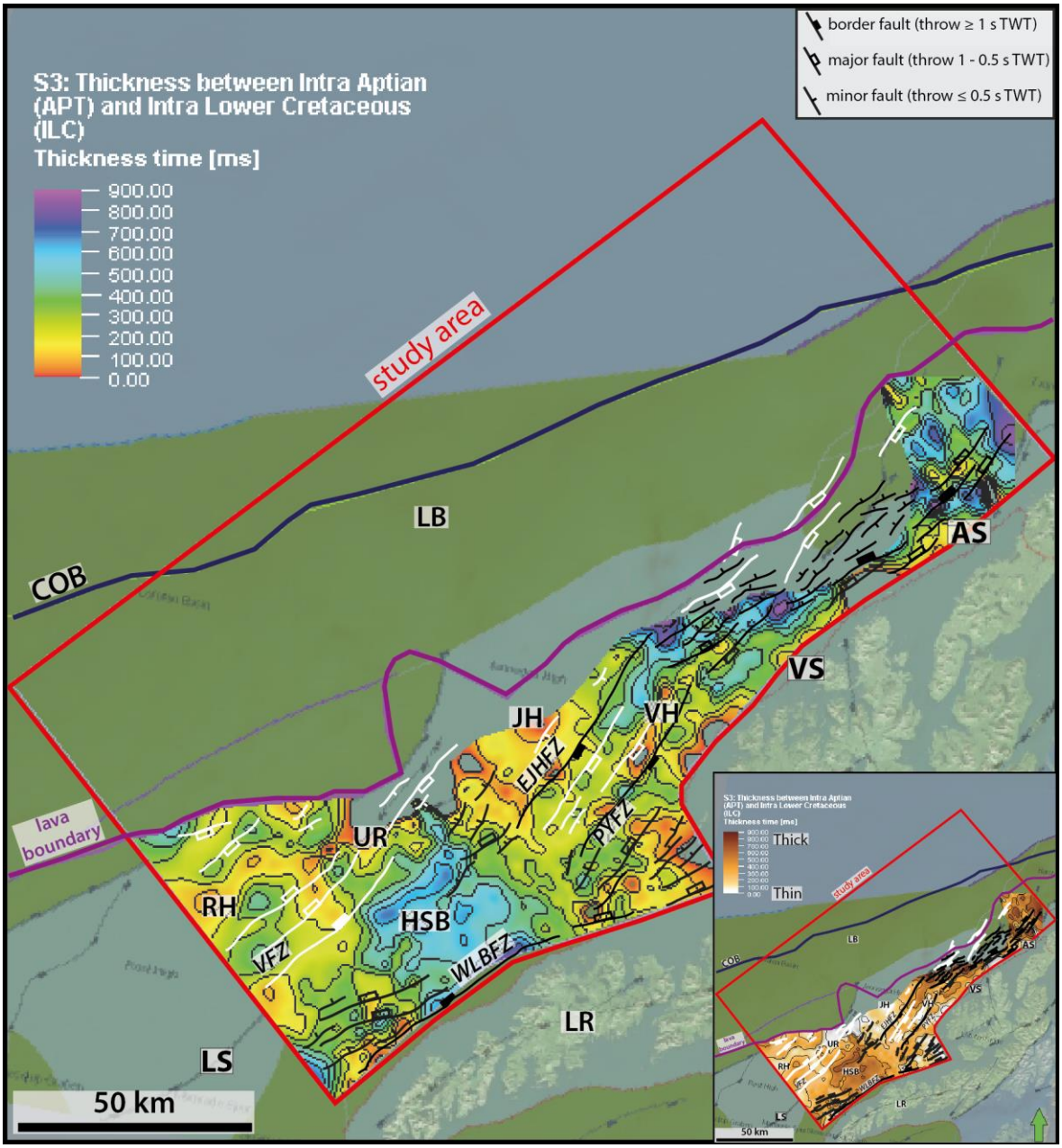

Fig. 5.3: *Time-thickness map of seismic sequence S3 (APT – ILC). Contour interval 100 ms. Inset: the same map in a monochromatic colour scale intonating thick (darker colours) versus thin (lighter colours) accumulations of the sequence. Abbreviations in Figs. 3.1 and 4.10.*

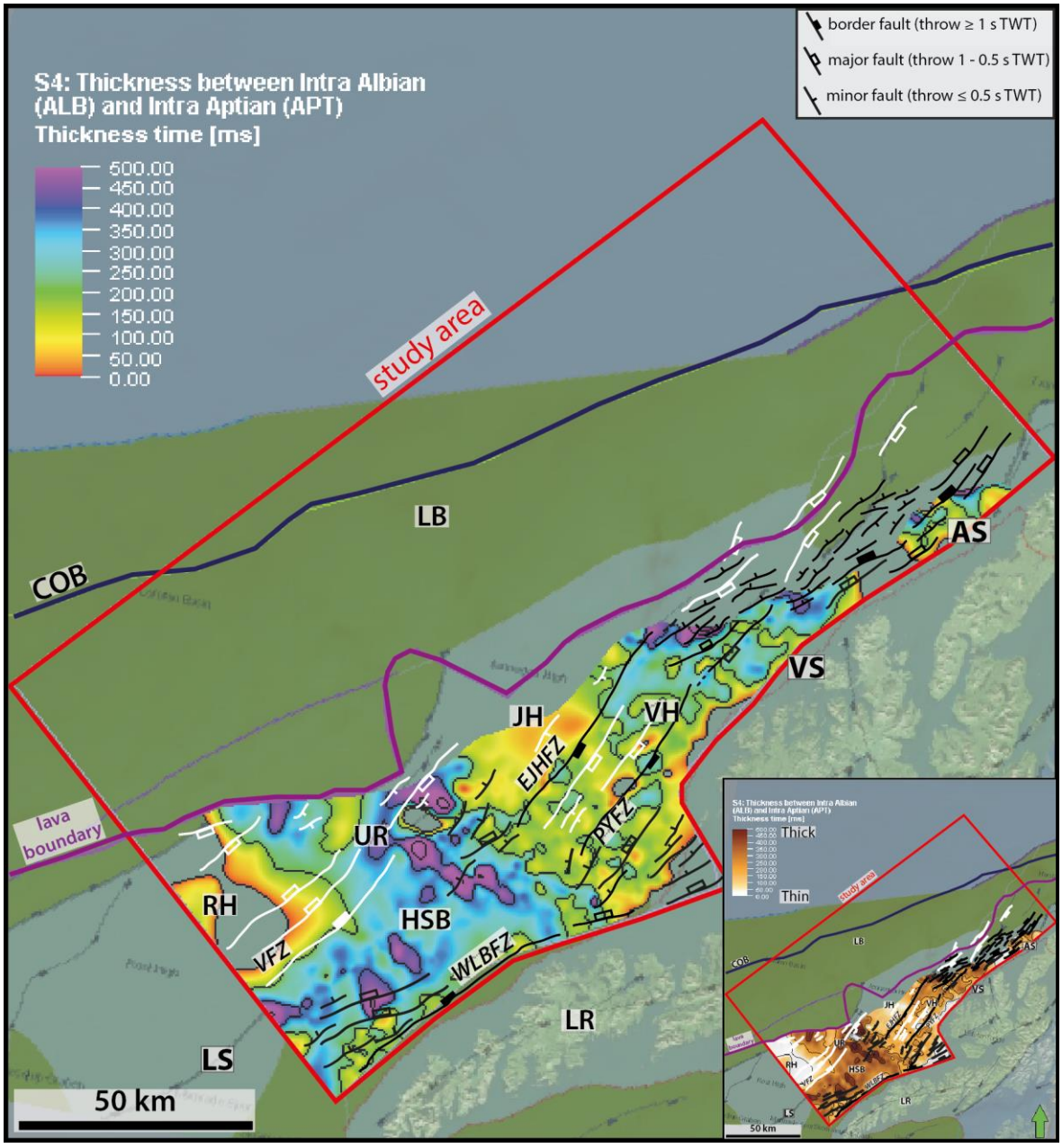

***Fig. 5.4**: Time-thickness map of seismic sequence S4 (ALB – APT). Contour interval 200 ms. Inset: the same map in a monochromatic colour scale intonating thick (darker colours) versus thin (lighter colours) accumulations of the sequence. Abbreviations in Figs. 3.1 and 4.10.*

5.1.4 Late Cretaceous

***Seismic sequence S5: ALB to ICEN* [Fig. 5.5]**

The Albian-Cenomanian time-thickness map illustrates a well-established Utrøst Ridge on the entire LVM. The overall stratigraphic character pictures a depositional trend for seismic sequence S5 limited to the Havbåen Sub-basin (> 600 ms time-thickness), and partly to the Vesterålen sub-basins 1 and 2 (< 400 ms time-thickness). In particular, the larger thickness of sequence S5 compared to units of Aptian-Albian age on the Havbåen Sub-basin indicates a local increase in the fault activity of the West Lofoten Border Fault Zone (WLBFZ). North of

the transition between the Lofoten and Vesterålen margin segments, little areal coverage of sequence S5 indicates a more intense deformation by the North Utrøst Ridge Fault Complex (NURFC). However, it is not easy to determine whether there is presence or not of thicker accumulations of sequence S5 within the latter.

Seismic sequence S6: ICEN to TTUR **[Fig. 5.6]**

By Late Cretaceous, an intense uplift/erosion is observed in the study area, and thus the only mapped major depocenter for sedimentary units of the seismic sequence S6 is located on the Havbåen Sub-basin (~600 ms time-thickness). E-dipping faults on the studied portion of the LVM are interpreted to be inactive due to lack of observed sedimentary successions (i.e. East Jennegga High Fault Zone, EJHFZ; and Pyramiden Fault Zone, PYFZ). Only the W-dipping faults associated to the West Lofoten Border Fault Zone (WLBFZ) on the Lofoten margin segment are interpreted to be active, together with the faults related to the development of the North Utrøst Ridge Fault Complex (NURFC) on the Vesterålen and Andøya margin segments. Sediments of sequence S6 might be present within this fault complex, in particular, on the northern parts, but it is not possible to differentiate them.

Seismic sequence S7: TTUR to BTU **[Fig. 5.7]**

The seismic sequence S7 time-thickness map represents the sedimentary successions that were deposited during late Turonian to earliest Cenozoic. In a general sense, this time-thickness map shows a similar tectono-stratigraphic character to that of the seismic sequence S6 time-thickness map (Fig. 5.6). The Havbåen Sub-basin area displays smoother and concentric contour lines than in sequence S6 time-thickness map, and reaches a maximum of sediment time-thickness of ~700 ms. Similar for seismic sequence S6, there may be additional depocenters for sequence S7 within the northern parts of the North Utrøst Ridge Fault Complex (NURFC), however, they cannot be correlated/mapped.

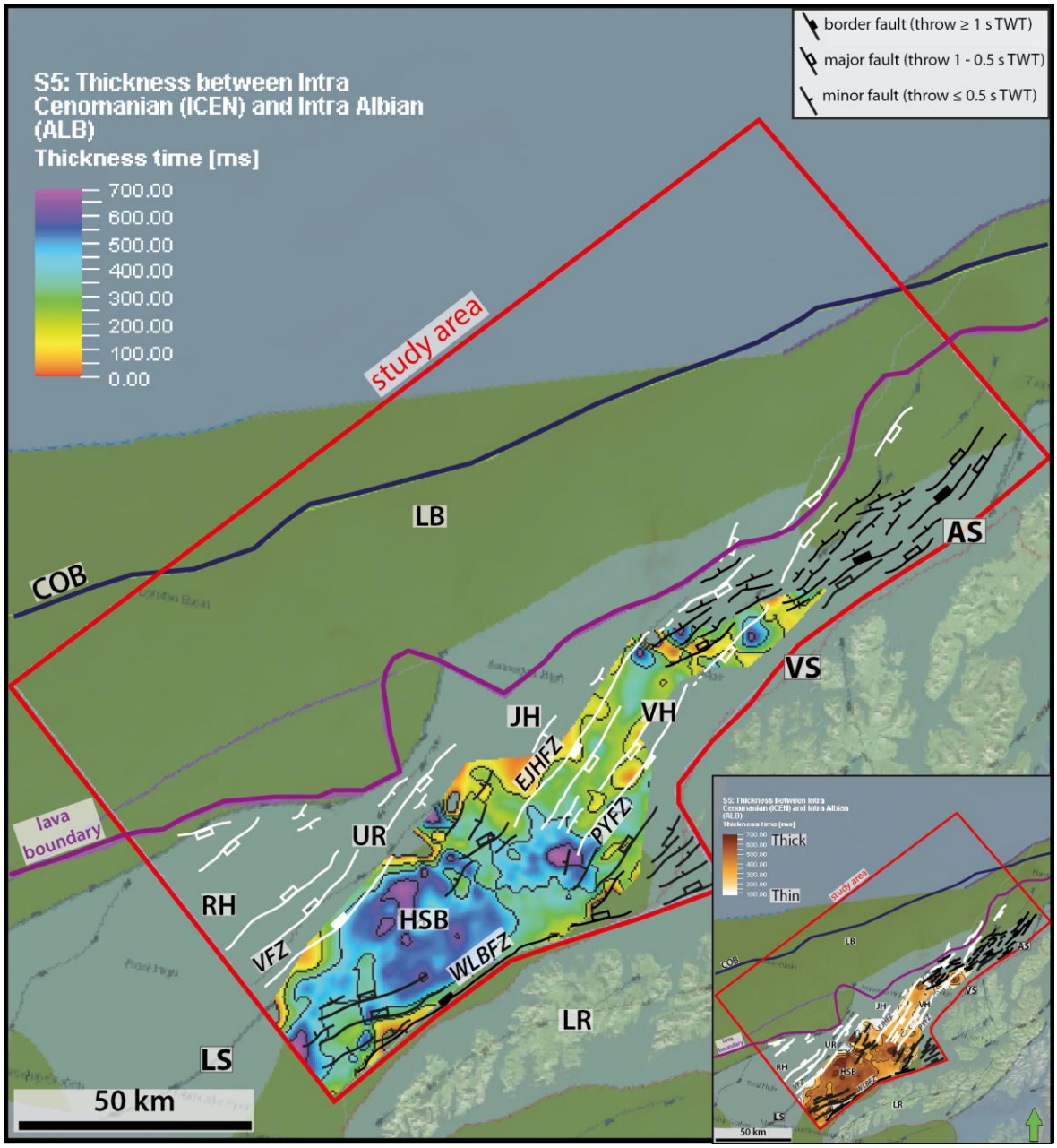

Fig. 5.5*: Time-thickness map of seismic sequence S5 (ICEN – ALB). Contour interval 200 ms. Inset: the same map in a monochromatic colour scale intonating thick (darker colours) versus thin (lighter colours) accumulations of the sequence. Abbreviations in Figs. 3.1 and 4.10.*

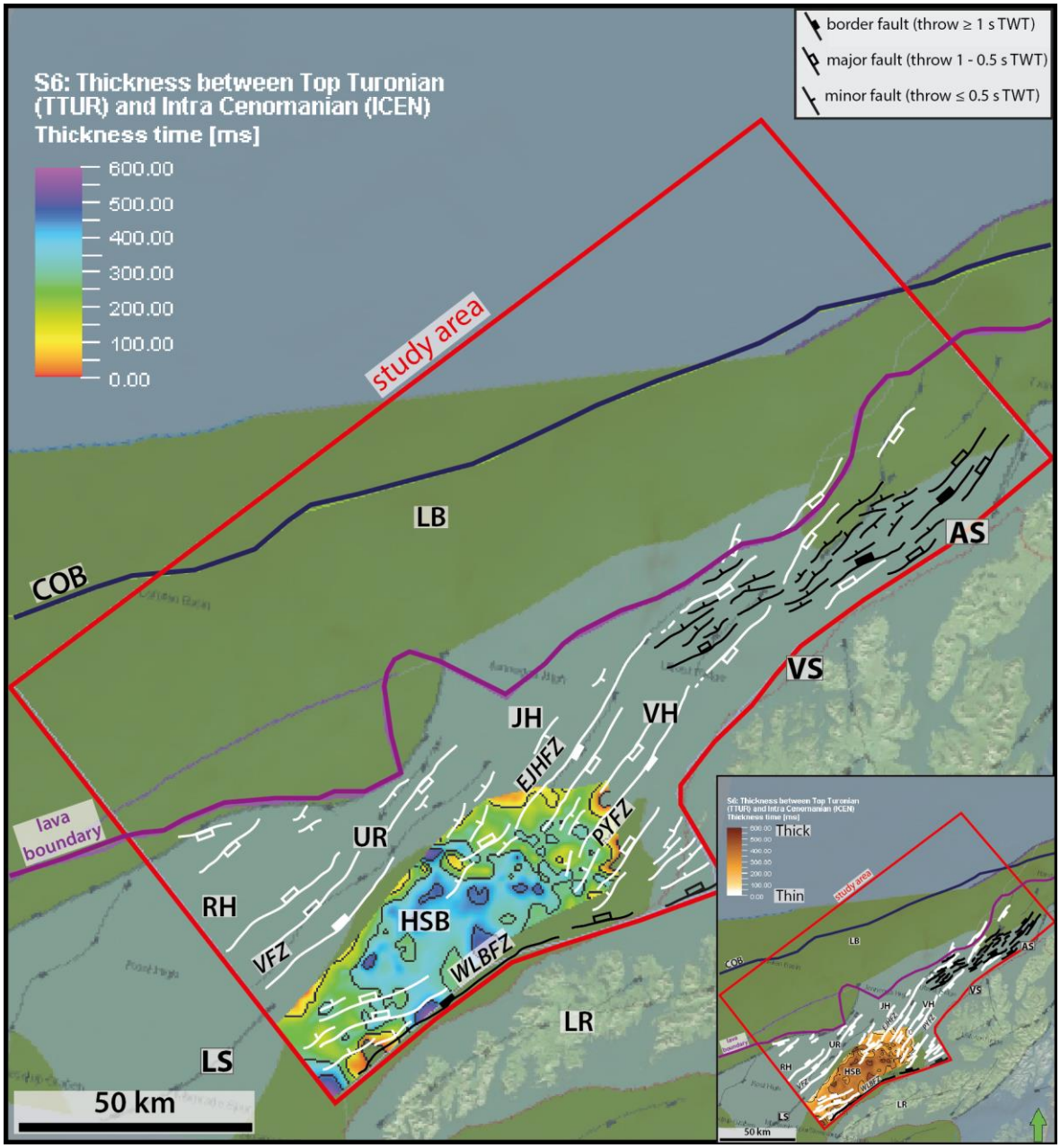

***Fig. 5.6**: Time-thickness map of seismic sequence S6 (TTUR – ICEN). Contour interval 150 ms. Inset: the same map in a monochromatic colour scale intonating thick (darker colours) versus thin (lighter colours) accumulations of the sequence. Abbreviations in Figs. 3.1 and 4.10.*

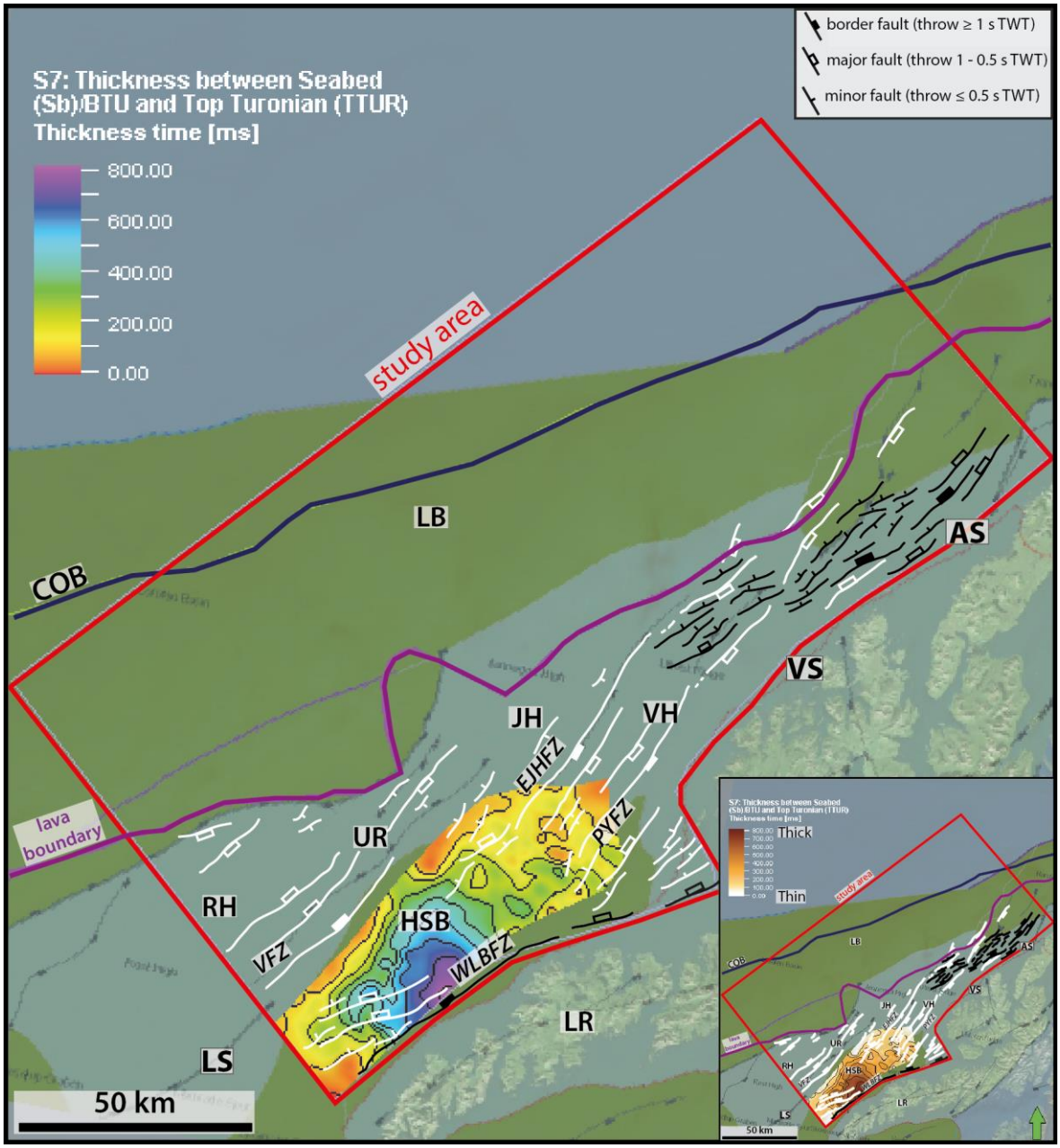

Fig. 5.7*: Time-thickness map of seismic sequence S7 (Sb/BTU – TTUR). Contour interval 100 ms. Inset: the same map in a monochromatic colour scale intonating thick (darker colours) versus thin (lighter colours) accumulations of the sequence. Abbreviations in Figs. 3.1 and 4.10.*

5.1.5 Cenozoic

The Cenozoic time-thickness maps are used to describe the tectono-stratigraphic evolution of the outer part of the LVM. In general, they illustrate periods of alternating doming/erosion and sedimentary infill associated to volcanic activity and different along-margin subsidence rates during Paleogene to early-mid Neogene (Figs. 5.8-5.13). On the contrary, the Late Mesozoic sedimentary infill-trend in the inner part of the LVM is rather stable in the studied area. It is represented by constant-area depocenters of the Havbåen Sub-basin in the Lofoten

margin, together with depocenters found on the northern parts of the study area, such as the Vesterålen sub-basins 1 and 2 and the undifferentiated units within the North Utrøst Fault Complex (NURFC) (Figs. 5.1-5.7). The latter observations differ from the Cretaceous-Paleocene tectono-stratigraphic evolution of the Vøring margin in the immediate south vicinity of the LVM, where depocenters have been observed with a northwards migration trend with time (Zastrozhnov et al., 2020).

Seismic sequence S8: BTU to TPAL **[Fig. 5.8]**

The seismic sequence S8 time-thickness map represents the sedimentary successions that were deposited during the Paleocene, and near the time of continental breakup. A general widespread deposition trend of, more or less, thick sedimentary units is observed within the Lofoten Basin on the outer part of the LVM. However, the Lofoten segment exhibits a larger thickness of sequence S8 compared to the northern parts of the study area. Maximum time-thickness values for sequence S8 are ~600-700 ms, while thinnest values are ~100-200 ms.

Seismic sequence S9: TPAL to TE **[Fig. 5.9]**

During Eocene, two well-defined, thick depocenters of seismic sequence S9 developed in the Lofoten Basin. One of those is located on the central part of the Lofoten Basin and near the transition of the Lofoten and Vesterålen margin segments. This depocenter is observed as a concentric accumulation of sediments of sequence S9, and it reaches a maximum time-thickness of ~700 ms within its central part. In addition, the same depocenter may have been sourced from sediments in the west from the Jennegga High area, or from farther east from the mainland and were transported across the shelf between the Lofoten and Vesterålen islands into their final burial/sink place. The second mapped depocenter in the Lofoten Basin is observed in the north-westernmost corner of the study area, and it exhibits a wide area for sediment accumulation of sequence S9. The two mapped depocenters are bounded in part of their flanks by areas of mainly absent sedimentary sequences, and appear to coincide with volcanic mounds that started to develop during Early Cenozoic.

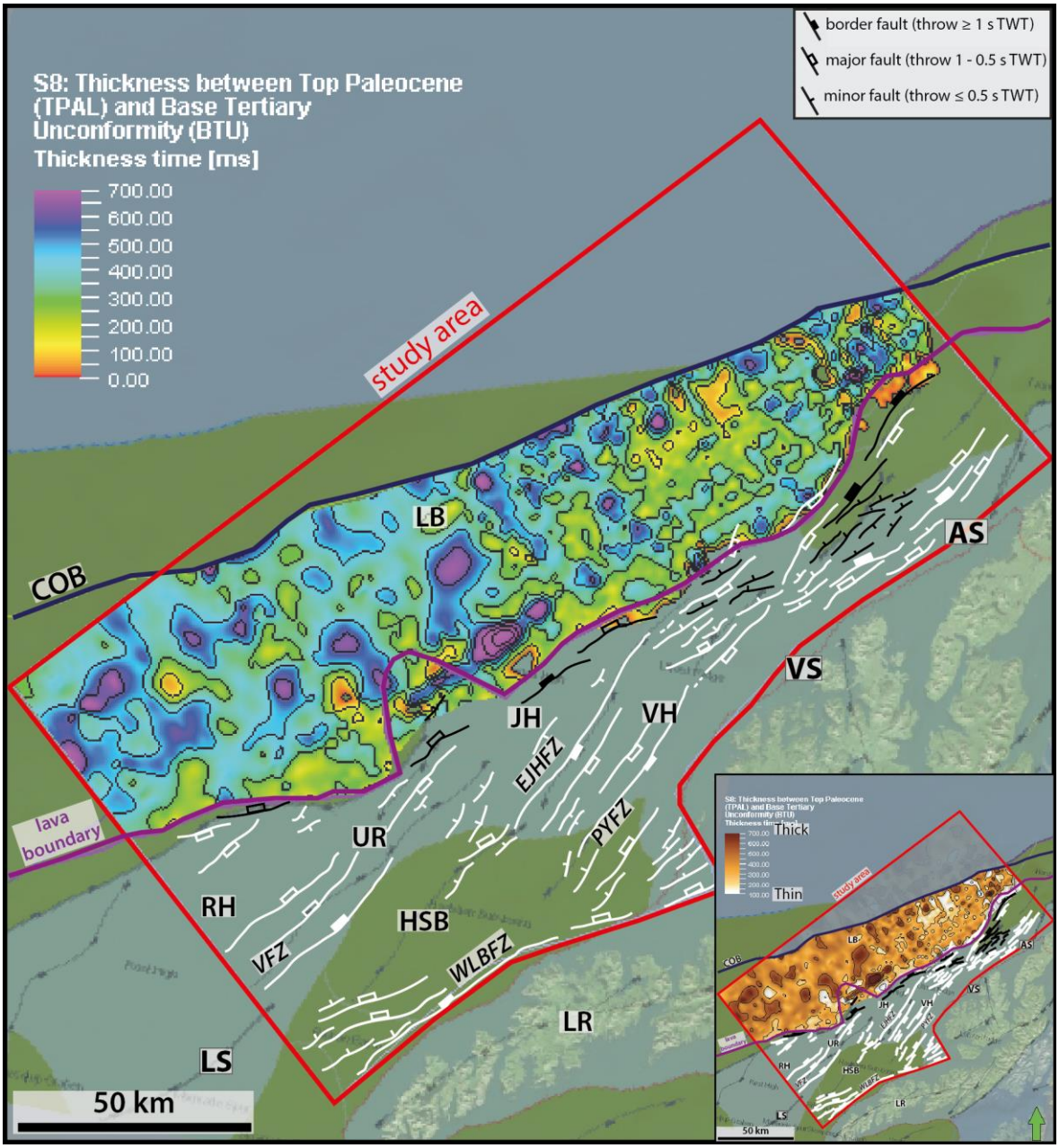

Fig. 5.8: *Time-thickness map of seismic sequence S8 (TPAL – BTU). Contour interval 150 ms. Inset: the same map in a monochromatic colour scale intonating thick (darker colours) versus thin (lighter colours) accumulations of the sequence. Abbreviations in Figs. 3.1 and 4.10.*

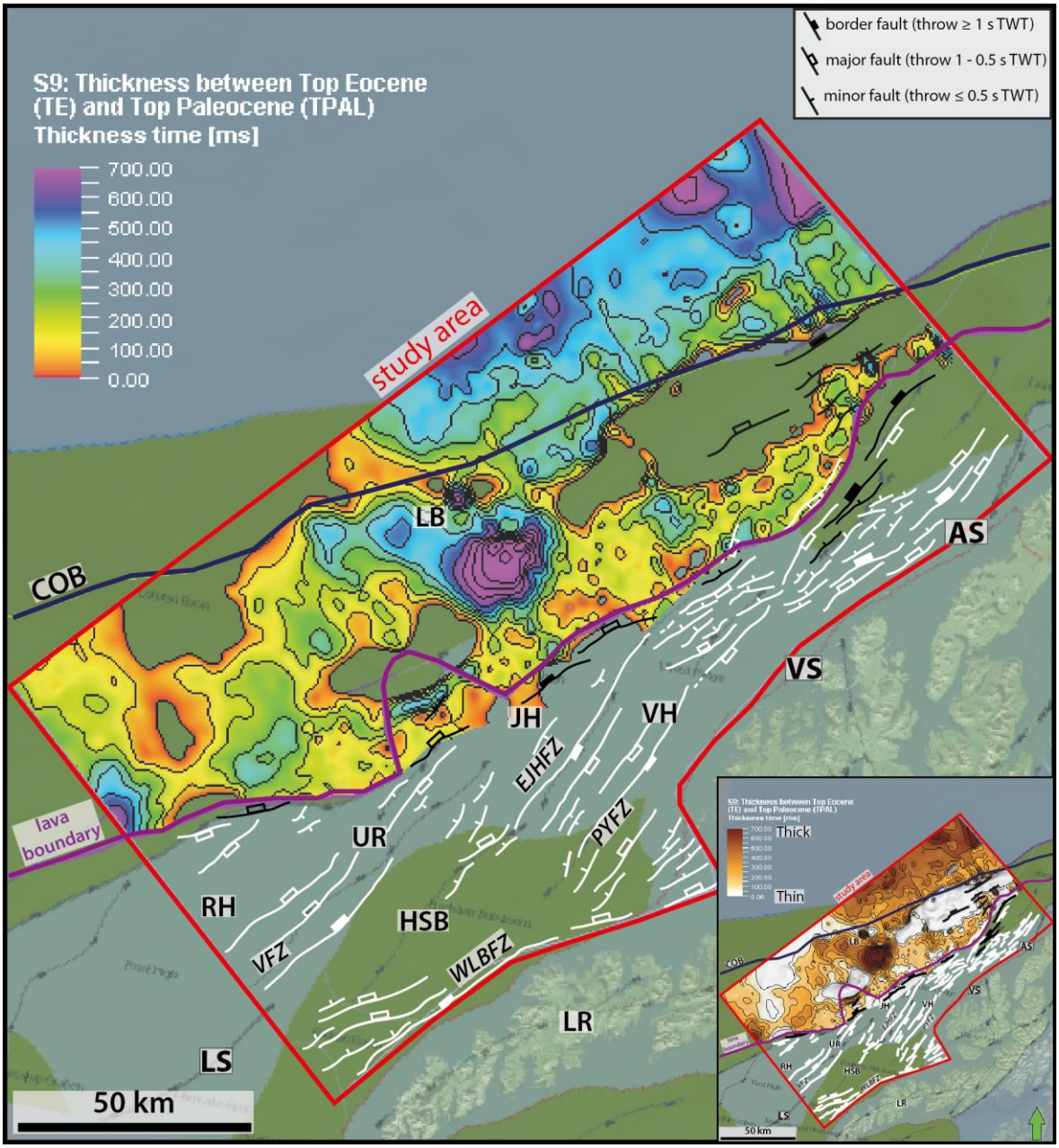

Fig. 5.9*: Time-thickness map of seismic sequence S9 (TE – TPAL). Contour interval 100 ms. Inset: the same map in a monochromatic colour scale intonating thick (darker colours) versus thin (lighter colours) accumulations of the sequence. Abbreviations in Figs. 3.1 and 4.10.*

Seismic sequence S10: TE to IO [Fig. 5.10]

The time-thickness map of seismic sequence S10 represents the sedimentary units deposited during the early Oligocene within the Lofoten Basin. The previously thin or sediment-starved portions for the Eocene seismic sequence S9 (Fig. 5.9) are now observed to be filled by strata of sequence S10 (~500-600 ms time-thickness). A large area of non-deposition is, however, observed in the central part of the outer margin near the transition between the Lofoten and Vesterålen margin segments. This region corresponds to one thick depocenter of sequence S9,

and may be interpreted to be mostly filled during Oligocene. The offshore region adjacent to the central part of Vesterålen island appears to be a pathway for sediment transport towards the outer margin. There, source areas for sediment input and transportation are observed towards the outer margin where finally the sediments reach and are buried.

Seismic sequence S11: IO to IM **[Fig. 5.11]**

The tectono-stratigraphic interval from late Oligocene to early Miocene is represented by the time-thickness map of seismic sequence S11. In general, a semi-widespread deposition trend is observed during late Paleogene-early Neogene, and it is represented by depocenters of sequence S11 that reaches a maximum time-thickness of ~400-500 ms. These depocenters are distributed through the entire studied portion of the Lofoten Basin.

Seismic sequence S12: IM to BPLIO **[Fig. 5.12]**

The time-thickness map of seismic sequence S12 represents the sedimentary units deposited during late Miocene until Plio-Pleistocene. This time-thickness map illustrates a similar depositional character as seismic sequence S11 (Fig. 5.11) with semi-widespread units (~200-300 ms time-thickness). However, in the southern part of the study area a more developed and better-delimited depocenter (~500 ms time-thickness) for seismic sequence S12 is observed and it reaches a maximum northwards extent towards the transition between the Lofoten and Vesterålen margin segments. In addition, a narrow and elongated area of non-deposition is observed in the northern part of the Lofoten Basin, and it coincides with the region where the Andøya Volcanic Mound is located.

Seismic sequence S13: BPLIO to Seabed **[Fig. 5.13]**

The time-thickness map of seismic sequence S13 represents the Plio-Pleistocene sediments related to the glacial period on the LVM. Major erosion is observed on the continental slope across the different margin segments, and it is characterized by very thin to absent sediments of sequence S13. The area of major sediment concentration (>1000 ms time-thickness) is located on the northwest corner of the study area and west of the continent-ocean boundary (COB) region.

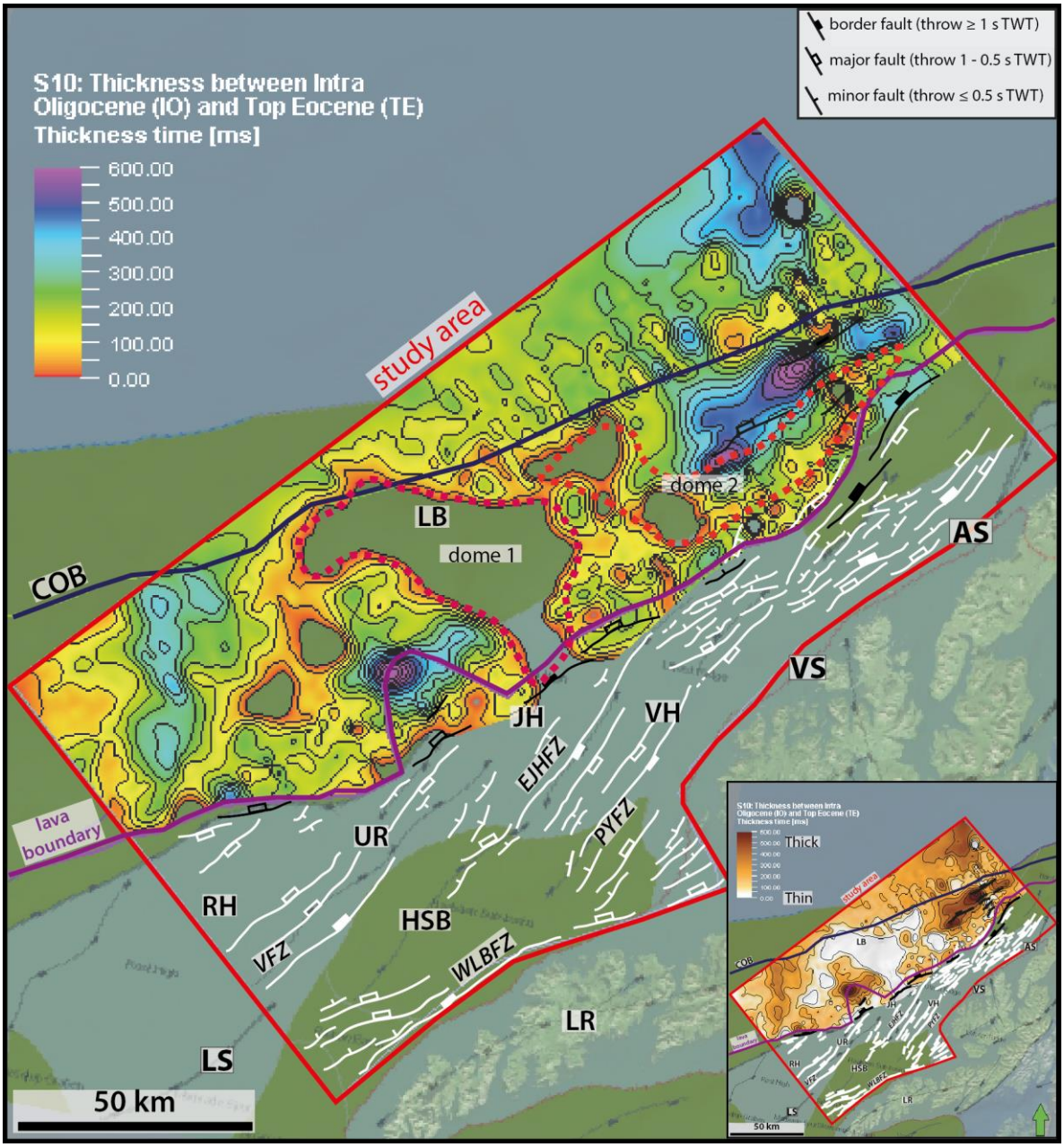

***Fig. 5.10**: Time-thickness map of seismic sequence S10 (IO – TE). Contour interval 50 ms. Inset: the same map in a monochromatic colour scale intonating thick (darker colours) versus thin (lighter colours) accumulations of the sequence. See text (sub-chapter 5.3.3) for discussion on dome 1 and dome 2. Abbreviations in Figs. 3.1 and 4.10.*

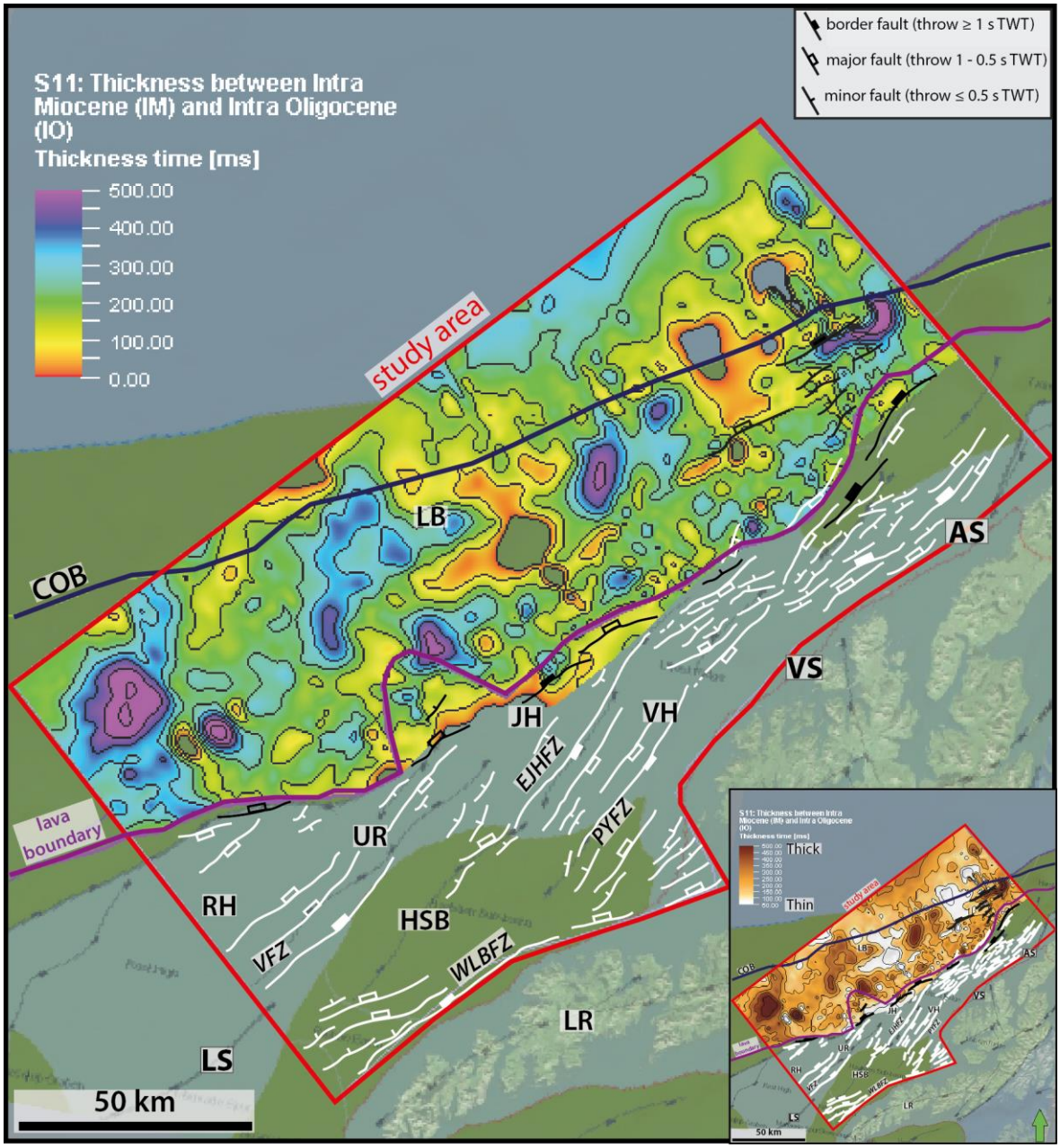

Fig. 5.11*: Time-thickness map of seismic sequence S11 (IM – IO). Contour interval 80 ms. Inset: the same map in a monochromatic colour scale intonating thick (darker colours) versus thin (lighter colours) accumulations of the sequence. Abbreviations in Figs. 3.1 and 4.10.*

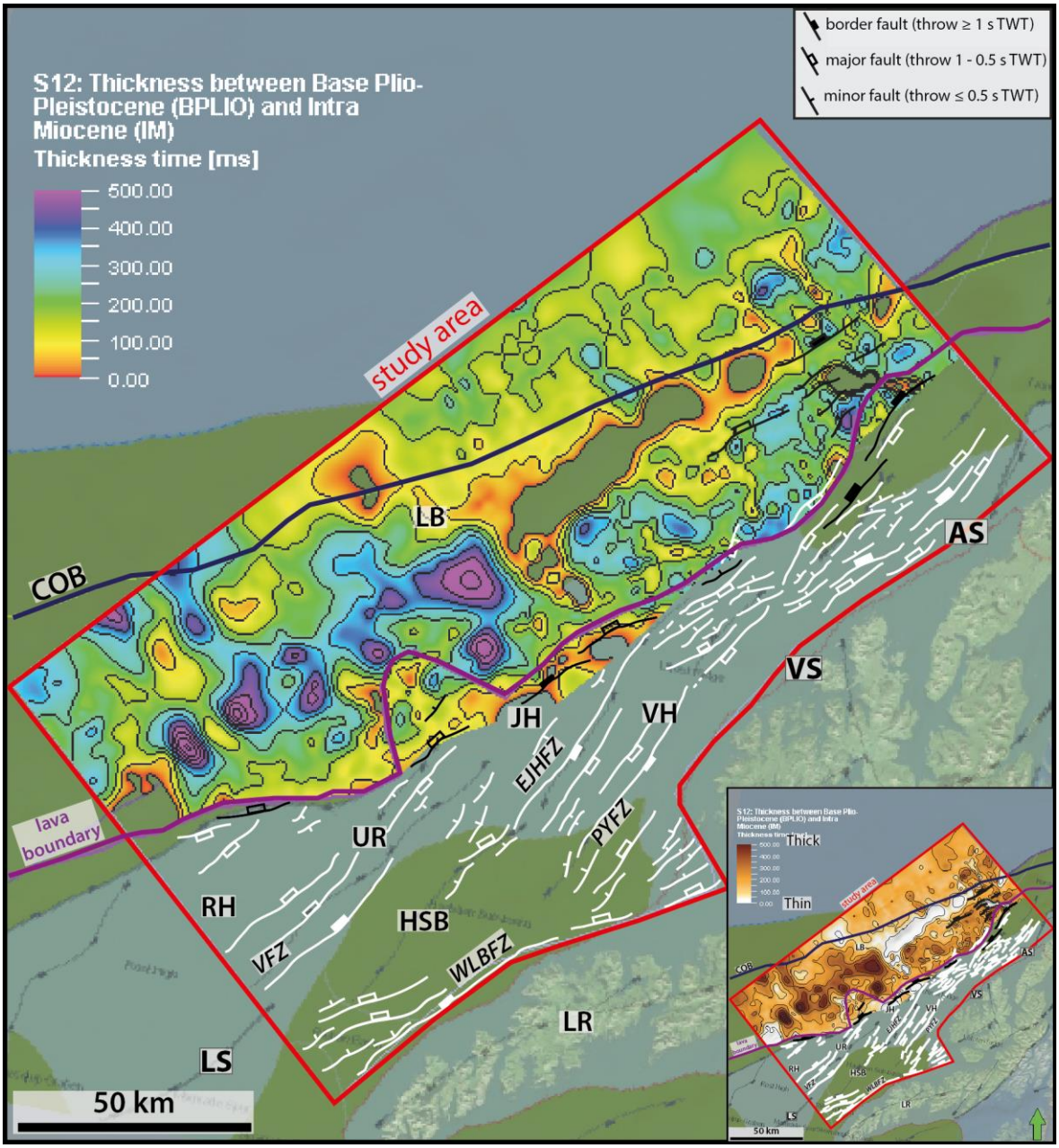

***Fig. 5.12**: Time-thickness map of seismic sequence S12 (BPLIO – IM). Contour interval 80 ms. Inset: the same map in a monochromatic colour scale intonating thick (darker colours) versus thin (lighter colours) accumulations of the sequence. Abbreviations in Figs. 3.1 and 4.10.*

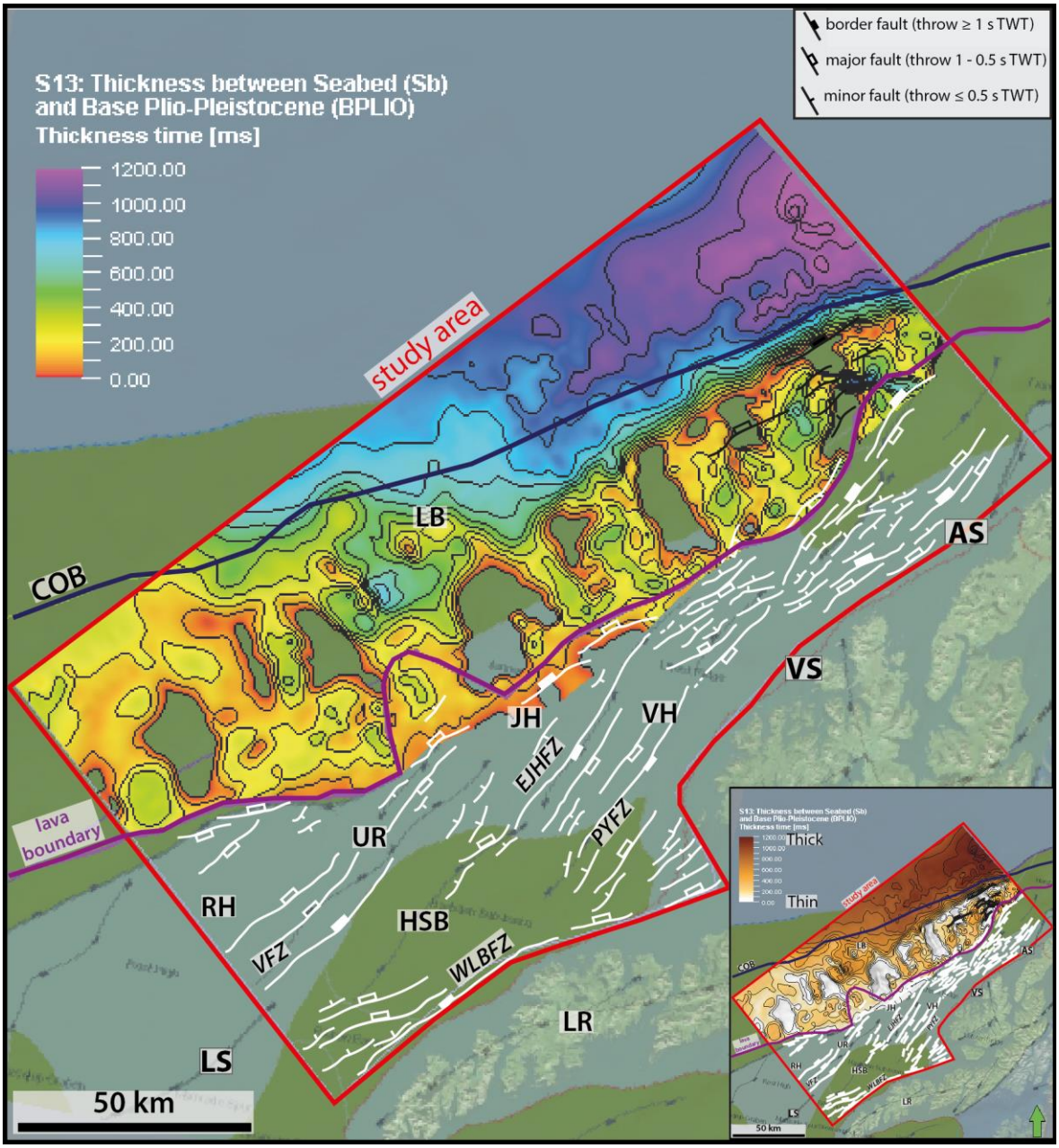

***Fig. 5.13**: Time-thickness map of seismic sequence S13 (Sb – BPLIO). Contour interval 100 ms. Inset: the same map in a monochromatic colour scale intonating thick (darker colours) versus thin (lighter colours) accumulations of the sequence. Abbreviations in Figs. 3.1 and 4.10.*

5.2 Basin architecture and margin segmentation

The LVM rift basin architecture is characterized by depocenters that are bounded by approximately NNE-SSW striking faults (Fig. 5.14). Major shifts in structural style are shown and are refined in this study in close correspondence with earlier published work, including changes in fault dip-polarity and fault-throw intensity between the Lofoten and Vesterålen margin segments (Løseth and Tveten, 1996; Tsikalas et al., 2001; Bergh et al., 2007; Færseth, 2012; Hansen et al., 2012). The Lofoten margin is dominated by west-dipping normal faults, and listric border faults separate the Lofoten Ridge and Utrøst Ridge from the offshore rift basins. The Vesterålen margin, on the other hand, is dominated by east-dipping normal faults and no separation occurs between the offshore rift basins and the Vesterålen islands. These east-dipping faults gradually die-out towards the Andøya margin, and some basement-involved west-dipping faults are observed again, together with the prominent North Utrøst Ridge Fault Complex (NURFC) on top of the Lower Cretaceous basins.

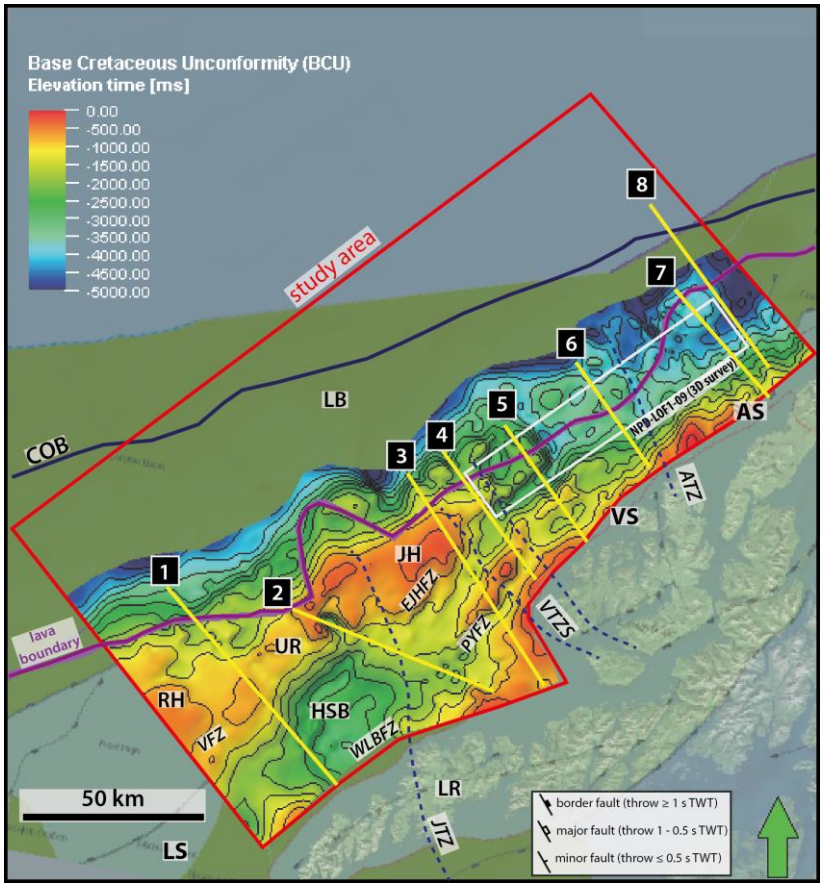

Fig 5.14: *Time-structure map of the Base Cretaceous Unconformity (BCU) used as a reference for the basin architecture description. Profile locations are shown in yellow lines (1 to 8). White polygon indicates 3D seismic survey (NPD-LOF1-09). Abbreviations in Fig. 4.10. Transfer zones are indicated in dashed blue lines, namely the Jennegga transfer zone (JTZ); Vesterålen transfer zone system (VTZS); and the Andøya transfer zone (ATZ).*

5.2.1 Definition and mapping of transfer zones

Tectonic boundaries, such as transfer zones, are often observed with a high degree of correlation with structural lineaments and/or shifts in potential-field anomaly (gravity and magnetic) maps (e.g. Jan Mayen Lineament: Doré et al., 1997; Bivrost Lineament: Tsikalas et al., 2019). The conducted structural interpretations, the constructed time-thickness maps, and the available gravity and magnetic anomaly maps, were all used to refine earlier proposed and to identify new possible transfer zones within the study area (Figs. 5.15 and 5.16).

The transfer zones defined in this study (*sensu* Rosendahl et al., 1986) coincide with intermediate positive gravity and magnetic anomalies (Fig. 5.15), and are believed to influence rift segmentation in the area (e.g. Olesen et al., 2002). As a result, three structural lineaments were mapped, namely (from south to north) the Jennegga transfer zone, the Vesterålen transfer zone system bounded by two lineaments, and the Andøya transfer zone; and broadly separates the studied area of the LVM into three major and distinct rifted segments: Lofoten, Vesterålen, and Andøya margin segments (Figs. 5.15).

Figure 5.16 displays composite Late Mesozoic time-thickness maps that are elaborated in order to better visualize the defined transfer zones and related rift segment domains and rift architecture. In general terms, the figure shows the transfer zones as NW-SE to NNW-SSE trending and curved lineaments with an apparent control on sedimentary infill, fault polarity, and basin geometry. For example, on the Lofoten margin segment the Jennegga transfer zone may be responsible that the Havbåen Sub-basin area has remained a constant depocenter for almost the entire Cretaceous, and even the Cenozoic (Figs. 4.10-4.16, 5.16). They are structures that, in addition, accommodate strain via oblique shear across individual grabens, and may evolve as transform faults/zone as rifting escalates with time (Rosendahl et al., 1986; Rosendahl, 1987; Lister et al., 1991). This latter statement is the case for the Vesterålen transfer zone system, where lateral offsets exit within the Vesterålen High (Fig. 5.16b).

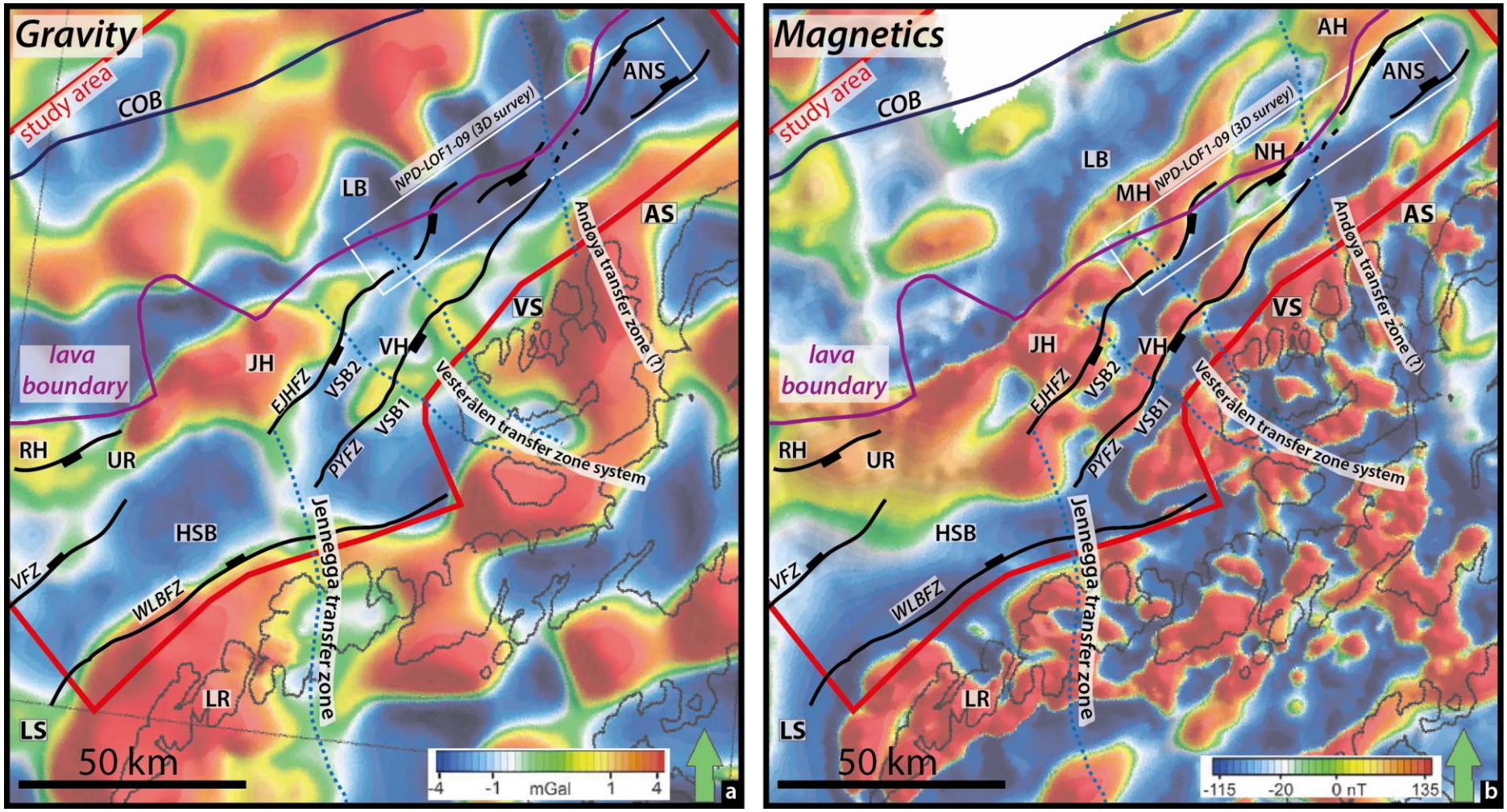

Fig. 5.15*: Potential field anomaly data (gravity and magnetics) with suggested transfer zones in the study area: Jennegga transfer zone, Vesterålen transfer zone system, and Andøya transfer zone; separating, respectively, three rifted segments: Lofoten, Vesterålen, and Andøya margin segments. Other annotations in Figs. 4.10 and 4.26.*

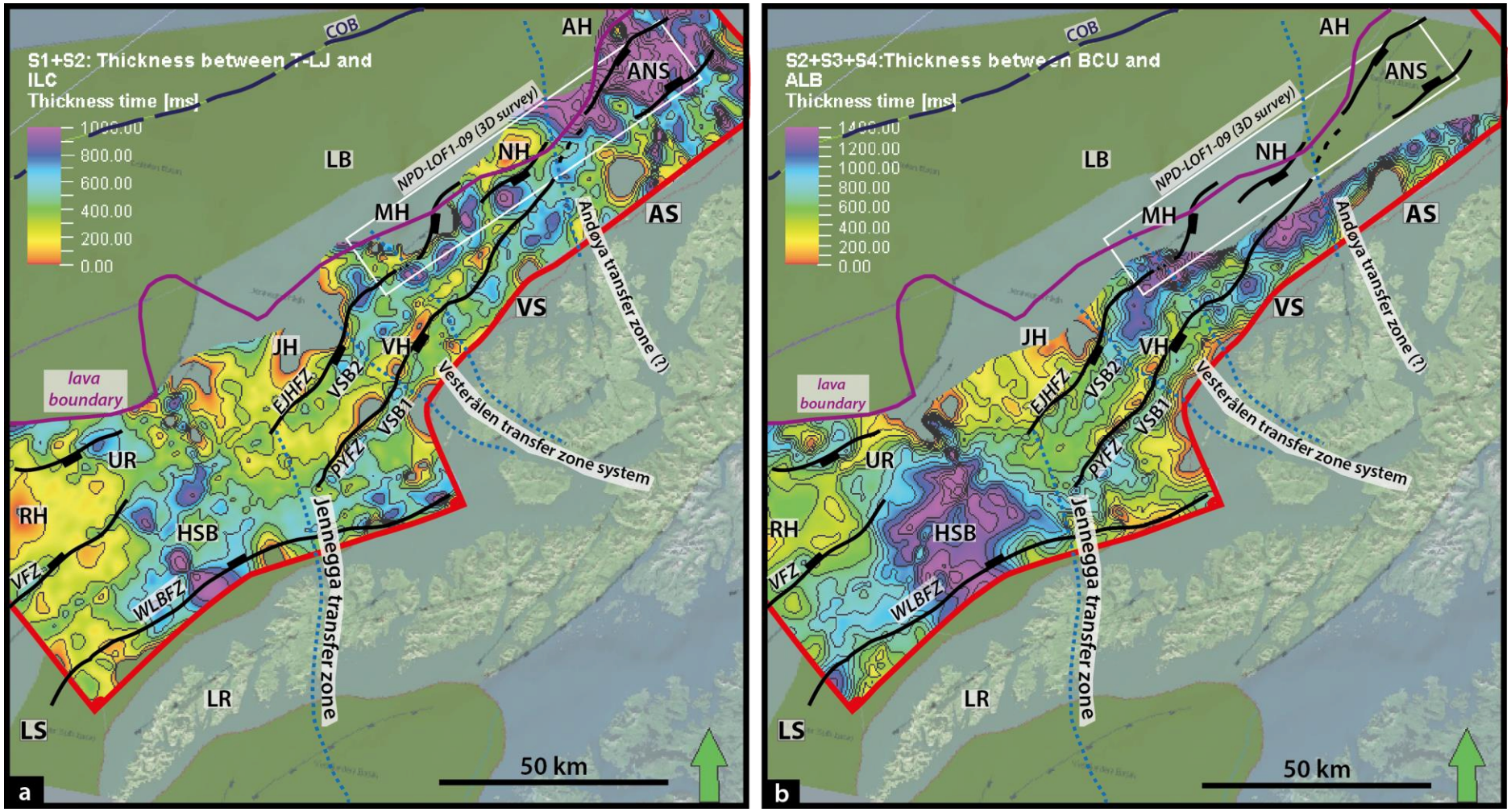

Fig. 5.16*: Composite time-thickness maps of interpreted seismic sequences with proposed transfer zones. NPD map included in the background (factpages.npd.no). Active major faults are displayed in black, while inactive in white. All faults are draped above the surface.* ***(a)*** *S1-S2 sequences (T-LJ to ILC). Contour interval 100 ms.* ***(b)*** *S2-S4 sequences (BCU to ALB). Contour interval 120 ms.* ***(c)*** *S4-S7 sequences (ALB to BTU). Contour interval 80 ms. Other annotations in Figs. 4.10 and 4.26.*

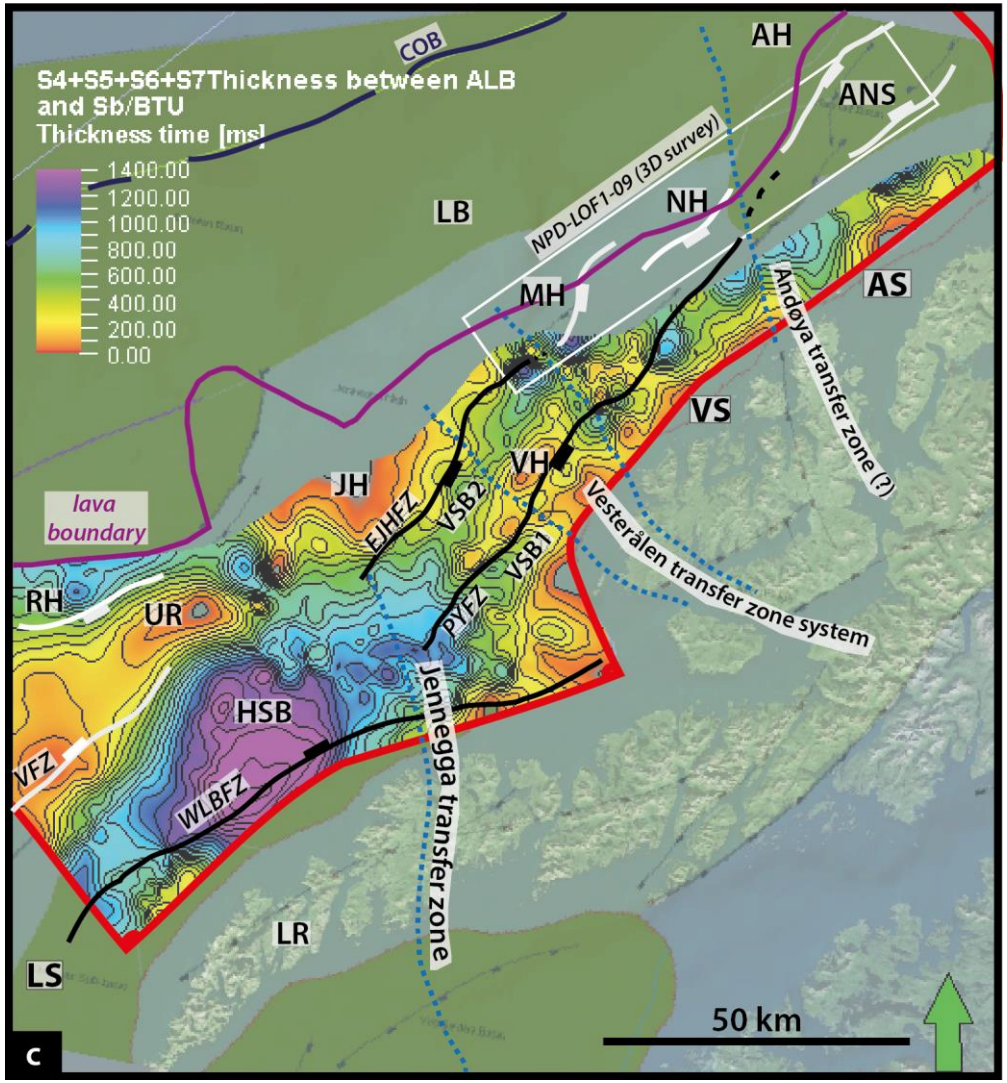

***Fig. 5.16**: (Continuation)*

5.2.2 Lofoten margin segment

Within the study area, on the Lofoten margin segment the main depocenter is the Havbåen Sub-basin that comprises the northern part of the Ribban Basin (Figs. 5.14 and 5.17). This sub-basin is bounded to the east by the West Lofoten Border Fault Zone (WLBFZ), which can be traced for up to ~50 km along the Lofoten Ridge (Fig. 5.14). The northern studied portion of this margin segment is dominated by the west-dipping faults of the WLBFZ, exhibiting throws larger than ~1.5 s TWT. Throw intensity, is however, progressively reduced towards the north of the margin segment to ~0.5 s TWT. Syn-sedimentary faulting is observed on the pre-Cretaceous and Lower Cretaceous strata as wedge-shaped geometries towards the WLBFZ and synthetic faults in its vicinity with similar westward-dip but smaller vertical offsets (< 0.5 s TWT). In particular, the Lower Cretaceous seismic sequences appear to be dragged upwards at their endings by the West Lofoten Border Fault Zone (WLBFZ), while no significant growth of Upper Cretaceous units have been observed towards the WLBFZ fault-plane. Farther west, the northern continuation of the Vesterdjupet Fault Zone (fault-throw of ~1 s TWT) is still seen in this part of the margin, and the fault zone delineates the eastern flank of the Utrøst Ridge/Røst High that bounds the western part of the Havbåen Sub-basin. Here, it can be seen how basement/intra-crustal reflectivity is depicting the elevated Utrøst Ridge under the folded Late Mesozoic sedimentary successions that progressively onlap onto it (Fig. 5.17 profile-1).

The Havbåen Sub-basin is flanked in the west by the composite Utrøst Ridge parts, the Røst High in the south and the Jennegga High in the north. The Røst High is an elevated structural element in the south of the study area, and delimits the inner part of the margin from the Cenozoic-filled Lofoten Basin and lava flows on the outer part of the margin. Towards the north, the Jennegga High is delineated in the eastern flank by the east-dipping East Jennegga High Fault Zone (EJHFZ), which progressively increases northward in vertical offset from ~0.5 to ~1 s TWT. Draping and folding of Lower Cretaceous strata (sequences S2 to S4) are also observed towards the fault-plane of the EJHFZ on the northern Lofoten margin segment, with diminishing in intensity towards the Upper Cretaceous units (Fig. 5.17 profile-3).

In the southernmost part of the study area, the Havbåen Sub-basin has the character of a relatively stable depocenter, and relatively thick (~1.5 s TWT) Upper Cretaceous sequences (S6 and S7) overlie the pre-Cretaceous (S1) and Lower Cretaceous units (S2-S5). The Jurassic units reach a maximum thickness of ~500 ms TWT, and are thin compared to the Cretaceous

units (> 2 s TWT). Both Jurassic and Lower Cretaceous strata are preserved at rotated fault-blocks that are related to the activity of the WLBFZ. The internal configuration for both the Jurassic and Lower Cretaceous units appears as stratified, sub-parallel and wavy reflections that onlap in the east and west onto the basin flanks. On the other hand, for the Upper Cretaceous sequences, the internal reflections appear with more chaotic and divergent seismic character.

5.2.3 Jennegga transfer zone

The Jennegga transfer zone has been delineated using potential field data (Fig. 5.15) and is confirmed by seismic interpretation (Fig. 5.16). This transfer zone has been previously interpreted as a tectonic lineation between the Jennegga High and the Lofoten Ridge that had an important role in crustal differentiation and rift segmentation (Tsikalas et al., 2001; Olesen et al., 2002). The supplemented gravity anomaly map (Fig. 3.2), not available in earlier studies, favours the roughly NW-SE orientation for this transfer zone, which can also be extended through the Lofoten Ridge and up to the central parts of the Vestfjorden Basin (Fig. 5.16). It can be argued that the lateral shifts attributed to the transfer zones are more evident in the gravity map (Fig. 5.15a) than in the magnetic anomaly map. The Jennegga transfer zone has been also identified in seismic data as a low-relief accommodation zone (LRAZ; *sensu* Rosendahl et al., 1987), and is expressed in 2D seismic profiles as an elevated near-flat relief at the northern margin of the Havbåen Sub-basin (Fig. 5.17 profile-3). Furthermore, interpretation of time-thickness maps (Fig. 5.16) suggests that south of the Jennegga transfer zone there is a clear structural and depositional control onto the Havbåen Sub-basin since Late Jurassic-Early Cretaceous (main phase) until, at least, mid-Late Cretaceous. The faulting style appears also to be influenced in part by the Jennegga transfer zone, and is represented by the onset of E-dipping master faults north of this lineament (Figs. 5.16, and 5.17 profile-3). Therefore, there is clear evidence for this transfer zone to be a major tectono-stratigraphic element.

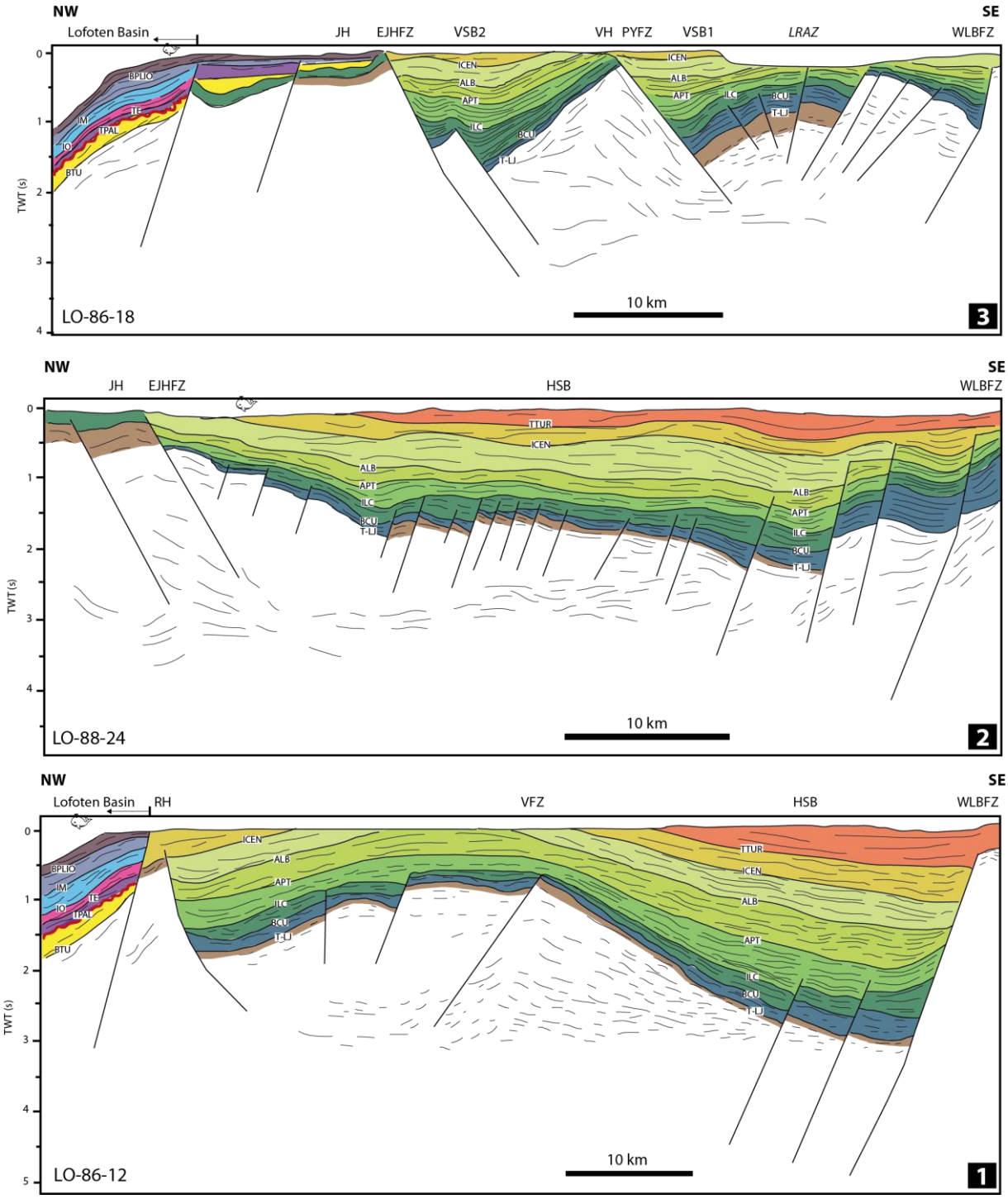

Fig 5.17: *Line-drawing interpretation of relevant seismic profiles for the northern Lofoten margin segment (profiles1 and 2) and for the southern Vesterålen margin segment (profile 3) illustrating the main structural elements. Colour legend and abbreviations as in Figs. 4.6 and 4.26. Profile locations in Fig. 5.14.*

5.2.4 Vesterålen transfer zone system

The Vesterålen transfer zone system is defined in this study as the area affected by two different structural lineaments, and is interpreted to originate in a proximal location in the region of the Vesterålen island. The term system (*sensu* Rosendahl et al., 1986) is denoted

here to emphasise the presence of two identified transfer zones. The Vesterålen margin segment is, therefore, subdivided into three sub-segments: South, Central, and North. These sub-segments are localized in-between the two lineaments that conform to the Vesterålen transfer zone system (Figs. 5.15 and 5.16). These sub-divisions are made to better describe the focus study area, however, the Vesterålen sub-segments do not display major changes in rift architecture across the transfer zones.

Both gravity and magnetic maps have contributed to identify the two offshore curvilinear and NW-SE trending lineaments, as these correlate with lateral anomaly shifts (Fig. 5.15). The westernmost extension of the lineaments seems to reach only a few kilometres into the outer margin. A more WNW-ESE trending character is, however, observed and interpreted for these two transfer zones towards the onshore Vesterålen islands part in the eastern side of the study area (Fig. 5.15). In addition, a clear, but with minimal offset, lateral shift on the Vesterålen High is evidenced in the magnetics map (Fig. 5.15-b) and has been further constrained by time-thickness maps (Fig. 5.16). The transfer zone in the south is located at the transition between the Lofoten and Vesterålen margin segments and shows a sinistral offset on the southern part of the Vesterålen High. On the contrary, the transfer zone in the northern part of the Vesterålen High shows a dextral offset (Figs. 5.15b and 5.16).

Towards the northern part of the study area at the transition between the Lofoten and Vesterålen margin segments, the basin architecture and the rift geometry have changed (South Vesterålen sub-segment). This shift in structural style occurs near the Jennegga High (Fig. 5.14) and north of the Jennegga transfer zone (Tsikalas et al., 2001; this study). The style of deformation on this part of the margin is characterized by significant rotation of fault-blocks with oppositely dipping normal fault polarities. Partial overlapping of the different set of faults and fault-blocks is observed with a low-relief in the footwall, or an intra-basin low-relief accommodation zone (LRAZ) (Rosendahl et al., 1986; Gawthorpe and Hurst, 1993). In general terms, these accommodation zones, also referred to transfer zones, direct the displacement and deformation among individual transverse or oblique basin-bounding fault segments or individual half-graben basins (Gawthorpe and Hurst, 1993). They also vary in style and size (e.g. relay-ramp, transfer fault), and have a marked influence on basin stratigraphy, drainage evolution, and/or even potential hydrocarbon trap generation, acting as axial conduits or transverse terraces for sediment transport during, or after, graben formation (Gabrielsen et al., 1995).

5.2.5 Vesterålen margin segment

The Vesterålen margin segment marks a change in dip polarity of the basin-bounding faults compared to that of the Lofoten margin segment. In the South Vesterålen sub-segment, the set of ENE-WSW striking and NW-dipping faults (Fig. 5.14) indicates the northern terminations of the West Lofoten Border Fault Zone and of the Havbåen Sub-basin (Figs. 4.10-4.16, 5.17-3). Once these faults die out in a northward direction (Central Vesterålen sub-segment), the displacement and deformation within the area is taken up by major NNE-SSW striking and east-dipping faults of the East Jennegga High Fault Zone and the Pyramiden Fault Zone (Fig. 5.18). The East Jennegga High Fault Zone and Pyramiden Fault Zone can be traced along-strike for more than ~60 km and ~80 km (Figs. 4.25, 5.14), and show maximum vertical offset of ~1 s and ~1.5 s TWT, respectively (Fig. 5.18).

In the South Vesterålen sub-segment, the sediment infill is observed to be more controlled by the east-dipping faults of the East Jennegga High Fault Zone, together with a fault zone here termed the Pyramiden Fault Zone (Fig. 5.17 profile-3). The Pyramiden Fault Zone, with a throw of ~1.5 s TWT, is a basement-involved fault to the east of a prominent rotated fault-block (i.e. Vesterålen High, VH; Fig. 4.27). The Vesterålen High is located in the central part of the area as an elongated intra-basin high, and its areal position defines to the east and west, respectively, two additional narrow and elongated sub-basins here named Vesterålen Sub-basin 1 and Vesterålen Sub-basin 2 (VSB1 and VSB2) with minimal extend into the Vesterålen margin segment (Figs. 4.25, 4.27). In these sub-basins, the Jurassic seismic sequence S1 has, in general, constant thickness of less than ~500 ms TWT, but minor thickness variations occur and are related to growth faulting (5.17 profile-3). The Middle Jurassic (MJ) reflector (in the places where it can be interpreted) appears as a dragged-up reflector within this seismic unit (S1) supporting the syn-rift origin (Fig. 5.18 profile-4). As in the south of the study area, there is evidence of syn-sedimentary faulting indicated by the internal seismic stratification and configuration of thin Jurassic (< 400 ms TWT) and thick Lower Cretaceous (~1.3 s TWT) units on both the eastern and western flanks of the Vesterålen High towards the Pyramiden Fault Zone and the East Jennegga High Fault Zone, respectively (Fig. 4.27). In contrast, prominent growth of the Lower Cretaceous seismic sequences (S2 and S3) is observed towards the fault-planes of the Pyramiden Fault Zone and the East Jennegga High Fault Zone (Fig. 5.18 profile-5). In addition, the sub-continuous and internally stratified Lower Cretaceous seismic sequences are observed blanketing the basement-imposed rift topography in all the area (Figs. 5.17 profile-3, and 5.18 profile-4 and

profile 5). Thus, there is evidence in this area for an initial rift episode that was initiated during Middle-Late Jurassic and escalated during Early Cretaceous with more developed faults. In the south part of this margin segment, a westward progradation of Jurassic and Lower Cretaceous sequences is observed with the sequences onlapping towards an apparent high, informally named the Myre High (MH) (Fig. 5.18 profile-4). Similarly, in the north of the margin these units are truncated by another less prominent high, informally named the Nøss High (NH) (Fig. 5.18 profile-6). No major accumulations of Upper Cretaceous seismic sequences are preserved at this part of the margin (< 500 ms TWT in thickness).

Towards the Central and near North Vesterålen sub-segments the Pyramiden Fault Zone is truncating and down-faulting the basement structure, and where reflectivity is observed below the Triassic-Lower Jurassic (T-LJ) horizon this has a wedge-shaped character (Figs. 5.18 profile-4 and profile-5). This internal geometrical character is thus evidence for local pre-Jurassic rifting. Farther north, the fault throw intensity of both the East Jennegga High Fault Zone and Pyramiden Fault Zone is substantially reduced to less than ~0.5 s TWT (Fig. 5.18 profile-6). Moreover, a series of intense, and younger NE-SW striking and NW-dipping faults within a fault complex, referred to here as the North Utrøst Ridge Fault Complex, detach onto a common low-angle fault-plane within undifferentiated Cretaceous units (Fig. 5.18). The North Utrøst Ridge Fault Complex rests on top of a fairly buried Jennegga High on the South Vesterålen sub-segment (Fig. 5.18 profile-4), and continues to propagate in a north-eastward manner as basement is further buried following the same trend.

In the same area, the Jurassic seismic sequence S1 exhibits minor internal reflectivity compared to the Lower Cretaceous sequences (S2 to S4) and to that observed in the south (Fig. 5.18 profile-4 and 5). Several faults with smaller vertical offset (~200 ms TWT) cross-cut the Jurassic unit and the lower part of sequence S2 at the Base Cretaceous Unconformity (BCU). However, towards the north of the margin these faults disappear. All these seismic units are observed to prograde in a general westward manner across the margin. Only the Jurassic (S1) and the lowermost Cretaceous (S2 and S3) sequences appear to be present under the North Utrøst Ridge Fault Complex, whereas the upper Lower Cretaceous (S4 and S5) sequences (and likewise the APT, ALB, and ICEN reflectors) are abruptly truncated by the prominent fault complex (e.g. Fig. 4.9). The latter sequences (S4 and S5), together with the limited accumulations (< 700 ms TWT thickness) of the Upper Cretaceous sequence S6, are not able to be mapped or to be correlated inside the North Utrøst Ridge Fault Complex due to

the extensive faulted nature and the intense reflectivity pattern of the strata within the fault complex. Evidence of syn-sedimentary faulting is observed towards the upper part of the North Utrøst Ridge Fault Complex, and some of the westernmost fault-planes are onlapped by Cenozoic units (S8 and S9) (Figs. 4.9 and 5.18). Furthermore, the truncation of lava flows to the west of the North Utrøst Ridge Fault Complex evidences that the fault complex must have been elevated enough at breakup time (~55 Ma) for the basalts not to be able to climb on top of the intense Cretaceous rotated fault-blocks (e.g. Figs. 4.9, 4.24). A similar seismic character is also observed in the south Lofoten margin segment on the West Røst High Fault Complex (WRHFC; Fig. 4.7) (Tsikalas et al., 2019), that provides similar evidence and details of composite Late Cretaceous-Paleogene rifting which is in agreement with previous interpretations (Tsikalas et al., 2001; Hansen et al., 2012).

The Cenozoic seismic sequences are found with thicker accumulations at this area (~2 s TWT thickness) compared to the south of the margin, as the outer part is widened in a north-easterly direction (Fig. 5.14). Discontinuous and sometimes chaotic internal reflectivity dominates within these units. Despite this, there is a general westward prograding trend indicated by some more continuous reflections towards the upper sequences. More continuous and brighter amplitude reflections are also occasionally observed below the lava flows that are correlated to the Top Paleocene (TPAL) reflector, indicating a likely local preservation of sedimentary successions below them.

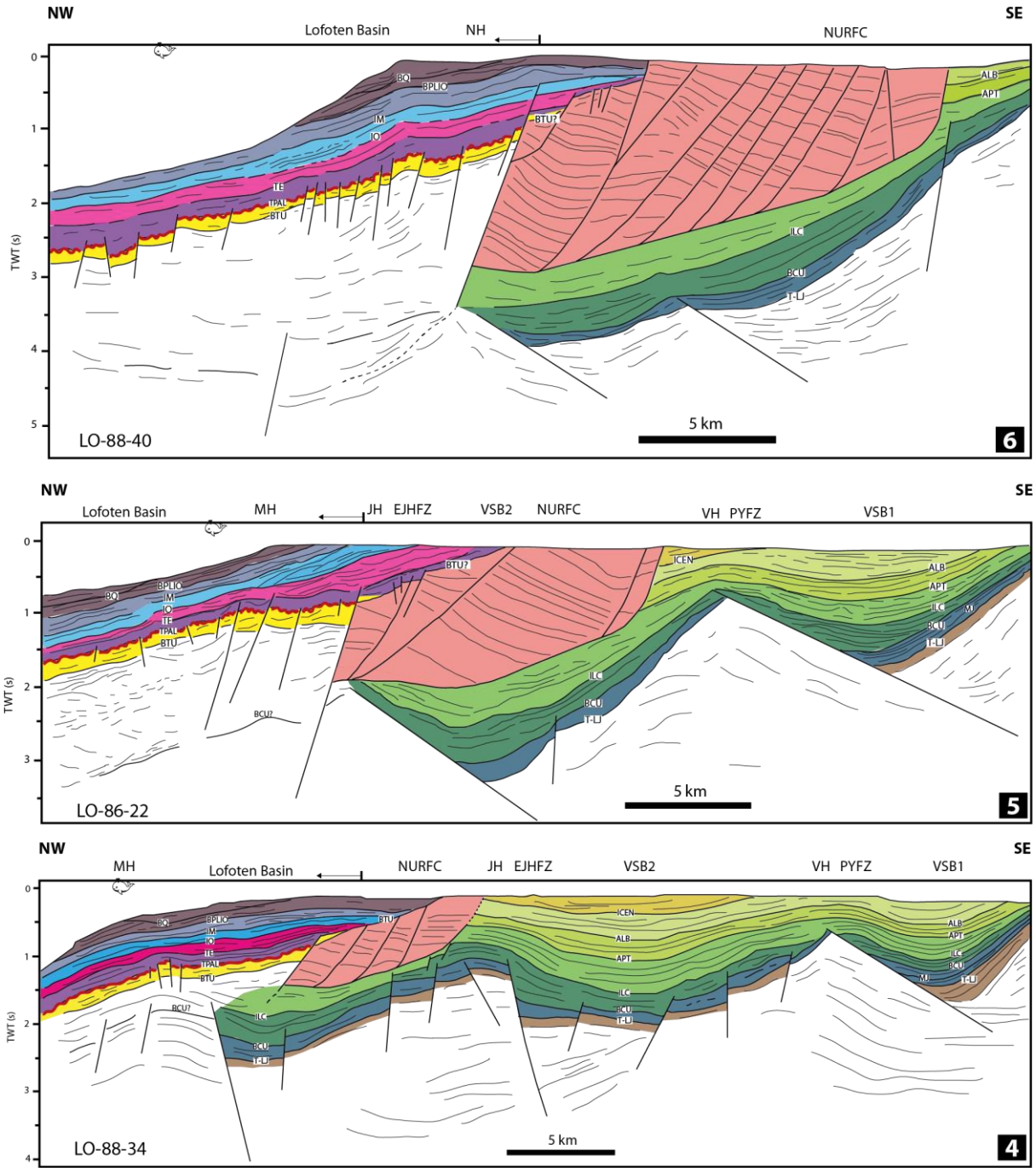

Fig 5.18: *Line-drawing interpretation of relevant seismic profiles for the Vesterålen margin segment illustrating the main structural elements. Colour legend and abbreviations as in Figs. 4.6 and 4.26. Profile locations in Fig. 5.14.*

5.2.6 Andøya transfer zone

The Andøya transfer zone is a tentative accommodation zone defined in this study, and some aspects were considered for its definition and suggested location. The first aspect is that E-dipping faults of the North Vesterålen sub-segment appear to gradually die-out towards the northern parts of the study area (Figs. 5.14 and 5.16). Nonetheless, no obvious/definite high- or low- relief accommodation zones were observed. Despite this, the presence, although

minimal, of basement-involved W-dipping faults may suggest that a shift in structural style occurs between this part of the study area and the northern parts of the Vesterålen segment. In addition, the magnetic map (Fig. 5.15b) displays a minimal lateral shift just north of the Nøss High.

5.2.7 Andøya margin segment

The structural complexity in the northern part of the study area, the Andøya margin segment, is substantially increased, and the margin physiography is dominated by the North Utrøst Ridge Fault Complex (Figs. 5.18-6 and 5.19). Thus, this part of the LVM has shifted to dominant NW-striking and W-dipping faults linked to the development of the prominent fault complex, and without evidence of the E-dipping faults of the East Jennegga High Fault Zone and Pyramiden Fault Zone. Basement elevation is also observed to have decreased at least by ~3 s TWT in the seismic profiles and in the time-structure map of BCU (Fig. 5.14) compared to that on the central part of the Vesterålen margin segment. Similar to the Lofoten margin segment, deep-rooted and W-dipping faults are also observed in the Andøya margin segment underneath the North Utrøst Ridge Fault Complex (Fig. 5.19). However, their occurrence is less frequent and they display significantly less fault-throw intensity compared to the other margin segments in the south (Figs. 5.17 and 5.18). Two additional structural elements have been also identified below the North Utrøst Ridge Fault Complex on seismic and potential-field data, and were informally named as the Andøya Syncline (ANS) and the Andenes High (AH) (Figs. 4.25, 4.26, 4.28; cf. subchapter 4.5). The AH area is observed to have undergone Cretaceous and Paleogene deformation in the form of an uplifted block characterized by intense sill intrusions, that was informally named the Andøya Volcanic Mound (AVM) (Fig. 4.25).

The Jurassic (S1) and the Lower Cretaceous (S2 to S4) seismic sequences increase in thickness in the Andøya Syncline and towards the fault-plane in the eastern flank of the Andenes High/Andøya Volcanic Mound. Furthermore, a north-eastward increasing rate of accommodation space with sedimentary successions underneath the North Utrøst Ridge Fault Complex is observed, and the previously (in the south) truncated APT and ALB seismic reflectors by this fault complex are now able to be interpreted below it at this margin segment (Fig. 5.19). Therefore, in this area there is evidence for Late Jurassic-Early Cretaceous extension.

Due to the structural dominance of the North Utrøst Ridge Fault Complex on the basin architecture of the Andøya margin segment, and the intense sedimentary reflectivity and faulting, no detailed stratigraphic correlations of the Upper Cretaceous seismic units are able to be differentiated here (Fig. 5.19). Higher uplift and erosion rates are evidenced for this part of the LVM that makes difficult the precise stratigraphic and structural correlation of the sedimentary units, especially within the fault complex. In general, the Cretaceous fault complex at this margin segment is observed to not be associated with elevated basement and basement-related faults (e.g. Tsikalas et al., 2001). Nonetheless, towards the westernmost parts of the North Utrøst Ridge Fault Complex the Andenes High/Andøya Volcanic Mound seems to be linked to deeper crustal parts, and as in the Vesterålen margin segment, the faults there are interpreted to deform Paleogene strata (Fig. 5.19).

Paleogene-related extension in the outer part of the margin is observed to be related to a prominent W-dipping fault-plane (~2.5 s TWT) in the western flank of the Andenes High/Andøya Volcanic Mound (Fig. 5.19 profile-8). This fault separates the thick (~2 s TWT) Cenozoic seismic sequences and the Lofoten Basin from the faulted Mesozoic terrain of the inner part of the Andøya margin segment. The lava flows are confined by this fault, and they cannot climb on top of the North Utrøst Ridge Fault Complex or to the more eroded layers of Cenozoic units on the continental slope (Figs. 4.25, 4.26 and 5.19). On the other hand, the continent-ocean boundary (COB) can be observed on the northernmost part of this margin segment and in the western vicinity of the prominent fault indicated by the presence of seaward dipping reflectors (SDR) (Fig. 5.19 profile-8).

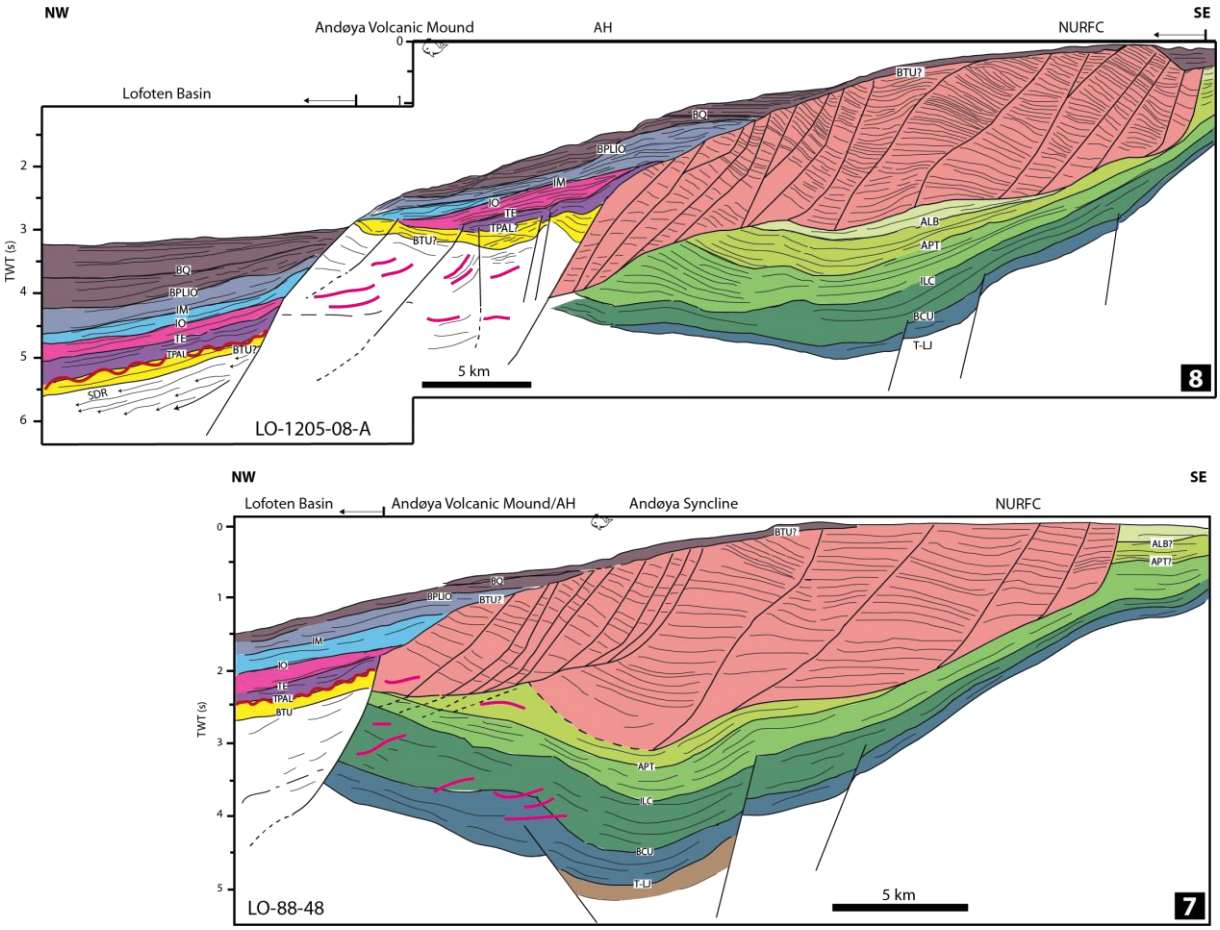

Fig 5.19: *Line-drawing interpretation of relevant seismic profiles for the Andøya margin segment illustrating the main structural elements. Colour legend and abbreviations as in Figs. 4.6 and 4.26. Profile locations in Fig. 5.14. SDR: sea-dipping reflections.*

5.3 North Utrøst Ridge Fault Complex: tectono-stratigraphic evolution

The 3D seismic survey (NPD-LOF1-09) is used to further study and to characterize in a better and more detailed manner the Late Cretaceous-Cenozoic deformation related to the development of the North Utrøst Ridge Fault Complex (NURFC) (Fig. 5.20).

5.3.1 Time constraints on rift phases

The faults of the NURFC are, in general, planar in shape in their upper parts, and sole out to become more low-angle with depth (Figs. 4.9, 4.24, 5.21-5.24). Thus, the geometry of the NURFC is that of a set of multiple and rotated fault-blocks with (undifferentiated) Cretaceous sequences. Seismic interpretation also suggests that the Upper Cretaceous seismic units progressively become more dominant (thicker/occupying the largest part of the sequences within the fault complex) within the NURFC towards the northeastern part of the LVM on the Andøya margin segment (Figs. 5.19 and 5.24 profiles l-n). Thus, the timing of the initiation of the NURFC can be constrained as early Late Cretaceous.

The intense sedimentary reflectivity and faulting (in combination with the moderate seismic resolution) makes impossible any systematic attempt to correlate the mapped stratigraphy in the rest of the study area within the numerous sub-parallel reflections composing each set of fault-blocks. Below and on top of the NURFC the lowermost Cretaceous seismic sequence S2 and the uppermost Cretaceous-Paleogene units are observed with wedge-shaped geometries, respectively, and they may be related to syn-sedimentary faulting (Figs. 5.21a-b, 5.22c, 5.23a, 5.24a-i). In the easternmost part of the complex, the faults form a detachment or décollement plane that mostly runs sub-parallel to the Base Cretaceous Unconformity (BCU) and the shale-dominated Lower Cretaceous units, and in particular sequence S3 in the Vesterålen margin segment (Figs. 4.24, 5.18 and Fig. 5.21a). Such detachment plane acts, in addition, as a pathway for fault propagation at depth (Figs. 5.21d, 5.22d).

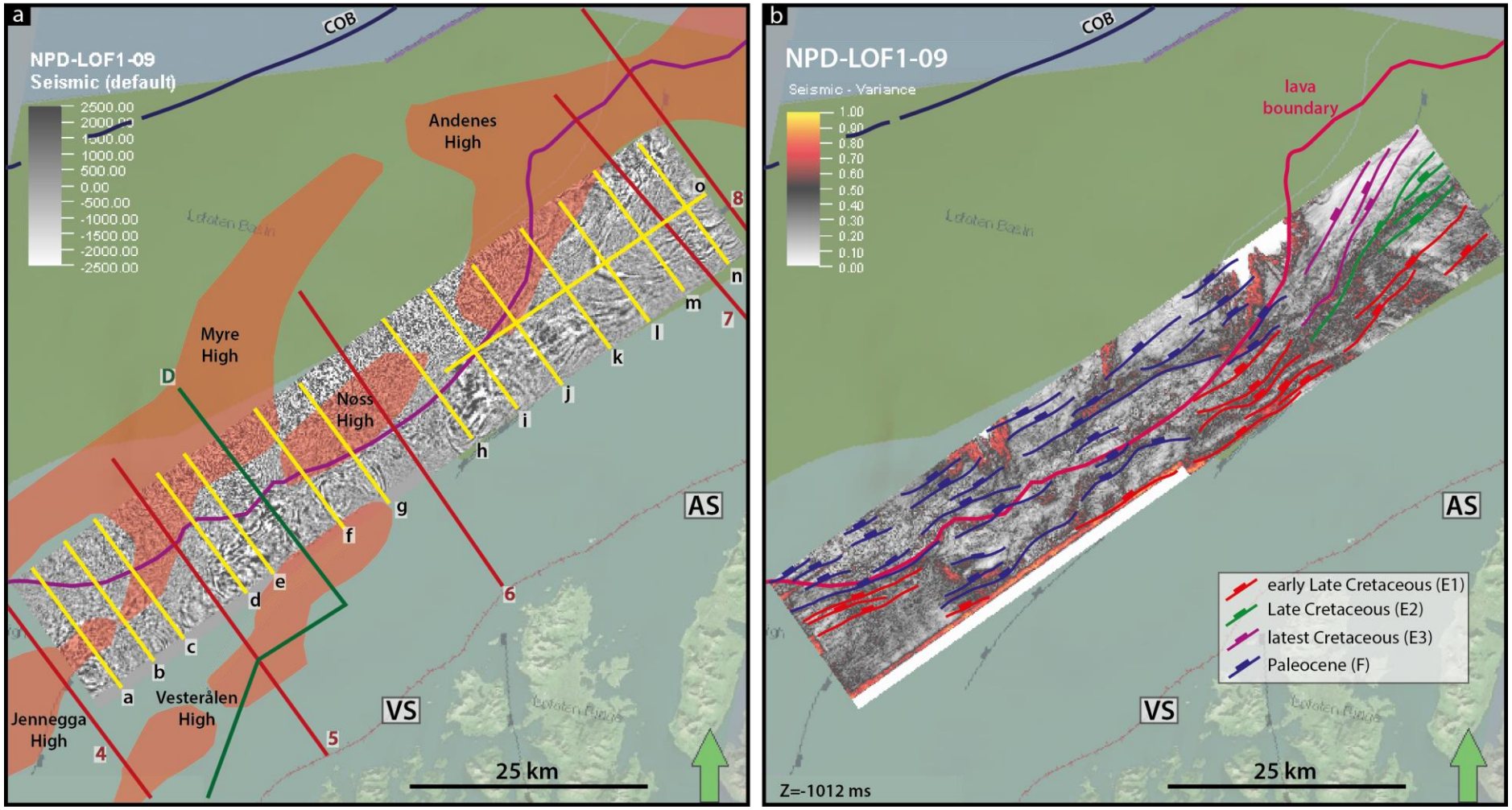

Fig 5.20: (a) *3D seismic survey (NPD-LOF1-09) with location of interpreted/line-drawing interpretation of seismic profiles with raster of new/refined structural elements coverage. Time-slice at 4180 ms, TWT.* ***(b)*** *Seismic attribute variance overlaid with west-dipping Late Cretaceous faults families (mostly located east of the lava boundary) and Paleocene faults family in blue (mostly located west of the lava boundary). Note the good match of interpreted faults within the high-variance regions in red. Time-slice at 1012 ms, TWT. Abbreviations in Figs. 4.10 and 4.26.*

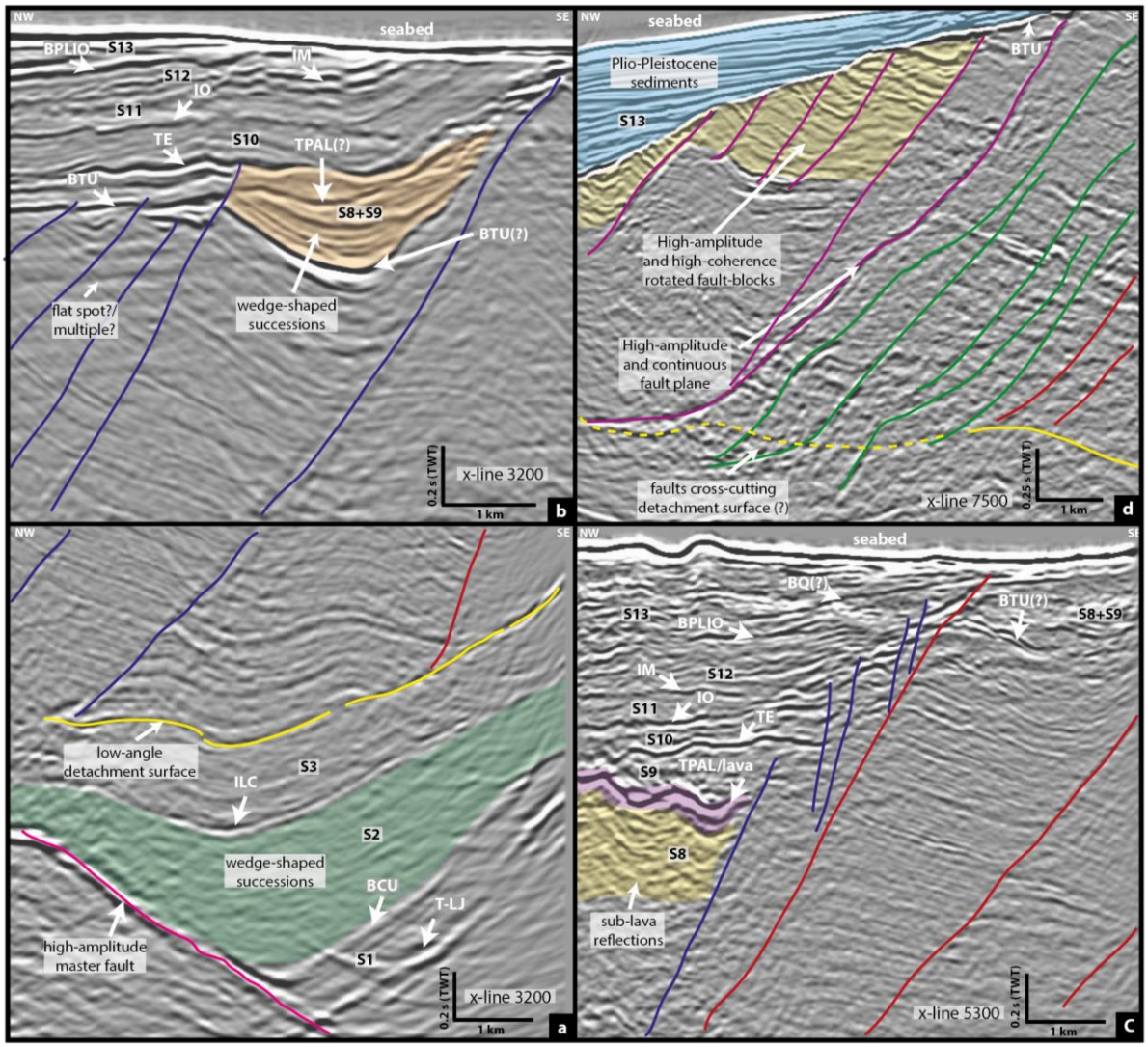

Fig 5.21: *Seismic expression of the North Utrøst Ridge Fault Complex (NURFC) and surrounding areas. Late Mesozoic faults are indicated in pink lines, while the detachment surface in yellow lines; colour legend for Late Cretaceous and Paleocene faults families in Fig. 5.20b. The interpreted key horizons are also indicated. Seismic examples from the NPD-LOF1-09 3D seismic survey. Profile locations on inset map of Fig. 4.24.*

Listric faults often indicate large-scale tectonism and displacement, associated with long-lasting faulting activity (Lister et al., 1991; Blaich et al., 2011). The maximum vertical offset of faults in the central parts of the NURFC is ~1 s TWT, and can be observed on the Vesterålen margin segment (Fig. 5.24a-h). Towards the north of the margin, the maximum vertical offset of faults in the central parts of the complex is slightly incremented (Fig. 5.24i-n). In addition, faults located towards the west of the NURFC seem to become steeper, as some appear to reactivate pre-existing structures or to generate more detachment surfaces (Fig. 5.19 profile-7). The seismic reflector that truncates the NURFC in all its extent is the Base Tertiary Unconformity (BTU), which is also interpreted as an erosional surface on top of

this fault complex (Figs. 5.21d, 5.22d, 5.23b). The BTU truncation character is also observed as Cretaceous strata toplap onto the seismic reflector (Figs. 5.21b-d and 5.22a). This indicates that fault complexes of this nature could have been more pronounced and affecting thicker packages of sedimentary units (Tsikalas et al., 2019). BTU is also offset by faults in the western part of the complex, although with minor throws (Figs. 5.18 profiles 5 and 6, 5.21b-c). Furthermore, as described earlier, the lava flows related to the Paleocene-Eocene lithospheric breakup cannot flow uphill the fault complex, hence this demonstrates the formation and presence of the NURFC as an elevated feature prior to breakup (Figs. 5.21c, 5.22a and 5.23c, 5.24a-j).

Many similarities exist, in terms of fault geometries and fault development, between the NURFC and the West Røst High Fault Complex (WRHFC) observed in the southernmost Lofoten segment (Fig. 4.7; Tsikalas et al., 2019). Similar fault-pattern observations and details on fault timing on the WRHFC have helped to confirm and constrain the Late Cretaceous-Paleocene rift-related activity in the northern parts of the LVM and the study area, and are tied to the development of the NURFC (Figs. 5.19b, 5.22b). In addition to the wedge-shaped geometries on top of the NURFC, latest Cretaceous-Paleocene rifting and mainly new Paleocene faults are also indicated by the presence of faults with Paleocene affinity down-faulting the Base Tertiary Unconformity (BTU) seismic reflector, mainly to the west of the NURFC (Figs. 5.18, 5.19, and 5.21). Those faults exhibit their largest throws near the edge of the landward breakup lava boundary and in the transition between the inner and outer margins (Figs. 5.19-5.21), and are observed with steeper angles in comparison to pre-Paleocene faults. Locally, the Paleocene faults represent re-activation of earlier Late Jurassic-earliest Cretaceous and Cretaceous faults (Tsikalas et al., 2019), but in several places initiation of several new fault sets took place (Figs. 5.20c and 5.21a-c). In some places, Paleocene faults clearly cross-cut the low-angle detachment surface and the Lower Cretaceous units (Figs. 5.20d, 5.21c-d, 5.23b-f). All these observations contribute to decipher the late phases of tectonic activity in the vicinity of the NURFC.

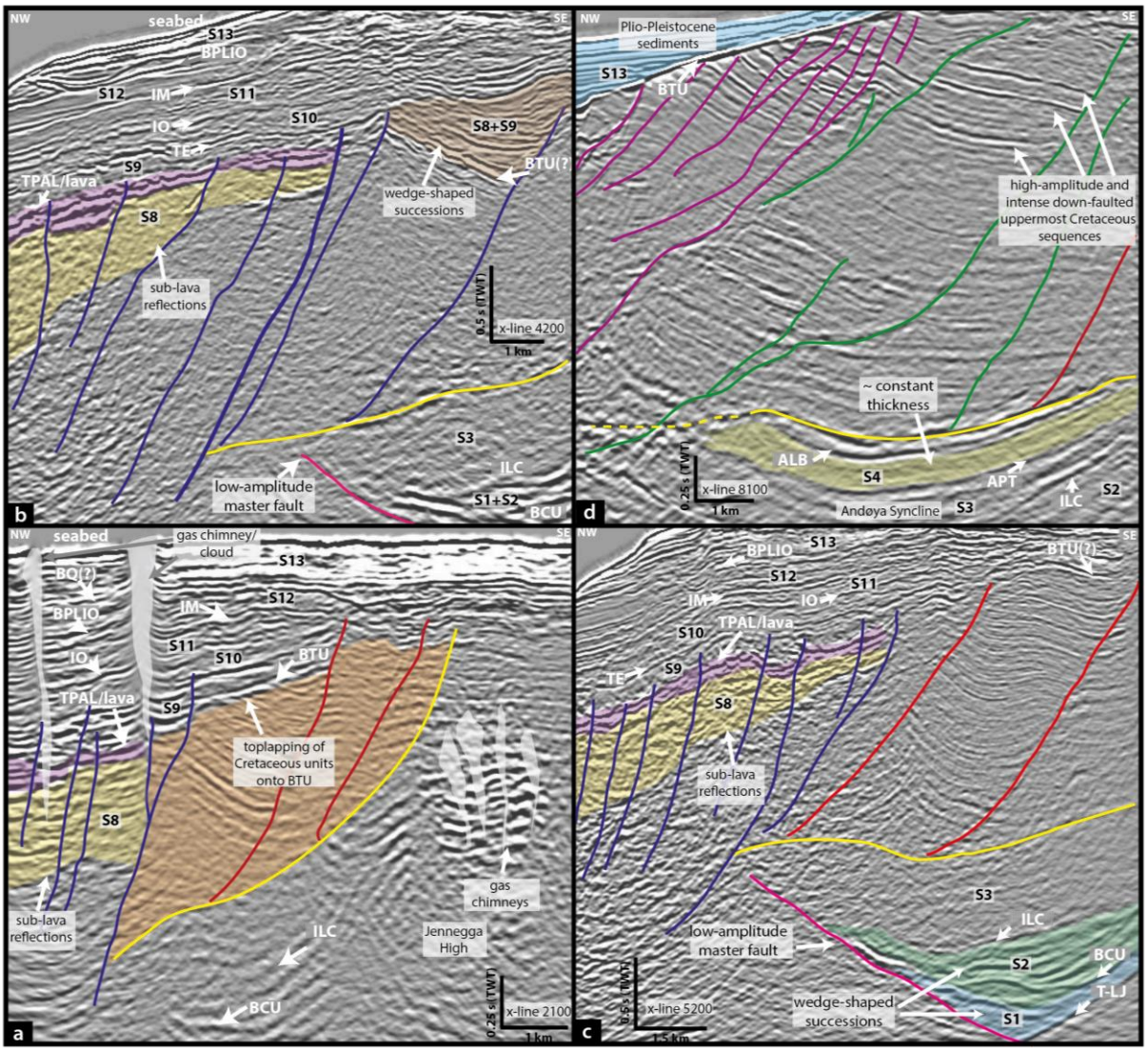

Fig 5.22: *Seismic expression of the North Utrøst Ridge Fault Complex (NURFC) and surrounding areas. Late Mesozoic faults are indicated in pink lines, while the detachment surface in yellow lines; colour legend for Late Cretaceous and Paleocene faults families in Fig. 5.20b. The interpreted key horizons are also indicated. Seismic examples from the NPD-LOF1-09 3D seismic survey. Profile locations on inset map of Fig. 4.24.*

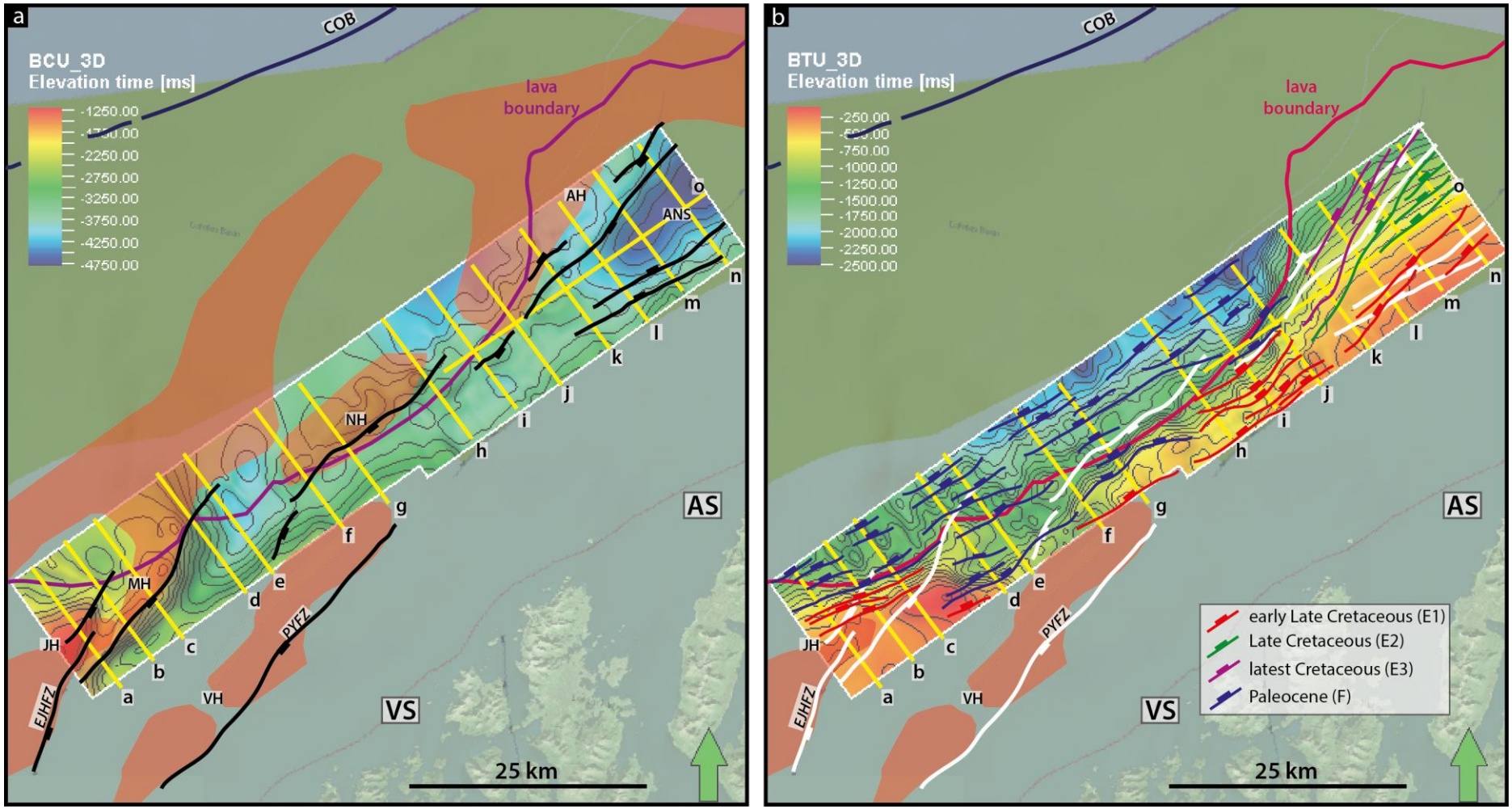

Fig 5.23: (a) *Base Cretaceous Unconformity (BCU) (contour interval: 200 ms) and* ***(b)*** *Base Tertiary Unconformity (BTU) (contour interval: 100 ms) time-structure maps gridded from the 3D seismic survey (NPD-LOF1-09). Active faults are indicated with colour, while inactive in white. Late Cretaceous faults families (mostly located east of the lava boundary) and Paleocene faults family (mostly located west of the lava boundary) on the BTU time-thickness map are all west-dipping. All faults are draped above the surface. Abbreviations in Figs. 4.10 and 4.26.*

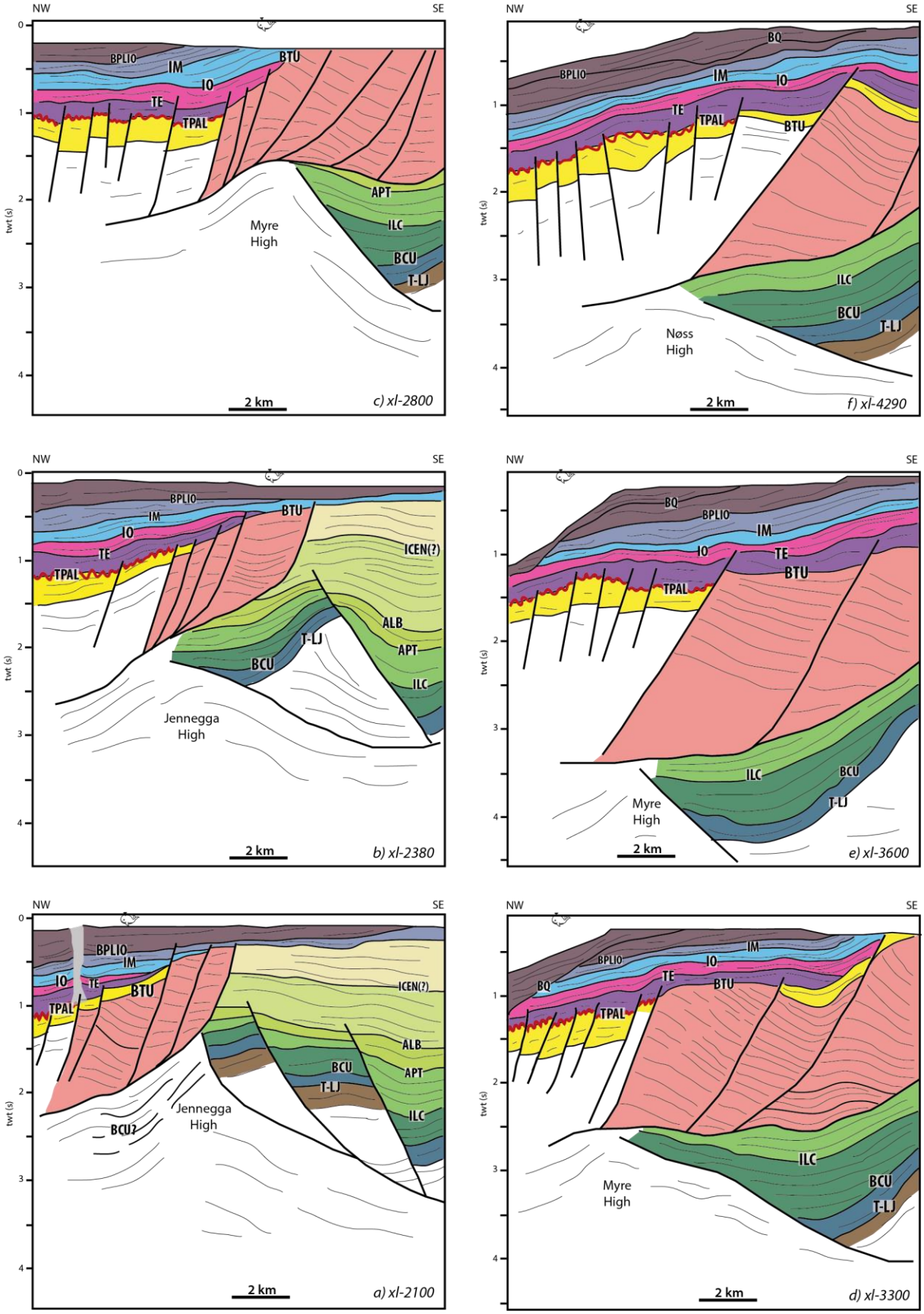

Fig 5.24: *Line-drawing interpretation of relevant seismic profiles from the 3D seismic survey (NPD-LOF1-09) illustrating the main structural elements and basin architecture. Colour legend and abbreviations as in Fig. 4.6. Profile locations in Figs. 5.20a and 5.23.*

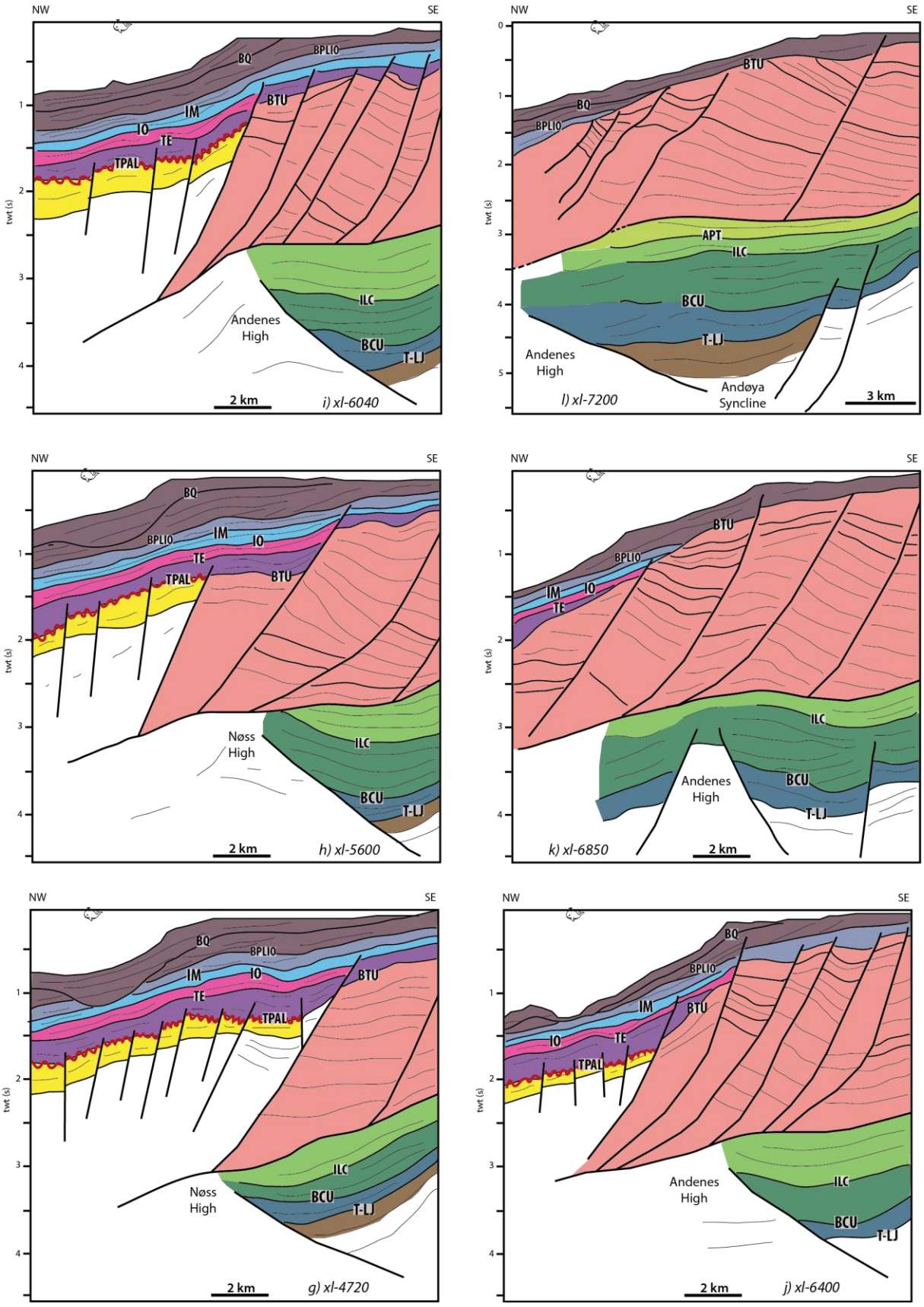

Fig. 5.24: *(continuation)*

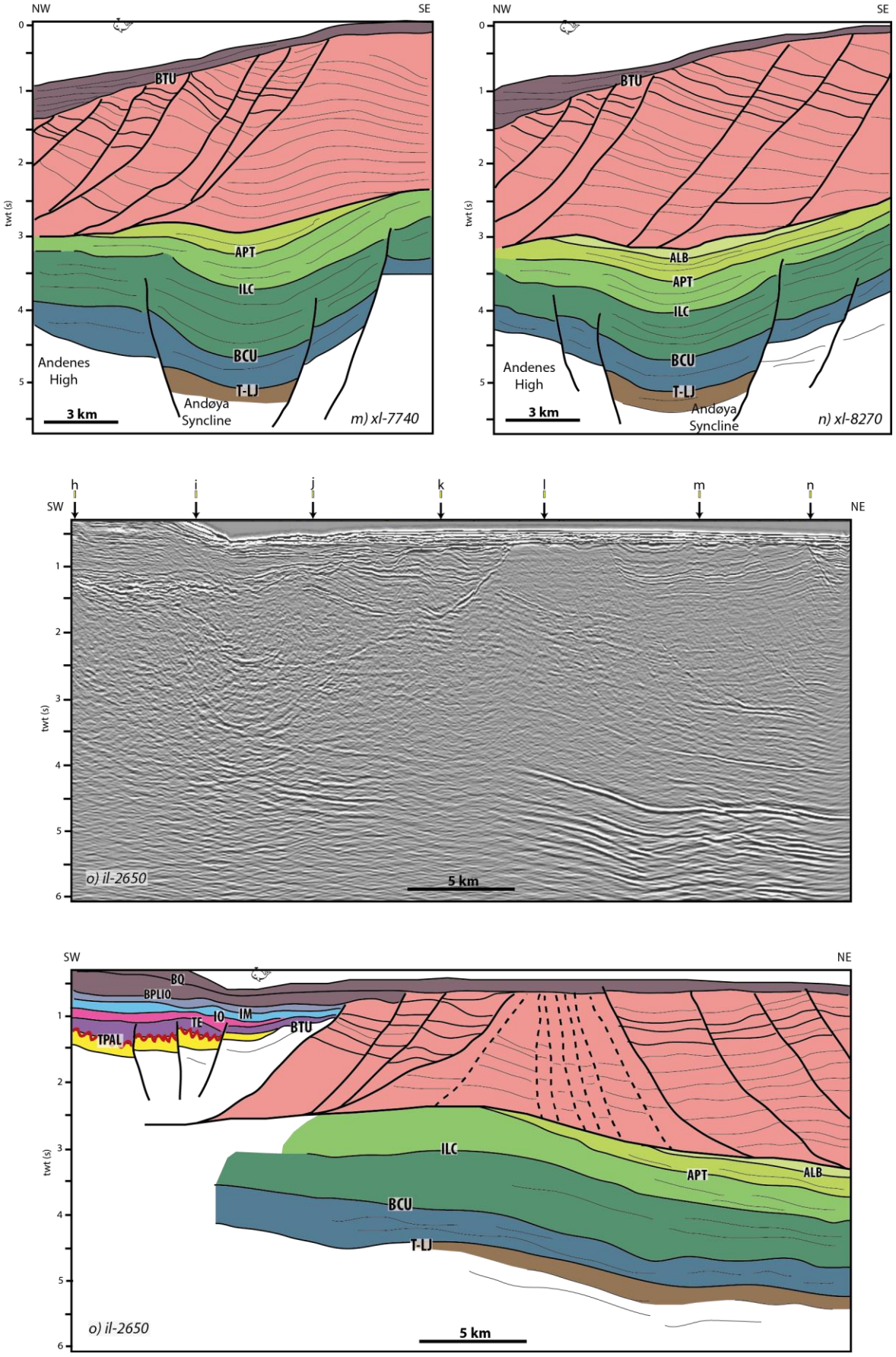

Fig. 5.24: *(continuation)*

5.3.2 Fault families

Key seismic profiles (Figs. 5.17-5.19, 5.24) and geometric correlations with the WRHFC and its vicinity in the south Lofoten margin (Tsikalas et al., 2019) have been used to identify the main fault families in the study area and to relate them to distinct rift pulses in the NURFC and its vicinity. The observations are supported through the observed lateral thickness variations (i.e. wedges) across faults and the fault character. In this context, the main fault families and evolution within the study area can be summarised as follows (Fig. 5.25) (main emphasis is given to the Late Cretaceous phases as these are revealed by the detailed study of the NURFC):

- pre-Jurassic (A)
- Late Jurassic-earliest Cretaceous (B)
- Early Cretaceous (Aptian-Albian) (C)
- mid-Cretaceous (Albian-Cenomanian) (D)
- early Late Cretaceous (E1): NURFC; initial rift phase with wider (in extent) fault-blocks in the east; décollement/detachment surface at slightly deeper levels
- Late Cretaceous (E2): NURFC; second rift phase with more intense faulting, narrower in extent fault-blocks; westward migration of rift activity; décollement/detachment surface at shallower levels; clear separation (in several seismic profiles) between the initial and second rift phases
- latest Cretaceous-Paleocene (E3): NURFC; third rift phase, local episode producing narrow in extent fault-blocks located on the uppermost parts of the fault complex; minimal offset of BTU is observed on top of these structures
- Paleocene (F): NURFC; steep faults located towards west in the outer margin offsetting considerably the BTU; cross-cut the earlier developed Late Cretaceous low-angle décollement/detachment surface(s); sediment wedges on top of the fault complex; landward limit of breakup lava boundary
- post-Paleocene (G): Andøya Volcanic Mound; uplift and erosion associated to volcanic up-building in the outer LVM; NW-oriented subsidence trend in the Lofoten Basin

Pre-Jurassic tectonism is observed in few places of the study area, in particular, the northern part of the Vesterålen segment and in the transition of the Vesterålen and Andøya margin

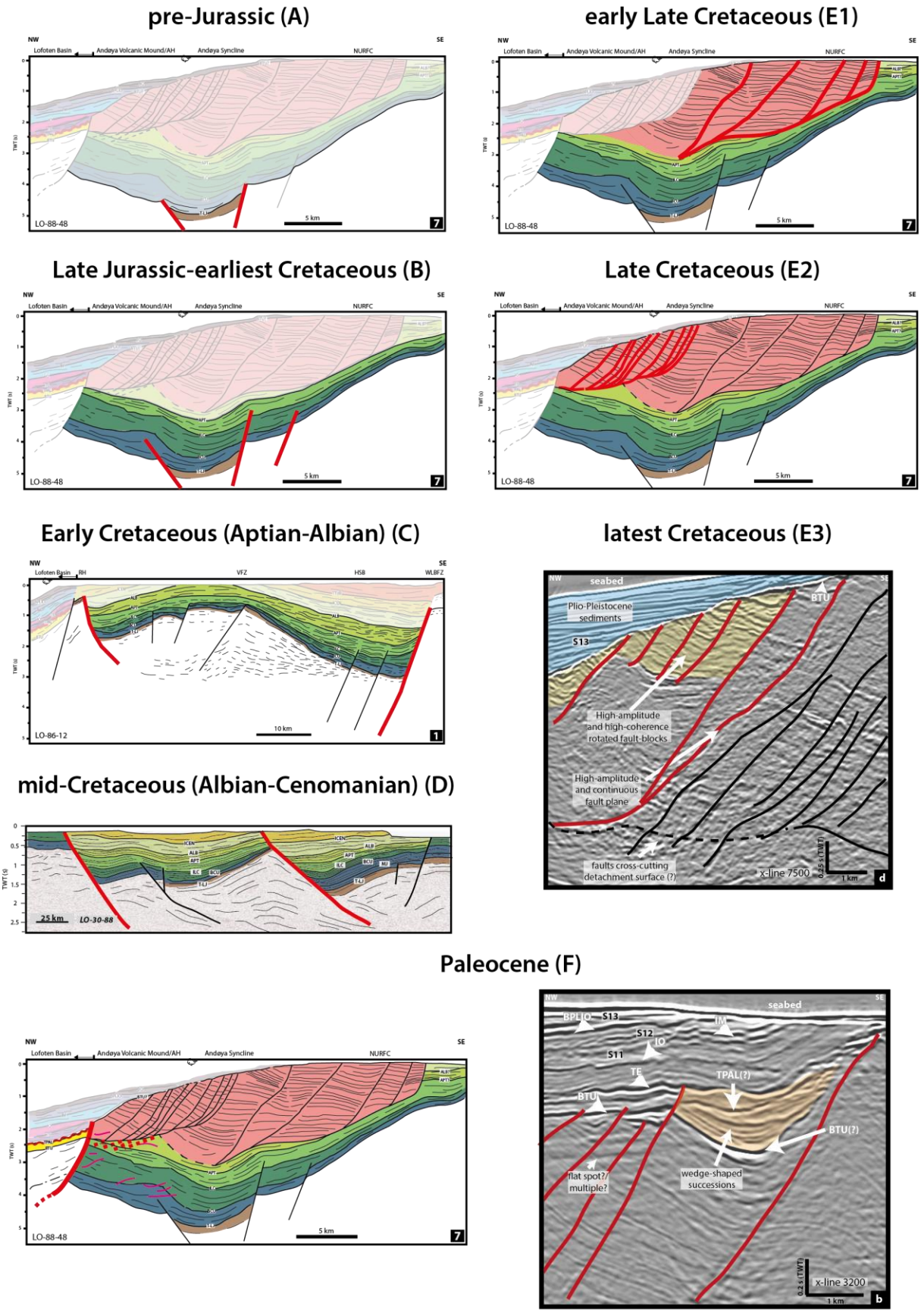

***Fig. 5.25**: Schematic evolution in time of identified fault families within and in the vicinity of NURFC.*

segments (Fig. 5.24c-h). Pre-Jurassic units related to syn-sedimentary faulting are preserved in hanging-walls located to the east side of elevated basement fault-blocks under the NURFC, and observed as semi-transparent or low-amplitude intensity wedge-shaped reflections (Fig. 5.24 profiles a, c, d, f to i). The bounding fault of these reflections is an east-dipping fault bordering the eastern flank of the Myre and Nøss highs (Fig. 5.23a). In addition, pre-Jurassic seismic sequences are believed to exist on the deepest basinal portions of the Andøya Syncline, but growth strata may be absent there (Fig. 5.24 profiles-l to o).

Late Jurassic-earliest Cretaceous rifting is considered as the most important tectonic event for the structuration of this studied portion of the LVM (Fig. 5.24), and it is in agreement with previous observations from Hansen et al. (2012) in terms of fault dominance (e.g. Figs. 4.6-4.9). This major extensional event is reflected in the considerable thickening of lowermost Cretaceous seismic sequence S2 (Fig. 5.24a-k). In the southern part of the 3D seismic survey, the Jennegga High appears to plunge at deeper depths in the form of a set of individual fault-blocks tilted to the west and bounded by east-dipping faults detaching to a single décollement plane underneath the NURFC (Figs. 4.24, 5.24a-b). As deformation continues towards north, the Jennegga High is observed to plunge towards north and to be buried beneath the Lower Cretaceous successions, while the Myre High becomes an elevated and more prominent high (Fig. 5.24b-e). The Myre High, in turn, is buried at deeper depths towards the north, and the deformation is taken up by an east-dipping fault bordering the eastern flank of the Nøss High (Figs. 4.26, 5.24f-j). Up to this point, it has been validated through seismic/structural interpretation that east-dipping faults in the studied area of the LVM have initiated prior to Jurassic and continued to be active until at least earliest Cretaceous. This latter observation contrasts the suggested Late Jurassic initiation of fault activity proposed by Bergh et al. (2007) for these east-dipping faults along the LVM. The Lower Cretaceous sequence S3 and the mid-Cretaceous sequence S4 (where it is possible to be mapped) appear rather constant in thickness towards the margin segments in the north (Figs. 4.6, 4.8, 5.22d, 5.24). Thus, a period from active syn-sedimentary faulting to tectonic quiescence is interpreted for these units. Subsequently, a distinct rift pulse is documented during Aptian-Albian in the southernmost part of the Lofoten margin segment, and may have escalated towards Cenomanian time (Tsikalas et al., 2019). Evidence for these pulses in the study area are present in the Havbåen Sub-basin as moderate-to-weak dragged-up sequences (S3-S5), and are controlled and guided by the West Lofoten Border Fault Zone (Fig. 5.17 profile-1). Fault re-activation is interpreted during Early to mid-Cretaceous times on the southernmost part of

the Vesterålen High (Figs. 4.27, 5.25), and within the area where the Jennegga High becomes a buried structural element (Fig. 5.24a-b). All these observations are attributed to an Early Cretaceous (C fault family) and a mid-Cretaceous (D fault family) rift phase, respectively.

The broad Late Cretaceous-Paleocene rifting episode within the LVM has been linked to the deformation related to the development of the NURFC. Since no detailed seismic correlations of the main horizons (Fig. 4.1 and Table 4.1) were able to be performed within the NURFC, the characterization of the Late Cretaceous-Paleocene rifting event is somehow reduced. Nevertheless, Figure 5.24 depicts a portion of the basin architecture of the Vesterålen and Andøya margin segments, and there is some good evidence to suggest that Aptian-Albian sequences are subordinate sedimentary successions within the fault complex (Figs. 5.18 profile-6, 5.19, 5.24 profiles j-o). The faults in the NURFC are steep in the upper part of the fault complex, and sole out in the deeper parts at a detachment/décollement surface (Fig. 5.24). Seismic interpretation also suggests that there is the possibility for more than one décollement surface/fault; in particular, towards the Andøya segment (Figs. 5.19 and 5.24k-n). Along this margin segment, a more SW-dipping orientation is observed for the faults of the NURFC in the North Vesterålen sub-segment, and the fault orientation gradually changes into a more NE-dipping trend towards the north (Fig. 5.24 in-line profile-o).

The faults in the NURFC are believed to have been initiated as steep planar normal faults and continuous faulting has led to two possible detachment evolutions, similar to the West Røst High Fault Complex in the south Lofoten margin (Tsikalas et al., 2019). As a consequence, the internal configuration and rotation of the individual fault-blocks composing the NURFC is directly influenced by the underlying Late Jurassic-Early Cretaceous rift topography. Therefore, at locations where prominently elevated basement highs, such as the Jennegga and/or Myre highs, were present underneath have made the detachment/décollement surface to be more rotated and to become more low-angle. This resulted in an increase of the internal rotation of Cretaceous fault-blocks (Figs. 5.18 profile-5, 5.24a-d). On the contrary, at locations where there was a less prominent basement high at depth, the décollement plane propagated sub-parallel to the underlying Lower Cretaceous strata (Figs. 5.19, 5.24 profiles j-o).

Observations on fault propagation within the West Røst High Fault Complex (WRHFC) have shown that faulting was initiated to the east and gradually propagated towards west (Tsikalas

et al., 2019; Fig. 4.7). Similarly, this is partly evidenced for the study area in the Vesterålen margin as Aptian-Albian seismic units, or younger Upper Cretaceous strata, are not able to be correlated farther to the west where the intensive faulting related to the NURFC commences (Figs. 5.18, 5.19, 5.24a-b). In addition, some down-faulted reflections with similar reflection character (hence a possible similar age correlation) have been identified across the individual rotated fault-blocks showing the same westwards fault propagation trend, together with an apparent westwards increase in fault throw intensity (E2 fault family; Figs. 5.21-d, 5.22-d, 5.24 profile-d, and profiles-h to o).

The final rift phase is recorded within the studied area of the LVM during Paleocene, and represents the late stage of the composite Late Cretaceous-Paleocene rift event (Fig. 5.25). This rift phase is represented by a distinct group of faults (F fault family) on the western side of the NURFC, and is characterized by steeper faults in comparison to the earlier Late Cretaceous faults (Figs. 5.21, 5.22, 5.24). These faults offset considerably (~0.5 s TWT) the BTU reflector, and locally cross-cut the low-angle detachment surface (Figs. 4.6-4.9, 4.24, 5.19 profile-7, 5.21-d, 5.22b-d, 5.24). Growth faults or apparent lateral thickness variations are observed towards the top of the NURFC, hence, the latest Cretaceous-Paleocene rifting event (E3 fault family) is expressed as steeper uppermost Cretaceous reflections and wedges of Paleogene sedimentary units (undifferentiated S8-S9) (Figs. 5.21b, 5.22b, 5.24 profiles d and f). The exact timing for this rift phase on the LVM and adjacent margins has been debated, however, it seems to be some consensus on a Campanian/Maastrichtian to Paleocene extension, such as in the case for the northern Vøring Basin/margin (e.g. Blystad et al., 1995; Ren et al., 2003; Zastrozhnov et al., 2018, 2020), the southern LVM (e.g. Tsikalas et al., 2019), and the northern LVM (e.g. Hansen et al., 2012; this study). Furthermore, these Paleocene faults worked as clear tectono-magmatic barriers for breakup-related lava flows, confining them to the outer margin (Figs. 5.17, 5.18, 5.19 profile-7, 5.21-c, 5.22b-d, 5.23-b, 5.24a-j), and separating the continental domain from the later evolved oceanic domain in the northernmost part of the study area (Fig. 5.19 profile-8).

5.3.3 Post-Paleocene evolution

Following the culmination of the Paleocene rift phase and continental breakup at the Paleocene-Eocene transition, the post-Paleocene LVM evolution is that of a continental passive margin (Eldholm et al., 2002). The Cenozoic units are found resting on top of the NURFC, and are observed to be gradually eroded towards the northern parts of the study area

in close proximity to the fault complex on the Andøya margin segment, where only thin glacial Plio-Pleistocene strata are still preserved (Fig. 5.24). In addition, mapping of these Cenozoic units has revealed dome-like features in the area at the transition between the inner and outer parts of the LVM. The presence, dimensions, shape and evolution of these features may be related to the development of massive volcanic bodies in the outer margin (Figs. 5.9-5.13). These dome and volcanic structures are interpreted on seismic data and further visualized in time-thickness maps of sequences S9 to S13, and represent thin time-thickness sediment accumulation areas or areas of non-deposition (Figs. 5.9-5.13, 5.19). The most prominent volcanic structure that was identified is a NE-SW oriented and elongated structure located in the northwestern part of the Vesterålen and Andøya segments, and is informally named in the current study as the Andøya Volcanic Mound (AVM; Figs. 4.25, 4.26). In particular, its western flank is observed to be near the continent-ocean boundary, where the volcanic mound is observed as a prominent elevated structure (Fig. 5.19 profile-8; Tsikalas et al., 2001; this study). Additional domal features that are possibly related to volcanic up-building activity are present in the outer part of the margin off Vesterålen and are believed to have taken place during late Eocene to mid-Oligocene (Fig. 5.10: dome-1 and dome-2).

The Eocene seismic sequence S9 is interpreted to span the time period with probably the most prominent volcanic-building processes in the study area, and it is depicted by the wide Andøya Volcanic Mound (AVM) (Fig. 5.9). Additional domes or elevated features are also observed in the vicinity of the AVM, and farther south (Fig. 5.9). In particular, south of the 3D seismic survey, the Eocene and some Paleocene units onlap the BTU horizon with a gradual doming pattern (Fig. 5.24a-f). Towards north, as the NURFC appears to be inflated and elevated, these sequences become thin or absent (Fig. 5.24 g-k, and o). Subsequently, the time-thickness map of the lower Oligocene sequence S10 shows that the AVM area was an active depocenter, and increased thinning of sediments is observed south of it (Fig. 5.10). In seismic profiles, this sequence is observed to bend upwards as it onlaps the elevated NURFC (Fig. 5.24a-k). The deposition of sequence S10 shifts farther west into the outer parts of the Lofoten Basin in the north of the margin, and the NURFC simultaneously becomes more prominent in its extent on the shelf and continental slope of the Andøya segment (Fig. 5.24l-n). Subsequently, the upper Oligocene to lowermost Miocene sequence S11, similar to sequence S10 in the south, bends just next to the NURFC and is observed top-lapping onto the seabed (Fig. 5.24c-d). Farther north, sequence S11 gently covers the previous elevated topography imposed by the older Cenozoic units and overlies the NURFC until the

southernmost part of the Andenes High (Fig. 5.24i-k). In the same area, tilting of the remaining Cenozoic sequences is increased, and this suggests progressive northwards migration of both depocenters and domes until Miocene (Fig. 5.24k-n). The time-thickness map representing the depositional time interval for sequence S11 (late Oligocene-early/middle Miocene) exhibits that the outer part of the margin was a broad elevated region, especially in the middle and north portions of the study area (Fig. 5.11). A last doming pulse is well delineated as uppermost Miocene in the time-thickness map representing the depositional time interval for sequence S12 (Fig. 5.12). This uplift episode is thought to be related to the final build-up of the AVM, although it appears to be narrower in areal coverage compared to that during Eocene (Fig. 5.9). The post-Miocene to Present tectonic history of the margin culminates with north-westward deepening of the Lofoten Basin (Fig. 5.13) and farther northwards expansion of the elevated Andøya margin (Fig. 5.24k-n). These later processes were accompanied by Plio-Pleistocene glaciations and related gravity mass-waste processes on the entire LVM continental slope (Faleide et al., 2015; Fig. 5.13). Additional observed features related to the Cenozoic evolution of the study area include gas chimneys/clouds located on several parts of the northern Jennegga High area, and these features appear to be related to deeper faulting (e.g. Figs. 5.22a, 5.24a). These latter described features may be related to petroleum systems at depth, however recent estimations for erosional events in the area off northern Vesterålen and its vicinity are believed to have removed up to 3.5 km of rock successions during Late Cretaceous to Early Eocene, together with the last Quaternary glacial event eroding up to 1.5 km of rock layers (e.g. Figs. 4.6-4.9), thus giving little margin for potential hydrocarbon reservoirs preservation (Breivik et al., 2020).

Following the observations described above, a multi-phase growth evolution is suggested for the AVM and associated domal features as there is evidence of distinct phases of vertical movements. This is in agreement with a similar evolution proposed for domal features in the southern Lofoten margin that was associated with possible compression/transpression affecting the area (Tsikalas et al., 2019). The initiation of doming in the study area could have possibly started during latest Cretaceous-Paleocene since the NURFC was already a prominent elevated structure. In addition, the Paleocene sequence S8 appears to be, in general, absent above the NURFC and this supports a pre-Paleocene vertical movement activity. Sequence S8 may have been deposited and later removed by erosion, or may not have been deposited at all as it is observed that the NURFC was an elevated structure/feature at that time and the breakup lavas climb upwards to the west side of NURFC but could not surpass it.

Subsequently, doming was later evolved further during early Cenozoic and reached its maximum extent by mid-to-late Miocene prior to its termination.

The observation of dome-like structures within the studied area of the LVM adds evidence for the well-stablished existence of compressional tectonic forces in the NE Atlantic margins, such as reverse faults, and broad basin inversion features observed in the mid-Norwegian margin (e.g. Blystad et al., 1995; Vågnes et al., 1998; Lundin and Doré, 2002; Tsikalas et al., 2005b, 2012, 2019; Doré et al., 2008). Doré et al. (2008) have reviewed possible mechanisms that are needed to account for sufficient stress to cause deformation, episodicity, and location of developed structures along the NE Atlantic margins. Among them, it was suggested a combination of far-field effects from the Late Mesozoic-Cenozoic Alpine Orogeny (Vågnes et al., 1998), horizontal compression caused by divergent asthenospheric flow (e.g. Breivik et al., 2006), and plume-spreading interaction generating plume-related body forces (Parnell-Turner et al., 2015). The closest similar dome-feature to the studied area is found in the south Lofoten margin, and named the southern Lofoten margin Dome (SLMD) (Tsikalas et al., 2019). Tsikalas et al. (2019) argued for a similar latest Cretaceous to late Miocene multi-phase growth evolution for this dome. For the SLMD, the presence of Bivrost Lineament in its proximity has been postulated to have acted as a structural pathway for the transfer of any imposed deformation related to any of the above processes. In a similar way, it can be suggested that the transfer zones identified within the study area (i.e. Jennegga, Vesterålen, and Andøya transfer zones) can also act as "structural corridors" and pathways to transfer any exerted regional deformation during Cenozoic within the study area. The latter is located at the rift-shear interaction between the dominantly rifted mid-Norwegian margin and the dominantly sheared western Barents Sea margin (e.g. Faleide et al., 2008; Tsikalas et al., 2012).

5.3.4 Extension estimates from fault heave measurements

The NURFC is the most prominent structural element within the study area composed of thick Cretaceous sequences that experienced composite tectonic deformation. In order to bring forward and be able to quantitative elaborate extension within the study area, extension estimates have been conducted based on fault components, such as heave and displacement measurements within the NURFC (Fig. 5.26 and Table 5.1).

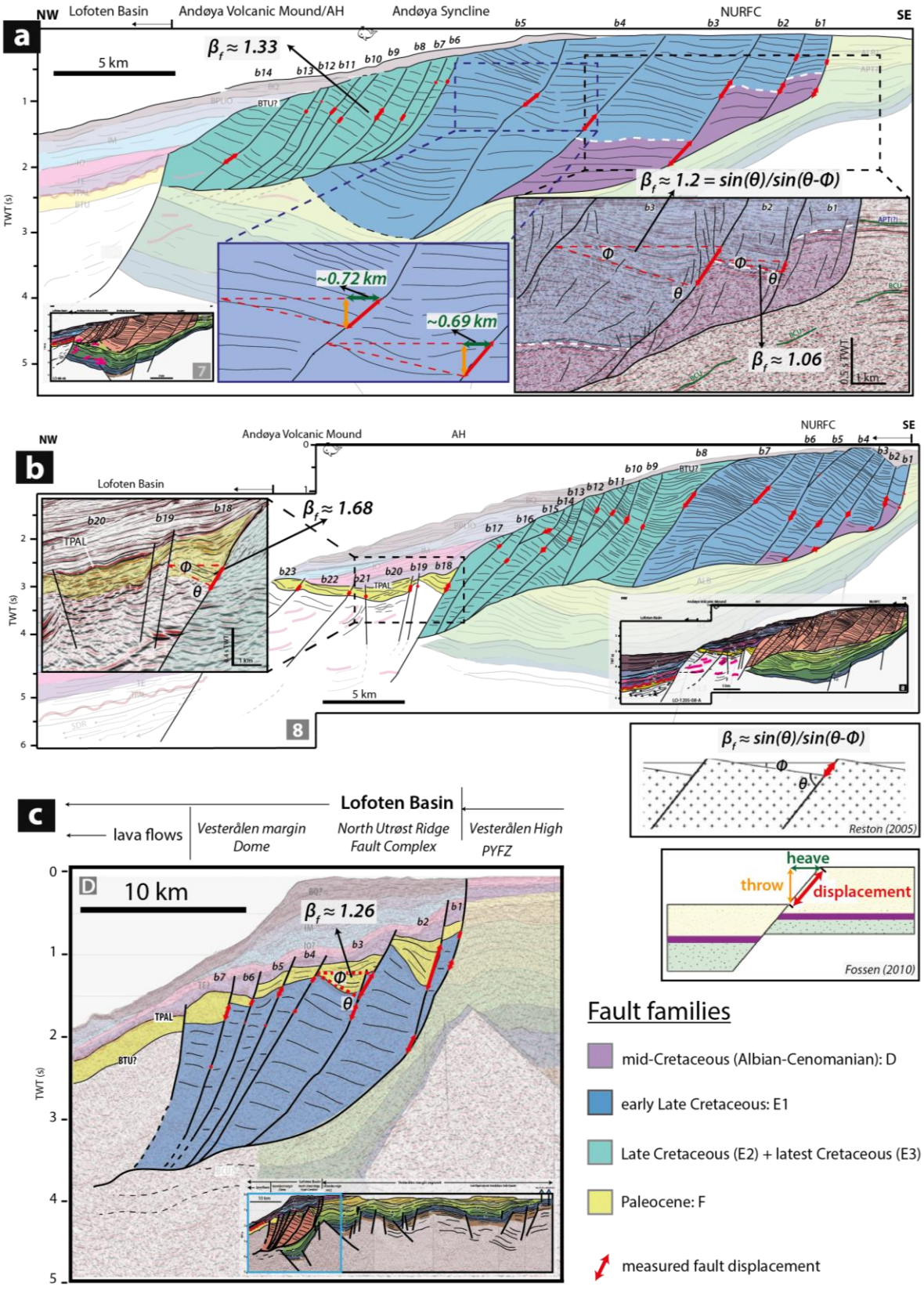

Fig. 5.26: *Fault heave and displacement measurements using identified fault families within and in vicinity of NURFC for all interpreted fault-blocks (b1-b14, b1-23, b1-7 for the three sections). Seismic panels with detailed seismic facies interpretation are displayed for profiles 7 and 8 to show close-ups (see descriptions in the text). Fault heave and displacement measurements are also exemplified on these seismic panels. Individual estimates on stretching factors (βf) are related to the fault geometry (see descriptions in the text).*

***Table 5.1**: Measurements of fault heaves and displacement within the NURFC. **(a)** Estimates for profile in Fig. 5.26a (original profile in Fig. 5.19-7); **(b)** Estimates for profile in Fig. 5.26b (original profile in Fig. 5.19-8); and **(c)** Estimates for profile in Fig. 5.26c (original profile in Fig. 4.9). An interval velocity of 2.75 and 2.45 km/s for the Upper Cretaceous and Tertiary sequences (cf. Table 3.3) was utilised in the fault displacement depth conversion, respectively.*

a

Profile_7						
Fault fam.	block	displ. (s, TWT)	displ. (km)	heave (km)	cumulative fault displ. per fault family (km)	cumulative fault heave per fault family (km)
D	1	0.18	0.25	0.17	1.3	1.10
	2	0.26	0.36	0.28		
	3	0.53	0.73	0.65		
E1	1	0.1	0.14	0.11	2.7	2.19
	2	0.16	0.22	0.17		
	3	0.53	0.73	0.50		
	4	0.6	0.83	0.69		
	5	0.55	0.76	0.72		
E2+E3	6	0.11	0.15	0.12	2.9	1.90
	7	0.09	0.12	0.11		
	8	0.27	0.37	0.18		
	9	0.34	0.47	0.35		
	10	0.11	0.15	0.13		
	11	0.14	0.19	0.17		
	12	0.13	0.18	0.05		
	13	0.36	0.50	0.16		
	14	0.55	0.76	0.63		
Total cumulative fault displacement and heave (km)					6.9	5.19

b

Profile_8						
Fault fam.	block	displ. (s, TWT)	displ. (km)	heave (km)	cumulative fault displ. per fault family (km)	cumulative fault heave per fault family (km)
D	1	0.1	0.14	0.10	0.9	0.78
	2	0.2	0.28	0.22		
	3	0.22	0.30	0.27		
	4	0.16	0.22	0.19		
E1	1	0.11	0.15	0.08	2.8	2.21
	2	0.3	0.41	0.27		
	3	0.24	0.33	0.24		
	4	0.26	0.36	0.29		
	5	0.09	0.12	0.07		
	6	0.32	0.44	0.42		
	7	0.7	0.96	0.84		
E2+E3	8	0.48	0.66	0.57	3.0	2.5
	9	0.17	0.23	0.17		
	10	0.24	0.33	0.26		
	11	0.17	0.23	0.19		
	12	0.17	0.23	0.18		
	13	0.15	0.21	0.19		
	14	0.19	0.26	0.21		
	15	0.29	0.40	0.34		
	16	0.18	0.25	0.2		
	17	0.15	0.21	0.19		
F	18	0.32	0.39	0.30	1.2	1.01
	19	0.11	0.13	0.08		
	20	0.17	0.21	0.19		
	21	0.09	0.11	0.10		
	22	0.13	0.16	0.14		
	23	0.17	0.21	0.20		
Total cumulative fault displacement and heave (km)					7.9	6.50

c

Profile_D						
Fault fam.	block	displ. (s, TWT)	displ. (km)	heave (km)	cumulative fault displ. per fault family (km)	cumulative fault heave per fault family (km)
E1	1	0.1	0.14	0.12	0.9	0.64
	2	0.22	0.30	0.29		
	3	0.22	0.30	0.13		
	4	0.05	0.07	0.06		
	5	0.02	0.03	0.01		
	6	0.02	0.03	0.01		
	7	0.02	0.03	0.02		
F	1	0.09	0.11	0.10	2.2	1.99
	2	0.53	0.65	0.59		
	3	0.47	0.58	0.56		
	4	0.14	0.17	0.15		
	5	0.18	0.22	0.20		
	6	0.13	0.16	0.12		
	7	0.25	0.31	0.27		
Total cumulative fault displacement and heave (km)					3.1	2.63

Figure 5.26 illustrates schematically the fault heave and displacement measurements undertaken within the NURFC along three profiles and for all individual fault-blocks. The location choice for the fault components to be measure was made based on the largest, more or less, observed rotated reflections within each fault-block. Fault heaves were measured along the horizontal separation of each reflection, whereas fault displacement was initially estimated in time (s, TWT) and then depth-converted using an interval velocity of 2.75 and 2.45 km/s for the Upper Cretaceous and Paleocene sequences, respectively (cf. Table 3.3). A detailed effort has been carried out in order to attribute the measured fault heaves and fault displacement estimates and their summations to the earlier described Cretaceous fault families. Initially, an even more detailed line-drawing interpretation was partly carried out (Fig. 5.26 part of profile 7 in close-up) in order to show a possible distinction of a mid-Cretaceous (Albian-Cenomanian, D fault family) seismic marker prior to the initiation of the composite and more intensive Late Cretaceous-Paleocene deformation. Further on, the measured fault components have been assigned to all previously described Late Cretaceous-Paleocene fault families (E1-E3 and F) (Fig. 5.26 and Table 5.1). Note that it was not possible in these 2D seismic profiles (optimally illustrating the entire extent of NURFC) to differentiate separately between fault families E2 and E3, thus these were treated together. Within the uncertainty imposed by the resolution of the seismic data, the outcome of this analysis is a progressively increasing fault heave and displacement intensity starting from fault family D (Albian-Cenomanian), escalating to fault family E1 (early Late Cretaceous) and the composite fault families E2+E3 (Late Cretaceous to latest Cretaceous-Paleocene), prior to a distinct drop at fault family F (Paleocene). The summed fault heave and fault displacement ranges for each fault family are indicated below, respectively:

- D (Albian-Cenomanian): 0.8-1.1 km and 0.9-1.3 km,
- E1 (early Late Cretaceous): 2.1-2.2 km and 2.7-2.8 km,
- E2+E3 (Late Cretaceous to latest Cretaceous-Paleocene): 1.9-2.5 km and 2.9-3 km
- F (Paleocene): 1-2 km and 1.2-2.2 km

Total cumulative fault displacement estimates are ~3 km in the southern parts of the NURFC, whereas as much as ~7-8 km in the northern parts of the fault complex. This shows that, in general, in the southern part of the fault complex extension is mainly accommodated by the Paleocene fault family (E), however towards the northern part of the study area extension is mainly accommodated by the combination of the identified Cretaceous fault families (D and

E1-E3) and less on the Paleocene fault family (F). A possible explanation accounting for the weak effect of Paleocene fault family (F) in the northern part of the study area and within the NURFC proper may be the larger erosion observed at this part of the margin, and consequently removal of any evidence of deformation related to early Cenozoic. Furthermore, the cumulative fault displacement estimates for NURFC when compared with extension estimates farther south in the Vøring Basin contrast with the high extension rates during the early Cenozoic observed in some parts of the margin, and have caused only minor faulting observed on conventional seismic reflection profiles (Skogseid et al., 1992b). Skogseid et al. (1992b) has attributed this behaviour to ductile crustal deformation, and to mobilization of Cretaceous shales and to breakup-related magmatic intrusions, features also observed within and in the vicinity of the NURFC. As for the total cumulative fault heave estimates, they display the same northwards increasing trend as the fault displacement estimates within the NURFC (Table 5.1), thus confirming the above discussed observations.

Stretching factor estimates can be also defined by fault geometry (β_f) (Reston, 2005) and such estimates were obtained on few selected rotated fault-blocks within the NURFC for further considerations on extension (Fig. 5.26). Reston (2005) described that broad domino-like fault-blocks are bounded by normal faults that develop at angles ~60-70^o and rotate during progressive extension to ~35^o, at which point it becomes mechanically more favourable to develop a new fault and the old fault locks up. Therefore, the resulting fault-block geometry, and fault heaves and throws, are a direct mean to measure the amount of extension (Reston, 2005). One approach to relate crustal extension to fault geometry is through the angular relationship that forms the top of the pre-rift marker with the horizontal reference surface (i.e. top of fault-block angle; φ), and the inclination of the fault-block (i.e. fault-plane inclination; θ), given by the formula (Reston, 2005) (Fig. 5.26):

$$\beta_f \cong \sin\theta \,/\, \sin(\theta - \varphi) \qquad \textbf{(eq. 1)}$$

This methodology is exemplified on the seismic close-ups of Figure 5.26 and Table 5.2. An estimate of ~1.2 is obtained for the β_f related to the early Late Cretaceous fault family (E1), whereas two different β_f related to the Paleocene fault family (F) are obtained, one of ~1.26 on the southeastern part of the NURFC, and a second one of ~1.68 on the northwestern part of the NURFC. Similarly, β_f of 1.06 and 1.33 are estimated for fault families D and E2+E3, respectively (Table 5.2). The fault heave/displacement estimates and the β_f values often refer

to as sub-seismic faulting (e.g. Reston, 2009) and may contribute to a relatively considerable and not accounted proportion of brittle crustal extension (Gómez-Romeu et al., 2020).

***Table 5.2**: Measurements of stretching factor estimates defined by fault geometry (β_f) utilizing eq. 1 (Reston, 2005) for selected rotated fault-blocks within the NURFC (see also seismic close-ups of Fig. 5.26).*

Fault family	θ (fault-plane inclination)	ϕ (top of fault-block angle)	β_f (eq. 1)
D	77°	10.47°	**1.06**
E1	63°	15.3°	**1.2**
E2 + E3	84°	35.74°	**1.33**
F (southeast NURFC)	81°	29.51°	**1.26**
F (northwest NURFC)	62°	30.13°	**1.68**

5.4 Vesterålen margin segment in a regional and conjugate setting

Conjugate setting perspectives are evaluated for the Vesterålen and NE Greenland margins, in order to complement the understanding of the basin development in a total rift perspective. This is done with the help of a recent conjugate crustal compilation and plate reconstruction (Fig. 5.27) combined with the seismic profiles interpreted in this study and previous publications, together with crustal transects and an updated tectonic model; all discussed in the following sections.

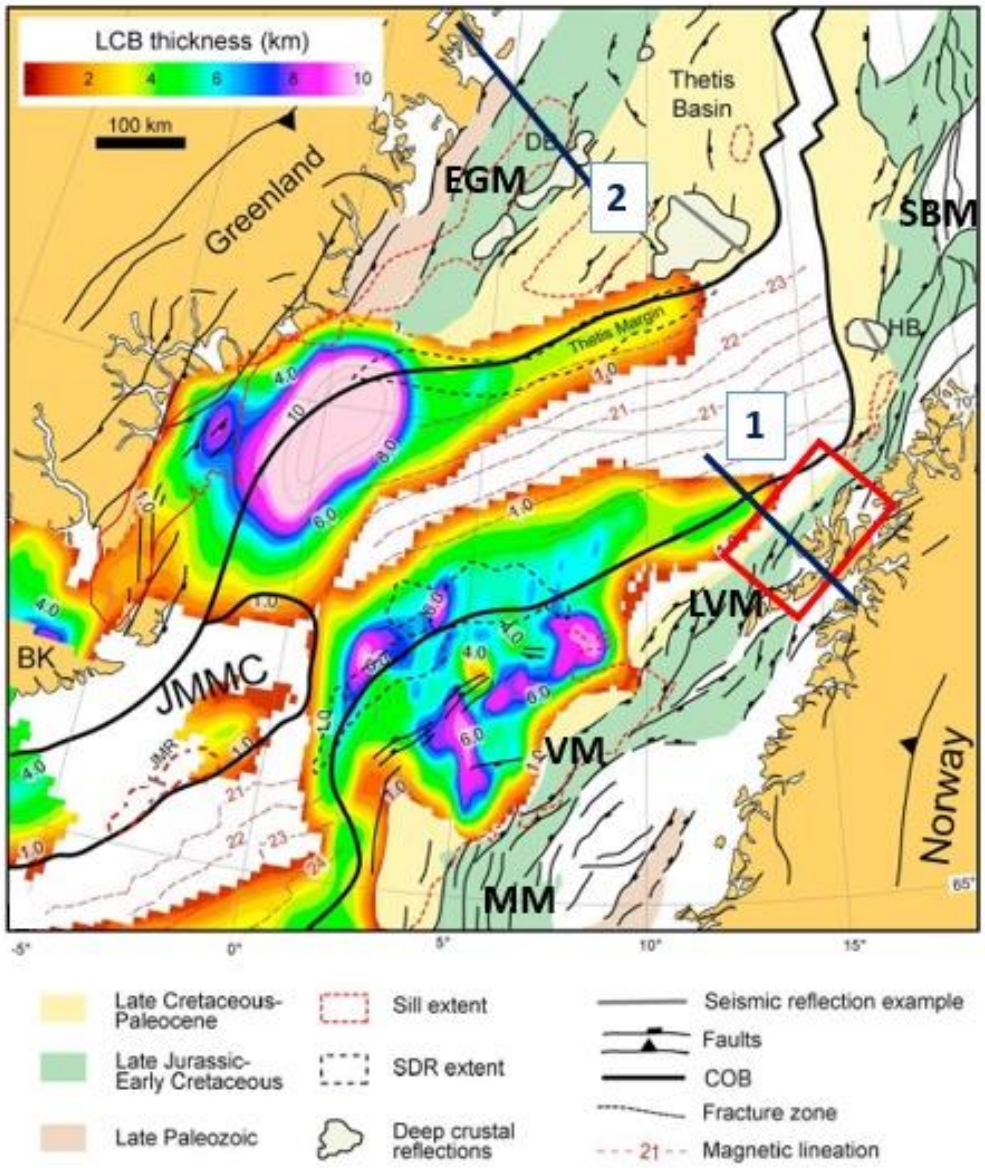

Fig. 5.27*: Lower crustal body (LCB) thickness map for the NE Atlantic conjugate margins restored to C21 (~47 Ma) (from Abdelmalak et al., 2017). Red box indicates study area. Profile locations for conjugate crustal transects (Fig. 5.29) are indicated in dark-blue lines. EGM: East Greenland margin; LVM: Lofoten-Vesterålen margin; MM: Møre margin; SBM: SW Barents Sea margin; VM: Vøring margin.*

5.4.1 Late Cretaceous-Cenozoic conjugate basin evolution

Late Cretaceous-Paleocene rifting with prominent low-angle detachment faults is observed both at the Vesterålen margin and the NE Greenland (NGM) conjugate margin counterpart, in addition to showing an apparent seaward propagation of fault activity (Fig. 5.28) (e.g. Tsikalas et al., 2005b). However, some differences exist between the North Utrøst Ridge Fault Complex (NURFC) and similar structures observed on the conjugate NE Greenland margin (Fig. 5.28). The main differences between the Late Cretaceous-Paleocene conjugate structures include the maximum extent of the deformation related to the development of the low-angle detachment fault structures, their fault geometries and intensities, and their relationship between thickness/distribution of the Cretaceous-Cenozoic sedimentary units above and below them.

Concerning the areal extent of the low-angle detachment faults, an evident NE-trending fault propagation is observed at NURFC towards the inner parts of the Vesterålen margin where the fault complex becomes more prominent as it increases in lateral extent and it is further elevated at shallower levels (Fig. 5.28c-e). The NE-oriented increase in deformation is enhanced due to the progressively deeper burial (with the same trend) within the study area of the northern part of Utrøst Ridge/Jennegga High, and supports the role of elevated basement highs acting as being obstacles for the intense North Utrøst Ridge Fault Complex faulting (Fig. 5.28d). On the contrary, low-angle detachment faults on the conjugate NE Greenland margin appear to be confined only to the east of the prominent Danmarkshavn Ridge, which may have acted as a barrier for Late Cretaceous fault propagation into the inner parts of the conjugate margin (Fig. 5.28a-b). Furthermore, the individual fault-blocks within the NURFC are observed to be less wide and thick compared to those massive and larger in dimension blocks found at the conjugate NE Greenland margin; the latter also displays less seismic internal reflectivity and layering (Fig. 5.28). Locally, somewhat more antithetic faults are observed in connection with the low-angle detachment structures in the NE Greenland margin seismic section (Fig. 5.28a-b). Although there is a bias towards more detailed observations on the Norwegian side (due to the amount of existing seismic data on this part), it can be postulated that the observed differences in fault geometries and intensities between the conjugate margins may be accounted, to some extent, to the fact that the Late Cretaceous low-angle detachment faults beneath the NURFC appear to have much more tilted and lower-angle than those few seen on the conjugate side (Fig. 5.28). It appears that the NURFC has experienced greater ductile deformation (possibly also with a longer duration), thus being

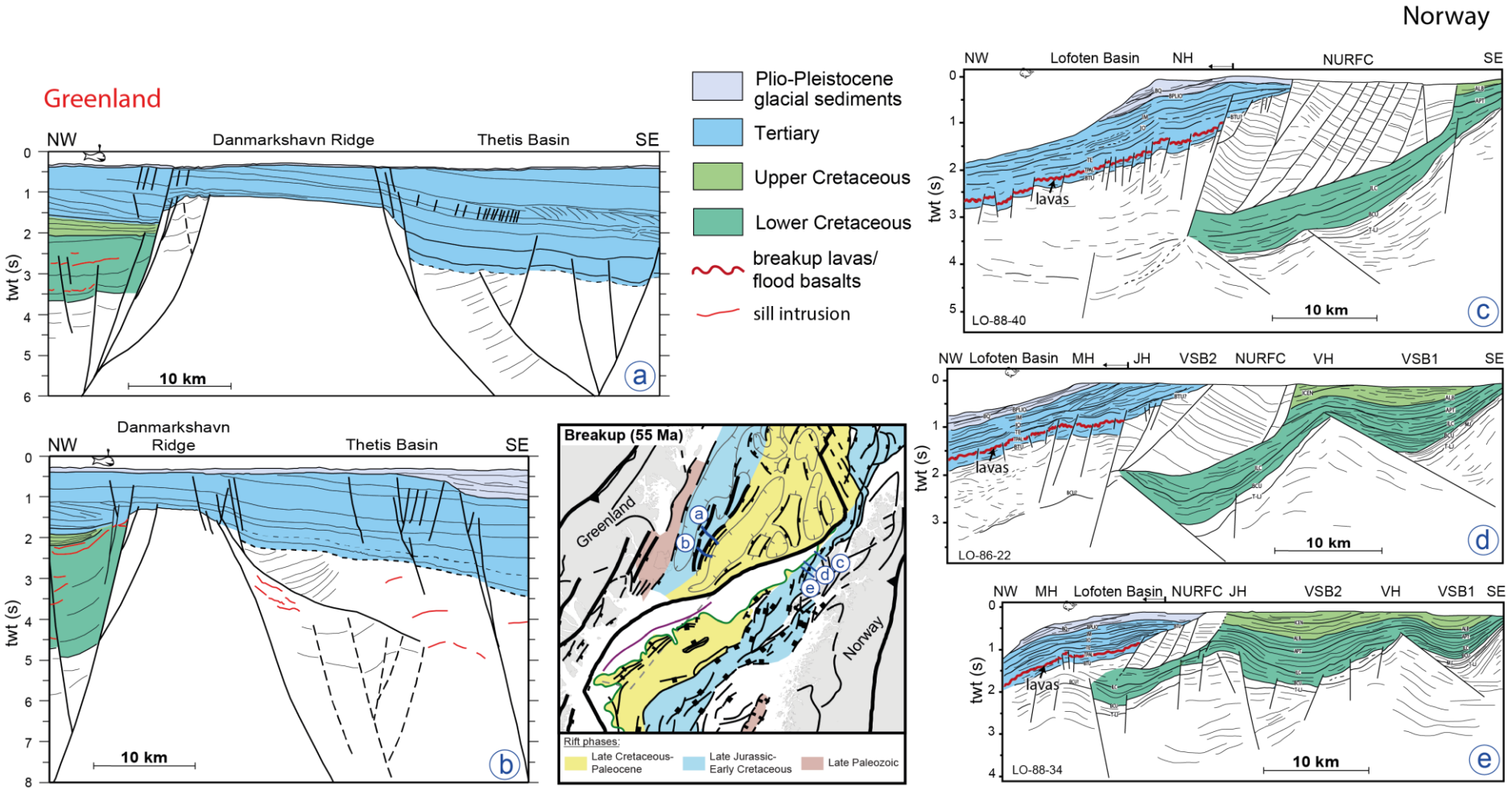

***Fig. 5.28**: Interpreted seismic profiles illustrating Late Cretaceous low-angle detachment fault systems from the conjugate NE Greenland (a-b; Tsikalas et al., 2005b) and Vesterålen (c-e; this study) margins. Profile locations in inset-map that illustrates the plate reconstruction at breakup (~55 Ma) (Tsikalas et al., 2012; Faleide et al., 2015). NURFC: North Utrøst Ridge Fault Complex. Other abbreviations in Figs. 3.1 and 4.10.*

.

more low-angle in comparison to the NE Greenland margin, and in addition the NURFC is located closer to the COB that represents the final breakup location.

The Cenozoic sedimentary cover appears different on the conjugate margin parts (Fig. 5.28). Late Cretaceous rifting was followed by smaller scale, but distinct rifting during Paleocene, with reactivation of earlier faults and locally initiation of new faults (Fig. 5.25). Paleocene is associated with regional uplift, erosion and intrusive igneous activity on both conjugate margins (Fig. 5.28) (Tsikalas et al., 2012). Paleocene uplift is indicated by early Cenozoic truncation of Cretaceous successions (Fig. 5.24), as the NURFC has an elevated and dome-shaped character and the landward breakup lava boundary lies very close to the western side of the fault complex (Fig. 5.29c-e). At the NE Greenland margin, however, the Late Cretaceous low-angle detachment faults are located at some distance away from the landward lava boundary (Fig. 5.28). In addition, the Late Cretaceous fault-blocks on the NE Greenland margin are overlain by very thick successions of Cenozoic sequences, with a wedge-shaped Plio-Pleistocene sequence above (Fig. 5.28a-b). The general northward decrease of the Cenozoic sequence, including the glacial sediments, in the immediate vicinity of the NURFC and conjugate side implies an increasing northward uplift and erosion along both margins, with the greatest erosion of Tertiary and pre-Tertiary sequences observed within the Vesterålen margin segment (Figs. 5.24 and 5.28).

5.4.2 Crustal structure and extension estimates

Early Cenozoic continental breakup between Greenland and Eurasia was in most parts very magma-rich, giving rise to the Northeast Atlantic Large Igneous Province (NALIP) (e.g. Eldholm and Coffin, 2000; Eldholm et al., 2002). Magmatic productivity varies along the margins to some extent as a function of the distance from the Iceland Plume hotspot, thus at the Vøring Plateau the magmatism is very voluminous compared to that at the Lofoten-Vesterålen margin (Fig. 5.28) (e.g. Skogseid et al., 2000; Breivik et al., 2012; Mjelde et al., 2005). These observations have been further studied considering the response of the moderately extended continental crust beneath the LVM, and the greatly extended lithosphere beneath the adjacent Vøring and SW Barents Sea margins, and the conjugate East Greenland margin (e.g. Faleide et al., 2008, 2010; Tsikalas et al., 2012). The continent-ocean boundary (COB) position, crustal thicknesses, depth-to-Moho, and high-velocity lower-crustal bodies (LCB) are some of the features used to commonly explain the relationship between the

mechanisms and geometries resulting from breakup (Fig. 5.28) (e.g. Tsikalas et al., 2005a; Breivik et al., 2017, 2020).

The narrow LVM is conjugate to a wide Northeast Greenland margin, while a wide Vøring margin is conjugate to a narrow Northeast Greenland margin (Fig. 5.27). In particular, the LVM exhibits maximum crustal thicknesses in the order of ~23-26 km beneath the slope, while it thickens towards mainland Norway reaching a maximum of ~36 km (Fig. 5.29) (Faleide et al., 2008, 2010; Breivik et al., 2017). In the southernmost part of the Lofoten margin, the Moho depth is about 20 km, whereas it increases to about 27 km underneath the southern Utrøst Ridge near the shelf edge, to become shallower again towards the outer margin (Fig. 5.29) (Mjelde et al., 1993). Furthermore, the thickness and distribution of the high-velocity (7+ km/s) lower-crustal body (LCB) beneath the crust varies along the conjugate margins (Fig. 5.27).

The Moho depth does not indicate the presence of mapped basement highs and basins on the LVM (Fig. 5.29). Breivik et al. (2020) suggested that this behaviour is because the depths of the basins are relatively shallow (~6 km deep) and, thus, crustal extension must have been minor. In this context, a distributed extension is proposed for the lower crust rather than a pure shear extension. Additionally, the basin infill has high density, which could reduce the Moho topography underneath through isostatic adjustments. Crustal modelling performed through ray-tracing inversion of OBS-velocity data has shown that the crust of the LVM shelf area is not strongly affected by the continental breakup. All the above processes may account to some degree for the different crustal structure observed on the LVM as the asymmetric conjugate counterpart of the NE Greenland margin (e.g. Tsikalas et al., 2005a). The latter is characterised by higher variations in crustal thickness and crustal densities, shallower maximum crustal depth (~26 km), and deeper Mesozoic sedimentary basins (Fig. 5.29).

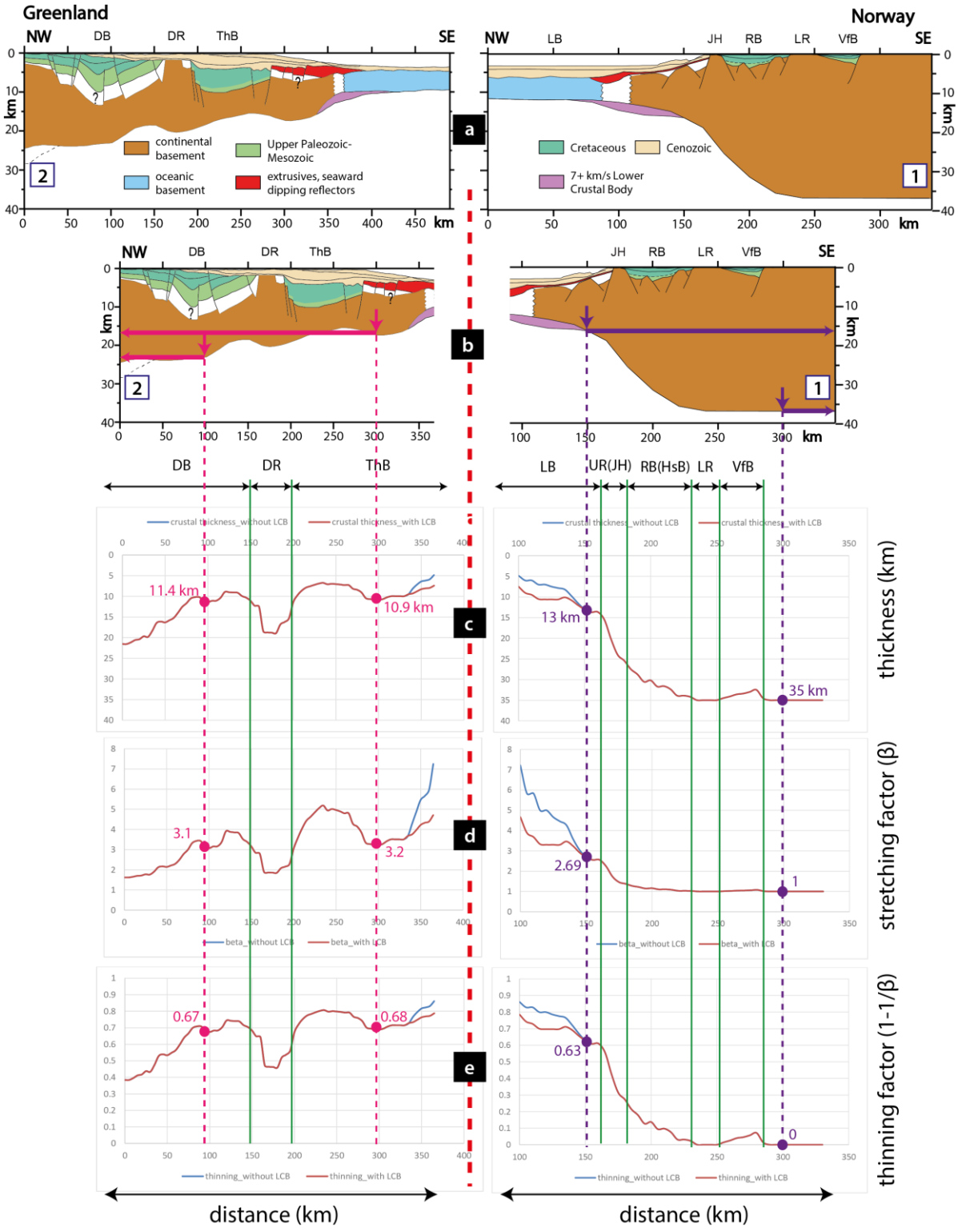

***Fig. 5.29**: **(a)-(b)** Conjugate crustal transects across the Vesterålen margin segment and NE Greenland margin illustrating pre- and post-breakup crustal architecture (from Tsikalas et al., 2012). DB, Danmarkshavn Basin; DR, Danmarkshavn Ridge; HsB, Havbåen Sub-basin; JH, Jennegga High; LB, Lofoten Basin; LR, Lofoten Ridge; RB, Ribban Basin; ThB, Thetis Basin; UR, Utrøst Ridge; VfB, Vestfjorden Basin. Profile locations in Fig. 5.27. **(c)-(e)** Crustal stretching and thinning factors in the conjugate margin setting between Vesterålen and NE Greenland margins with and without consideration of a lower crustal body (LCB) as part of the continental crust. Crystalline crust thickness was estimated from crustal transects in **(b)** and is displayed in **(c)**. In **(d)** and **(e)** are the estimated stretching and thinning factors, respectively. An initial reference thickness of crust of 35 km is used for both LVM-NE Greenland margins.*

***Table 5.3**: Summary of stretching, thinning, and extension estimates for the conjugate NE Greenland and Vesterålen margins.*

NE Greenland					**Norway**
final stretched length (km)	F_G	350	200	F_N	final stretched length (km)
average beta factor_without LCB	β_G	3.40	2.01	β_N	average beta factor_without LCB
average thinning factor_without LCB	h_G	0.66	0.27	h_N	average thinning factor_without LCB
pre-rift length_without LCB (km)	$L_G = F_G/\beta_G$	102.83	98.95	$L_N = F_N/\beta_N$	pre-rift length_without LCB (km)
total extension_without LCB (km)	$E_G = F_G - L_G$	**247.17**	**101.05**	$E_N = F_N - L_N$	**total extension_without LCB (km)**
average beta factor_with LCB	β_G'	3.29	1.71	β_N'	average beta factor_with LCB
average thinning factor_with LCB	h_G'	0.66	0.25	h_N'	average thinning factor_with LCB
pre-rift length_with LCB (km)	$L_G' = F_G'/\beta_G'$	106.25	115.78	$L_N' = F_N'/\beta_N'$	pre-rift length_with LCB (km)
total extension_with LCB (km)	$E_G' = F_G' - L_G'$	**243.75**	**84.22**	$E_N' = F_N' - L_N'$	**total extension_with LCB (km)**
Conjugate total extension_without LCB (km)			$E_G + E_N$		**348.22**
Conjugate total extension_with LCB (km)			$E_G' + E_N'$		**327.97**

The compiled conjugate crustal transects are used to perform crustal extension estimates. Crustal stretching and thinning factors in the conjugate margin setting between Vesterålen and NE Greenland margins have been calculated with and without consideration of a lower crustal body (LCB) as part of the continental crust (Fig. 5.29). Extension estimates suggest that the conjugate margin counterparts depict the asymmetry in extension, and in particular during Late Cretaceous-Paleocene rifting (Fig. 5.29 and Table 5.3). Skogseid (1994) has defined the dimensions (i.e. width) of the Late Cretaceous-Paleocene rift zone and magnitude of extensional deformation through distribution of Cenozoic subsidence and subsidence-derived stretching estimates. As a result, a NE Atlantic rift zone with more than 300 km width was estimated, with a considerable contribution of the Late Cretaceous-Paleocene rifting (~140 km) (Skogseid, 1994; Skogseid et al., 2000). These observations are in agreement with the estimates of conjugate total extension in this study, with a syn-rift displacement reaching as much as ~327 km (considering the LCB as part of the continental crust), or ~348 km (without considering LCB as part of the continental crust) (Fig. 5.29 and Table 5.3). A general seaward increase in Cenozoic tectonic subsidence was also reported, reflecting the increased tectonic activity as the zone of final continental separation between Greenland and Norway was approached (Skogseid et al., 1992b; Skogseid, 1994), and which is reflected as the stretching/thinning factors increase gradually towards the line of continental separation (Fig. 5.29).

5.4.3 Ductile mode of extensional deformation towards breakup

Late Cretaceous-Paleocene crustal extension at the outer LVM was intensive around breakup (Fig. 5. 29), and resulted into a thinner continental crust than the adjacent margins to the south (e.g. Mjelde et al., 1993, 2005, 2009; Tsikalas et al., 2008). In particular, Figure 5.30a shows an updated ocean-bottom seismometer (OBS) velocity crustal model across the Vesterålen margin (Breivik et al., 2017). Seismic interpretation in this study (Fig. 5.30b) is consistent with this model in the inner margin part that extends from the west flank of the Lofoten Ridge up to the west side of the Utrøst Ridge/Jennegga High (Fig. 5.30a). Towards the outer part of the margin and farther west, the intensive of the Late Cretaceous-Paleocene deformation took place, and the prominent low-angle/listric detachment faults developed (Fig. 5.30b). Figure 5.30c illustrates a close-up of the OBS-velocity crustal model (Fig. 5.30a) overlaid by a tectonic model which can explain the geometry of the Late Cretaceous-Paleocene low-angle detachment faults leading to continental breakup (Breivik et al., 2017). The same tectonic model (Fig. 5.30c) supports the observations of brittle faulting within upper-crustal levels, while ductile deformation is assumed within the crystalline lower crust. A stretching factor (β) of at least ~3, will explain the thin crust and the above mentioned processes observed in the Vesterålen margin at the onset of breakup. In addition, ~26-30 km of extension are estimated from the measured fault heaves (~13-15 km) of the two inner detachment faults (Fig. 5.30c) (Breivik et al., 2017).

In a similar way, the stretching factor (β) estimates from the utilised crustal transects (Fig. 5.29) appear to be in agreement with the above reported extension and stretching estimates at the outer part of the Vesterålen margin, west of the Utrøst Ridge/Jennegga High. Measuring extension as a function of depth at rifted margins must include upper crust (i.e. fault heaves) extension estimates, in order to avoid under-prediction, for example, of sediment temperature, heat flow and hydrocarbon maturation (e.g. Skogseid et al., 1992b; Kusznir et al., 2005). Furthermore, rifted margins are often characterised by an extension discrepancy, which refers to the amount of extension measurable from the observed faulting (i.e. β_f) is far less than that required to explain the crustal stretching or thinning (i.e. β_c) (Reston, 2005). The extension discrepancy may be a combination of several factors, including differential compaction of sediments during and after rifting, non-uniform stretching of the lithosphere, rheological layering of the crust, and significant plastic/ductile deformation in the rock volume (Walsh et al., 1991; Reston, 2009).

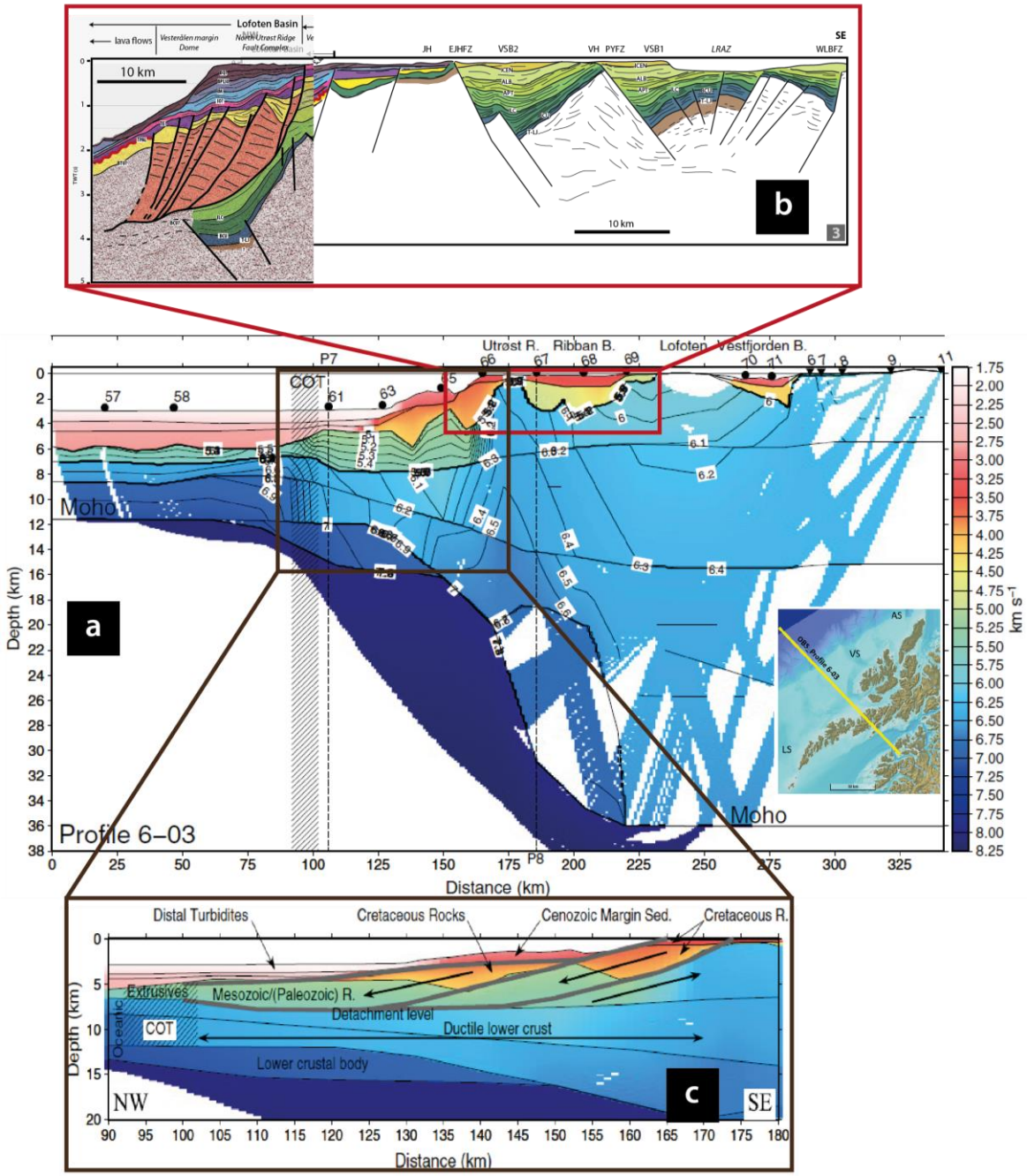

***Fig. 5.30**: **(a)** Ocean-bottom seismometer (OBS) crustal velocity model for the Vesterålen margin. **(b)** Inner part of the Vesterålen margin as interpreted from seismic profiles in this study. **(c)** Tectonic model for the Vesterålen margin segment superimposed on velocity model in **(a)**. Grey bands indicate low-angle detachment faults, and the thick arrows show relative direction of movement. Detachments are interpreted to sole out on the top of the ductile lower crust. The hanging wall block is missing from the upper detachment, presumably left on the Northeast Greenland margin, exposing the lower sedimentary layer at the outer margin. **(a)** and **(c)** from Breivik et al. (2017). Inset map from the Norwegian Mapping Authority (www.kartverket.no).*

The extension discrepancy is further confirmed by an apparent discrepancy between individual Late Cretaceous-Paleocene β-factor estimates from fault geometry (e.g. max. $\beta_f \approx 1.7$; Table 5.2 and sub-chapter 5.3.4), and those from crustal stretching ($\beta_c \geq 3$). In this

context, a simple version of fault population analysis was performed in order to explore whether there is a possibility for sub-seismic faulting and if this may substantially contribute to an under-estimation of brittle crustal extension (Fig. 5.31). This analysis, following the methodologies described in Walsh et al. (1991), Pickering et al. (1996), Ackermann et al. (2001), and Gómez-Romeu et al. (2020), determines the proportion of faults which have displacements too small to be imaged by conventional seismic reflection data. The applied fault population analysis in this study (Fig. 5.31) consists on statistical expressions of power-law and exponential distributions of the sampled fault heave estimates (Fig. 5.26 and Table 5.1). Figure 5.31a shows a generalized example of the method as a cumulative frequency analysis with sampling artefacts related to a limited sampling area (data censoring), and to non-imaged faults below seismic resolution (data truncation). The idealised fault distribution shown by the cumulative frequency analysis consists of a central steep segment with negative gradient, and represents the average fault population. The slope of a power-law distribution curve gives the fractal dimension and is usually between −0.7 and −0.9 suggesting that a proportion of faults are not being seismically observed whereas an exponential distribution type indicates that the majority of faults are being seismically observed (Fig. 5.31a).

Figure 5.31b shows the results obtained in this study from the fault population analysis of all the interpreted faults/fault families within the NURFC (Fig. 5.26 and Table 5.1). The figure demonstrates that the sampled faults fit better with an exponential distribution. However, the behaviour of the faults in the data censoring area appears to be above the predicted (exponential) frequency curve, and not below as expected by the method. Thus, the misfit suggest that a power-law frequency distribution needs to be considered (Gómez-Romeu et al., 2020). As a result, the value of the slope (red-line in Fig. 5.31b), or the fractal dimension obtained is approximately -0.8. Such a value implies a lower-limit of resolution of ~50 m in order for faulting to be recognized on seismic data (i.e. data truncation in Fig. 5.31b). Adding to that, only ~14% of the extension would be seen on seismic profiles/sections (Fig. 5.31c). Nonetheless, the power-law distribution shows that the data (blue-dots in Fig. 5.31b) do not entirely fall on the slope (red-line in Fig. 5.31b) of this statistical fit. Such behaviour might be explained by several factors, including an imperfect interpretation. Despite this, seismic interpretation supports the presence of more than one fault family within the NURFC, and one may fit more than one power-law lines to better represent the slope segments on the fault population graph in Figure 5.31b. In this sense, multiple rift phases from Late Cretaceous to Paleocene are interpreted for the development and evolution of the NURFC in the Vesterålen

margin, similar to the cases in the Galicia margin (Reston, 2005) and in the Iberia-Newfoundland conjugate margins (Gómez-Romeu et al., 2020). All these observations confirm the existence of sub-seismic density faulting that, for instance, may help to predict integrity of reservoir intervals considering faults below the seismic resolution and to estimate total tectonic extension due to fault heave (Pickering et al., 1996).

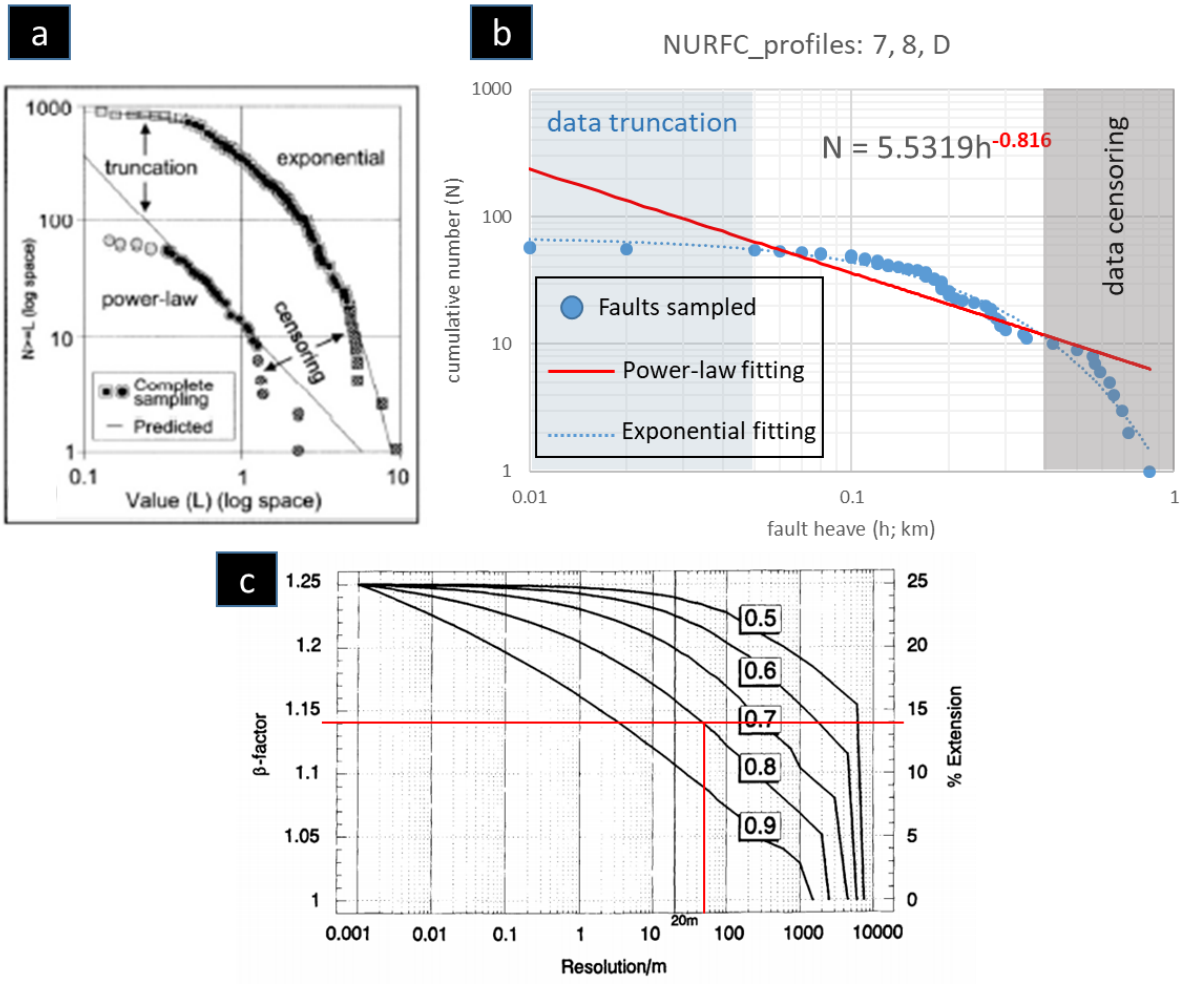

***Fig. 5.31**: **(a)** Fault population plot showing power-law and exponential cumulative frequencies against fault size (measured as length, L) and sampling artefacts from truncation and censoring (from Ackermann et al., 2001). **(b)** Fault population analysis showing cumulative number (N) versus all the measured fault heaves (h, km; Table 5.1) in this study from seismic interpretation of profiles in Fig. 5.26. Possible fits to power-law and an exponential relationship are shown. The fractal dimension for the power-fitting is the exponent in red of the equation in **(b)**. **(c)** Graph of the proportional measured extension for the lower-limit of seismic resolution for different ideally power-law populations of faults (from Pickering et al., 1996). The red lines in **(c)** show that for a lower-limit of 50 m and a fractal dimension of -0.8 the extension that would be seen on seismic section is ~14% of the total.*

Finally, a model for lithospheric extension is presented in Figure 5.32, and shows a tectonic multiphase evolution model for the Vesterålen-NE Greenland conjugate margins. A primary first stage (Fig. 5.32a) is interpreted to be related to a thinning phase during Late Cretaceous-

Paleocene that is characterized by low-angle detachment faulting and possibly depth-depending stretching as proposed for the NE Atlantic margins (e.g. Kusznir et al., 2005) and similar rifted margins worldwide (e.g. Blaich et al., 2011). A second stage related to breakup is then followed, together with an increase in magmatic activity and abandonment of the detachment system (Fig. 5.32b) (Blaich et al., 2011). The resulting asymmetric rift geometry of the Vesterålen-NE Greenland conjugate margins is controlled by listric faults and the configuration of a detachment system through an upper plate or flexural margin (NE Greenland margin), and a lower plate or tilted-block margin configuration (Vesterålen margin) (Fig. 5.32a) (e.g. Mosar et al., 2002). The obliquity in the breakup axis location along the LVM-NE Greenland conjugate margins (Fig. 5.27) can be explained by this model.

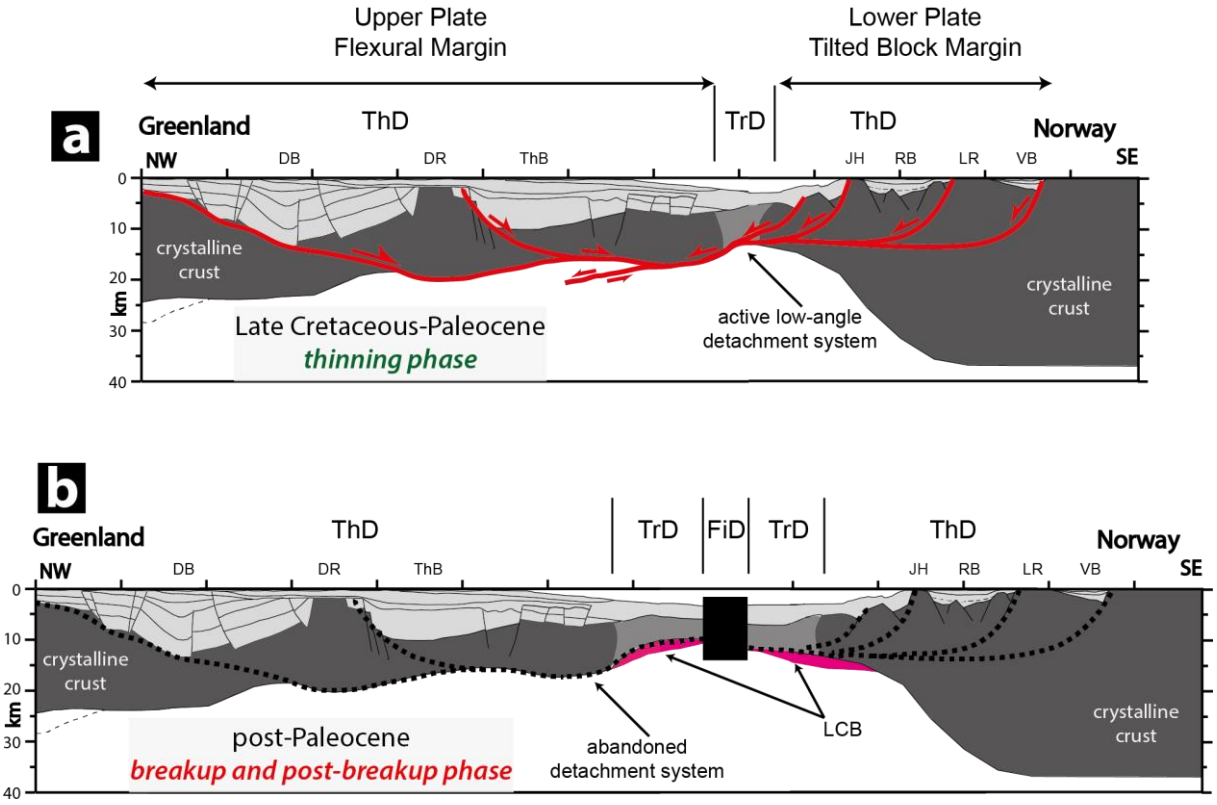

***Fig. 5.32**: Conceptual tectonic model illustrating the multi-phase evolution of the NE Greenland-Norway (Vesterålen) conjugate margins. (a) Late Cretaceous-Paleocene thinning phase showing a lower and upper plate rift geometry triggering a low-angle detachment system that developed through the ductile lower crust and lithospheric mantle. Possibly, depth-dependent stretching is the main mechanism responsible for crustal thinning in the area (i.e. ThD and part of the TrD following the concepts of Blaich et al., 2011 for the South Atlantic margins). (b) Post-Paleocene breakup and post-breakup phase accompanied by intense volcanic activity (i.e. FiD) and abandonment of the detachment system. The low-angle detachment system was possibly interrupted by the emplacement of oceanic crust into the margin that subsequently resulted in an increase of crustal densities leading to post-breakup subsidence of the area by volcanic loading (e.g. Blaich et al., 2011). A lower-crustal body (LCB), typical for magma-rich margins, is placed underneath the crust and it is contemporaneous with the latter described events. FiD: fully igneous crust; ThD: thinned crystalline crust domain; TrD: transitional domain.*

6 Summary and conclusions

The Late Mesozoic-Cenozoic tectono-stratigraphic evolution of the Vesterålen margin segment (part of the Lofoten-Vesterålen margin offshore northern Norway) has been studied in detail utilizing and integrating several datasets that included available reprocessed vintage and the most recently acquired 2D multi-channel seismic reflection profiles, a 3D seismic survey (first time available to academia), limited well data (exploration and stratigraphic shallow boreholes), and potential field (gravity and magnetic) data. The main focus of the work has been on structural and stratigraphic interpretations in order to refine details of the rift phases affecting the study area, as well as to study the role of transfer zones in the along-margin tectono-stratigraphic basin segmentation and evolution. In order to bring forward and be able to quantitative elaborate extension within the study area, extension estimates have been conducted based on fault components, such as heave and displacement measurements. Furthermore, a comparison with the conjugate NE Greenland margin through the evaluation of crustal extensional processes was carried out to complement and add to the understanding of the Vesterålen margin within the context of a total rift setting.

An updated structural and stratigraphic framework, together with new and better refined structural elements for the Vesterålen margin is presented in this study, and it is given in the form of interpreted seismic sections, and time-structure and time-thickness maps. On the basis of seismic and potential field data integration, new and better refined structural elements include the (informally named) Jennegga, Myre, Vesterålen, Nøss and Andenes highs; depocenters including the Vesterålen Sub-basins 1 and 2 and the Andøya Syncline; and the prominent North Utrøst Ridge Fault Complex (NURFC). The study area has been divided into three main margin segments (from south to north), namely the northern Lofoten, Vesterålen, and Andøya segments. The criteria for segmentation relay on the observed changes of basin architectural elements, such as shift in fault dip-polarity, northwards diminishing fault-throw intensity, northwards burial of ridges and basement highs, and to the presence of NW-SE trending curvilinear lineaments informally named as Jennegga transfer zone, Vesterålen transfer zone system, and Andøya transfer zone. Each of these transfer zones constitutes low-relief accommodation structural pathways for the distribution of deformation initiated prior to Jurassic and lasting until early Cenozoic times.

Five main rift phases of varying intensity have been recognised and refined in the study area, and are evidenced by eight fault families. The pre-Jurassic rifting is clear in few parts of the central and northern portions of the Vesterålen segment, particularly in the vicinity of the Vesterålen High. Late Jurassic-earliest Cretaceous rifting controlled the initial structuring of the main structural elements. Evidence for an Aptian-Albian rift phase exists as dragged-up reflections at the West Lofoten Border Fault Zone within the Havbåen Sub-basin. Mid-Cretaceous rifting (Albian-Cenomanian) was responsible for the initiation of faulting at the NURFC in the southern part of the Vesterålen segment, while extension there continued during the composite Late Cretaceous rifting with a westward propagation of three distinct rift phases and corresponding fault families. Paleocene rifting generated new faults and reactivated several Late Jurassic-earliest Cretaceous and Cretaceous faults, prior to continental breakup and seafloor spreading initiation at the Paleocene-Eocene transition. The post-Paleocene evolution is that of a continental passive margin, and specifically for the Vesterålen margin intense uplift and erosion phases took place together with related gravity mass-waste processes.

Fault heave and displacement measurements were undertaken within the NURFC along three profiles and for all individual fault-blocks. The analysis demonstrated a progressively northwards increase of fault heave and displacement intensity, with respective values as follows: starting from fault family D (Albian-Cenomanian) with 1.1 and 1.3 km, escalating to fault family E1 (early Late Cretaceous) with 2.2 and 2.8 km and the composite fault families E2+E3 (Late Cretaceous to latest Cretaceous-Paleocene) with 2.5 and 3 km, prior to a distinct drop at fault family F (Paleocene) with 2 and 2.2 km. Total cumulative fault displacement estimates are ~3 km in the southern parts of the NURFC, whereas as much as ~7-8 km in the northern parts of the fault complex. This shows that, in general, in the southern part of the fault complex extension is mainly accommodated by the Paleocene fault family (E), whereas towards the northern part extension is mainly accommodated by the combination of the identified Cretaceous fault families (D and E1-E3) and less on the Paleocene fault family (F). In addition, stretching factor estimates defined by fault geometry (β_f) in the NURFC reach as much as ~1.7.

Late Cretaceous-Paleocene rifting resulted in the formation of low-angle detachment structures on both the NE Greenland and Vesterålen conjugate margins. In the Vesterålen side, it appears that the NURFC has experienced greater ductile deformation, possibly also

with a longer duration, thus being more low-angle in comparison to the fault complexes at the NE Greenland margin. Paleocene uplift is indicated by early Cenozoic truncation of Cretaceous successions, as the NURFC has an elevated and dome-shaped character and the landward breakup lava boundary lies very close to the western side of the fault complex. In addition, the much thinner Cenozoic units covering the NURFC suggest greater uplift and erosional rates at the Vesterålen margin compared to its conjugate counterpart at NE Greenland. Furthermore, crustal stretching and thinning factors in the conjugate margin setting were estimated. As a result, the conjugate total (post-Caledonian) extension estimates obtained for a crust with and without consideration of a lower crustal body (LCB) are ~328 and ~348 km, respectively, with a β-factor exceeding values of ~3 at the time of Late Cretaceous-Paleocene thinning phase. An apparent extension discrepancy is seen when seismically observed fault heaves and displacement are summed up. Fault population analysis suggests that only ~14% of extension is seen from the faults on seismic profiles in the detailed analysis of the NURFC.

Finally, a conceptual tectonic multiphase evolution model for lithospheric extension is proposed for the NE Greenland-Vesterålen conjugate margins. The model consists of a Late Cretaceous-Paleocene thinning phase that shows lower and upper plate rift geometry. This geometry has triggered a low-angle detachment system that developed through the ductile lower crust and probably the lithospheric mantle. Possibly, depth-dependent stretching is the main mechanism responsible for crustal thinning in the area. Following that, post-Paleocene breakup and post-breakup evolution were accompanied by intense volcanic activity and abandonment of the detachment system. The low-angle detachment system was possibly interrupted by the emplacement of oceanic crust that subsequently resulted in an increase of crustal densities leading to post-breakup subsidence. The study of the Vesterålen margin has demonstrated that this margin segment represents a key area to study the Late Mesozoic-Cenozoic rift-basin architecture and the tectono-stratigraphic evolution of the NE Atlantic margins.

References

Abdelmalak, M. M., Faleide, J. I., Planke, S., Gernigon, L., Zastrozhnov, D., Shephard, G. E., Myklebust, R., 2017. The T-reflection and the deep crustal structure of the Vøring Margin, offshore mid-Norway. Tectonics, 36(11), 2497-2523.

Ackermann, R. V., Schlische, R. W., Withjack, M. O., 2001. The geometric and statistical evolution of normal fault systems: an experimental study of the effects of mechanical layer thickness on scaling laws. Journal of Structural Geology, 23(11), 1803-1819.

Bergh, S. G., Eig, K., Kløvjan, O. S., Henningsen, T., Olesen, O., Hansen, J. A., 2007. The Lofoten-Vesterålen continental margin: a multiphase Mesozoic-Palaeogene rifted shelf as shown by offshore-onshore brittle fault-fracture analysis. Norwegian Journal of Geology/Norsk Geologisk Forening, 87.

Berndt, C., 2002. Residual Bouguer satellite gravity anomalies reveal basement grain and structural elements of the Vøring Margin, off Norway. Norwegian Journal of Geology, 82, 31-36.

Blaich, O. A., Faleide, J. I., Tsikalas, F., 2011. Crustal breakup and continent-ocean transition at South Atlantic conjugate margins. Journal of Geophysical Research: Solid Earth, 116(B1).

Blystad, P., Brekke, H., Færseth, R.B., Larsen, B.T., Skogseid, J., Tørudbakken, B., 1995. Structural elements of the Norwegian continental shelf, Part II: The Norwegian Sea region. NPD-Bul. Nor. Pet. Dir. 8.

Breivik, A.J., Mjelde, R., Faleide, J.I., Murai, Y., 2006. Rates of continental breakup magmatism and seafloor in the Norway Basin-Iceland plume interaction. J. Geophys. Res. 111, B07102.

Breivik, A.J., Mjelde, R., Faleide, J.I., Murai, Y., 2012. The eastern Jan Mayen microcontinent volcanic margin. Geophys. J. Int. 188, 798–818.

Breivik, A. J., Faleide, J. I., Mjelde, R., Flueh, E. R., Murai, Y., 2017. A new tectono-magmatic model for the Lofoten/Vesterålen Margin at the outer limit of the Iceland Plume influence. Tectonophysics, 718, 25-44.

Breivik, A. J., Faleide, J. I., Mjelde, R., Flueh, E. R., Murai, Y., 2020. Crustal structure and erosion of the Lofoten/Vesterålen shelf, northern Norwegian margin. Tectonophysics, 228318.

Brekke, H., Sjulstad, H. I., Magnus, C., Williams, R. W., 2001. Sedimentary environments offshore Norway—an overview. In Norwegian Petroleum Society Special Publications (Vol. 10, pp. 7-37). Elsevier.

Dalland, A., 1981. In: Bøe, R., Fossen, H., Smelror, M. 2010. Mesozoic sediments and structures onshore Norway and in the coastal zone. Norges geologiske undersøkelse Bulletin, 450, 15-32.

Doré, A. G., Lundin, E. R., Fichler, C., Olesen, O., 1997. Patterns of basement structure and reactivation along the NE Atlantic margin. Journal of the Geological Society, 154(1), 85-92.

Doré, A.G., Lundin, E.R., Kusznir, N.J., Pascal, C., 2008. Potential mechanisms for the genesis of Cenozoic domal structures on the NE Atlantic margin: pros, cons and some new ideas. In: In: Johnson, H., Doré, A.G., Gatliff, R.W., Holdsworth, R., Lundin, E.R., Ritchie, J.D. (Eds.), The Nature and Origin of Compression in Passive Margins, vol. 306. Geological society, London, Special Publications, pp. 1–26.

Eig, K., Bergh, S. G., 2011. Late Cretaceous–Cenozoic fracturing in Lofoten, North Norway: Tectonic significance, fracture mechanisms and controlling factors. Tectonophysics, 499(1-4), 190-205.

Eldholm, O., Tsikalas, F., Faleide, J. I., 2002. Continental margin off Norway 62–75 N: Palaeogene tectono-magmatic segmentation and sedimentation. Geological Society, London, Special Publications, 197(1), 39-68.

Færseth, R. B., 2012. Structural development of the continental shelf offshore Lofoten–Vesterålen, northern Norway. Norwegian Journal of Geology/Norsk Geologisk Forening, 92(1).

Faleide, J.I., Tsikalas, F., Breivik, A.J., Mjelde, R., Ritzmann, O., Engen, O., Wilson, J., Eldholm, O., 2008. Structure and evolution of the continental margin off Norway and the Barents Sea. Episodes 31, 82–91.

Faleide, J. I., Bjørlykke, K., Gabrielsen, R. H., 2015. Geology of the Norwegian continental shelf. In Petroleum Geoscience (pp. 603-637). Springer, Berlin, Heidelberg.

Fossen, H., 2010. Structural geology. Cambridge University Press.

Gabrielsen, R. H., Steel, R. J., Nottvedt, A., 1995. Subtle traps in extensional terranes; a model with reference to the North Sea. Petroleum Geoscience, 1(3), 223-235.

Gawthorpe, R. L., Hurst, J. M., 1993. Transfer zones in extensional basins: their structural style and influence on drainage development and stratigraphy. Journal of the Geological Society, 150(6), 1137-1152.

Gómez-Romeu, J., Kusznir, N., Roberts, A., Manatschal, G., 2020. Measurements of the extension required for crustal breakup on the magma-poor Iberia-Newfoundland conjugate margins. Marine and Petroleum Geology, 104403.

Hansen, J. A., Bergh, S. G., Henningsen, T., 2011. Mesozoic rifting and basin evolution on the Lofoten and Vesterålen Margin, North-Norway; time constraints and regional implications. Norwegian Journal of Geology/Norsk Geologisk Forening, 91(4).

Henstra, G. A., Rotevatn, A., Gawthorpe, R. L., Ravnås, R., 2015. Evolution of a major segmented normal fault during multiphase rifting: The origin of plan-view zigzag geometry. Journal of Structural Geology, 74, 45-63.

Henstra, G. A., Kristensen, T. B., Rotevatn, A., Gawthorpe, R. L., 2019. How do pre-existing normal faults influence rift geometry? A comparison of adjacent basins with contrasting underlying structure on the Lofoten Margin, Norway. Basin Research, 31(6), 1083-1097.

Kalač, A., 2017. Cretaceous and Cenozoic Tectono-Stratigraphic Evolution of the Southern Lofoten and Northern Vøring Margins, Offshore Northern Norway. Master thesis. University of Oslo, pp. 106.

Kusznir, N. J., Hunsdale, R., Roberts, A. M., 2005. Timing and magnitude of depth-dependent lithosphere stretching on the southern Lofoten and northern Vøring continental margins offshore mid-Norway: implications for subsidence and hydrocarbon

maturation at volcanic rifted margins. In Geological Society, London, Petroleum Geology Conference series (Vol. 6, No. 1, pp. 767-783). Geological Society of London.

Lister, G. S., Etheridge, M. A., Symonds, P. A., 1991. Detachment models for the formation of passive continental margins. Tectonics, 10(5), 1038-1064.

Løseth, H., Tveten, E., 1996. Post-Caledonian structural evolution of the Lofoten and Vesteralen offshore and onshore areas. Norsk Geologisk Tidsskrift, 76(4), 215-229.

Lundin, E., Doré, A. G., 2002. Mid-Cenozoic post-breakup deformation in the 'passive' margins bordering the Norwegian–Greenland Sea. Marine and Petroleum Geology, 19(1), 79-93.

Mjelde, R., Sellevoll, M. A., 1993. Seismic anisotropy inferred from wide-angle reflections off Lofoten, Norway, indicative of shear-aligned minerals in the upper mantle. Tectonophysics, 222(1), 21-32.

Mjelde, R., Shimamura, H., Kanazawa, T., Kodaira, S., Raum, T., Shiobara, H., 2003. Crustal lineaments, distribution of lower crustal intrusives and structural evolution of the Vøring Margin, NE Atlantic; new insight from wide-angle seismic models. Tectonophysics, 369(3-4), 199-218.

Mjelde, R., Raum, T., Breivik, A., Shimamura, H., Murai, Y., Takanami, T., Faleide, J. I., 2005. Crustal structure of the Vøring Margin, NE Atlantic: a review of geological implications based on recent OBS data. In Geological Society, London, Petroleum Geology Conference Series (Vol. 6, No. 1, pp. 803-813). Geological Society of London.

Mjelde, R., Raum, T., Kandilarov, A., Murai, Y., Takanami, T., 2009. Crustal structure and evolution of the outer Møre Margin, NE Atlantic. Tectonophysics, 468(1-4), 224-243.

Mosar, J., Eide, E. A., Osmundsen, P. T., Sommaruga, A., Torsvik, T. H., 2002. Greenland–Norway separation: a geodynamic model for the North Atlantic. In Norwegian Journal of Geology (Vol. 82, p. 282).

Norlex, 2012. *Standard Lithostratigraphy of Offshore Norway*. Available from: http://nhm2.uio.no/norlex/StandardLithostratigraphicWallchartOffshoreNorway.pdf.

Norwegian Petroleum Directorate (NPD), 2010. *Petroleumsressurser i havområdene utenfor Lofoten, Vesterålen og Senja*. Available from: http://www.npd.no/Publikasjoner/Rapporter/Petroleumsressurser-i-havomradene-utenfor-Lofoten-Vesteralen-og-Senja---Geofaglig-vurdering/Regional-geologi-og-petroleumsgeologi-Lofoten-Vesteralen-og-Troms-II/

Norwegian Petroleum Directorate (NPD), 2020. *FactMaps Norwegian Petroleum Directorate*. Available from: http://gis.npd.no/factmaps/html_21/

Norwegian Petroleum Directorate (NPD), 2020a. *FactPages Norwegian Petroleum Directorate*. Available from: https://www.npd.no/en/facts/resource-accounts-and-analysis/resource-accounts-as-of-31-december-2019/

Norwegian Petroleum Directorate (NPD), 2020b. *FactPages Norwegian Petroleum Directorate*. Available from: https://factpages.npd.no/en/wellbore/pageview/exploration/all/2932

Olesen, O., Lundin, E., Nordgulen, Ø., Osmundsen, P. T., Skilbrei, J. R., Smethurst, M. A., Solli, A., Bugge, T., Fichler, C., 2002. Bridging the gap between the onshore and offshore geology in Nordland, northern Norway. Norwegian Journal of Geology/Norsk Geologisk Forening, 82(4).

Olesen, O., Ebbing, J., Lundin, E., Mauring, E., Skilbrei, J. R., Torsvik, T. H., Hansen, E. K., Henningsen, T., Midbøe, P., Sand, M., 2007. An improved tectonic model for the Eocene opening of the Norwegian–Greenland Sea: Use of modern magnetic data. Marine and Petroleum Geology, 24(1), 53-66.

Olesen, O., Brönner, M., Ebbing, J., Gellein, J., Gernigon, L., Koziel, J., Lauritsen, T., Myklebust, R., Pascal, C., Sand, M., 2010. New aeromagnetic and gravity compilations from Norway and adjacent areas: methods and applications. In: Geological Society, London, Petroleum Geology Conference Series. Geological Society of London, pp. 559–586.

Parnell-Turner, R., White, N.J., McCave, I.N., Henstock, T.J., Murton, B., Jones, S.M., 2015. Architecture of North Atlantic contourite drifts modified by transient circulation of the Icelandic mantle plume. Geochem. Geophys. Geosyst. 16, 3414–3435.

Paterson, N. R., Reeves, C. V., 1985. Applications of gravity and magnetic surveys; the state-of-the-art in 1985. Geophysics, 50(12), 2558-2594.

Pickering, G., Bull, J. M., Sanderson, D. J., 1996. Scaling of fault displacements and implications for the estimation of sub-seismic strain. Geological Society, London, Special Publications, 99(1), 11-26.

Planke, S., Skogseid, J., Eldholm, O., 1991. Crustal structure off Norway, 62 to 70 north. Tectonophysics, 189(1-4), 91-107.

Ren, S., Faleide, J. I., Eldholm, O., Skogseid, J., Gradstein, F., 2003. Late Cretaceous–Paleocene tectonic development of the NW Vøring basin. Marine and Petroleum Geology, 20(2), 177-206.

Reston, T. J., 2005. Polyphase faulting during the development of the west Galicia rifted margin. Earth and Planetary Science Letters, 237(3-4), 561-576.

Reston, T. J., 2009. The extension discrepancy and syn-rift subsidence deficit at rifted margins. Petroleum Geoscience, 15(3), 217-237.

Rise, L., Bøe, R., Riis, F., Bellec, V. K., Laberg, J. S., Eidvin, T., Elvenes, S., Thorsnes, T., 2013. The Lofoten-Vesterålen continental margin, North Norway: Canyons and mass-movement activity. Marine and Petroleum Geology, 45, 134-149.

Rosendahl, B. R., Reynolds, D. J., Lorber, P. M., Burgess, C. F., McGill, J., Scott, D., Lambiase, J. J., Derksen, S. J., 1986. Structural expressions of rifting: lessons from Lake Tanganyika, Africa. Geological Society, London, Special Publications, 25(1), 29-43.

Rosendahl, B. R., 1987. Architecture of continental rifts with special reference to East Africa. Annual Review of Earth and Planetary Sciences, 15(1), 445-503.

Sellevoll, M. A., Mokhtari, M., 1988. An intra-oceanic crustal seismic reflecting zone below the dipping reflectors on Lofoten margin. Geology, 16(7), 666-668.

Skogseid, J., 1994. Dimensions of the late Cretaceous-Paleocene northeast Atlantic rift derived from Cenozoic subsidence. Tectonophysics, 240(1-4), 225-247.

Skogseid, J., Pedersen, T., Larsen, V. B., 1992b. Vøring Basin: subsidence and tectonic evolution. In Structural and tectonic modelling and its application to petroleum geology (pp. 55-82). Elsevier.

Skogseid, J., Planke, S., Faleide, J. I., Pedersen, T., Eldholm, O., Neverdal, F., 2000. NE Atlantic continental rifting and volcanic margin formation. Geological Society, London, Special Publications, 167(1), 295-326.

Smelror, M., Mørk, A., Mørk, M. B. E., Weiss, H. M., Løseth, H., 2001. Middle Jurassic-Lower Cretaceous transgressive-regressive sequences and facies distribution off northern Nordland and Troms, Norway. In Norwegian Petroleum Society Special Publications (Vol. 10, pp. 211-232). Elsevier.

Tasrianto, R., Escalona, A., 2015. Rift architecture of the Lofoten-Vesterålen margin, offshore Norway. Marine and Petroleum Geology, 64, 1-16.

Theissen-Krah, S., Zastrozhnov, D., Abdelmalak, M. M., Schmid, D. W., Faleide, J. I., Gernigon, L., 2017. Tectonic evolution and extension at the Møre Margin–Offshore mid-Norway. Tectonophysics, 721, 227-238.

Tsikalas, F., Faleide, J. I., Eldholm, O., 2001. Lateral variations in tectono-magmatic style along the Lofoten–Vesterålen volcanic margin off Norway. Marine and Petroleum Geology, 18(7), 807-832.

Tsikalas, F., Eldholm, O., Faleide, J. I., 2005a. Crustal structure of the Lofoten–Vesterålen continental margin, off Norway. Tectonophysics, 404(3-4), 151-174.

Tsikalas, F., Faleide, J. I., Eldholm, O., Wilson, J., 2005b. Late Mesozoic–Cenozoic structural and stratigraphic correlations between the conjugate mid-Norway and NE Greenland continental margins. In Geological Society, London, Petroleum Geology Conference series (Vol. 6, No. 1, pp. 785-801). Geological Society of London.

Tsikalas, F., Faleide, J. I., Kusznir, N. J., 2008. Along-strike variations in rifted margin crustal architecture and lithosphere thinning between northern Vøring and Lofoten margin segments off mid-Norway. Tectonophysics, 458(1-4), 68-81.

Tsikalas, F., Faleide, J. I., Eldholm, O., Blaich, O. A., 2012. The NE Atlantic conjugate margins. Regional geology and tectonics: Phanerozoic passive margins, cratonic basins and global tectonic maps, 1, 140-201.

Tsikalas, F., Faleide, J. I., Kalač, A., 2019. New insights into the Cretaceous-Cenozoic tectono-stratigraphic evolution of the southern Lofoten margin, offshore Norway. Marine and Petroleum Geology, 110, 832-855.

Vågnes, E., Gabrielsen, R. H., Haremo, P., 1998. Late Cretaceous–Cenozoic intraplate contractional deformation at the Norwegian continental shelf: timing, magnitude and regional implications. Tectonophysics, 300(1-4), 29-46.

Walsh, J., Watterson, J., Yielding, G., 1991. The importance of small-scale faulting in regional extension. Nature, 351(6325), 391-393.

Wilhelmsen-Rolstad, H.C., 2016. Cretaceous Tectono-Stratigraphic Evolution of the Ribban and Northern Træna Basins at the Lofoten Margin, Offshore Northern Norway. Master thesis. University of Oslo, pp. 105.

Wilson, R. W., McCaffrey, K. J., Holdsworth, R. E., Imber, J., Jones, R. R., Welbon, A. I., Roberts, D., 2006. Complex fault patterns, transtension and structural segmentation of

the Lofoten Ridge, Norwegian margin: using digital mapping to link onshore and offshore geology. Tectonics, 25(4).

Zastrozhnov, D., Gernigon, L., Gogin, I., Abdelmalak, M. M., Planke, S., Faleide, J. I., Eide, S., Myklebust, R., 2018. Cretaceous-Paleocene Evolution and Crustal Structure of the Northern Vøring Margin (Offshore Mid-Norway): Results from Integrated Geological and Geophysical Study. Tectonics, 37(2), 497-528.

Zastrozhnov, D., Gernigon, L., Gogin, I., Planke, S., Abdelmalak, M. M., Polteau, S., Faleide, J. I., Manton, B., Myklebust, R., 2020. Regional structure and polyphased Cretaceous-Paleocene rift and basin development of the mid-Norwegian volcanic passive margin. Marine and Petroleum Geology, 115, 104269.